

# Advances

## in Clinical and Experimental Medicine

MONTHLY ISSN 1899-5276 (PRINT) ISSN 2451-2680 (ONLINE)

[www.advances.umed.wroc.pl](http://www.advances.umed.wroc.pl)

2020, Vol. 29, No. 5 (May)

Impact Factor (IF) – 1.227  
Ministry of Science and Higher Education – 40 pts.  
Index Copernicus (ICV) – 155.19 pts.



WROCLAW  
MEDICAL UNIVERSITY

Advances  
in Clinical and Experimental  
Medicine



# Advances in Clinical and Experimental Medicine

ISSN 1899-5276 (PRINT)

ISSN 2451-2680 (ONLINE)

www.advances.umed.wroc.pl

**MONTHLY 2020**  
**Vol. 29, No. 5**  
**(May)**

Advances in Clinical and Experimental Medicine is a peer-reviewed open access journal published by Wrocław Medical University. Its abbreviated title is Adv Clin Exp Med. Journal publishes original papers and reviews encompassing all aspects of medicine, including molecular biology, biochemistry, genetics, biotechnology, and other areas. It is published monthly, one volume per year.

---

## Editorial Office

ul. Marcinkowskiego 2–6  
50-368 Wrocław, Poland  
Tel.: +48 71 784 11 36  
E-mail: redakcja@umed.wroc.pl

## Publisher

Wrocław Medical University  
Wybrzeże L. Pasteura 1  
50-367 Wrocław, Poland

© Copyright by Wrocław Medical University,  
Wrocław 2020

Online edition is the original version of the journal

---

## Editor-in-Chief

Maciej Bagłaj

## Vice-Editor-in-Chief

Dorota Frydecka

---

## Editorial Board

Piotr Dziągpiel  
Marian Klinger  
Halina Milnerowicz  
Jerzy Mozrzymas

---

## Thematic Editors

Marzenna Bartoszewicz (microbiology)  
Marzena Dominiak (dentistry)  
Paweł Domosławski (surgery)  
Maria Ejma (neurology)  
Jacek Gajek (cardiology)  
Mariusz Kuształ  
(nephrology and transplantology)  
Rafał Matkowski (oncology)  
Ewa Milnerowicz-Nabzdyk (gynecology)  
Katarzyna Neubauer (gastroenterology)  
Marcin Ruciński (basic sciences)  
Robert Śmigiel (pediatrics)  
Paweł Tabakow (experimental medicine)  
Anna Wiela-Hojeńska  
(pharmaceutical sciences)  
Dariusz Wołowicz (internal medicine)

---

## International Advisory Board

Reinhard Berner (Germany)  
Vladimir Bobek (Czech Republic)  
Marcin Czyz (UK)  
Buddhadeb Dawn (USA)  
Kishore Kumar Jella (USA)

---

## Secretary

Katarzyna Neubauer

---

Piotr Ponikowski  
Marek Sąsiadek  
Leszek Szenborn  
Jacek Szepietowski

---

## Statistical Editors

Dorota Diakowska  
Leszek Noga  
Lesław Rusiecki

## Technical Editorship

Paulina Kunicka  
Marek Misiak

## English Language Copy Editors

Eric Hilton  
Sherill Howard Pociecha  
Jason Schock  
Marcin Tereszewski

---

Pavel Kopel (Czech Republic)  
Tomasz B. Owczarek (USA)  
Ivan Rychlík (Czech Republic)  
Anton Sculean (Switzerland)  
Andriy B. Zimenkovsky (Ukraine)

## Editorial Policy

Advances in Clinical and Experimental Medicine (Adv Clin Exp Med) is an independent multidisciplinary forum for exchange of scientific and clinical information, publishing original research and news encompassing all aspects of medicine, including molecular biology, biochemistry, genetics, biotechnology and other areas. During the review process, the Editorial Board conforms to the "Uniform Requirements for Manuscripts Submitted to Biomedical Journals: Writing and Editing for Biomedical Publication" approved by the International Committee of Medical Journal Editors ([www.ICMJE.org/](http://www.ICMJE.org/)). The journal publishes (in English only) original papers and reviews. Short works considered original, novel and significant are given priority. Experimental studies must include a statement that the experimental protocol and informed consent procedure were in compliance with the Helsinki Convention and were approved by an ethics committee.

For all subscription-related queries please contact our Editorial Office:  
[redakcja@umed.wroc.pl](mailto:redakcja@umed.wroc.pl)

For more information visit the journal's website:  
[www.advances.umed.wroc.pl](http://www.advances.umed.wroc.pl)

Pursuant to the ordinance No. 134/XV R/2017 of the Rector of Wrocław Medical University (as of December 28, 2017) from January 1, 2018 authors are required to pay a fee amounting to 700 euros for each manuscript accepted for publication in the journal Advances in Clinical and Experimental Medicine.

„Podniesienie poziomu naukowego i poziomu umiędzynarodowienia wydawanych czasopism naukowych oraz upowszechniania informacji o wynikach badań naukowych lub prac rozwojowych – zadanie finansowane w ramach umowy 784/p-DUN/2017 ze środków Ministra Nauki i Szkolnictwa Wyższego przeznaczonych na działalność upowszechniającą naukę”.



Indexed in: MEDLINE, Science Citation Index Expanded, Journal Citation Reports/Science Edition, Scopus, EMBASE/Excerpta Medica, Ulrich's™ International Periodicals Directory, Index Copernicus

Typographic design: Monika Kołęda, Piotr Gil  
DTP: Wydawnictwo UMW  
Cover: Monika Kołęda  
Printing and binding: EXDRUK

## Contents

### Original papers

- 525 Xingli Jiang, Zhiguang Gao, Linli Tian, Ming Liu  
**Expressions of miR-122a and miR-3195 in laryngeal cancer and their effects on the proliferation and apoptosis of laryngeal cancer cell Hep-2**
- 535 Huifen Huang, Xiaolin Tian, Xiao Peng, Liangtong Huang, Lerong Mei, Yanli Zhan, Siying Chen, Huihua Wu, Guofang Wei, Xueli Cai  
**Antifungal itraconazole ameliorates experimental autoimmune encephalomyelitis through a novel mechanism of action**
- 547 Iwona Bednarz-Misa, Katarzyna Neubauer, Ewa Zacharska, Bartosz Kapturkiewicz, Małgorzata Krzystek-Korpacka  
**Whole blood *ACTB*, *B2M* and *GAPDH* expression reflects activity of inflammatory bowel disease, advancement of colorectal cancer, and correlates with circulating inflammatory and angiogenic factors: Relevance for real-time quantitative PCR**
- 557 Patrycja Downarowicz, Paweł Noszczyk, Marcin Mikulewicz, Rafał Nowak  
**Thermal effect of Er:YAG and Er,Cr:YSGG used for debonding ceramic and metal orthodontic brackets: An experimental analysis**
- 565 Małgorzata Matusiewicz, Maciej Rachwałik, Małgorzata Krzystek-Korpacka, Grzegorz Bielicki, Izabela Berdowska, Rafał Nowicki, Andrzej Gamian, Marek Jasiński  
**Upregulated sulfatase and downregulated MMP-3 in thoracic aortic aneurysm**
- 573 Sławomir Woźniak, Radosław Kempirski, Joanna Grzelak, Zygmunt Domagała, Friedrich Paulsen  
**Anatomy-related ratios predict colonoscopy incompleteness in similar examination conditions**
- 581 Grzegorz Raba, Izabela Zawlik, Marcin Braun, Sylwia Paszek, Natalia Potocka, Marzena Skrzypa, Bogdan Obrzut, Marek Kluz, Katarzyna Kluz, Barbara Zych, Magdalena Janowska, Tomasz Kluz  
**Evaluation of the association between angiotensin converting enzyme insertion/deletion polymorphism and the risk of endometrial cancer in and characteristics of Polish women**
- 587 Ryszard Antkowiak, Łukasz Antkowiak, Sławomir Grzegorzczyn, Klaudia Nalik-Iwaniak, Natalia Kabała, Zbigniew Arent, Edyta Warmusz-Reichman, Katarzyna Stęplewska, Paweł Domosławski  
**Efficacy of intra-arterial lidocaine infusion in the treatment of cerulein-induced acute pancreatitis**
- 597 Andrea Freer-Rojas, Luis Carlos Martínez-Garibay, Fernando Torres-Méndez, Claudia Edith Dávila-Pérez, Gabriel Alejandro Martínez-Castañón, Nuria Patiño-Marín, Jorge Alejandro Alegría-Torres  
**Macrophage migration inhibitory factor gene polymorphisms as exacerbating factors of apical periodontitis**
- 603 Anna Jakubowska, Katarzyna Kiliś-Pstrusińska  
**Annexin V in children with idiopathic nephrotic syndrome treated with cyclosporine A**
- 611 Anna Medyńska, Katarzyna Kiliś-Pstrusińska, Irena Makulska, Danuta Zwolińska  
**Kidney transplantation and other methods of renal replacement therapy in children: 30 years of observations in one center**

### Reviews

- 615 Stefano Cosma, Chiara Benedetto  
**Classification algorithm of patients with endometriosis: Proposal for tailored management**
- 623 Andrzej Żyłuk  
**The role of genetic factors in carpal tunnel syndrome etiology: A review**
- 629 Agnieszka Sas-Strózik, Magdalena Krajewska, Mirosław Banasik  
**The significance of angiotensin II type 1 receptor (AT1 receptor) in renal transplant injury**



# Expressions of miR-122a and miR-3195 in laryngeal cancer and their effects on the proliferation and apoptosis of laryngeal cancer cell Hep-2

Xingli Jiang<sup>1,A–F</sup>, Zhiguang Gao<sup>2,A–C</sup>, Linli Tian<sup>1,D,F</sup>, Ming Liu<sup>1,A,E,F</sup>

<sup>1</sup> Department of Otorhinolaryngology, and Head and Neck Surgery, The Second Affiliated Hospital of Harbin Medical University, China

<sup>2</sup> Department of Otorhinolaryngology, and Head and Neck Surgery, Heilongjiang Provincial Hospital Affiliated to Harbin Institute of Technology, China

A – research concept and design; B – collection and/or assembly of data; C – data analysis and interpretation;

D – writing the article; E – critical revision of the article; F – final approval of the article

Advances in Clinical and Experimental Medicine, ISSN 1899–5276 (print), ISSN 2451–2680 (online)

*Adv Clin Exp Med.* 2020;29(5):525–534

## Address for correspondence

Ming Liu

E-mail: liuming83b@163.com

## Funding sources

None declared

## Conflict of interest

None declared

Received on August 9, 2019

Reviewed on November 13, 2019

Accepted on March 10, 2020

Published online on May 28, 2020

## Cite as

Jiang X, Gao Z, Tian L, Liu M. Expressions of miR-122a and miR-3195 in laryngeal cancer and their effects on the proliferation and apoptosis of laryngeal cancer cell Hep-2.

*Adv Clin Exp Med.* 2020;29(5):525–534.

doi:10.17219/acem/118848

## DOI

10.17219/acem/118848

## Copyright

© 2020 by Wrocław Medical University

This is an article distributed under the terms of the Creative Commons Attribution 3.0 Unported (CC BY 3.0)

(<https://creativecommons.org/licenses/by/3.0/>)

## Abstract

**Background.** Laryngeal cancer (LC) is one of the common malignant tumors in the head and neck area, and the survival rate for patients is low.

**Objectives.** To investigate miR-122a and miR-3195 expressions in LC tissue, their correlations with clinicopathological features, and their impacts on Hep-2 proliferation and apoptosis.

**Material and methods.** Thirty LC and 20 peritumoral tissue specimens were analyzed. miR-122a, miR-122a-negative control sequence, miR-3195, and miR-3195-NG sequence were transfected into Hep-2 in the miR-122a-mimics, miR-122a-NG, miR-3195-mimics, and miR-3195-NG groups, respectively. The miR-122a-mimics-non-transfected and miR-3195-mimics-non-transfected groups used non-transfected Hep-2.

**Results.** There were lower miR-122a, miR-3195 and occludin protein, and higher TBX1 protein expressions in LC than in the peritumoral tissue; the miR-122a level was associated with clinical stage (all  $p < 0.001$ ). Positive correlations between miR-122a and miR-3195, and miR-122a and occludin expressions, and a negative correlation between miR-3195 and TBX1 expressions were observed ( $r = 0.418$ ,  $r = 0.541$ ,  $r = -0.428$ , all  $p < 0.001$ ). The miR-122a and miR-3195 levels in the 2 mimics groups increased respectively compared to their NG and the non-transfected groups. At different time points after 24 h of transfection, the optical density in the 2 mimics groups was lower than in their NG groups. The miR-122a-mimics group had an increased occludin level and the miR-3195-mimics group had a decreased TBX1 level, and both groups had greater apoptosis rates than their NG groups and in the non-transfected groups (all  $p < 0.001$ ).

**Conclusions.** miR-122a is associated with clinical stage. miR-122a and miR-3195 may act as tumor suppressors and play a role in LC pathogenesis. They can suppress Hep-2 proliferation and promote its apoptosis, probably owing to the upregulation of occludin by miR-122a and suppression of TBX1 by miR-3195.

**Key words:** apoptosis, microRNAs, cell proliferation, laryngeal neoplasms

## Introduction

Laryngeal cancer (LC) is one of the common malignant tumors in the head and neck area, which accounts for 85–90% of the malignant tumors in the larynx; currently, surgery, chemotherapy and radiotherapy are the main methods for treating LC.<sup>1</sup> Although technologies in cancer treatment have been advancing over the past few decades, many patients still experience metastasis of tumor cells into important organs, leading to low survival rates.<sup>2</sup> This problem is mainly caused by a lack of early diagnosis and leads to a decrease in treatment efficacy; apart from that, patients' weak tolerance to chemotherapy or radiotherapy and postoperative recurrence and metastasis of tumor also contribute to the high mortality.<sup>3</sup> Therefore, it is of great significance to find molecular biomarkers that are related to the early diagnosis of LC, the molecular mechanisms in LC pathogenesis, and the biological marker and therapeutic target that can inhibit LC occurrence and progression in order to improve early diagnosis and prognosis in patients.

The microRNA (miRNA), existing widely in eukaryotes, is a highly conserved endogenous non-coding hairpin-shaped nucleotide transcript (containing 19–25 base and 18–25 nucleotides).<sup>4,5</sup> Some studies have found that miRNA is closely associated with LC occurrence and progression. Liu et al. have reported that miR-125a can target hematopoietic stem cell-specific protein 1-associated protein X-1 (HAX-1) and reverse the cisplatin resistance in Hep-2 cancer stem cell.<sup>6</sup> Although miR-122a has been reported by Chen et al. to be able to suppress the proliferation of LC cell Hep-2, the effect of miR-122a on Hep-2 apoptosis remains unclear.<sup>7</sup> Previous studies have demonstrated that miR-3195 can act as a tumor suppressor gene. For instance, Yoon et al. reported a reduction in miR-3195 expression level in gastric cancer tissue.<sup>8</sup> However, there have yet been no studies on the expression of miR-3195 in LC.

Thus, in the present study, we measured the expressions of miR-122a and miR-3195 in LC tissue and Hep-2 cell and investigated these 2 miRNAs in LC pathogenesis and their impacts on the cell proliferation and apoptosis, with the hope of gaining a better understanding on the biological function of these 2 miRNAs in LC. Furthermore, as a preliminary analysis of the molecular mechanisms of miR-122a and miR-3195, bioinformatics was also used to examine the potential target genes that may be regulated by these miRNAs.

## Material and methods

### Basic information

A total of 30 LC specimens from patients undergoing surgical excision in our hospital and 20 peritumoral tissue specimens (>2 cm from the tumor) were collected for

the study (21 men, 9 women, age range: 46–80 years, mean age: 62.7 ± 8.3 years). The study was approved by the Ethics Committee of our hospital, and informed consent was obtained from all patients or their family members.

Inclusion criteria: the specimens of LC and peritumoral tissues were confirmed by pathological examination<sup>9</sup>; patients or their family members signed the informed consent.

Exclusion criteria: chemotherapy, radiotherapy or immunotherapy received in the past; severe liver and kidney dysfunction, connective tissue diseases, endocrine and metabolic diseases, nervous system disease, hematopoietic disorder, immune disease, and other tumors; or a history or a family history of mental illness.

We used TargetScan Release v. 7.2 online software (<http://www.targetscan.org>) to predict the target gene of miR-122a and miR-3195 and found that miR-122a can regulate occludin and miR-3195 can regulate *TBX1*.

### Main instruments and reagents

Main instruments and reagents were as follows: quantitative fluorescence polymerase chain reaction (PCR) (7500; Applied Biosystems, Foster City, USA), total RNA extraction kit (EasyPure miRNA Kit; Transgen, Beijing, China). PCR-reverse transcription kit (TransScript<sup>®</sup> Green miRNA Two-Step qRT-PCR SuperMix; TransGen Biotech, Beijing, China), Lipofectamine 2000 and Annexin V-FITC cell apoptosis kit (Invitrogen, Carlsbad, USA), incubator (RPMI-1640; Hyclone, Logan, USA), rabbit anti-human *TBX1* primary antibody (Abcam, Cambridge, UK), rabbit anti-human occludin polyclonal antibody (Santa Cruz Biotechnology, Santa Cruz, USA), mouse anti-human  $\beta$ -catenin primary antibody (Boster Biological Technology, Wuhan, China), miR-122a mimics, miR-122a NG, miR-3195 mimics, and miR-3195 NG (Sangon Biotech, Shanghai, China), horseradish peroxidase (HRP)-conjugated goat anti-mouse secondary antibody, MTT cell proliferation kit (Beyotime Biotechnology, Shanghai, China), FACSCanto flow cytometer (Becton Dickinson, Franklin Lakes, USA), and a microplate reader (Elx-800; BioTek, Winooski, USA). Primers of miR-122a, miR-3195 and U6 were designed and synthesized by Shanghai GenePharma Co., Ltd (Shanghai, China) (Table 1).

### Cell culture

Hep-2 cells were seeded in a culture plate followed by the addition of RPMI-1640 medium containing 15% fetal bovine serum (FBS) and 1% mycillin/streptomycin.<sup>10</sup> The cells were incubated in an incubator under saturated humidity and constant temperature (37°C, 5% CO<sub>2</sub>). The medium was changed in a timely manner, and the cells were digested with trypsin for subculture. The cells in logarithmic growth phase were collected for subsequent experiments.



Table 1. Primer sequence

Primers	Forward primer	Reverse primer
miR-122a	5'-CCTTTGTGTAAGTGTACGGCC-3'	5'-CTTTGGCAGTAAATAGCTGATTGAC-3'
miR-3195	5'-AACACGGCTCACGCTTAC-3'	5'-CCAGACCCTCAGACTTGC-3'
U6	5'-GCGCGTCGTGAAGCGTTC-3'	5'-GTGCAGGGTCCGAGGT-3'

## Cell transfection

Cells in logarithmic growth phase were seeded in a 6-well plate for culture ( $1 \times 10^5$ /well). When fusion reached 60–70%, transfection was performed according to the manufacturer's instructions for Lipofectamine 2000. Eighty nmol/L of miR-122a, miR-122a NG sequence, miR-3195, and miR-3195 NG sequence were transfected into Hep-2 cell in the miR-122a-mimics, miR-122a-NG, miR-3195-mimics, and miR-3195-NG groups, respectively, followed by the cell culture for 24 h. Meanwhile, 2 non-transfected groups, miR-122a-mimics-non-transfected and miR-3195-mimics-non-transfected groups with non-transfected Hep-2 cells were set up and cultured for 24 h. Subsequently, the medium was replaced with 50 ng/mL macrophage colony-stimulating factors for all cells (twice per day).

## qRT-PCR

Total RNA extraction from all the tissues and cells was performed using EasyPure miRNA kit (TransGen Biotech). The purity, concentration and integrity of RNA were checked with a UV spectrophotometer and agarose gel electrophoresis, and the total RNAs were reversely transcribed using TransScript<sup>®</sup> miRNA RT Enzyme Mix and 2 × TS miRNA Reaction Mix (TransGen Biotech) according to the manufacturer's instructions. Next, PCR was conducted for amplification, and the reaction system included 1 μL of cDNA, 0.4 μL of forward primer, 0.4 μL of reverse primer, 10 μL of 2 × TransTaq<sup>®</sup> Tip Green qPCR SuperMix, 0.4 μL of 50 × passive reference dye, and distilled deionized water that made the whole volume into 20 μL. The PCR running parameters were set as follows: 94°C for 30 s (pre-denaturation), 94°C for 5 s (denaturation) and 60°C for 30 s (annealing and extension) for 40 cycles. Each sample was set in triplicate, and the experiment was repeated 3 times. U6 was used as an internal control. Data was calculated using the  $2^{-\Delta\Delta C_t}$  method.

## Western blot

The total proteins were isolated from the tissues and cells using radioimmunoprecipitation assay lysis buffer. The protein concentration was measured with bicinchoninic acid method, and the concentration was adjusted to 4 μg/μL. After running 12% SDS-PAGE for separation, samples were transferred to polyvinylidene fluoride

(PVDF) membranes and stained with Ponceau solution followed by washing in phosphate-buffered saline/Tween (PBST) for 5 min and blocking in 5% skim milk for 2 h. Next, samples were incubated with primary antibodies overnight at 4°C (1:1,000). The membrane was then washed to remove the primary antibodies, and the samples were incubated with HRP-conjugated goat anti-mouse secondary antibody (1:5,000) for 1 h at 37°C followed by 3 washes in Tris-buffered saline/Tween; 5 min per wash). Afterward, the membrane was placed in a darkroom for developing. Extra fluid on the membrane was dried using filter papers, and the samples were treated with enhanced chemiluminescence (ECL) for imaging. Protein band was scanned and analyzed with Gel-Pro Analyzer v. 4.0 software (Molecular Devices Corp, Bay Area, USA) to measure the grayscale. The relative protein expression was calculated as the grayscale value of the target protein band/grayscale value of the β-catenin protein band.

## Cell proliferation

Cell suspension ( $1 \times 10^5$ ) was prepared with cells in a logarithmic growth phase. After adjusting the cell density to  $2 \times 10^4$  mL, the cells were seeded in a 96-well plate ( $2 \times 10^3$ /well). The MTT assay was performed every 24 h 5 times to measure the cell viability (the final test was done at 120 h). During the test, MTT solution (10 μL, 5 mg/mL) was added into each well followed by 4 h of incubation. Next, formazan dissolution (150 μL) was added into each well, and the plate was agitated under room temperature for 10 min. The crystal was dissolved completely as observed under a light microscope. The optical density (OD) value at 570 nm was measured using a microplate reader, and the measurement was repeated 3 times for each well.

## Cell apoptosis

Forty-eight hours after transfection, the cells were digested using trypsin, and cold PBS (0.01 mol/L) was used to wash the collected cells. After centrifugation ( $111.8 \times g$ , 25°C), the supernatant was discarded, and the cells were resuspended with 100 μL  $1 \times$  binding buffer. Next, the samples were transferred to flow cytometry tubes, and 5 μL 7AAD and 5 μL PE annexin V was added to each tube for a 15 min incubation away from light under room temperature before the addition of 400 μL  $1 \times$  binding buffer. The flow cytometry was completed within 1 h. Each sample was measured 3 times.

## Outcome measures

Main outcome measures included protein expressions of occludin and TBX1 in LC Hep-2 after transfection and impacts of miR-122a and miR-3195 expressions in LC tissue and Hep-2 on cell proliferation and apoptosis.

Secondary outcome measures were associations of the miR-122a and miR-3195 expressions in LC tissue with clinicopathological features as well as the occludin and TBX1 protein expressions in LC tissue.

## Statistical analysis

Statistical software SPSS v. 19.0 (IBM Corp., Armonk, USA) was applied for data analysis. Graphs were plotted using GraphPad Prism v.7 (GraphPad Software Inc., San Diego, USA). Measurement data is presented as mean  $\pm$  standard deviation (SD). Comparisons between groups were conducted using independent samples t-test, while comparisons of mean values across multiple groups were performed with one-way analysis of variance (ANOVA) followed by Dunnett's t-test for two-group comparison. Pearson test was used to assess the correlation. A value of  $p < 0.05$  was considered to indicate a statistically significant difference.

## Results

### miR-122a and miR-3195 expressions in LC and peritumoral tissues and their correlations

The qRT-PCR results showed that expression levels of miR-122a and miR-3195 in LC tissue were lower than those in peritumoral tissue (both  $p < 0.001$ ). Pearson analysis found that miR-122a and miR-3195 expressions were positively associated ( $r = 0.418$ ,  $p < 0.001$ ; Table 2, Fig. 1).

Table 2. miR-122a and miR-3195 expressions in LC and peritumoral tissues ( $\bar{x} \pm \text{SD}$ )

Group	n	miR-122a	miR-3195
LC tissue	30	0.731 $\pm$ 0.117	0.831 $\pm$ 0.201
Peritumoral tissue	20	1.187 $\pm$ 0.315	1.135 $\pm$ 0.304
t		7.244	4.264
p		<0.001	<0.001

LC – laryngeal cancer.

### Associations of miR-122a and miR-3195 expressions with clinicopathological features

The study results exhibited that the expression level of miR-122a in LC tissue was associated with patients' clinical stage ( $p < 0.001$ ) but not associated with patients' gender, age, pathological grade, and lymphatic metastasis (all  $p > 0.05$ ). Meanwhile, the expression level of miR-3195 in LC tissue was not associated with all of these factors (all  $p > 0.05$ ; Table 3).

### Correlation between occludin protein expression in LC tissue and miR-122a

The occludin protein expression level in the LC issue was much lower than in peritumoral tissue ( $p < 0.001$ ). Pearson analysis showed that miR-122a expression level was positively associated with occludin protein expression level ( $r = 0.541$ ,  $p < 0.001$ ; Fig. 2).

### Correlation between TBX1 protein expression in LC tissue and miR-3195

It was found that TBX1 protein expression level in LC tissue was much higher than in peritumoral tissue ( $p < 0.001$ ). Pearson analysis showed that miR-3195 expression level in LC tissue was negatively correlated with TBX1 protein ( $r = -0.428$ ,  $p < 0.001$ ; Fig. 3).

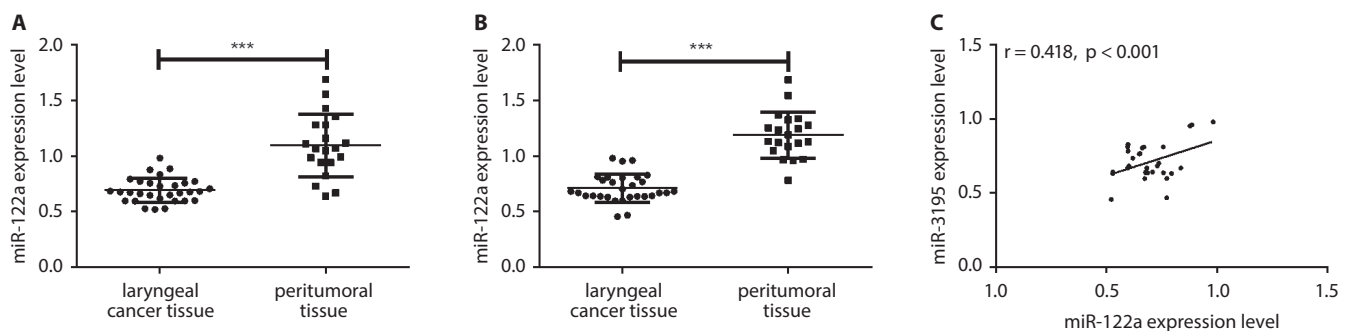
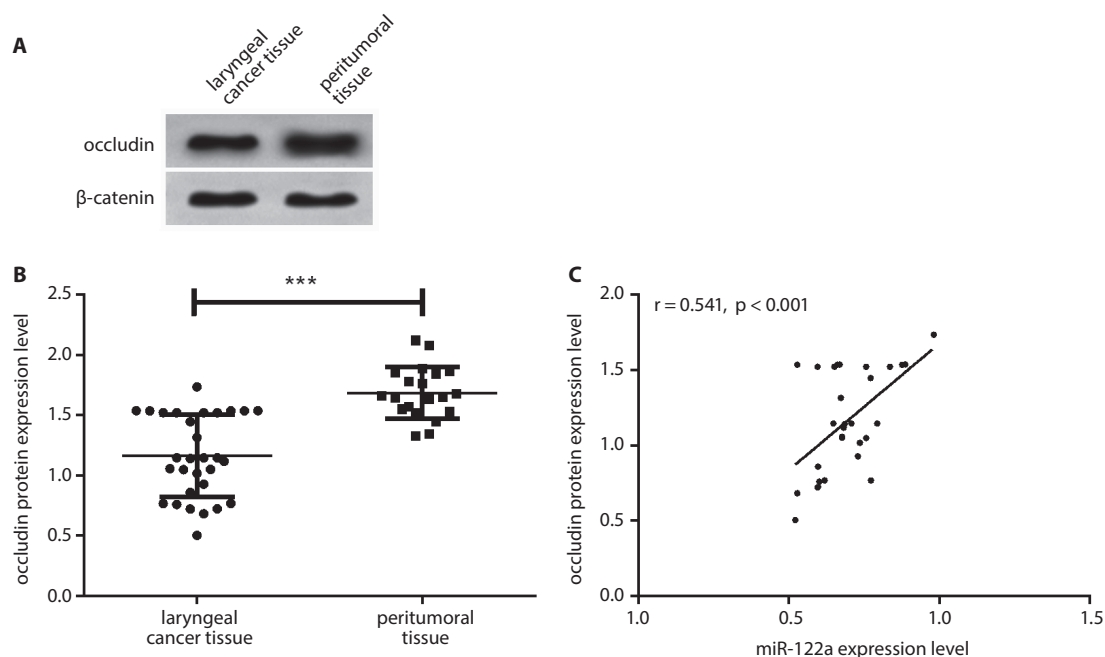


Fig. 1. miR-122a and miR-3195 expressions in the LC and peritumoral tissue and their associations. A. miR-122a expressions in the LC and peritumoral tissue. B. miR-3195 expressions in the LC and peritumoral tissue. C. Correlation between miR-122a and miR-3195 expression levels in the LC tissue

LC – laryngeal cancer; \*\*\*  $p < 0.001$ .

**Table 3.** Associations of miR-122a and miR-3195 expressions with clinicopathological features (x ±SD)

Features	n	miR-122a	F	p-value	miR-3195	F	p-value
Gender			0.538	0.595		0.329	0.744
male	21	0.754 ±0.128			0.826 ±0.193		
female	9	0.726 ±0.137			0.851 ±0.184		
Age			1.585	0.124		0.365	0.718
≤62 years	16	0.767 ±0.136			0.846 ±0.208		
>62 years	14	0.691 ±0.125			0.819 ±0.195		
Pathological grade			0.167	0.847		0.046	0.956
G1	11	0.732 ±0.109			0.842 ±0.124		
G2	15	0.739 ±0.128			0.834 ±0.153		
G3	4	0.701 ±0.083			0.817 ±0.148		
Lymphatic metastasis			1.036	0.309		0.926	0.363
yes	10	0.698 ±0.097			0.794 ±0.113		
no	20	0.746 ±0.129			0.846 ±0.158		
Clinical stage			4.678	<0.001		1.127	0.269
I–II	12	0.926 ±0.157			0.836 ±0.119		
III–IV	18	0.702 ±0.106			0.789 ±0.107		



**Fig. 2.** Expression level of occludin protein in the LC tissue and its association with miR-122a. A. Protein band image. B. Occludin protein expression in LC and peritumoral tissue. C. Correlation between miR-122a expression level and occludin protein expression level in the LC tissue

LC – laryngeal cancer; \*\*\* p < 0.001.

### miR-122a and miR-3195 expressions in Hep-2

The qRT-PCR results showed that there were no differences in miR-122a and miR-3195 expression levels in Hep-2 between the non-transfected and the NG groups (both p > 0.05). The miR-122a expression level in the miR-122a-mimics group was greater than in the miR-122a-NG and the miR-122a-mimics-non-transfected groups, and the miR-3195

expression level in the miR-3195-mimics group was greater than in the miR-3195-NG and the miR-3195-mimics-non-transfected groups (all p < 0.001; Fig. 4).

### Effect of miR-122a and miR-3195 overexpression on Hep-2 proliferation

Effects of miR-122a and miR-3195 transfections after 24 h, 48 h, 72 h, and 96 h on the proliferation of LC Hep-2

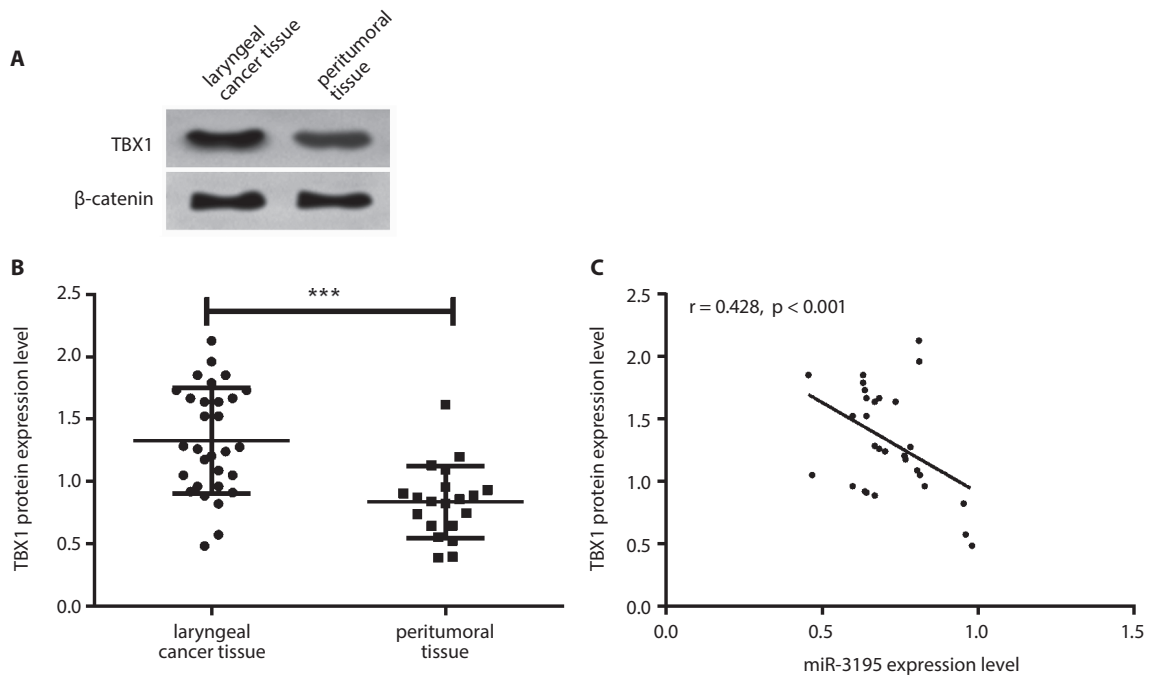


**Fig. 3.** Expression level of TBX1 protein in the LC tissue and its association with miR-3195. A. Protein band image. B. TBX1 protein expression in the LC and peritumoral tissue. C. Correlation between miR-3195 expression level and TBX1 protein expression level in the LC tissue

LC – laryngeal cancer; \*\*\*  $p < 0.001$ .

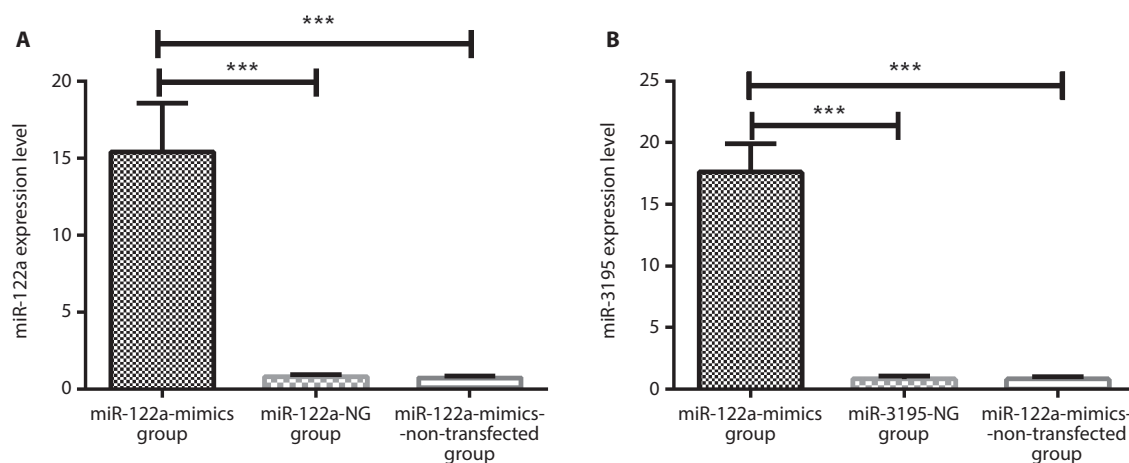


**Fig. 4.** miR-122a and miR-3195 expressions in LC Hep-2 cell. A. miR-122a expression in Hep-2. B. miR-3195 expression in Hep-2

LC – laryngeal cancer; \*\*\*  $p < 0.001$ .

were investigated using MTT assay. The results showed that at different time points after 24 h, the OD values in the miR-122a-mimics and the miR-3195-mimics groups were lower than in the miR-122a-NG and the miR-3195-NG groups respectively (all  $p < 0.001$ ; Fig. 5).

### Effect of miR-122a and miR-3195 overexpression on Hep-2 apoptosis

Effects of miR-122a and miR-3195 transfections on the apoptosis of LC Hep-2 were studied. We used flow cytometry to measure the Hep-2 apoptosis rate after miR-122a and miR-3195 transfections. The results

displayed that the cell apoptosis rate in the miR-122a-mimics group was higher than that in the miR-122a-NG and the miR-122a-mimics-non-transfected groups (both  $p < 0.001$ ); and the apoptosis rate in the miR-3195-mimics group was higher than that in the miR-3195-NG and the miR-3195-mimics-non-transfected groups (both  $p < 0.001$ ; Fig. 6).

### Effect of miR-122a overexpression on occluding expression in Hep-2 cell

In order to explore the biological mechanisms of miR-122a in regulating Hep-2 cell proliferation

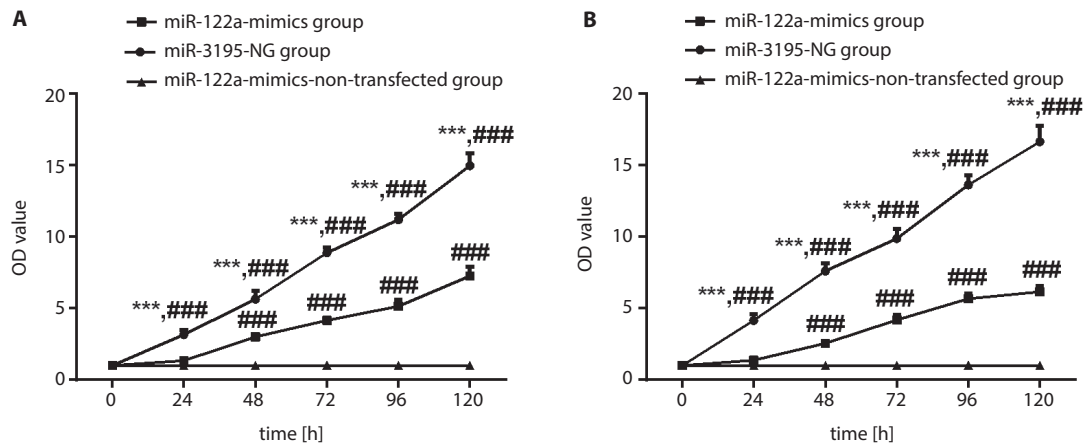


Fig. 5. Effect of miR-122a and miR-3195 overexpression on proliferation of LC Hep-2 cell. A. Effect of miR-122a overexpression on Hep-2 proliferation; \*\*  $p < 0.001$  vs the miR-122a-mimics group at the same time point; ###  $p < 0.001$  vs other time points within the same group. B. Effect of miR-3195 overexpression on HEP-2 cell proliferation; \*\*\*  $p < 0.001$  vs the miR-3195-mimics group at the same time point; ###  $p < 0.001$  vs other time points within the same group

LC – laryngeal cancer.

and apoptosis, we performed western blot to measure the changes in occludin protein expression in Hep-2 following miR-122a overexpression. The results showed that, compared with the miR-122a-NG and the miR-122a-mimics-non-transfected groups, occludin protein expression level in the miR-122a-mimics group was higher ( $p < 0.001$ ; Fig. 7).

### Effect of miR-3195 overexpression on TBX1 expression in Hep-2 cell

In order to investigate the biological mechanisms of miR-3195 in regulating Hep-2 cell proliferation and apoptosis, we performed western blot to measure the changes in TBX1 protein expression level in Hep-2 after miR-3195 overexpression. The results showed that, compared with the miR-3195-NG and the miR-3195-mimics-non-transfected groups, the TBX1 protein expression level in the miR-3195-mimics group was lower ( $p < 0.001$ ; Fig. 8).

## Discussion

The miRNA serves a critical role in the development of various cells and is closely related to cell differentiation, morphogenesis and tumor occurrence.<sup>11</sup> The miRNA can either act as a tumor promoter or suppressor in the pathogenesis of different tumors. Since miRNA is closely associated with tumor occurrence and progression, miRNAs can become effective molecular biomarkers for the diagnosis, treatment and prognostic evaluation of tumor.<sup>12,13</sup> As a liver-specific miRNA, miRNA-122a often acts as a tumor suppressor in cancer. In a study by Gramantieri et al., miR-122a was reported to be frequently downregulated in a cancerous human liver cell, and cyclin-G1 is its target protein.<sup>14</sup> Zeisel et al. documented that miR-122 can

regulate cholesterol metabolism and promote replication of hepatitis C virus. Meanwhile, the reduction in miR-122 expression in hepatocellular carcinoma is associated with metastasis and poor prognosis.<sup>15</sup> Lu et al., through analyzing miRNA genomic expression profile and bioinformatics target genes in LC, found a marked downregulation of miR-3195 level.<sup>16</sup> Our study showed that miR-122a and miR-3195 expression levels in LC tissue were much lower than in peritumoral tissue, and the lowering of miR-122a was associated with the clinical stage of LC patients, which aligned with other study results. Both miR-122a and miR-3195 may act as tumor suppressors and be involved in the pathogenesis of LC. Moreover, we found that the expression levels of these 2 miRNAs in LC tissue were positively correlated with each other, suggesting a mutual regulation. However, there have been no studies in this area yet, and verification would be necessary in the future.

Much research has been carried out on the biological function of miR-122a in malignant tumors. Wang et al. have reported that miR-122a is downregulated in gastrointestinal cancer cell line and primary cancer tissue, while miR-122a mimics can inhibit cell growth.<sup>17</sup> However, studies on the biological function of miR-3195 in tumor are scarce. In the present study, we analyzed the impact of miR-122a and miR-3195 transfections on the proliferation and apoptosis of Hep-2. The results showed that at different time points after 24 h, the OD values in both miR-122a-mimics and miR-3195-mimics groups were much lower than in the NG groups, and the apoptosis rate in the 2 mimics groups was higher than in the NG and non-transfected groups. These findings indicated that overexpression of miR-122a and miR-3195 could markedly inhibit the proliferation of LC Hep-2 and promote its apoptosis.

Occludin is an integral membrane protein located at tight junction. Martin et al. observed that occludin could have an aberrant expression in cancerous human breast tissue and cancer cell line, and occludin expression loss is related

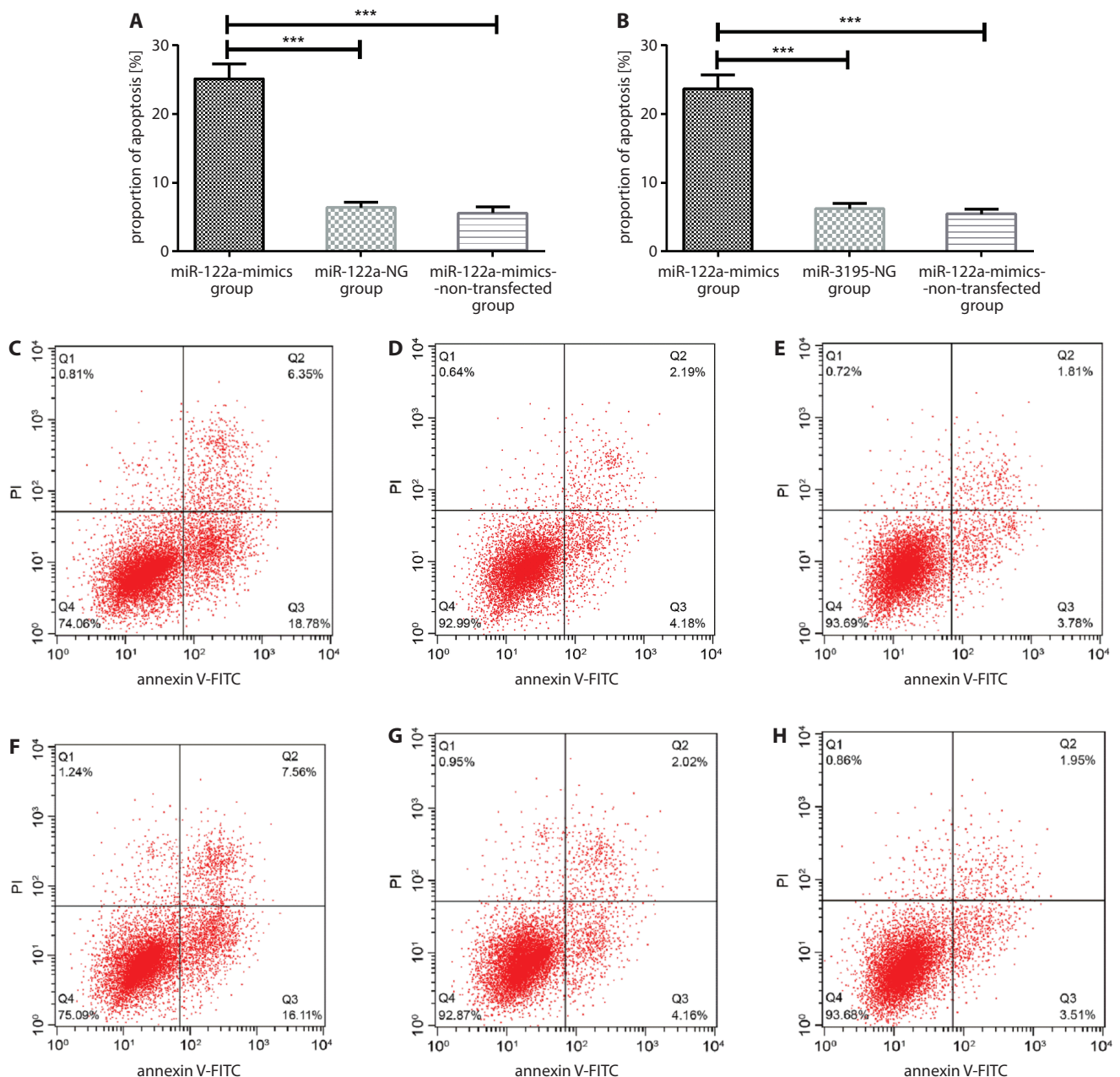


**Fig. 6.** Effect of miR-122a and miR-3195 overexpression on apoptosis of LC Hep-2 cell. A. Effect of miR-122a overexpression on Hep-2 apoptosis. B. Effect of miR-3195 overexpression on Hep-2 apoptosis. C. Hep-2 apoptosis rate in the miR-122a-mimics group. D. Hep-2 apoptosis rate in the miR-122a-mimics-NG group. E. Hep-2 apoptosis rate in the miR-122a-mimics-non-transfected group. F. Hep-2 apoptosis rate in the miR-3195-mimics group. G. Hep-2 apoptosis rate in the miR-3195-mimics-NG group. H. Hep-2 apoptosis rate in the miR-3195-mimics-non-transfected group

LC – laryngeal cancer; \*\*\*  $p < 0.001$ .

to bone metastasis.<sup>18</sup> In a study by Ye et al., it was reported that the binding of miR-122a to occludin 3'UTR can regulate occludin expression, and tumor necrosis factor  $\alpha$  (TNF- $\alpha$ ) can adjust intestinal permeability through inducing miR-122a-mediated degradation of occludin, which substantiates the possibility of targeting miR-122a in vivo to maintain intestinal barrier function.<sup>19</sup> Our results showed that the occludin protein expression level in LC tissue was lower compared with those in peritumoral tissues. Pearson analysis displayed that the miR-122a expression level was positively associated with the occludin protein

level in LC tissue, suggesting that there may be a regulative relation between miR-122a and occludin. As a result, we performed western blot to measure the changes in occludin protein expression levels in Hep-2 after miR-122a overexpression. The results showed that, compared with the NG and non-transfected groups, the occludin protein level in the miR-122a-mimics group was higher. Therefore, miR-122a may inhibit Hep-2 cell proliferation and promote its apoptosis through upregulating occludin expression. Jingushi et al. have demonstrated that miR-122 can directly regulate occludin expression; moreover, their study

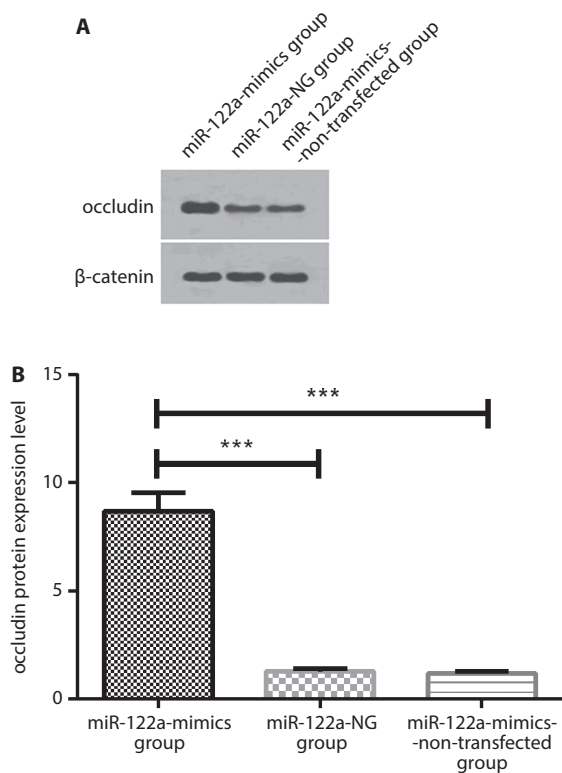


Fig. 7. Effect of miR-122a overexpression on occludin protein expression in LC Hep-2 cell. A. Protein band image. B. Occludin protein expression level in Hep-2 cell after miR-122a overexpression was detected using western blot

LC – laryngeal cancer; \*\*\*  $p < 0.001$ .

also indicated that miR-122 level can be upregulated significantly in clear cell renal cell carcinoma (CCRCC), and the expression level of miR-122 is negatively associated with occludin protein expression level; the knockdown of occludin can promote CCRCC cell migration ability, but cannot enhance proliferation and invasion ability of CCRCC cell.<sup>20</sup> This finding may be due to the difference in growth, invasion and regulatory mechanism between CCRCC and LC, and the mechanism is yet to be investigated.

*TBX1* gene is mainly located on human chromosome 22q 11.21. The dysfunction of this gene can cause 22q11 deletion syndrome. *TBX1* can activate or inhibit transcription and negatively regulate cardiomyocyte differentiation.<sup>21</sup> Aberrant expression of *TBX1* can be found in various tumors. Jiang et al. have reported that *TBX1* miRNA and protein are highly expressed in CCRCC and overexpression of *TBX1* may contribute to CCRCC pathogenesis.<sup>22</sup> Through measuring *TBX1* protein expression in LC tissue, we found that *TBX1* protein expression increased significantly in LC tissue, which was consistent with previous reports. Further studies demonstrated that miR-3195 was negatively associated with *TBX1* protein expression in LC tissue. Thus, we speculate that there may be a regulative relation between miR-3195 and *TBX1* protein. However, the correlation between them had not been elucidated in previous studies. Therefore, we predicted target genes

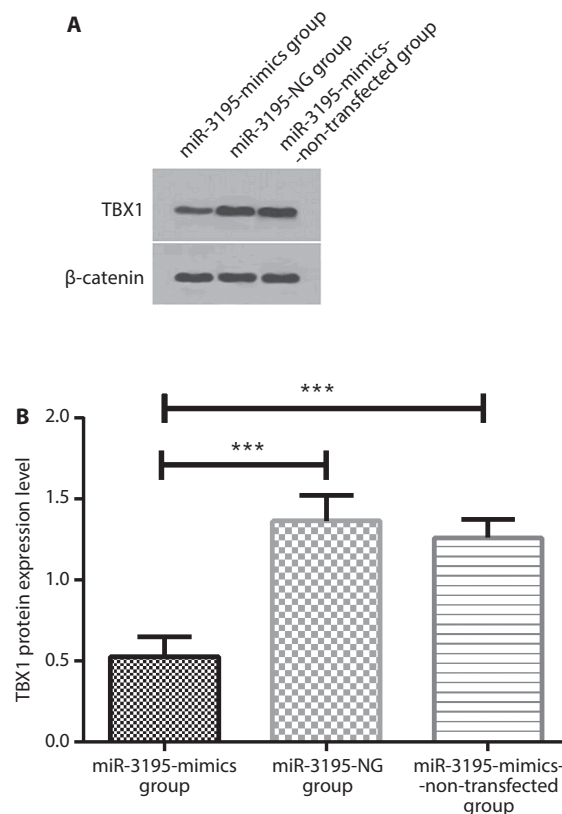


Fig. 8. Effect of miR-3195 overexpression on TBX1 protein expression in LC Hep-2 cell. A. Protein band image. B. TBX1 protein expression level in Hep-2 cell after miR-3195 overexpression was detected using western blot

LC – laryngeal cancer; \*\*\*  $p < 0.001$ .





for miR-3195 and found *TBX1* protein in the miR-3195 binding site. Western blot was used to detect changes in *TBX1* protein expression in Hep-2 after miR-3195 overexpression. The results showed that, compared with the NG and non-transfected groups, *TBX1* protein expression level was lower in the miR-3195-mimics group, indicating that miR-3195 may suppress Hep-2 cell proliferation and promote its apoptosis through inhibiting *TBX1* expression. However, more studies would be necessary in the future to elucidate its detailed mechanism.

In the present study, we observed that miR-122a and miR-3195 overexpression could suppress Hep-2 cell proliferation and promote its apoptosis, and we carried out preliminary analysis on the mechanisms. However, there were still some limitations in the study design. First, we did not verify the relations between miR-122a and occludin, and between miR-3195 and *TBX1* using dual-luciferase reporter assay. Second, the effects of miR-122a and miR-3195 on LC Hep-2 migration and invasion abilities were not further investigated, and the regulating mechanism remains unclear. Therefore, more studies would be required in the future to overcome these shortcomings and to verify our results.

In conclusion, both miR-122a and miR-3195 can act as tumor suppressors in LC. miR-122a is related to patients’ clinical stage, and the 2 miRNAs may be involved in the pathogenesis of LC. Both miR-122a and miR-3195 can

substantially inhibit Hep-2 cell proliferation and promote its apoptosis. These effects may be achieved by the upregulation of occludin expression by miR-122a and suppression of TBX1 expression by miR-3195. Therefore, miR-122a and miR-3195 may become potential targets for the treatment of LC.

### ORCID iDs

Xingli Jiang  <https://orcid.org/0000-0002-8584-926X>  
 Zhiguang Gao  <https://orcid.org/0000-0003-4025-7743>  
 Linli Tian  <https://orcid.org/0000-0001-8378-109X>  
 Ming Liu  <https://orcid.org/0000-0002-9366-2577>

### References

1. Tomeh C, Holsinger FC. Laryngeal cancer. *Curr Opin Otolaryngol Head Neck Surg*. 2014;22(2):147–153.
2. Miao S, Mao X, Zhao S, et al. miR-217 inhibits laryngeal cancer metastasis by repressing AEG-1 and PD-L1 expression. *Oncotarget*. 2017; 8(37):62143–62153.
3. Yu X, Li Z. The role of microRNAs expression in laryngeal cancer. *Oncotarget*. 2015;6(27):23297–23305.
4. Nie W, Ge HJ, Yang XQ, et al. LncRNA-UCA1 exerts oncogenic functions in non-small cell lung cancer by targeting miR-193a-3p. *Cancer Lett*. 2016;371(1):99–106.
5. Fernandez S, Risolino M, Mandia N, et al. miR-340 inhibits tumor cell proliferation and induces apoptosis by targeting multiple negative regulators of p27 in non-small cell lung cancer. *Oncogene*. 2015; 34(25):3240–3250.
6. Liu J, Tang Q, Li S, Yang X. Inhibition of HAX-1 by miR-125a reverses cisplatin resistance in laryngeal cancer stem cells. *Oncotarget*. 2016; 7(52):86446–86456.
7. Chen YH, Yu YF. Impact of miR-122a on inhibition proliferation of laryngeal carcinoma cell line Hep2 [in Chinese]. *Chinese Journal of Immunology*. 2017;33:352–355.
8. Yoon SO, Kim EK, Lee M, et al. NOVA1 inhibition by miR-146b-5p in the remnant tissue microenvironment defines occult residual disease after gastric cancer removal. *Oncotarget*. 2016;7(3):2475–2495.
9. Forastiere AA, Ismaila N, Wolf GT. Use of larynx-preservation strategies in the treatment of laryngeal cancer: American Society of Clinical Oncology Clinical Practice Guideline Update Summary. *J Oncol Pract*. 2018;14:123–128.
10. Munoz M, Rosso M, Aguilar FJ, Gonzalez-Moles MA, Redondo M, Esteban F. NK-1 receptor antagonists induce apoptosis and counteract substance P-related mitogenesis in human laryngeal cancer cell line HEp-2. *Invest New Drugs*. 2008;26(2):111–118.
11. Wan GL, Chen H, Zhou L, Huang JM. Overexpressed miR-128a inhibits the proliferation of laryngeal cancer cells. *Transl Cancer Res*. 2018;7(4): 901–911.
12. Wu T, Qu L, He G, et al. Regulation of laryngeal squamous cell cancer progression by the lncRNA H19/miR-148a-3p/DNMT1 axis. *Oncotarget*. 2016;7(10):11553–11566.
13. Jin C, Zhang Y, Li J. Upregulation of MiR-196a promotes cell proliferation by downregulating p27(kip1) in laryngeal cancer. *Biol Res*. 2016; 49(1):40.
14. Gramantieri L, Ferracin M, Fornari F, et al. Cyclin G1 is a target of miR-122a, a microRNA frequently downregulated in human hepatocellular carcinoma. *Cancer Res*. 2007;67(13):6092–6099.
15. Zeisel MB, Pfeffer S, Baumert TF. miR-122 acts as a tumor suppressor in hepatocarcinogenesis in vivo. *J Hepatol*. 2013;58(4):821–823.
16. Lu ZM, Lin YF, Jiang L, et al. Micro-ribonucleic acid expression profiling and bioinformatic target gene analyses in laryngeal carcinoma. *Onco Targets Ther*. 2014;7:525–533.
17. Wang X, Lam EK, Zhang J, Jin H, Sung JJ. MicroRNA-122a functions as a novel tumor suppressor downstream of adenomatous polyposis coli in gastrointestinal cancers. *Biochem Biophys Res Commun*. 2009;387(2):376–380.
18. Martin TA, Jordan N, Davies EL, Jiang WG. Metastasis to bone in human cancer is associated with loss of occludin expression. *Anticancer Res*. 2016;36(3):1287–1293.
19. Ye D, Guo S, Al-Sadi R, Ma TY. MicroRNA regulation of intestinal epithelial tight junction permeability. *Gastroenterology*. 2011;141(4): 1323–1333.
20. Jinguishi K, Kashiwagi Y, Ueda Y, et al. High miR-122 expression promotes malignant phenotypes in ccRCC by targeting occludin. *Int J Oncol*. 2017;51(1):289–297.
21. Pane LS, Fulcoli FG, Cirino A, et al. Tbx1 represses Mef2c gene expression and is correlated with histone 3 deacetylation of the anterior heart field enhancer. *Dis Model Mech*. 2018;11(9). pii: dmm.029967
22. Jiang H, Tian H, Guo Y, et al. Expression of TBX1 gene in kidney tissues in patients with clear cell renal cell carcinoma and its clinical significance. *Journal of China Medical University*. 2016.



# Antifungal itraconazole ameliorates experimental autoimmune encephalomyelitis through a novel mechanism of action

\*Huifen Huang<sup>1,B-D,F</sup>, \*Xiaolin Tian<sup>2,B,C,F</sup>, Xiao Peng<sup>1,C,F</sup>, Liangtong Huang<sup>1,D-F</sup>, Lerong Mei<sup>1,C,F</sup>, Yanli Zhan<sup>1,D,F</sup>, Siying Chen<sup>1,B,F</sup>, Huihua Wu<sup>1,B,F</sup>, Guofang Wei<sup>1,D-F</sup>, Xueli Cai<sup>1,A,F</sup>

<sup>1</sup> Department of Neurology, Lishui Hospital, Zhejiang University School of Medicine, China

<sup>2</sup> Department of Rehabilitation Medicine, Second Hospital of Tianjin Medical University, China

A – research concept and design; B – collection and/or assembly of data; C – data analysis and interpretation; D – writing the article; E – critical revision of the article; F – final approval of the article

Advances in Clinical and Experimental Medicine, ISSN 1899–5276 (print), ISSN 2451–2680 (online)

*Adv Clin Exp Med.* 2020;29(5):535–545

## Address for correspondence

Xueli Cai

E-mail: caixueli@163.com

## Funding sources

This research was supported by the Lishui public welfare technology application research self-funded project (project name: Study on the effect and mechanism of new AMPK activator against oligodendrocyte injury in multiple sclerosis; project No. 2019SJZC30).

## Conflict of interest

None declared

\* Huifen Huang and Xiaolin Tian contributed equally to this work.

Received on September 5, 2019

Reviewed on March 9, 2020

Accepted on April 24, 2020

Published online on May 27, 2020

## Abstract

**Background.** Multiple sclerosis (MS) is an autoimmune disease characterized by a loss of myelin, limb disabilities and dysregulation of gene expression. Unfortunately, there still is no treatment to cure MS.

**Objectives.** To explore a novel way to treat MS using currently available antifungal drugs.

**Material and methods.** We built an experimental autoimmune encephalomyelitis (EAE) model to mimic MS and tested the effect of an antifungal drug – itraconazole – on EAE by comparing it with a phosphate-buffered saline (PBS) control group. We assessed the animal limb deficits with Weaver's scoring and used histology staining (including luxol fast blue (LFB) and hematoxylin & eosin (H&E) methods) to determine the demyelination in the spinal tissues. We also performed western blotting to quantify the expression changes of proteins related to endoplasmic reticulum (ER) stress response and apoptosis.

**Results.** The limb disabilities were greatly diminished and the demyelination in the spinal tissues of the EAE mice was mostly reduced following itraconazole treatment. The hyperactivation of the ER stress response and apoptosis pathway in EAE was also significantly diminished by the itraconazole treatment. In addition, the AMPK pathway was downregulated in EAE, its expression level bi-directionally affected the activity of the ER stress response, and its downregulation removed the beneficial effect of itraconazole.

**Conclusions.** Our study revealed a new method for treating MS using currently approved antifungal drugs.

**Key words:** apoptosis, EAE, itraconazole, ER stress, AMPK

## Cite as

Huang H, Tian X, Peng X, et al. Antifungal itraconazole ameliorates experimental autoimmune encephalomyelitis through a novel mechanism of action. *Adv Clin Exp Med.* 2020;29(5):535–545. doi:10.17219/acem/121008

## DOI

10.17219/acem/121008

## Copyright

© 2020 by Wrocław Medical University

This is an article distributed under the terms of the Creative Commons Attribution 3.0 Unported (CC BY 3.0) (<https://creativecommons.org/licenses/by/3.0/>)

## Introduction

Multiple sclerosis (MS) is an autoimmune disease which affects millions of people worldwide; in MS, the immune system improperly attacks its own tissues.<sup>1</sup> Specifically, the immune system attacks the protective myelin – which envelopes the nerve fibres and facilitates fast neuronal impulses – and eventually affects the fast-neuronal conduction in myelinated fibers. Multiple sclerosis has 4 key pathological features<sup>2</sup>:

- inflammation, which is considered to be the main trigger of the neuronal injuries;
- demyelination, the mark of MS;
- loss or damage of axons; and
- gliosis.<sup>3</sup>

Experimental autoimmune encephalomyelitis (EAE), a primary animal model of autoimmune inflammatory diseases established over 80 years ago,<sup>4</sup> is widely used in research on MS because it resembles MS in terms of inflammation, demyelination, apoptosis, and gliosis.<sup>5</sup> Based on the gene expression in the EAE brain,<sup>6,7</sup> some novel treatments involved in neuroprotection and immunosuppression have been developed. However, there is still no standard treatment that can fully cure MS due to the various symptoms of MS differing greatly from person to person and to the unclear molecular mechanism behind it.<sup>8</sup> Therefore, it is valuable to further develop novel therapies in MS.

During the pathogenesis of EAE, several components of endoplasmic reticulum (ER) stress response have been found to be upregulated.<sup>9</sup> The ER stress response, also known as the unfolded protein response, is critical for ameliorating the accumulation of unfolded or misfolded proteins and its prolonged activation can induce an inflammatory signal.<sup>10</sup> The ER stress activates 3 branches of response to mitigate the stress, represented by activating transcription factor 6 (ATF6), inositol requiring enzyme 1 (IRE1) and PKR-like endoplasmic reticulum kinase (PERK) pathways.<sup>11</sup> ATF6 helps increase the capacity of ER protein folding by being cleaved into transcription factor ATF6(N) and promoting the synthesis of folding-assisting proteins.<sup>12</sup> PERK indirectly inhibits mRNA translation by phosphorylating itself and eIF2a (a ubiquitous translation initiation factor), thereby decreasing the load of proteins into the ER. Besides, PERK can also contribute to cell apoptosis by sequentially driving transcription factors ATF4 and CHOP (transcription factor C/EBP homologous protein) once the ER stress can no longer be handled.<sup>13</sup> Phosphorylated IRE1 mitigates the ER response by degrading ER-binding mRNAs and enhancing transcriptional responses to increase the protein-folding capacity.<sup>14</sup> Considering the hyperactivity of the ER stress response in EAE, it is worth attempting to treat MS by suppressing the ER stress responses.

Given that developing drugs from scratch is both time-consuming and costly, screening currently available drugs is a reasonably promising idea. There is evidence which

suggests that fungal infection can lead to MS and can cause an elevation of some biomarkers of MS, like interleukin 17 (IL-17) and chitotriosidase.<sup>15</sup> Additionally, among several antifungal drugs, itraconazole has been shown to improve the condition of patients with psoriasis, which is another autoimmune disease, by binding to the fungal cytochrome p450 enzymes and inhibiting the production of ergosterol.<sup>16–18</sup> Thus, we explored the novel effect of antifungal itraconazole on ameliorating MS-related symptoms and molecular changes using the EAE animal model and oligodendroglia OLN-93 cell line.

In this study, we successfully built an animal EAE model in which the animals exhibited severe limb disabilities and their spinal tissues lost myelin. We then tested the effect of itraconazole on the pathogenesis of EAE and found that the tissue lesions and animal motor deficit was dramatically diminished by itraconazole. Meanwhile, the pathways of the ER stress response and apoptosis were highly activated in EAE mice, and itraconazole application significantly restored the hyperactivation of these pathways. Furthermore, we confirmed the suppressive effect of itraconazole on the ER stress response and apoptosis by using an ER stress cell model induced by thapsigargin (Tg), a known cytotoxic inducer of ER stress.<sup>19</sup> We additionally explored the novel mechanism of itraconazole mitigating EAE and found that the neuroprotective AMPK pathway was essential in this process, as knockdown of AMPK completely abolished the beneficial effect of itraconazole. Collectively, our results showed that this currently available antifungal drug might be used to help mitigate MS and provide a new direction in the future treatment of MS.

All the experimental procedures were approved by the ethics committee of Zhejiang University School of Medicine, China.

## Material and methods

### EAE model

The adult male C57BL/6J mice (8 weeks old) used in this study were ordered from Shanghai Laboratory Animal Center, China. The EAE model was built using antigen myelin oligodendrocyte glycoprotein (MOG) protein 35–55 (SCP0195; Sigma-Aldrich, St. Louis, USA) as previously described.<sup>20</sup> Briefly, the mice were immunized by subcutaneous (s.c.) injection of 1.5 mg/mL of MOG 35–55 in complete Freund's adjuvant (CFA) on both the upper and lower back of each animal (0.2 mL in total). Two hours later, each animal was intraperitoneally (i.p.) injected with 2 µg/mL of pertussis toxin (PTX, 0.1 mL; Sigma-Aldrich). Forty-eight hours later, the mice received another i.p. injection of 2 µg/mL of PTX (0.1 mL). For the sham controls, phosphate-buffered saline (PBS) was delivered in each corresponding injection. To test the effect of the drug on the development of EAE, from

the onset of immunization to the termination of the study, the animals were randomly grouped and received daily i.p. injection of 100  $\mu$ L of PBS, itraconazole (10 mg/kg), Compound C (also known as dorsomorphin, 20 mg/kg), AICAR (5-aminoimidazole-4-carboxamide ribonucleotide, 500 mg/kg), or combinations of the above. The EAE mice were examined daily from day 1 to 21 and scored for clinical symptoms. To test the effect of itraconazole on the acute ER stress response, another batch of mice received daily i.p. injections of Tg (0.4 mg/kg), or Tg+itraconazole (10 mg/kg) without immunization. All drugs were purchased from Sigma-Aldrich. Twenty-one days after the first immunization or 15 days after the first Tg treatment, the mice were anesthetized with a mixture of ketamine (80 mg/kg) and xylazine (10 mg/kg). They were then perfused with saline and 4% paraformaldehyde and the spinal tissues were obtained for subsequent immunostaining or western blot analysis. The cytotoxicity of itraconazole was examined by staining the livers from the same animals.

### Downregulation or upregulation of AMPK in vivo

The sequence of mus AMP-activated, alpha 1 catalytic subunit (AMPK $\alpha$ 1, NM\_001013367.3) was constructed into the pcDNA3.1 vector for overexpressing AMPK. The oligonucleotide sh-AMPK1 (GGAGAGCUAUUUGAUUUAUUU) and its control sh-NC (ACA CAA CGC GGA AUC UCG AAU), was synthesized and also constructed into pcDNA3.1 to knockdown AMPK1. All the constructs were then packaged into adeno-associated virus vectors (AAV) for in vivo experiments by GenePharma Co., Ltd. (Shanghai, China). To manipulate the level of AMPK, AAV-sh-AMPK or AAV-AMPK was transferred to some mice via tail vein injection of AAVs 10 days before the first immunization as previously described.<sup>21</sup> The AAVs packed with a mock (sh-NC) or vector sequence were used as controls.

### Luxol fast blue and hematoxylin & eosin staining

The lumbar sections of the spinal cord (15  $\mu$ m) were prepared and stained using Luxol Fast Blue (LFB) Stain Kit (ab1506751; Abcam, Cambridge, UK) according to the manual. The prepared liver sections were stained using the hematoxylin & eosin (H&E) method: the sections were first soaked in 0.4% HCl (in EtOH) for 15 s, washed once, and then stained with eosin for 3 min. The LFB and H&E slides were then imaged to examine the pathological changes of tissues.

### Weaver score

From day 0 to day 21 after immunization, the mice were scored daily to quantify their limb disabilities using Weaver's scoring method.<sup>22,23</sup> Briefly, the total score is the sum

of the response from the tail and all 4 limbs as follows: tail – 0 for normal, 1 for partially paralyzed and 2 for fully paralyzed; each limb – 0 for normal, 1 for weak gait, 2 for paresis, and 3 for fully paralyzed. Therefore, the total score ranges from 0–15.

### ELISA assay

First, the total proteins were obtained by centrifuging the fresh liver tissues obtained from the EAE mice. The concentration of the proteins of interest (AST, ALT and ALP) was measured using sandwich-type enzyme-linked immunosorbent assay (ELISA) kits (Boster Bio, Pleasanton, USA). Briefly, the proteins of interest were sequentially captured with monoclonal antibody coated on a 96-well plate and linked with a biotin-conjugated detection antibody. Then, the biotin signal was amplified with avidin conjugated HRP and read using a microplate reader (Synergy2; BioTek, Winooski, USA) at 450 nm. The concentration of the proteins was calculated using the standard curve method.

### Western blot

The spinal cord segments or OLD cells were first treated with radioimmunoprecipitation assay (RIPA) buffer to lyse the cells (Thermo Fisher Scientific, Waltham, USA) following the manufacturer's instructions. The proteins were then separated using gel electrophoresis, followed by incubation with primary and secondary antibodies conjugated with horseradish peroxidase (HRP) and visualization. The protein level was quantified using ImageJ software (National Institutes of Health, Bethesda, USA), normalized to the value of internal control, GAPDH or Actin- $\beta$ , and expressed as the fold of the control. The primary antibodies were purchased from Thermo Fisher Scientific (p-PERK, #MA5-15033; ATF4, #PA5-86112; p-IRE1 $\alpha$ , #PA1-16927; GAPDH, #39-8600; Bax, #MA5-14003;  $\beta$ -actin, #MA5-11869; AMPK-  $\alpha$ 1, #MA5-15815; and ATF6, # MA1-25358), Cell Signaling Technology (Danvers, USA; CHOP, #2895; p-eIF2 $\alpha$ , #9721; and p-AMPK $\alpha$ , #2531), and Abcam (caspase-3, ab13847; Bcl-2, ab182858; and p53, ab26)

### Cell culture and Cell Counting Kit-8 assay

Due to the critical role of oligodendrocytes (OLs) in producing and maintaining the myelin around axons,<sup>24</sup> for cellular study we used the OLN-93 cell line (Otwo Biotech, Shenzhen, China), which is derived from rat brain cultures.<sup>25</sup> The OLN cells were cultured in Gibco Dulbecco's modified Eagle's medium (DMEM) basal media containing a high level of glucose (Thermo Fisher Scientific) at 37°C. The dosage-dependent cytotoxicity of Tg and itraconazole was determined with a Cell Counting Kit-8 (CCK-8; Dojindo Laboratories, Kumamoto, Japan; CK04).

Briefly, the OLN cells were precultured in 96-well plates for 12 h (5,000 cells/well) and then treated with various concentrations (0, 1, 5, 10, 20, and 40 nM) of Tg and itraconazole for 24 h. Next, 10  $\mu$ L of CCK-8 solution was added, and the cells were cultured for another 3 h. Finally, the cellular optical density (OD) was measured at 450 nm, and the percentage of cell viability was calculated as the ratio of samples to controls. To test the effect of itraconazole on the activity of the ER stress response evoked by Tg, Tg (20 nM) or a combination of Tg and itraconazole (5 nM) was added and the cells were cultured for another 48 h before protein analysis using western blotting.

## Flow cytometry

For the apoptosis test, the OLN cells were treated with PBS, Tg (20 nM), or Tg+itraconazole (20 nM+5 nM) for 48 h. Then, the OLN cells were washed twice with PBS, digested using EDTA-free trypsin, and treated using fluorescent annexin V conjugates (Thermo Fisher Scientific) according to the instructions. The percentage of cell apoptosis was quantified using a flow cytometer (Beckman Coulter Inc., Brea, USA) with an excitation wavelength of 488 nm.

## Statistical analysis

The sample size in each drug/virus treatment group was 6 animals. In total, there were 19 groups and 114 mice (Fig. 1–6; all animals used for behavior assessment were also used for tissue staining and western blotting). An example band from 1 or 2 animals was shown in western blotting. For the cellular study (testing drug toxicity using CCK-8, examining apoptosis using flow cytometry and measuring the activity of the ER stress response or apoptosis induced by Tg), experiments were repeated 3 times for quantification. The data is expressed as means  $\pm$  standard deviation (SD). The confidence level was set at 0.05. Statistical differences were analyzed using Student's *t*-test between 2 groups or one-way analysis of variance (ANOVA) followed by Dunnett's test among multiple groups, using Prism 6 (GraphPad Software Inc., San Diego, USA).

## Results

### Itraconazole functionally mitigated the tissue damage and limb disabilities in EAE mice

We first built the EAE animal model by immunizing the mice with MOG and found that the tissue damage (indicated by infiltration and demyelination) in the lumbar spinal cord was severe (Fig. 1A). Meanwhile, the mice exhibited significant limb deficits as shown by an increase

in the clinical Weaver scores (Fig. 1B). These behavioral and histological changes suggested that the EAE model had been successfully built. Next, we tested whether the application of the antifungal itraconazole could rescue these phenotypes. We found that the demyelination in EAE was largely restored (Fig. 1A), and the animal limb disabilities were significantly lessened (Fig. 1B). To make sure that the chosen dosage of itraconazole did not cause any cytotoxicity that was not observed in the spinal tissues, we performed H&E staining using the livers obtained from the same EAE animals; no obvious liver pathogenesis was observed (Fig. 1C). Meanwhile, the level of liver failure markers – AST, ALT and ALP – was also not significantly different between the EAE+itraconazole group and the EAE+PBS group (Fig. 1D). Together, this data suggested that the nontoxic dosage of antifungal itraconazole very effectively diminished the tissue damage and limb disabilities in EAE.

### Itraconazole diminished the overactivation of the ER stress response and cell apoptosis in EAE

We next explored the novel mechanism of itraconazole in regulating the symptoms of EAE. We measured the level of ER stress response-related proteins and found that the levels of cleaved ATF6, phosphorylated-PERK (p-PERK), p-eIF-2 $\alpha$ , ATF4, CHOP, and p-IRE $\alpha$  were all much higher in EAE (Fig. 2A,B). These changes indicated that all 3 branches of ER stress response were concurrently dysregulated in EAE and the endogenous mechanisms to mitigate the stress were disrupted. Importantly, the application of itraconazole largely restored the overactivity of the proteins involved in ER stress response (Fig. 2A,B). As cell apoptosis is also one of the main symptoms in EAE, we also examined the expression change of apoptotic indicators. We found that apoptotic activators, including caspase-3, Bax and TP53, exhibited high expression levels while there were lower levels of the apoptotic inhibitor Bcl-2 in EAE. Accordingly, these changes were also significantly reduced by itraconazole (Fig. 2C,D). Interestingly, the level of p-AMPK, which is key in cellular energy metabolism, was also decreased in EAE and improved by administering itraconazole (Fig. 2A,B). Together, these results indicate that itraconazole effectively restored the dysregulated gene expression network involved in the EAE-related ER stress response and cell apoptosis.

### Itraconazole mitigated the cell apoptosis and hyperactivity of ER stress response induced by Tg in OLN cells

To further confirm the mitigating effect of itraconazole on the ER stress response, which might be important in the development of EAE, we acutely induced an ER stress response in OLN cells using Tg. We first tested the dosage effect of Tg and itraconazole on cell survival

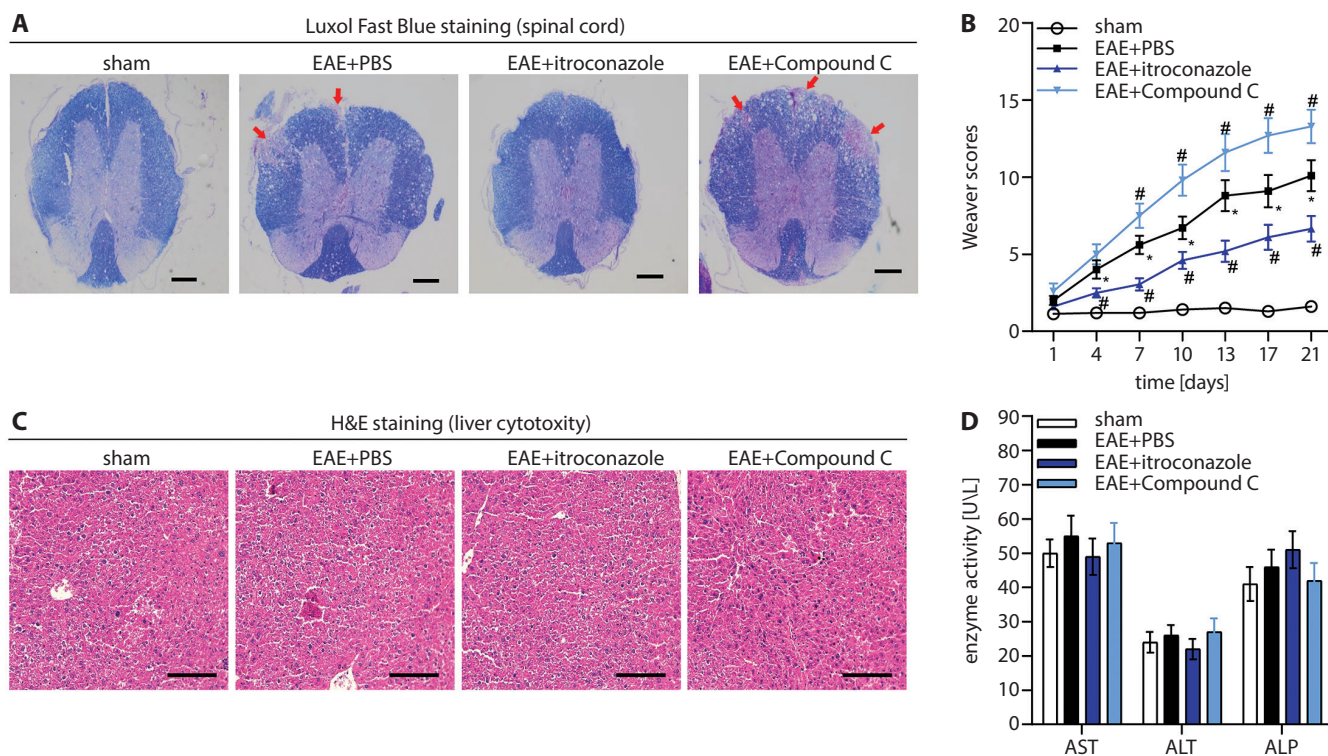


**Fig. 1.** Itraconazole effectively diminished the tissue damage and limb disabilities in EAE. **A.** Representative LFB-stained transverse sections of spinal cord showing the demyelination (pallor and vacuolation indicated by arrow) induced by EAE. The demyelination was corrected and exacerbated by itraconazole and Compound C (an AMPK pathway inhibitor) treatment, respectively. Scale bar, 200  $\mu$ m. **B.** Itraconazole dramatically alleviated the limb disabilities, as shown by lowered Weavers scores, while Compound C exacerbated the disabilities. **C.** Representative H&E-stained liver sections showing that the dosages of both itraconazole and Compound C used in the study were not cytotoxic to the liver. Scale bar, 100  $\mu$ m. **D.** The levels of liver failure markers, such as AST, ALT and ALP, was not significantly affected by itraconazole or Compound C treatment, as assessed using ELISA. One-way ANOVA followed by Dunnett's test

\*  $p < 0.01$  vs the sham group; #  $p < 0.01$  vs the EAE+PBS group.

and found that they displayed significant cytotoxicity at 20–40 nM but not at a lower dosage (5 nM; Fig. 3A). We next examined whether the nontoxic dosage of itraconazole (5 nM) could reverse the cell apoptosis induced by 20 nM of Tg and found that the percentage of cell death decreased from ~20% in the Tg group to ~7.5% in the Tg+itraconazole group (Fig. 3B). At the protein level, 20 nM of Tg increased the expression of apoptotic activators (caspase-3, Bax and TP5) and decreased the expression of inhibitors (Bcl-2) in OLN cells (Fig. 3C,D). In contrast, these changes were dramatically diminished by itraconazole administration (Fig. 3C,D). We further confirmed the potential anti-apoptotic effect of itraconazole using tissues obtained from animals pretreated with PBS, Tg or Tg+itraconazole. Consistently, we found the dysregulation of apoptotic mediators significantly ameliorated by itraconazole (Fig. 3E,F). We further examined whether itraconazole could reverse the overactivation of the ER stress response in the same tissues and found that the upregulation of ER stress response mediators caused by Tg was significantly decreased by itraconazole (Fig. 4). Overall, these results further demonstrated that itraconazole could suppress the activity of cell apoptosis and the ER stress response.

## AMPK was a novel mediator of itraconazole mitigating the hyperactivity of the ER stress response and apoptosis

We next explored the novel mediator of itraconazole restoring the dysregulated gene network relevant to the apoptosis and ER stress response in EAE. We noticed that the level of p-AMPK dropped significantly in the spinal cords of EAE mice (Fig. 2A,B). Previous studies reported that the activity of AMPK was reduced in the brain from EAE disease and the genetic ablation of AMPK caused severe clinical impairments in EAE animals.<sup>26–28</sup> We first validated the functional role of the AMPK pathway in the development of EAE. Consistent with the effect of genetic ablation of AMPK, suppressing the AMPK pathway with Compound C significantly exacerbated the demyelination in the spinal cord and further impacted the clinical score compared with the EAE+PBS group (Fig. 1A,B), although the same dosage was not cytotoxic for the liver (Fig. 1C,D). Besides, the level of AMPK pathway also affected the activity of the ER stress response, as AICAR – an activator of AMP-activated protein kinase (AMPK) – statistically diminished the hyperactivation of ER-stress-related proteins

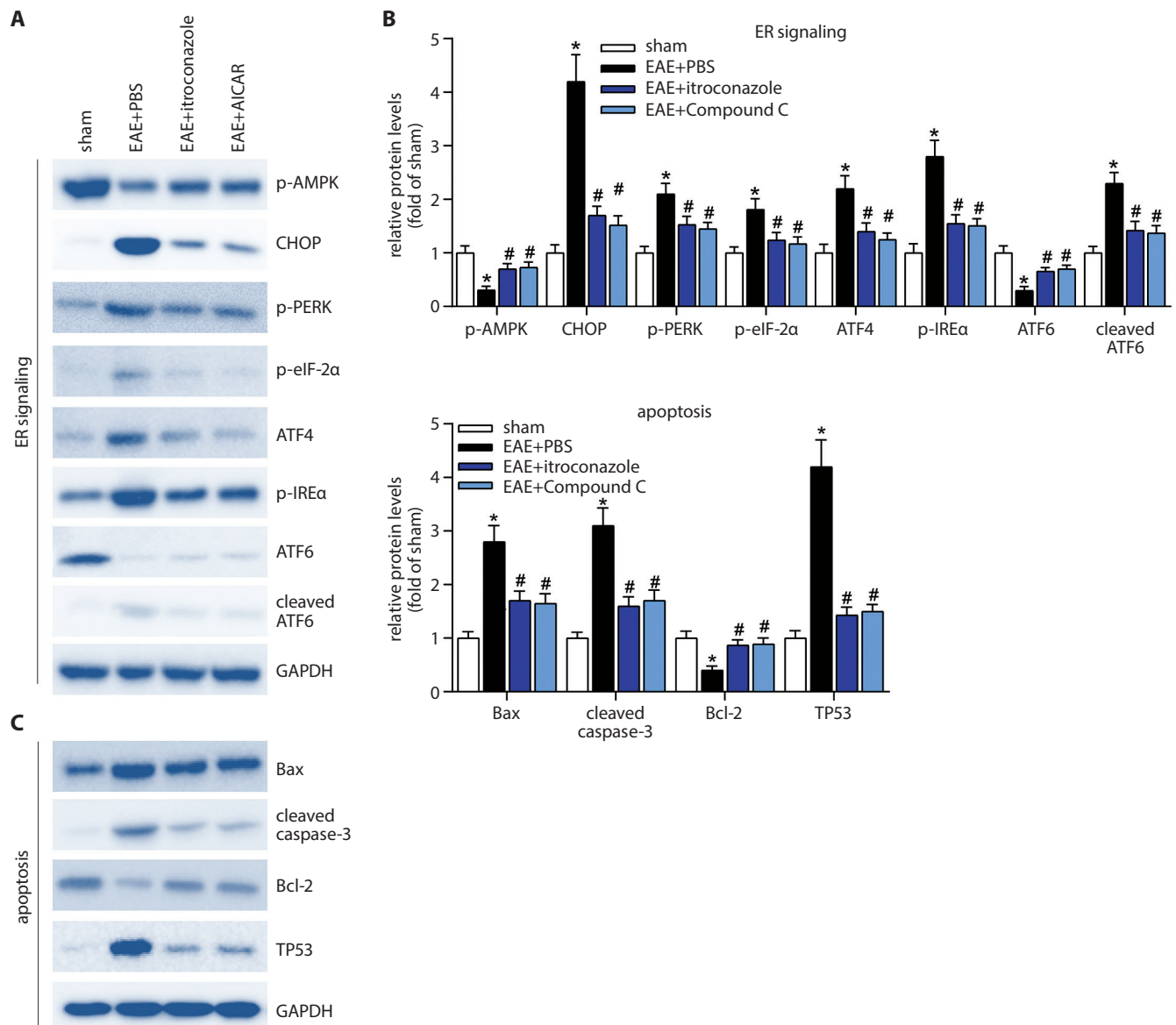


**Fig. 2.** Itraconazole mitigated the hyperactivity of the ER stress response and cell apoptosis in EAE. **A.** The levels of ER stress response mediators, including ATF6, PERK and IRE, were upregulated, while the level of p-AMPK was downregulated in spinal tissues of EAE mice. Both itraconazole and AICAR (activator of AMPK pathway) restored the changes. **B.** Quantitative analysis of the proteins' levels in (A). **C** and **D.** Expression change of apoptotic mediators was significantly improved by itraconazole and AICAR. One-way ANOVA followed by Dunnett's test

\*  $p < 0.01$  vs the sham group; #  $p < 0.01$  vs the EAE+PBS group.

(Fig. 2A–D). Meanwhile, similar effects were obtained in the mice treated with the acute ER stress inducer Tg (Fig. 4). As Compound C is also a BMP pathway inhibitor, we further determined the role of AMPK in EAE by delivering AAV transgenes to the mice to specifically knockdown (AAV-sh-AMPK) or overexpress AMPK (AAV-AMPK) before EAE. Consistent with the pharmacological results, the knockdown of AMPK further enhanced the activity of ER stress response and apoptosis, while overexpression of AMPK largely reduced those responses (Fig. 5A–D). Taken together, these complementary manipulations demonstrated that the AMPK pathway could bi-directionally regulate the development of EAE at the animal motor, tissue and molecular levels.

In our study, we found that the downregulation of p-AMPK was reversed by itraconazole in EAE (Fig. 2A,B). Therefore, we hypothesized that an elevation of p-AMPK might be required for the beneficial effect mediated by itraconazole. As expected, we found that the downregulation of AMPK further enhanced the hyperactivity of the ER stress response, while itraconazole decreased the response in the spinal tissues of Tg-treated animals (Fig. 6A,B). Importantly, the beneficial effect of itraconazole was abolished by AMPK knockdown (Fig. 6A,B). Therefore, AMPK might be a key downstream target of itraconazole in order to mitigate the hyperactivity of apoptosis and the ER stress response in EAE.

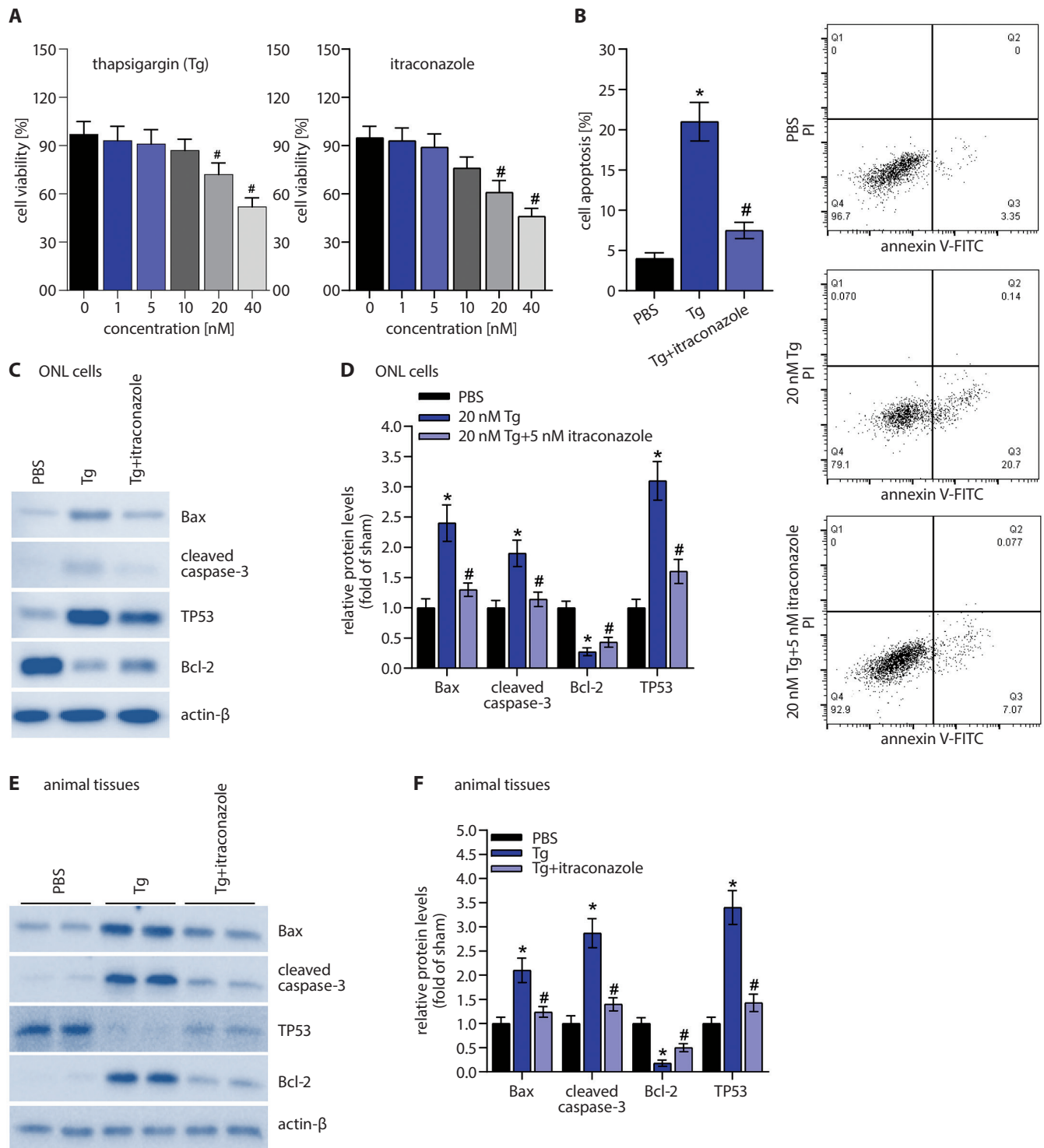


**Fig. 3.** Itraconazole mitigated the cell apoptosis caused by ER stress inducer Tg at the cellular and protein levels. **A.** Dosage effects of Tg and itraconazole on the cell viability of OLN cells as assessed using a CCK-8 assay. The cell viability gradually decreased with increasing concentration of Tg and itraconazole. One-way ANOVA followed by Dunnett’s test; #  $p < 0.05$  vs 0 mM. **B.** The application of itraconazole significantly decreased the percentage of OLN cell apoptosis evoked by Tg determined using flow cytometer. The altered levels of apoptotic mediators induced by Tg in the OLN cells (**C** and **D**) or animal tissues (**E** and **F**) was significantly reversed by itraconazole. One-way ANOVA followed by Dunnett’s test

\*  $p < 0.01$  vs the PBS group; #  $p < 0.01$  vs the Tg group.

## Discussion

Multiple sclerosis is an autoimmune disease in which the immune system destroys the insulation covering

of nerves, thus affecting the fast conduction of neural impulse in myelinated fibers. Along with the development, MS is sequentially characterized by inflammation, demyelination, axonal loss, gliosis, and limb motor deficit,<sup>3</sup>

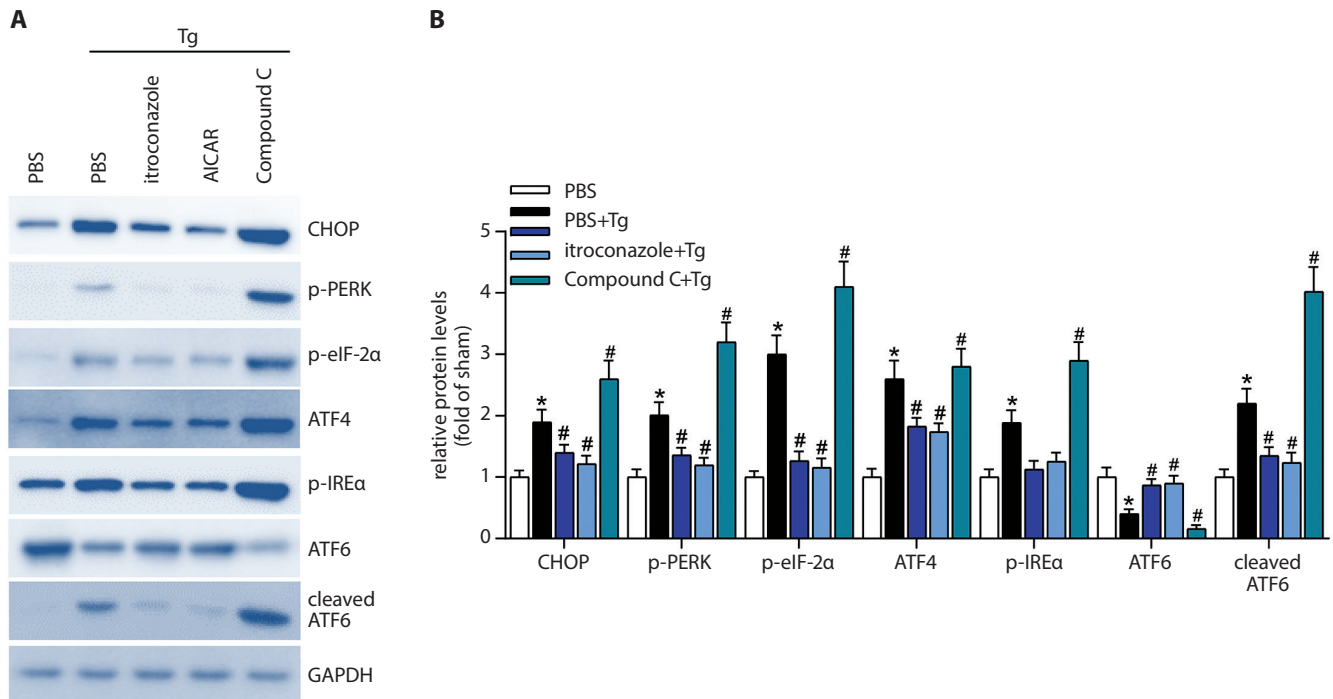


**Fig. 4.** Itraconazole mitigated the overactivity of the ER stress response evoked by Tg in spinal tissues. A and B. Itraconazole and AMPK signal activator AICAR diminished the overactivation of the ER stress pathway, while AMPK signal inhibitor Compound C further enhanced the overactivation. One-way ANOVA followed by Dunnett's test

\*  $p < 0.01$  vs the PBS group; #  $p < 0.01$  vs the PBS+Tg group.

while the inflammatory and apoptotic responses at the cellular level gradually increased in MS patients.<sup>29</sup> In our EAE model, we successfully replicated these symptoms: demyelination in the tissue of the lumbar spinal cord (Fig. 1A), severe limb disabilities (Fig. 1B), and overactivity of ER stress and apoptotic responses (Fig. 2). According to the development of MS, some EAE therapies have focused on suppressing the immune response and protecting the loss of nerves. For example, mitoxantrone was used for general immunosuppression<sup>30</sup> and flecainide (Na channel blocker) was used for axonal protection.<sup>31</sup> In our case, we significantly diminished neural damage and animal limb deficit using the antifungal itraconazole (Fig. 1A,B). A previous study found that fungal infection can lead to MS, and that some fungal-infection-related molecules are biomarkers of MS, laying the foundation to treat MS using antifungal drugs.<sup>15</sup> Although our study opens a new window to treat MS using currently approved antifungal drugs, the translation from animal study to clinical trials needs further assessment, as the EAE model cannot completely mimic the symptoms of MS, and the biological process of MS and the effective dosage of itraconazole might greatly differ between animals and humans.

Due to the complexity of causes and symptoms in MS, the underlying biological mechanism is still very unclear. Studies using animal EAE model have uncovered that several components of the ER stress response are dysregulated at the cellular level. The ER stress response is a bifunctional process, determining the fidelity

of protein folding in healthy cells and promoting cellular apoptosis once the prolonged ER stress cannot be resolved through 3 molecular branches.<sup>32</sup> In our study, the level of mediators of all 3 branches in the ER stress response was changed in the spinal tissues of EAE mice (Fig. 2A). The increase of cleaved ATF6 and phosphorylation of IRE $\alpha$  indicated that the injured cells had tried to increase the protein-folding capacity in order to mitigate the ER stress in EAE. The increase of phosphorylated PERK, eIF-2 $\alpha$  and IRE $\alpha$  reflected that the cells attempted to reduce the flux of protein into ER to alleviate the ER stress, as these proteins can inhibit the mRNA translation and degrade ER-bound mRNAs. Meanwhile, the increase of transcription factor ATF4 and CHOP indicated that the self-death procedure was initiated as these factors can promote the transcription of apoptotic genes. Combined with the fact that the ER stress response has also been found to be an important feature in many other human diseases,<sup>33–36</sup> our data suggest that the ER stress response might play important roles in endogenous self-repair and apoptosis in MS. Importantly, the antifungal itraconazole effectively inhibited the overactivation of ER stress response evoked by EAE (Fig. 2A,B) or Tg (Fig. 4A,B). Furthermore, the upregulation of apoptotic pathways in EAE or Tg treatment was also largely reversed by itraconazole (Fig. 2C,D and 3B–F). These results indicate that itraconazole can effectively restore the dysregulated molecular network caused by EAE, laying the molecular basis for alleviating EAE.



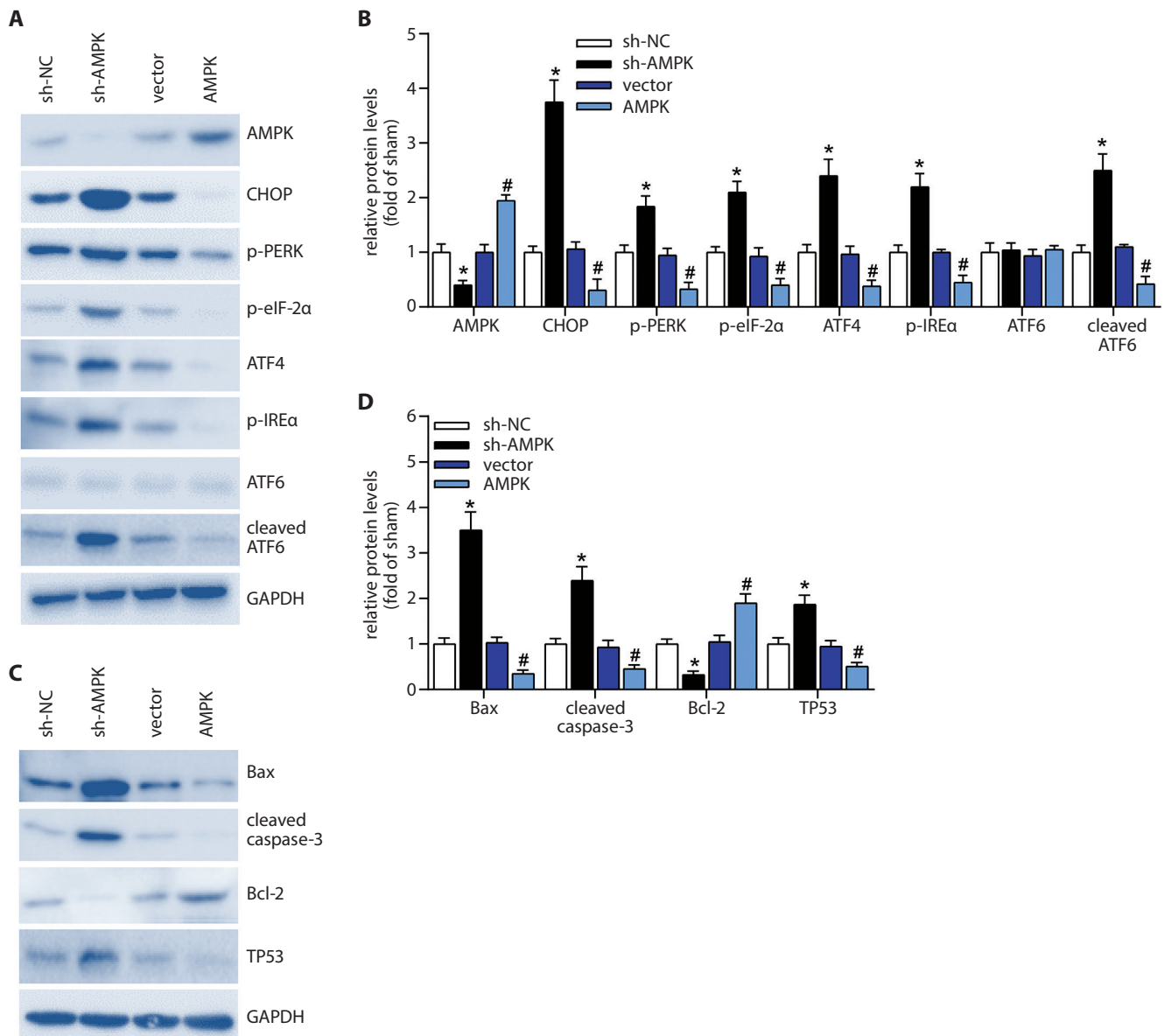


**Fig. 5.** The level of AMPK bi-directionally affected the activity of the ER stress response and apoptosis in spinal tissues of EAE. A and B. Knockdown or overexpression of AMPK by AAV delivery increased or decreased the activity of the ER stress response pathway, respectively. C and D. Knockdown or overexpression of AMPK increased or decreased the level of apoptotic biomarkers, respectively. Student's t-test

\* p < 0.01 vs the sh-NC group; # p < 0.01 vs the vector group.

We found that one potential mediator of itraconazole ameliorating EAE was AMPK. The AMPK pathway is responsible for maintaining energy homeostasis by promoting the uptake of glucose and fatty acids and is also one of the central regulators of growth.<sup>37–39</sup> Additionally, AMPK was relevant to the development of EAE, as its activity was reduced in the brain of EAE animals and the genetic ablation of AMPK exacerbated the clinical impairments in EAE animals.<sup>26–28,40</sup> Consistent with these studies, our data showed that the phosphorylated level of AMPK largely decreased in EAE animals (Fig. 2A), further strengthening the correlation between the dysregulation of the AMPK pathway and EAE development. In addition, our study first showed that pharmacologically enhancing the AMPK

pathway by AICAR significantly restored the hyperactivity of the ER stress response and apoptosis induced by EAE or Tg (Fig. 2,4), consistent with a previous finding that AICAR treatment protected inflammation-induced myelin loss and axonal abnormalities in EAE mice.<sup>41</sup> Besides, specific downregulation or overexpression of AMPK with AAVs bi-directionally altered the endogenous activity of the ER stress response and cellular apoptosis in EAE animal tissues (Fig. 5). Therefore, our complimentary experiments demonstrated that the level of AMPK was critical for the molecular changes associated with EAE. Furthermore, the downregulation of endogenous AMPK abolished the mitigating effect of itraconazole on the acute ER stress response (Fig. 6). This result should not be simply

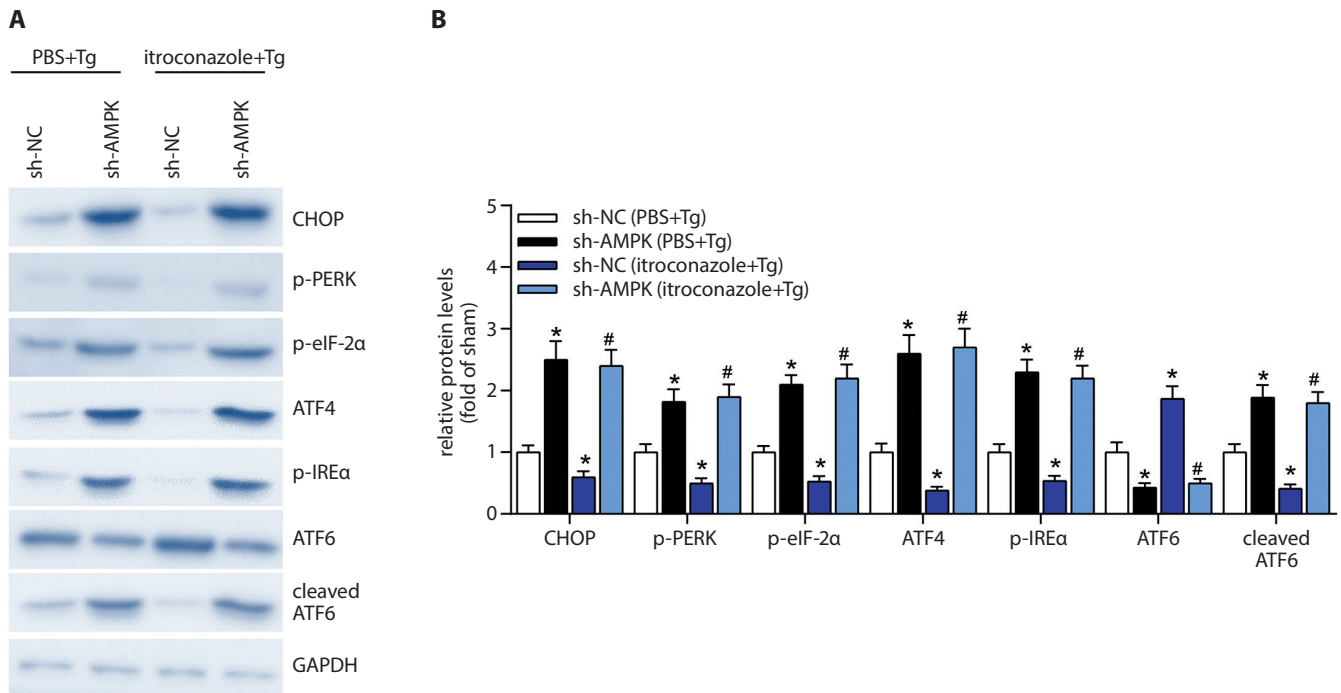


**Fig. 6.** Downregulation of AMPK removed the suppression effect of itraconazole on the overactivation of the ER stress response evoked by Tg in spinal tissues. A and B. The knockdown of AMPK further increased the hyperactivity of the ER stress response pathway induced by Tg and completely blocked the beneficial effect mediated by itraconazole. One-way ANOVA followed by Dunnett's test

\*  $p < 0.01$  vs the sh-NC (PBS+Tg) group; #  $p < 0.01$  vs the sh-NC (itraconazole+Tg) group.

explained away by the fact that the beneficial effect of itraconazole was masked by the knockdown effect of AMPK. If that is the case, the levels of the proteins should be lower in the sh-AMPK (itraconazole+Tg) group than in the sh-AMPK (PBS+Tg) group, since AMPK and itraconazole independently regulated the response. This data indicates that the AMPK pathway might be an essential downstream mediator of itraconazole which mitigates ER stress and suggests that this pathway might be a good target for alleviating MS. It is crucial to explore how itraconazole regulates the AMPK pathway in order to find ways to enhance the therapeutic effect of itraconazole in MS.

## Conclusion

We showed that the antifungal itraconazole effectively ameliorated the EAE symptoms at the behavioral, tissue, cellular, and molecular level. Specifically, the limb disabilities were significantly lessened as demonstrated by decreased clinical score. The demyelination in the spinal cord of EAE mice and the cell apoptosis percentage induced by Tg was largely decreased. Meanwhile, the hyperactivation of related molecular pathways, including ER stress response and cell apoptosis, was mostly reset to the basal level after itraconazole application. Furthermore, we verified that the AMPK pathway is involved in regulating EAE and is a novel target of itraconazole, since the beneficial effect of itraconazole was removed by knockdown of AMPK.

Together, these results demonstrated that the antifungal itraconazole mitigated EAE and showed a new direction to find ways to treat MS using the available antifungal drug.

## ORCID iDs

Huifen Huang <https://orcid.org/0000-0003-2132-3733>  
 Xiaolin Tian <https://orcid.org/0000-0003-2397-8151>  
 Xiao Peng <https://orcid.org/0000-0003-2597-9473>  
 Liangtong Huang <https://orcid.org/0000-0002-3105-8606>  
 Lerong Mei <https://orcid.org/0000-0002-7227-8787>  
 Yanli Zhan <https://orcid.org/0000-0002-8382-2880>  
 Siying Chen <https://orcid.org/0000-0002-9563-2726>  
 Huihua Wu <https://orcid.org/0000-0002-6345-2325>  
 Guofang Wei <https://orcid.org/0000-0002-0512-1181>  
 Xueli Cai <https://orcid.org/0000-0003-1670-3539>

## References

- Browne P, Chandraratna D, Angood C, et al. Atlas of Multiple Sclerosis 2013: A growing global problem with widespread inequity. *Neurology*. 2014;83(11):1022–1024.
- Goverman J. Autoimmune T cell responses in the central nervous system. *Nat Rev Immunol*. 2009;9(6):393–407.
- Constantinescu CS, Farooqi N, O'Brien K, Gran B. Experimental autoimmune encephalomyelitis (EAE) as a model for multiple sclerosis (MS). *Br J Pharmacol*. 2011;164(4):1079–1106.
- Rivers TM, Sprunt DH, Berry GP. Observations on attempts to produce acute disseminated encephalomyelitis in monkeys. *J Exp Med*. 1933;58(1):39–53.
- Farooqi N, Gran B, Constantinescu CS. Are current disease-modifying therapeutics in multiple sclerosis justified on the basis of studies in experimental autoimmune encephalomyelitis? *J Neurochem*. 2010;115(4):829–844.
- Han MH, Hwang SI, Roy DB, et al. Proteomic analysis of active multiple sclerosis lesions reveals therapeutic targets. *Nature*. 2008;451(7182):1076–1081.

7. Steinman L. A molecular trio in relapse and remission in multiple sclerosis. *Nat Rev Immunol*. 2009;9(6):440–447.
8. English C, Aloji JJ. New FDA-approved disease-modifying therapies for multiple sclerosis. *Clin Ther*. 2015;37(4):691–715.
9. Kamarehei M, Kabudanian Ardestani S, Firouzi M, et al. Increased expression of endoplasmic reticulum stress-related caspase-12 and CHOP in the hippocampus of EAE mice. *Brain Res Bull*. 2019;147:174–182.
10. Schroder M. Endoplasmic reticulum stress responses. *Cell Mol Life Sci*. 2008;65(6):862–894.
11. Walter P, Ron D. The unfolded protein response: From stress pathway to homeostatic regulation. *Science*. 2011;334(6059):1081–1086.
12. Haze K, Yoshida H, Yanagi H, Yura T, Mori K. Mammalian transcription factor ATF6 is synthesized as a transmembrane protein and activated by proteolysis in response to endoplasmic reticulum stress. *Mol Biol Cell*. 1999;10(11):3787–3799.
13. Marciniak SJ, Yun CY, Oyadomari S, et al. CHOP induces death by promoting protein synthesis and oxidation in the stressed endoplasmic reticulum. *Genes Dev*. 2004;18(24):3066–3077.
14. Reimold AM, Iwakoshi NN, Manis J, et al. Plasma cell differentiation requires the transcription factor XBP-1. *Nature*. 2001;412(6844):300–307.
15. Benito-Leon J, Laurence M. The role of fungi in the etiology of multiple sclerosis. *Front Neurol*. 2017;8:535.
16. Faergemann J. Treatment of seborrheic dermatitis with itraconazole. *Mykosen*. 1985;28(12):612–618.
17. Boehncke WH, Schon MP. Psoriasis. *Lancet*. 2015;386(9997):983–994.
18. Ahmad N, Mukhtar H. Cytochrome p450: A target for drug development for skin diseases. *J Invest Dermatol*. 2004;123(3):417–425.
19. Denmeade SR, Isaacs JT. The SERCA pump as a therapeutic target: Making a “smart bomb” for prostate cancer. *Cancer Biol Ther*. 2005;4(1):14–22.
20. Berard JL, Wolak K, Fournier S, David S. Characterization of relapsing-remitting and chronic forms of experimental autoimmune encephalomyelitis in C57BL/6 mice. *Glia*. 2010;58(4):434–445.
21. Gramez MS, Jackson KL, Dayton RD, Stanford JA, Klein RL. Methods and tips for intravenous administration of adeno-associated virus to rats and evaluation of central nervous system transduction. *J Vis Exp*. 2017(126):55994. doi:10.37971/55994
22. Weaver A, Goncalves da Silva A, Nuttall RK, et al. An elevated matrix metalloproteinase (MMP) in an animal model of multiple sclerosis is protective by affecting Th1/Th2 polarization. *FASEB J*. 2005;19(12):1668–1670.
23. Dasilva AG, Yong VW. Expression and regulation of matrix metalloproteinase-12 in experimental autoimmune encephalomyelitis and by bone marrow derived macrophages in vitro. *J Neuroimmunol*. 2008;199(1–2):24–34.
24. Groves AK, Barnett SC, Franklin RJ, et al. Repair of demyelinated lesions by transplantation of purified O-2A progenitor cells. *Nature*. 1993;362(6419):453–455.
25. Richter-Landsberg C, Heinrich M. OLN-93: A new permanent oligodendroglia cell line derived from primary rat brain glial cultures. *J Neurosci Res*. 1996;45(2):161–173.
26. Prasad R, Giri S, Nath N, Singh I, Singh AK. 5-aminoimidazole-4-carboxamide-1-beta-4-ribofuranoside attenuates experimental autoimmune encephalomyelitis via modulation of endothelial-monocyte interaction. *J Neurosci Res*. 2006;84(3):614–625.
27. Meares GP, Qin H, Liu Y, Holdbrooks AT, Benveniste EN. AMP-activated protein kinase restricts IFN-gamma signaling. *J Immunol*. 2013;190(1):372–380.
28. Mangalam AK, Rattan R, Suhail H, et al. AMP-activated protein kinase suppresses autoimmune central nervous system disease by regulating M1-type macrophage-Th17 axis. *J Immunol*. 2016;197(3):747–760.
29. Macchi B, Marino-Merlo F, Nocentini U, et al. Role of inflammation and apoptosis in multiple sclerosis: Comparative analysis between the periphery and the central nervous system. *J Neuroimmunol*. 2015;287:80–87.
30. Mangano K, Nicoletti A, Patti F, et al. Variable effects of cyclophosphamide in rodent models of experimental allergic encephalomyelitis. *Clin Exp Immunol*. 2010;159(2):159–168.
31. Bechtold DA, Kapoor R, Smith KJ. Axonal protection using flecainide in experimental autoimmune encephalomyelitis. *Ann Neurol*. 2004;55(5):607–616.
32. Tabas I, Ron D. Integrating the mechanisms of apoptosis induced by endoplasmic reticulum stress. *Nat Cell Biol*. 2011;13(3):184–190.
33. Carrasco DR, Sukhdeo K, Protopopova M, et al. The differentiation and stress response factor XBP-1 drives multiple myeloma pathogenesis. *Cancer Cell*. 2007;11(4):349–360.
34. Wang M, Kaufman RJ. The impact of the endoplasmic reticulum protein-folding environment on cancer development. *Nat Rev Cancer*. 2014;14(9):581–597.
35. Hetz C, Mollereau B. Disturbance of endoplasmic reticulum proteostasis in neurodegenerative diseases. *Nat Rev Neurosci*. 2014;15(4):233–249.
36. Lin W, Lin Y, Li J, et al. Oligodendrocyte-specific activation of PERK signaling protects mice against experimental autoimmune encephalomyelitis. *J Neurosci*. 2013;33(14):5980–5991.
37. Paintlia AS, Paintlia MK, Mohan S, Singh AK, Singh I. AMP-activated protein kinase signaling protects oligodendrocytes that restore central nervous system functions in an experimental autoimmune encephalomyelitis model. *Am J Pathol*. 2013;183(2):526–541.
38. Wang P, Xu TY, Guan YF, et al. Nicotinamide phosphoribosyltransferase protects against ischemic stroke through SIRT1-dependent adenosine monophosphate-activated kinase pathway. *Ann Neurol*. 2011;69(2):360–374.
39. Mihaylova MM, Shaw RJ. The AMPK signalling pathway coordinates cell growth, autophagy and metabolism. *Nat Cell Biol*. 2011;13(9):1016–1023.
40. Nath N, Khan M, Paintlia MK, Singh I, Hoda MN, Giri S. Metformin attenuated the autoimmune disease of the central nervous system in animal models of multiple sclerosis. *J Immunol*. 2009;182(12):8005–8014.
41. Singh I, Samuvel DJ, Choi S, Saxena N, Singh AK, Won J. Combination therapy of lovastatin and AMP-activated protein kinase activator improves mitochondrial and peroxisomal functions and clinical disease in experimental autoimmune encephalomyelitis model. *Immunology*. 2018;154(3):434–451.



# Whole blood *ACTB*, *B2M* and *GAPDH* expression reflects activity of inflammatory bowel disease, advancement of colorectal cancer, and correlates with circulating inflammatory and angiogenic factors: Relevance for real-time quantitative PCR

Iwona Bednarz-Misa<sup>1,A–D,F</sup>, Katarzyna Neubauer<sup>2,B,C,E,F</sup>, Ewa Zacharska<sup>3,B,E,F</sup>,  
Bartosz Kapturkiewicz<sup>4,B,E,F</sup>, Małgorzata Krzystek-Korpacka<sup>1,A–D,F</sup>

<sup>1</sup> Department of Medical Biochemistry, Wrocław Medical University, Poland

<sup>2</sup> Department of Gastroenterology and Hepatology, Wrocław Medical University, Poland

<sup>3</sup> Department of Food Hygiene and Consumer Health, Wrocław University of Environmental and Life Sciences, Poland

<sup>4</sup> First Department of Oncological Surgery of Lower Silesian Oncology Center, Wrocław, Poland

A – research concept and design; B – collection and/or assembly of data; C – data analysis and interpretation;  
D – writing the article; E – critical revision of the article; F – final approval of the article

Advances in Clinical and Experimental Medicine, ISSN 1899–5276 (print), ISSN 2451–2680 (online)

*Adv Clin Exp Med.* 2020;29(5):547–556

## Address for correspondence

Iwona Bednarz-Misa

E-mail: iwona.bednarz-misa@umed.wroc.pl

## Funding sources

The research was funded by National Science Centre (grant No. DEC-2011/01/D/NZ5/02835).

## Conflict of interest

None declared

Received on November 5, 2019

Reviewed on November 18, 2019

Accepted on March 10, 2020

Published online on May 19, 2020

## Cite as

Bednarz-Misa I, Neubauer K, Zacharska E, Kapturkiewicz B, Krzystek-Korpacka M. Whole blood *ACTB*, *B2M* and *GAPDH* expression reflects activity of inflammatory bowel disease, advancement of colorectal cancer, and correlates with circulating inflammatory and angiogenic factors: Relevance for real-time quantitative PCR. *Adv Clin Exp Med.* 2020;29(5):547–556. doi:10.17219/acem/118845

## DOI

10.17219/acem/118845

## Copyright

© 2020 by Wrocław Medical University

This is an article distributed under the terms of the Creative Commons Attribution 3.0 Unported (CC BY 3.0) (<https://creativecommons.org/licenses/by/3.0/>)

## Abstract

**Background.** The effect of bowel inflammation and cancer on the expression of the most prevalent internal controls: *ACTB*, *GAPDH* and *B2M* in whole blood is unknown, although at least *GAPDH* occurred to be tightly regulated and suspected of supporting cancer growth, challenging its suitability as a reference.

**Objectives.** To evaluate the effect of colorectal cancer (CRC) and active inflammatory bowel disease (IBD) on the stability of *ACTB*, *B2M*, *GAPDH*, *HPRT1*, *SDHA*, and *TBP* leukocyte expression.

**Material and methods.** Gene expression in controls and CRC and IBD patients (n = 21/18/25) was evaluated in real-time quantitative polymerase chain reaction (RT-qPCR) using NormFinder, geNorm, BestKeeper, and comparative  $\Delta\text{Ct}$  method, and validated by comparison with absolute quantification of interleukin 1 $\beta$  (IL-1 $\beta$ ) and CCL4.

**Results.** *HPRT1*, *SDHA* and *TBP* were superior normalizers in CRC and IBD. The highest expression variability was noted in active IBD. *B2M* was significantly lower in CRC but higher in IBD. *GAPDH* was higher in CRC and IBD. *ACTB* and *GAPDH* corresponded with CRC advancement ( $p = 0.52$  and  $p = 0.53$ ) and with clinical activity in Crohn's disease ( $p = 0.44$  and  $p = 0.57$ ) and ulcerative colitis (*GAPDH*:  $p = 0.72$ ). *ACTB*, *B2M* and *GAPDH* correlated with circulating inflammatory/angiogenic indices, differently in IBD and CRC.

**Conclusions.** Leukocyte *GAPDH*, *ACTB*, and *B2M* expression is affected by bowel inflammation and cancer, rendering them unsuitable as a reference in CRC and IBD.

**Key words:** geNorm, NormFinder, BestKeeper, whole blood transcriptome, expression stability

## Introduction

Real time quantitative polymerase chain reaction (RT-qPCR) is a powerful tool used to detect even subtle alterations in gene expression in order to unravel pathomechanisms of diseases and to aid research on new biomarkers and/or therapeutic targets. Normalization of target gene expression against reference gene(s), assumed to be uniformly expressed and hence referred to as housekeeping genes (HKG), is a common method of accounting for non-biological variation introduced during sample handling and attributed to differences in amount of loaded templates, transcription efficiencies, contamination with inhibitors, etc. Considering the high sensitivity of the method, the choice of appropriate reference genes is a prerequisite for obtaining valid and reproducible results in studies employing RT-qPCR.<sup>1</sup> However, there is now solid evidence that HKG expression is in fact regulated and might not only differ between cells or tissues but also change in response to endo- or exogenous factors. Particularly, the stability of the most popular reference genes, *GAPDH*, *ACTB* and *B2M*, has recently been challenged, both in cancer disease<sup>2,3</sup> and in inflammation.<sup>4,5</sup> Consequently, a need for validating candidate normalizers prior to their application as internal control in order to find these minimally regulated under given experimental conditions has been repeatedly stressed.<sup>6,7</sup>

Inflammatory bowel disease (IBD) and colorectal cancer (CRC) evoke a response from circulating immune cells, which is why analyzing gene expression patterns in whole blood, owing to its availability, might be advantageous over more relevant but less accessible bowel tissues. Accordingly, profiling gene expression in blood is gaining interest. Recently, it has been proved useful in evaluating various pathological conditions and immune responses, including identifying new biomarkers<sup>8–10</sup> in IBD<sup>11</sup> and CRC.<sup>12</sup> We have previously shown that both bowel inflammation and cancer affect tissue expression of common reference genes.<sup>13</sup> However, their potential effect in whole blood has not been investigated yet. Hence, we designed our present study to find and validate optimal reference genes for whole blood transcriptome studies involving patients with CRC and IBD, active and non-active, and to examine and compare the effect, if any, bowel cancer and inflammation might have on the expression of popular reference genes in whole blood. We showed that the most popular genes used for whole blood transcriptome analysis are not suitable for CRC and IBD patients due to the high level of variation in their expression. Moreover, we showed that this variation was directional; namely, it reflected the advancement/severity of diseases and the expression of genes associated with inflammatory and angiogenic responses.

## Material and methods

### Study population

Sixty-four individuals were enrolled in the current study: 18 CRC patients with histologically confirmed adenocarcinoma, 25 patients with active IBD (13 with Crohn's disease (CD) and 12 with ulcerative colitis (UC)), and 21 controls recruited from patients with adenomas (n = 4), colonic diverticulosis (n = 1) or IBD in remission (n = 16). There were 3 patients with T2N0M0, 1 with T2N × M0, 2 with T3N0M0, 5 with T3N1M0, 2 with T4N0M0, 3 with T4N1M0, 1 with T4N2M1, and 1 with T4N1M1 in cancer group. For the assessment of CD activity, the Crohn's Disease Activity Index (CDAI) combining the evaluation of vital parameters, clinical findings and medical history was applied, and CDAI ≥150 was indicative of active disease. For the assessment of UC activity, the Rachmilewitz Index (RI; clinical activity index – CAI), encompassing stool frequency, number of stools with blood, general well-being, abdominal pain/cramp, fever, extraintestinal manifestations, and laboratory tests (erythrocyte sedimentation rate and hemoglobin concentration) was applied and RI ≥ 6 was indicative of active disease.

Female to male ratio in control/CRC/IBD groups was as follows: 7/14, 3/15 and 10/15,  $p = 0.257$  and age distribution was as follows: median 46 years (range: 20–78), 62 years (46–77) and 34.8 years (19–60),  $p < 0.001$ . None of HKG correlated with age.

### Ethical considerations

The study protocol was approved by the Medical Ethics Committee of Wroclaw Medical University (approval No. KB-575/2011 from 10 November 2011) and the study was conducted in accordance with the Helsinki Declaration of 1975, as revised in 1983, and informed consent was obtained from all patients.

### Analytical methods

#### Sample selection and RNA isolation, quantification and quality assessment

Whole blood samples (3 mL) were collected into PAX-gene Blood RNA Tubes prior to any treatment and stored at  $-80^{\circ}\text{C}$ . RNA was isolated and purified with complementary PAXgene Blood RNA Kit (Qiagen, Hilden, Germany) according to manufacturer's instructions, then quantified in duplicates with NanoDrop 2000 (Thermo Fisher Scientific, Waltham, USA) and its purity assessed by calculating ratios of absorbance at 260 nm, 280 nm, and 230 nm. RNA integrity was evaluated with RNA quality indicator (RQI; from 1 – degraded to 10 – intact RNA) using the Experion platform incorporating LabChip microfluidic technology and Experion RNA StdSens analysis kits (BioRad,

Hercules, USA). Only RNA isolates with RQI  $\geq 7$  were used for RT-qPCR. Possible presence of inhibitors in each RNA isolate was tested by calculating RT-qPCR efficiencies from standard curves prepared by serial dilutions of respective cDNA samples (five-fold dilutions, 6 point-curve, conducted in duplicates using SG qPCR Master Mix from EURx, Gdańsk, Poland). Working dilution of cDNA 1:5 was found to effectively dilute reaction inhibitors and assure near 100% qPCR efficiencies.

### Reverse transcription

To assure the same load of RNA template, for all samples 0.25  $\mu\text{g}$  of whole blood RNA per reaction (20  $\mu\text{L}$ ), previously quantified in duplicates with NanoDrop 2000 and verified in Experion electrophoresis, was reversely transcribed in C1000 thermocycler (BioRad) using Maxima First Strand cDNA Synthesis Kit for RT-qPCR (Thermo Fisher Scientific) according to the protocol suggested by manufacturer. All samples were accompanied by matching negative transcription (“no-RT”) controls, devoid of reverse transcriptase, subsequently tested to assure lack of contamination with genomic DNA.

### Quantitative real-time PCR

Quantitative real-time PCR (qPCRs) were conducted with CFX96 Real-Time PCR system (BioRad) using SsoFast EvaGreen<sup>®</sup> Supermix (BioRad) and the following cycling conditions: 30 s activation at 95°C, 5 s denaturation at 95°C, annealing/extension for 5 s at 61°C, 40 cycles, followed by melting step (60–95°C with fluorescent reading every 0.5°C). Reaction mixture contained 2  $\mu\text{L}$  of cDNA

(diluted 1:5), 10  $\mu\text{L}$  of  $\times 2$  SsoFast EvaGreen<sup>®</sup> Supermix 1  $\mu\text{L}$  of each 10 nM forward and reverse target-specific primers, and water up to 20  $\mu\text{L}$ . Sequences and specificities (evaluated with RT-qPCR and calculated from a four-fold dilution series with 6 measuring points in triplicates, plotted as Cq vs logarithms of dilution values of the DNA templates) of optimized and validated primers spanning at least 1 intron are presented in Table 1. Primers were synthesized by Generi Biotech (Hradec Králové, Czech Republic). A mixture of all cDNA samples investigated was used as a template for calculating primers' specificities. Samples were assessed in 3 technical replicates and accompanied by “no template” control.

### Absolute quantification

For absolute quantification, plasmids with *IL-1 $\beta$*  and *CCL4* inserts were prepared in the following manner: PCR products (10 ng) were cloned into pJET1.2/blunt cloning vector following manufacturer's protocol (Fermentas UAB, Vilnius, Lithuania) and subsequently used to transform NovaBlue GigaSinglets<sup>™</sup> Competent Cells-Novagen (Sigma-Aldrich, St. Louis, USA). Amplified constructs with *IL-1 $\beta$*  and *CCL4* inserts were isolated using Plasmid DNA Purification Kit (Macherey-Nagel, Düren, Germany) and quantified using NanoDrop 2000. Mean concentrations of *IL-1 $\beta$*  and *CCL4* plasmids were 4.47  $\mu\text{g}/\mu\text{L}$  and 5.89  $\mu\text{g}/\mu\text{L}$ , respectively, and 260/280 and 260/230 ratios were 2.03 and 2.4 for *IL-1 $\beta$*  and 1.99 and 2.36 for *CCL4*. Ten-fold dilution series was prepared for each plasmid ( $E = 102.1\%$ ,  $R^2 = 1.0$  for *IL-1 $\beta$*  and  $E = 100.7\%$  and  $R^2 = 0.999$  for *CCL4*) and used for constructing standard curves, in which Cq values were plotted against log of copy

**Table 1.** Sequences and performance characteristics of primers used in the current study

Symbol	Gene name; function of encoded protein	Accession No.	Primer sequence 5'→3' (forward/reverse)	Amp. size	E [%]
<i>ACTB</i> <sup>1</sup>	actin, $\beta$ ; cytoskeletal structural protein	NM_001101.3	F: caccattggcaatgagcgggt R: aggtctttgaggatgtccact	135 bp	100.9
<i>B2M</i> <sup>1</sup>	$\beta$ -2-microglobulin; $\beta$ -chain of MHC class I molecules	NM_004048.2	F: cactgaaaagatgagatgct R: ccaatcfaatgaggatcttca	126 bp	104.3
<i>GAPDH</i> <sup>1</sup>	glyceraldehyde-3-phosphate dehydrogenase; glycolytic enzyme	NM_002046.4	F: gtctccttgacttcaacagcg R: accaccctgttgctgtagccaa	131 bp	105.4
<i>HPRT1</i>	hypoxanthine phosphoribosyl-transferase; purine metabolism	NM_000194.2	F: tgacactggcaaaacaatgca R: ggtcctttcaccagcaagct	94 bp	103.2
<i>SDHA</i>	succinate dehydrogenase subunit A; subunit of respiratory chain complex	NM_004168.2	F: agaggcaggaaggagtcac R: caccatcttgctcatcagtagg	267 bp	94.8
<i>TBP</i>	TATA-box-binding protein; general transcription factor	NM_003194.4	F: tataatcccaagcggttgtg R: ctggtcataactactaaattgtg	283 bp	109.7
<i>IL-1<math>\beta</math></i> <sup>1</sup>	interleukin (IL)-1 $\beta$	NM_000576.2	F: ccacagaccttcaggagaatg R: gtgcagttcagtgatgtagcagg	131 bp	100.1
<i>CCL4</i> <sup>1</sup>	macrophage inflammatory protein (MIP)-1 $\beta$	NM_002984.2	F: ggtcatacagctactcctggac R: gctcctcgcaactttgtgtag	140 bp	103.5

Amp – amplicon; E – efficiency; <sup>1</sup> primer sequences were as proposed by Origene ([www.origene.com](http://www.origene.com)). Remaining primers were designed using Beacon Designer Probe/Primer Design Software (BioRad) as previously described (manuscript submitted). Forward and reverse primer sequences are denoted by “F” and “R”, respectively.

number. The qPCR were run in triplicates using SsoFast EvaGreen® Supermix (BioRad) and conditions described in the above section.

## Circulating cytokines and growth factors

For the purpose of correlation analysis, data on circulating cytokines and growth factors: IL1- $\beta$ , IL-4, IL-6, IL-8, IL-12, G-CSF, GM-CSF, FGF2, MCP-1 (CCL2), macrophage inflammatory protein (MIP)-1 $\alpha$  (CCL3), PDGF-BB, and tumor necrosis factor  $\alpha$  (TNF- $\alpha$ ), were retrieved from our earlier study and were available for 26 patients (16 with CRC and 10 with IBD).<sup>14</sup> Cytokines/growth factors were measured by means of flow cytometry-based method incorporating Luminex xMAP® technology, which utilizes magnetic microspheres conjugated with monoclonal antibodies. Measurements were conducted on BioPlex 200 platform with HRF (BioRad) using custom-made multiplexes validated by the manufacturer (BioRad).

Data on C-reactive protein (CRP) levels at the time of blood sample collection for current study was retrieved from patients' medical records.

## Statistical analysis

Technical replicates were averaged prior to any analyses and differences in primer efficiencies (Table 1) were taken into account by calculating efficiency (E)-corrected Cq values (CqE) using the following formula:  $CqE = \log(E^{\wedge}Cq)$  base 2, where  $E = 10^{(-1/\text{slope of standard curve})}$ .

Expression stability was evaluated using the 4 most popular algorithms: geNorm utility in qbasePLUS v. 2.4 software (Biogazelle BE, Ghent, Belgium),<sup>15</sup> calculating stability M value described as the average pair-wise variation of a specific gene as compared with other candidate genes, NormFinder software v. 0.953 (available as MS Excel Add-in at [www.mdl.dk/publicationsnormfinder.htm](http://www.mdl.dk/publicationsnormfinder.htm)),<sup>16</sup> calculating intra- and inter-group variability combined into stability value, BestKeeper,<sup>17</sup> using pair-wise correlation analysis of candidate genes yielding BestKeeper index, and comparative  $\Delta C_t$  method,<sup>18</sup> comparing relative expression

of pairs of genes within each sample and calculating mean standard deviation (SD) for each gene. RefFinder comprehensive tool (available at [www.leonxie.com](http://www.leonxie.com)) was used to create the final ranking integrating the results obtained with geNorm, NormFinder, BestKeeper, and comparative  $\Delta C_t$  method by assigning an appropriate weight to an individual gene, calculating the geometric mean of their weights and re-ranking the candidate genes accordingly. The smaller geometric mean, the more stably expressed reference gene.

Number of genes sufficient as normalizers was determined with geNorm algorithm. Remaining analyses were conducted using MedCalc Statistical Software v. 12.7.7 (MedCalc Software bvba, Ostend, Belgium) on absolute or normalized relative quantities (NRQ) calculated with qbasePLUS. Normalized relative quantities is a Cq of a given sample referred to the average Cq across all samples for specific gene, with differences in PCR amplification efficiencies taken into account, and normalized against geometric mean Cq of a set of genes selected as reference. If not otherwise stated, data was presented as geometric means with 95% confidence interval (95% CI). Between-group differences were analyzed using one-way analysis of variance (ANOVA) with post-hoc analysis with the Tukey–Kramer test (multigroup comparisons) or using t-test for independent samples with Welch correction when necessary (two-group comparisons). Correlation analysis was conducted using Pearson or Spearman rank correlation tests. Data distribution was tested using  $\chi^2$  test and the homogeneity of variances was tested using Levene's test. Frequency analysis was conducted using  $\chi^2$  test. All calculated probabilities were two-tailed and p-values  $\leq 0.05$  were considered statistically significant.

## Results

### Finding optimal reference genes for studying whole blood transcriptome from IBD and CRC patients

The expression stability of 6 common reference genes, namely *ACTB*, *B2M*, *GAPDH*, *HPRT1*, *SDHA*, and *TBP*, was

**Table 2.** The expression stability of selected reference genes as calculated using different algorithms: NormFinder, geNorm, BestKeeper, and comparative  $\Delta C_t$  method and integrated using RefFinder

NormFinder		geNorm		BestKeeper		Comparative $\Delta C_t$		Comprehensive ranking (RefFinder)	
gene	S <sup>1</sup>	gene	S <sup>1</sup>	gene	S <sup>1</sup>	gene	S <sup>1</sup>	gene	S <sup>1</sup>
<i>HPRT1</i>	0.281	<i>TBP</i>	0.332	<i>ACTB</i>	0.462	<i>TBP</i>	0.561	<i>TBP</i>	1.682
<i>TBP</i>	0.296	<i>SDHA</i>	0.34	<i>GAPDH</i>	0.489	<i>SDHA</i>	0.585	<i>SDHA</i>	2.06
<i>SDHA</i>	0.361	<i>HPRT1</i>	0.385	<i>SDHA</i>	0.515	<i>HPRT1</i>	0.59	<i>HPRT1</i>	2.59
<i>ACTB</i>	0.496	<i>ACTB</i>	0.502	<i>TBP</i>	0.528	<i>ACTB</i>	0.667	<i>ACTB</i>	2.828
<i>GAPDH</i>	0.499	<i>GAPDH</i>	0.545	<i>HPRT1</i>	0.623	<i>GAPDH</i>	0.68	<i>GAPDH</i>	3.976
<i>B2M</i>	0.829	<i>B2M</i>	0.661	<i>B2M</i>	0.907	<i>B2M</i>	0.912	<i>B2M</i>	6

<sup>1</sup>stability value calculated using different algorithms and interpreted as follows: the lower S, the more stable the expression of a given gene. Genes listed in descending order.



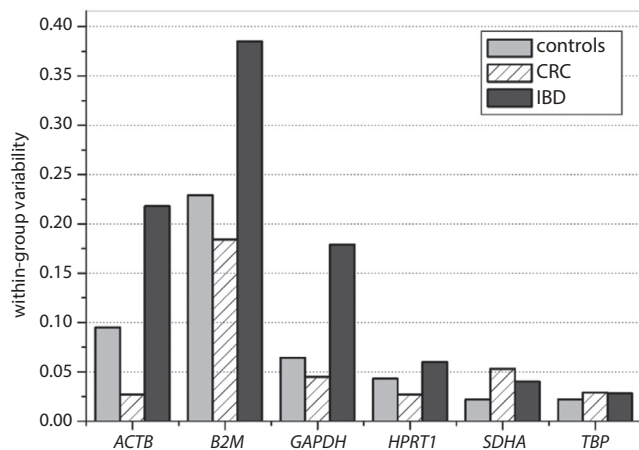


Fig. 1. Expression variability of selected reference genes between controls and patients with CRC or active IBD. Bars present intra-group variability in each of studied groups calculated using NormFinder

CRC – colorectal cancer; IBD – inflammatory bowel disease.

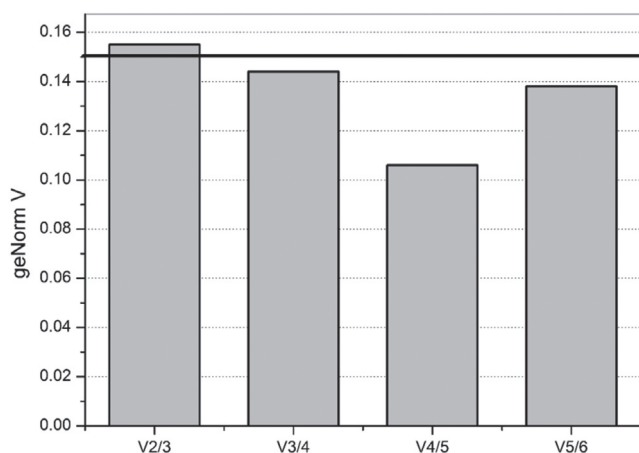


Fig. 2. Determination of optimal number of reference genes to be used as normalizers in studies on whole blood transcriptome in IBD and CRC

Optimal number was determined using geNorm algorithm based on pairwise variation analysis. Bars represent the magnitude of the change in normalization factor following the inclusion of an additional reference gene. GeNorm V values exceeding 0.15 are indicative of a significant effect, pointing at the necessity to include the added gene in a panel of normalizers.

evaluated using the 4 most popular algorithms: NormFinder, geNorm, BestKeeper, and comparative  $\Delta C_t$  method, and integrated using RefFinder in a form of comprehensive ranking (Table 2). Although the exact order differed, most approaches yielded concordant results with *SDHA*, *TBP* and *HPRT1* expression found more stable than that of *GAPDH* or *ACTB*. Regardless of the evaluation method, *B2M* was uniformly found to be the least stable gene in the sample set investigated (Table 2). It also displayed the highest variability within each of the examined cohort, while *GAPDH* and *ACTB* expression varied particularly in IBD group (Fig. 1).

GeNorm algorithm was employed to evaluate the optimal number of reference genes to be used as normalizers.

For studies on whole blood transcriptome in mixed cohorts of CRC and IBD patients or for studies on IBD patients, respective V value dropped below 0.15 (threshold) when normalization factors based on the 3 or 4 most stable reference genes were compared, indicating that normalization of target gene expression should be based on 3 most stable reference genes (Fig. 2), that is, *SDHA*, *TBP* and *HPRT1*. For studies on CRC patients, normalization against *SDHA* and *TBP* was found sufficient.

## Validation of selected normalizers

The performance of reference genes was tested on 2 target genes, *CCL4* and *IL-1 $\beta$* , known to be differently expressed in CRC and IBD. Results obtained using relative quantification method in which target gene expression was normalized either against geometric mean of *SDHA*, *TBP* and *HPRT1* or against individual popular normalizers – *ACTB*, *B2M* or *GAPDH*, were compared with these yielded by absolute quantification method with transcript copy number.

*CCL4* was significantly overexpressed in CRC as compared to IBD and insignificantly downregulated in IBD as compared to controls (Fig. 3A). While results obtained using relative quantification with *SDHA*, *TBP* and *HPRT1* as normalizers were concordant with those obtained using absolute quantification, normalization against *B2M* and *GAPDH* substantially overestimated between-group differences in *CCL4* expression.

*IL-1 $\beta$*  was significantly underexpressed in CRC as compared to IBD, while the slight upregulation in IBD as compared to controls was not significant (Fig. 3B). Again, the results obtained with the absolute method and using the proposed panel of reference genes were concordant, while those obtained using either *B2M* or *GAPDH* underestimated CRC-IBD difference and wrongly implied the downregulation of *IL-1 $\beta$*  in IBD as compared to controls. For both target genes, of the most popular reference genes, normalization against *ACTB* yielded the closest results to those obtained with absolute quantification or by using a panel of normalizers.

## Effect of inflammation and cancer on *GAPDH*, *ACTB* and *B2M* expression in whole blood

Using the panel of normalizers validated here, we compared the effect, if any, of bowel inflammation and cancer on the whole blood expression of *ACTB*, *B2M* and *GAPDH*. As depicted in Table 3, both *B2M* and *GAPDH* expressions differed significantly between groups. *GAPDH* expression was regulated in active IBD as compared to controls by 1.7-fold (95% CI = 1.3–2.1;  $p < 0.001$ ). It was also upregulated as compared to CRC – by 1.8-fold (1.3–2.5;  $p < 0.001$ ). *B2M* expression in active IBD was upregulated by 1.5-fold (1.1–2;  $p = 0.009$ ) and by 1.5-fold (1.1–1.9;

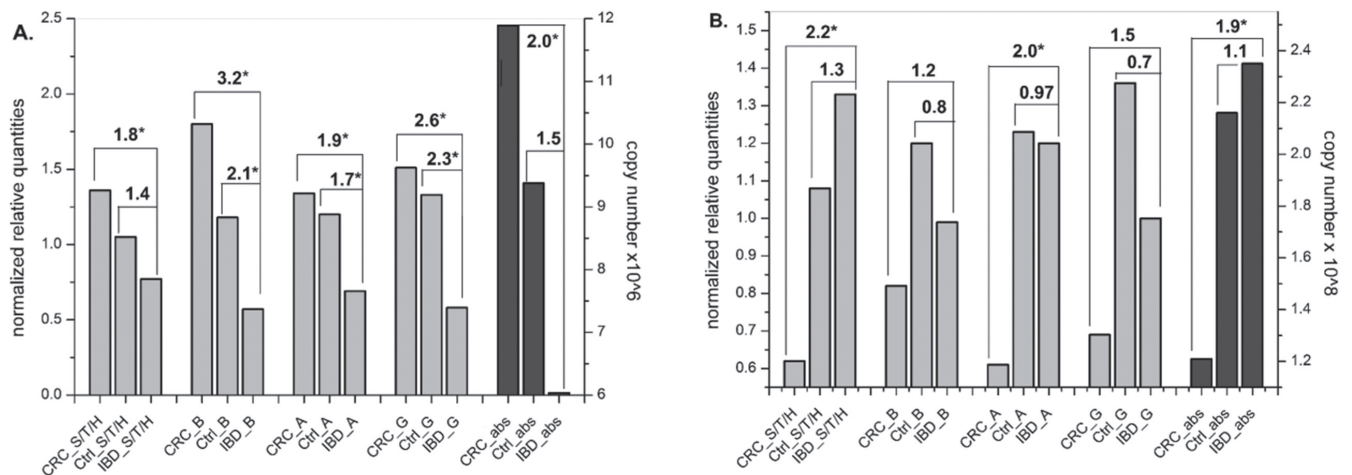


**Fig. 3.** Expression of target genes in CRC and IBD as compared to controls quantified using absolute and relative quantification methods with various reference genes as normalizers: (a) *CCL4*; (b) *IL-1 $\beta$*

Light grey bars represent geometric means of normalized relative quantities (scale on left Y axis) calculated for colorectal cancer patients (denoted as CRC\_), controls (Ctrl\_) or inflammatory bowel disease patients (IBD\_) using geometric mean of *SDHA*, *TBP* and *HPRT1* expression as reference (\_S/T/H) or individual expression of *B2M* (\_B), *ACTB* (\_A), or *GAPDH* (\_G) as reference. Dark grey bars represent geometric means of absolute quantities (scale on right Y axis; denoted as “\_abs”) obtained from standard curves based on serial dilutions of plasmid DNA with *CCL4* and *IL-1 $\beta$*  inserts. Expression ratios, CRC-to-IBD and controls-to-IBD (for *CCL4* in part A) or IBD-to-CRC and IBD-to-controls (for *IL-1 $\beta$*  in part B), are given above the bars. Statistical significance ( $p < 0.05$ ) is denoted with asterisks.

**Table 3.** Relationship between the whole blood expression of *ACTB*, *B2M* and *GAPDH*, and the disease characteristics

Characteristics	n	<i>ACTB</i>	<i>B2M</i>	<i>GAPDH</i>
Cohort:		$p = 0.127$	$p = 0.001$	$p < 0.001$
controls	21	0.87 (0.78–0.98)	0.89 (0.73–1.1) <sup>1,2</sup>	0.79 (0.69–0.91) <sup>1,2</sup>
CRC	18	1.01 (0.85–1.21)	0.75 (0.6–0.94) <sup>2,3</sup>	0.9 (0.76–1.05) <sup>2,3</sup>
active IBD	25	1.11 (0.9–1.36)	1.35 (1.07–1.69) <sup>1,3</sup>	1.32 (1.09–1.6) <sup>1,3</sup>
CRC stage		$\rho = 0.52, p = 0.029$	$\rho = 0.02, p = 0.951$	$\rho = 0.53, p = 0.025$
Local progression (T)		$\rho = 0.16, p = 0.520$	$\rho = 0, p = 0.965$	$\rho = 0, p = 0.972$
Lymph node status (N):		$p = 0.084$	$p = 0.958$	$p = 0.051$
N0	7	0.89 (0.7–1.07)	0.77 (0.51–1.17)	0.79 (0.65–0.92)
N1/2	10	1.2 (0.91–1.49)	0.78 (0.56–1.09)	1.05 (0.8–1.3)
Distant metastases (M):		$p = 0.242$	$p = 0.561$	$p = 0.097$
M0	16	1.04 (0.85–1.22)	0.74 (0.58–0.94)	0.9 (0.75–1.05) <sup>2,3</sup>
M1	2	1.36	1.36	1.27
IBD phenotype:		$p = 0.347$	$p = 0.339$	$p = 0.755$
CD	14	1.22 (1.01–1.46)	1.22 (0.85–1.8)	1.28 (1.08–1.53)
UC	11	0.99 (0.63–1.54)	1.52 (1.19–1.95)	1.37 (0.9–2.07)
IBD activity <sup>4</sup> :				
CD: CDAI	20	$\rho = 0.44, p = 0.052$	$\rho = 0.36, p = 0.118$	$\rho = 0.57, p = 0.009$
UC: RI	12	$\rho = 0.34, p = 0.274$	$\rho = 0, p = 1$	$\rho = 0.72, p = 0.009$

<sup>1</sup>significantly different from CRC; <sup>2</sup>significantly different from active IBD; <sup>3</sup>significantly different from controls; <sup>4</sup>correlation with clinical activity was calculated for all patients for whom it was available, also these with clinically inactive disease (CDAI < 150 or RI < 6). Data presented as means of normalized relative quantities (against geometric mean of *SDHA*, *TBP* and *HPRT1*) with 95% confidence intervals (95% CI) or as Spearman rank correlation coefficients ( $\rho$ ). CD – Crohn’s disease; UC – ulcerative colitis; CDAI – Crohn’s disease activity index; RI – Rachmilewitz index.

$p = 0.004$ ) as compared to controls and CRC, respectively. While *GAPDH* in CRC was significantly higher than in controls, the expression of *B2M* was significantly lower. Between-group differences in *ACTB* expression did not reach statistical significance when analyzed with ANOVA and Tukey–Kramer post-hoc test, but when the controls and IBD patients were compared using t-test for independent samples, the difference was significant ( $p = 0.043$ ).

In CRC, *ACTB* and *GAPDH* expressions increased along with the disease advancement, being associated with the metastatic potential rather than local progression. In IBD, gene expression was not affected by the disease phenotype (CD vs UC), but *ACTB* positively correlated with clinical activity of CD and *GAPDH* also with the activity of UC.

**Table 4.** Association between the whole blood expression of *ACTB*, *B2M* and *GAPDH*, and the systemic levels of inflammatory markers and growth factors

Marker	<i>ACTB</i>	<i>B2M</i>	<i>GAPDH</i>
CRP	$r = 0.51, p = 0.012^1$	–	$r = 0.63, p = 0.001^1$
IL-1 $\beta$	$r = 0.64, p = 0.010^2$	–	$r = 0.74, p < 0.0001$
IL-4	–	–	$p = 0.62, p = 0.053^1$
IL-6	$r = 0.54, p = 0.032^2$	–	$r = 0.63, p = 0.009^2$
IL-8	$r = 0.49, p = 0.053^2$	–	$r = 0.64, p = 0.046^1$
IL-12	–	–	$r = 0.71, p = 0.023^1$
FGF2	$r = 0.65, p = 0.007^2$	$r = -0.49, p = 0.055^2$ $r = 0.56, p = 0.094^1$	$r = 0.53, p = 0.035^2$
G-CSF	$r = 0.66, p = 0.005^2$	$r = -0.56, p = 0.025^2$	$r = 0.81, p < 0.0001$
GM-CSF	$r = 0.65, p = 0.006^2$	–	$r = 0.43, p = 0.096^2$
MIP-1 $\alpha$	$r = 0.63, p = 0.009^2$	$r = 0.65, p = 0.044^1$	$r = 0.54, p = 0.032^2$
TNF- $\alpha$	$r = 0.57, p = 0.020^2$	$r = -0.65, p = 0.006^2$	$r = 0.79, p < 0.001$

<sup>1</sup>correlation observed in IBD patients; <sup>2</sup>correlation observed in CRC patients. Data on circulating cytokines and growth factors was available for 26 patients (16 with CRC and 10 with IBD). Data presented as Pearson correlation (*r*) or Spearman rank correlation (*p*) coefficients.

## *GAPDH*, *ACTB* and *B2M* correlation with inflammatory and angiogenic indices

To further explore the association between popular reference genes and inflammation or tumor angiogenic potential, we investigated whether their expression was related to the levels of *IL-1 $\beta$*  and *CCL4* transcripts in whole blood and whether there was a correlation with circulating mediators of inflammation and angiogenesis.

Concerning whole blood, *ACTB* positively correlated with *CCL4*, exclusively in CRC patients ( $r = 0.57, p = 0.014$ ), and with *IL-1 $\beta$*  in active IBD ( $r = 0.41, p = 0.42$ ). It also tended to correlate with *IL-1 $\beta$*  in CRC ( $r = 0.45, p = 0.061$ ). *B2M* correlated with *CCL4* and *IL-1 $\beta$*  neither in CRC nor in IBD patients. *GAPDH*, in turn, correlated exclusively with *CCL4* expression: positively in CRC ( $r = 0.58, p = 0.013$ ) but negatively in IBD ( $r = -0.45, p = 0.023$ ).

We also examined possible associations between the expression of popular reference genes in whole blood and the levels of circulating inflammatory and angiogenic indices and hematopoietic factors: CRP, IL-1 $\beta$ , IL-4, IL-6, IL-8, IL-12, G-CSF, GM-CSF, FGF2, MCP-1 (*CCL2*), MIP-1 $\alpha$  (*CCL3*), PDGF-BB, TNF- $\alpha$ , and VEGF-A. As shown in Table 4, *ACTB* and *GAPDH* both correlated with a marker of systemic inflammation, CRP, yet exclusively in IBD patients. *ACTB* displayed a number of positive correlations with inflammatory indices, which, however, were significant solely in CRC patients. *GAPDH*, in turn, correlated with IL-6, FGF2, GM-CSF, and MIP-1 $\alpha$  exclusively in CRC, with IL-4, IL-8, and IL-12 solely in IBD and with IL-1 $\beta$ , G-CSF, and TNF- $\alpha$  in both groups of patients. *B2M* expression was associated only with FGF2 and MIP-1 $\alpha$  in IBD, and with G-CSF, FGF2 and TNF- $\alpha$  in CRC. While the observed associations of *B2M* were positive in IBD, they were negative in CRC patients. None of the examined popular reference genes correlated with circulating MCP-1, VEGF-A or PDGF-BB.

## Discussion

A body of evidence has been gathered showing that there is no universal reference gene(s) that would be suitable for all tissues or pathophysiological conditions and that using invalidated normalizers, the expression of which is regulated under experimental conditions, might compromise the study leading to erroneous conclusions.<sup>1,6</sup> There are no previous reports validating reference genes for whole blood analysis (encompassing a mixture of RNA from numerous blood cell types) in a mixed cohort including patients with inflammatory and cancer disease. Thus, we started our research from selection and validation of potential reference genes. As shown by the literature survey, *GAPDH*, *ACTB* and *B2M* are the most popular reference genes, frequently used singlehandedly. Of these, *GAPDH* was rather poorly rated in blood-derived RNA studies, displaying high variability in neonatal whole blood with varying degrees of hypoxia and acidosis,<sup>19</sup> whole blood of patients with multiple sclerosis,<sup>20</sup> in neutrophils from healthy individuals,<sup>21</sup> and in platelets<sup>22</sup> or peripheral blood mononuclear cells<sup>23</sup> from patients with a history of cardiac inflammatory conditions. It also fluctuated during the activation of T lymphocytes<sup>24</sup> or LPS-stimulation of monocytes.<sup>25</sup> Under some of these conditions, *ACTB*<sup>19,21,22,26</sup> or *B2M*<sup>20,21,25</sup> have been expressed stably, but similarly to *GAPDH*, *ACTB* expression has been altered upon the activation of lymphocytes<sup>24,27</sup> or monocytes.<sup>25</sup> In reticulocytes, in turn, *GAPDH* and not *B2M* have been found to be a better reference gene.<sup>18</sup> Of other evaluated reference genes, *HPRT1*,<sup>18,21,26</sup> *TBP*<sup>25</sup> and *SDHA*<sup>18</sup> have been repeatedly ranked well and, as such, they have been included in the current study.

There are several software programs available, which, using various algorithms, are dedicated to aiding in the evaluation of expression stability. We used the 4 most popular ones: NormFinder,<sup>16</sup> geNorm utility in qBasePLUS,<sup>15</sup> BestKeeper,<sup>17</sup> and comparative  $\Delta$ Ct method,<sup>18</sup> and employed

RefFinder to summarize the results. Except for BestKeeper, all algorithms yielded concordant results with *HPRT1*, *SDHA* and *TBP*, outperforming *ACTB*, *B2M* and *GAPDH*. *B2M* was uniformly found the least stable of evaluated reference genes. All genes displayed the highest level of variability in IBD. Consequently, in studies involving patients with active disease normalization against 3 genes is optimal, while 2 – *TBP* and *SDHA* – are sufficient for CRC patients. To validate selected reference genes as normalizers, we analyzed expression of 2 target genes – *IL-1 $\beta$*  and *CCL4* – using both absolute and relative quantification, the latter employing either a set of stable reference genes (*HPRT1/SDHA/TBP*) or *ACTB*, *B2M* and *GAPDH* individually. Only normalization against a set of reference genes yielded results of relative *IL-1 $\beta$*  and *CCL4* expression analysis comparable to these obtained with absolute quantification of copy number. Normalization against *GAPDH* or *B2M* substantially overestimated between-group differences in *CCL4* and underestimated differences in *IL-1 $\beta$*  expression, rendering these genes not suitable for whole blood expression analysis in IBD and CRC patients. However, the results obtained with *ACTB* as a reference did not differ much, although normalization against *ACTB* overestimated *CCL4* downregulation in active IBD, falsely signifying the difference.

Random fluctuations in reference genes are likely to mask subtle alterations in expression of target genes but directional changes in genes used for normalization might result in invalid conclusions.<sup>6</sup> It is evident now that, contrary to previous assumptions, *GAPDH* expression is tightly regulated at transcriptional and posttranslational levels.<sup>28,29</sup> Consistently, several studies have demonstrated that *GAPDH* might be upregulated in response to hypoxia, a common feature of cancer and inflammation.<sup>30</sup> Moreover, it has been implied that *GAPDH* overexpression may constitute a growth advantage for tumor cells.<sup>31</sup> However, the effect of inflammation and cancer on whole blood expression of *GAPDH* as well as that of *ACTB* or *B2M* has not been evaluated yet. Hence, having validated set of stably expressed reference genes, we examined whether variability in *GAPDH*, *B2M* and *ACTB* in whole blood of CRC and IBD patients was random or specifically affected by the examined conditions.

Complementing the findings on *GAPDH* overexpression in colonic tumors at protein level,<sup>32</sup> we found *GAPDH* expression to be upregulated in whole blood of CRC patients. The elevation was even more profound in IBD patients. Moreover, we showed that *GAPDH* upregulation was not random but corresponded with clinical activity of both CD and UC in IBD patients as well as with cancer advancement in CRC patients, in whom it tended to be associated with gaining metastatic potential rather than with local progression of the tumor. Furthermore, it positively and strongly correlated with a number of circulating inflammatory indices, either exclusively in IBD patients (CRP, IL-8, IL-12) or CRC patients (IL-6, FGF2, MIP-1 $\alpha$ ) or both

(IL-1 $\beta$ , G-CSF, TNF- $\alpha$ ), most of which display pro-angiogenic properties as well. As all these cytokines are inter-related, it is likely that some of *GAPDH* associations are mediated by others. Unfortunately, the number of observations is not sufficient to allow for a multivariate analysis, impeding identification of variables independently associated with whole blood *GAPDH* expression.

Our observations are consistent with the phenomena of tumor metabolism reprogramming, which occurs to satisfy increased energetic demands of proliferating cancer cells under diminished oxygen availability. One of its manifestations is the acceleration of glycolysis upon combined actions of mutations in *c-myc* proto-oncogene and the upregulation of hypoxia-inducible factor (HIF)-1 $\alpha$ , the binding sites which can be found in *GAPDH* promoter.<sup>29</sup> It also contains a binding site for *c-jun/AP-1*, transcription factor involved in inflammatory responses<sup>33</sup> as well as tumor angiogenesis.<sup>34</sup> Accordingly, new non-glycolytic functions have recently been attributed to *GAPDH*, e.g., in cell death regulation. Although the exact role it may play remains unclear, as *GAPDH* has been demonstrated to both induce cancer cell senescence<sup>35</sup> and contribute to cancer progression<sup>28</sup> in colon adenocarcinoma cell lines, *GAPDH* has been demonstrated to display pro-survival activities.<sup>36</sup>

*B2M* was uniformly selected as the least stable reference gene in the whole cohort, independently from statistical method of evaluation. It also displayed the highest degree of variability within each study group. Similarly to our previous observations in colorectal tissue (manuscript submitted), whole blood *B2M* was significantly downregulated in cancer but upregulated in active IBD. Accordingly, Bianchini et al.<sup>37</sup> identified *B2M* as the most downregulated gene from among 19.2K genes screened and suggested that the phenomenon might be related to the escape mechanism from NK-mediated lysis developed by tumor cells. Shrouf et al.<sup>3</sup> showed that *B2M* downregulation in colorectal tumors was a strong prognostic indicator of lymph node metastases. In the investigated sample set, whole blood *B2M* did not correspond with cancer advancement nor was it correlated with clinical scores of IBD activity. Nevertheless, consistently with its observed underexpression in CRC and overexpression in IBD, *B2M* expression negatively correlated with FGF2, G-CSF and TNF- $\alpha$  in the former and positively with FGF2 and MIP-1 $\alpha$  in the latter.

Expression of *ACTB* in whole blood was the least variable of the 3 most popular reference genes, and normalization against *ACTB* was even found superior using BestKeeper. However, although the differences between groups did not reach statistical significance when analyzed with ANOVA, *ACTB* clearly tended to be higher in active IBD than in controls (the difference was significant when t-test was used). Moreover, it positively correlated with CRP levels and clinical severity score in CD, rendering it unsuitable as a reference in IBD. In CRC, in turn, it tended to be higher in patients with lymph node metastases and

positively correlated with inflammatory and angiogenic factors: IL-1 $\beta$ , IL-6, FGF2, G-CSF, GM-CSF, MIP-1 $\alpha$ , and TNF- $\alpha$ .

Taken together, our results demonstrate that none of the most popular reference genes, namely, *GAPDH*, *ACTB* or *B2M*, are suitable for transcriptional studies on whole blood from CRC and/or IBD patients. Firstly, their expression differs between conditions, showing that bowel inflammation and cancer affect not only their tissue,<sup>13</sup> but also whole blood expression. Even more importantly, however, the observed variability is not random, as the alterations in their expression levels correspond, to a varying degree, with CRC advancement and the clinical activity of IBD (*GAPDH* and *ACTB*) as well as correlate with the levels of circulating mediators of inflammation and angiogenesis. The clinical relevance of this observation needs to be elucidated; however, regardless of whether the *ACTB*, *B2M*, and *GAPDH* regulation is unintended or plays an active role in inflammatory responses and/or cancer, they definitely does not constitute good internal controls. The set of normalizers proposed here instead, that is, *TBP*, *SDHA* and *HPRT1*, have recently been successfully used by our group for the analysis of whole blood transcriptome of IBD patients.<sup>38,39</sup>

## Conclusions

The expression of frequently used normalizers for whole blood transcriptomic analysis, that is, *GAPDH*, *ACTB*, and *B2M*, is directionally affected by bowel inflammation and cancer, rendering them unsuitable as references in CRC and IBD. The expression of *HPRT1*, *SDHA* and *TBP* was stable across CRC and IBD patients, allowing for their recommendation as normalizers in studies involving both groups of patients.

### ORCID iDs

Iwona Bednarz-Misa  <https://orcid.org/0000-0001-7244-2017>  
 Katarzyna Neubauer  <https://orcid.org/0000-0003-3650-9311>  
 Ewa Zacharska  <https://orcid.org/0000-0002-1840-9731>  
 Bartosz Kapturkiewicz  <https://orcid.org/0000-0002-2894-4834>  
 Małgorzata Krzystek-Korpacka  <https://orcid.org/0000-0002-2753-8092>

### References

- Bustin SA, Murphy J. RNA biomarkers in colorectal cancer. *Methods*. 2013;59(1):116–125.
- Rubie C, Kempf K, Hans J, et al. Housekeeping gene variability in normal and cancerous colorectal, pancreatic, esophageal, gastric and hepatic tissues. *Mol Cell Probes*. 2005;19(2):101–109.
- Shrout J, Yousefzadeh M, Dodd A, et al. Beta(2)microglobulin mRNA expression levels are prognostic for lymph node metastasis in colorectal cancer patients. *Br J Cancer*. 2008;98(12):1999–2005.
- Glare EM, Divjak M, Bailey MJ.  $\beta$ -Actin and GAPDH housekeeping gene expression in asthmatic airways is variable and not suitable for normalising mRNA levels. *Thorax*. 2002;57(9):765–770.
- Congiu M, Slavin JL, Desmond PV. Expression of common housekeeping genes is affected by disease in human hepatitis C virus-infected liver. *Liver Int*. 2011;31(3):386–390.
- Dheda K, Huggett JF, Bustin SA, Johnson MA, Rook G, Zumla A. Validation of housekeeping genes for normalizing RNA expression in real-time PCR. *Biotechniques*. 2004;37(1):112–119.
- Radonić A, Thulke S, Mackay IM, Landt O, Siebert W, Nitsche A. Guideline to reference gene selection for quantitative real-time PCR. *Biochem Biophys Res Commun*. 2004;313(4):856–862.
- Vartanian K, Slottke R, Johnstone T, et al. Gene expression profiling of whole blood: Comparison of target preparation methods for accurate and reproducible microarray analysis. *BMC Genomics*. 2009;10:2.
- Ghosh S, Dent R, Harper ME, Gorman SA, Stuart JS, McPherson R. Gene expression profiling in whole blood identifies distinct biological pathways associated with obesity. *BMC Med Genomics*. 2010;3:56.
- Batliwalla FM, Baechler EC, Xiao X, et al. Peripheral blood gene expression profiling in rheumatoid arthritis. *Genes Immun*. 2005;6(5):388–397.
- Burczynski ME, Peterson RL, Twine NC, et al. Molecular classification of Crohn's disease and ulcerative colitis patients using transcriptional profiles in peripheral blood mononuclear cells. *J Mol Diag*. 2006;8(1):51–61.
- DePrimo SE, Wong LM, Khatry DB, et al. Expression profiling of blood samples from an SU5416 Phase III metastatic colorectal cancer clinical trial: A novel strategy for biomarker identification. *BMC Cancer*. 2003;3:3.
- Krzystek-Korpacka M, Diakowska D, Bania J, Gamian A. Expression stability of common housekeeping genes is differently affected by bowel inflammation and cancer: Implications for finding suitable normalizers for inflammatory bowel disease studies. *Inflamm Bowel Dis*. 2014;20(7):1147–1156.
- Krzystek-Korpacka M, Diakowska D, Kapturkiewicz B, Bębenek M, Gamian A. Profiles of circulating inflammatory cytokines in colorectal cancer (CRC), high cancer risk conditions, and health are distinct. *Cancer Lett*. 2013;337(1):107–114.
- Vandesompele J, De Preter K, Pattyn F, et al. Accurate normalization of real-time quantitative RT-PCR data by geometric averaging of multiple internal control genes. *Genome Biol*. 2002;3(7):RESEARCH0034.
- Andersen CL, Jensen JL, Ørntoft TF. Normalization of real-time quantitative reverse transcription-PCR data: A model-based variance estimation approach to identify genes suited for normalization, applied to bladder and colon cancer data sets. *Cancer Res*. 2004;64(15):5245–5250.
- Pfaffl MW, Tichopad A, Prgomet C, Neuvians TP. Determination of stable housekeeping genes, differentially regulated target genes and sample integrity: BestKeeper-Excel-based tool using pair-wise correlations. *Biotechnol Lett*. 2004;26(6):509–515.
- Silver N, Best S, Jiang J, Thein SL. Selection of housekeeping genes for gene expression studies in human reticulocytes using real-time PCR. *BMC Mol Biol*. 2006;7:33.
- Maron JL, Arya MA, Seefeldt KJ, et al. pH but not hypoxia affects neonatal gene expression: Relevance for housekeeping gene selection. *Matern Fetal Neonatal Med*. 2008;21(7):443–447.
- Stamova BS, Apperson M, Walker WL, et al. Identification and validation of suitable endogenous reference genes for gene expression studies in human peripheral blood. *BMC Med Genomics*. 2009;2:49.
- Zhang X, Ding L, Sandford AJ. Selection of reference genes for gene expression studies in human neutrophils by real-time PCR. *BMC Mol Biol*. 2005;6:4.
- Zsóri KS, Muszbek L, Csiki Z, Shemirani AH. Validation of reference genes for the determination of platelet transcript level in healthy individuals and in patients with the history of myocardial infarction. *Int J Mol Sci*. 2013;14(2):3456–3466.
- Dabek J, Wilczok J, Kulach A, Gasior Z. Altered transcriptional activity of gene encoding GAPDH in peripheral blood mononuclear cells from patients with cardiac syndrome X – an important part in pathology of microvascular angina? *Arch Med Sci*. 2010;6(5):709–712.
- Bas A, Forsberg G, Hammarström S, Hammarström ML. Utility of the housekeeping genes 18S rRNA, beta-actin and glyceraldehyde-3-phosphate-dehydrogenase for normalization in real-time quantitative reverse transcriptase-polymerase chain reaction analysis of gene expression in human T lymphocytes. *Scand J Immunol*. 2004;59(6):566–573.
- Piehlér AP, Grimholt RM, Ovstebø R, Berg JP. Gene expression results in lipopolysaccharide-stimulated monocytes depend significantly on the choice of reference genes. *BMC Immunol*. 2010;11:21.
- Spinsanti G, Zannolli R, Panti C, et al. Quantitative real-time PCR detection of TRPV1-4 gene expression in human leukocytes from healthy and hyposensitive subjects. *Mol Pain*. 2008;4:51.

27. Røge R, Thorsen J, Tørring C, Ozbay A, Møller BK, Carstens J. Commonly used reference genes are actively regulated in in vitro stimulated lymphocytes. *Scand J Immunol.* 2007;65(2):202–209.
28. Colell A, Green DR, Ricci JE. Novel roles for GAPDH in cell death and carcinogenesis. *Cell Death Differ.* 2009;16(12):1573–1581.
29. Krasnov GS, Dmitriev AA, Snezhkina AV, Kudryavtseva AV. Deregulation of glycolysis in cancer: Glyceraldehyde-3-phosphate dehydrogenase as a therapeutic target. *Expert Opin Ther Targets.* 2013;17(6):681–693.
30. Eltzschig HK, Carmeliet P. Hypoxia and inflammation. *N Engl J Med.* 2011;364(7):656–665.
31. Guo C, Liu S, Sun MZ. Novel insight into the role of GAPDH playing in tumor. *Clin Transl Oncol.* 2013;15(3):167–172.
32. Cuezva JM, Krajewska M, de Heredia ML, et al. The bioenergetic signature of cancer: A marker of tumor progression. *Cancer Res.* 2002;62(22):6674–6681.
33. Schonhaler HB, Guinea-Viniegra J, Wagner EF. Targeting inflammation by modulating the Jun/AP-1 pathway. *Ann Rheum Dis.* 2011;70(Suppl 1):i109–112.
34. Yin Y, Wang S, Sun Y, et al. JNK/AP-1 pathway is involved in tumor necrosis factor- $\alpha$  induced expression of vascular endothelial growth factor in MCF7 cells. *Biomed Pharmacother.* 2009;63(6):429–435.
35. Nicholls C, Pinto AR, Li H, et al. Glyceraldehyde-3-phosphate dehydrogenase (GAPDH) induces cancer cell senescence by interacting with telomerase RNA component. *Proc Natl Acad Sci U S A.* 2012;109(33):13308–13313.
36. Azam S, Jouvret N, Jilani A, et al. Human glyceraldehyde-3-phosphate dehydrogenase plays a direct role in reactivating oxidized forms of the DNA repair enzyme APE1. *J Biol Chem.* 2008;283(45):30632–30641.
37. Bianchini M, Levy E, Zucchini C, et al. Comparative study of gene expression by cDNA microarray in human colorectal cancer tissues and normal mucosa. *Int J Oncol.* 2006;29(1):83–94.
38. Neubauer K, Misa IB, Diakowska D, Kapturkiewicz B, Gamian A, Krzystek-Korpacka M. Nampt/PBEF/visfatin upregulation in colorectal tumors, mirrored in normal tissue and whole blood of colorectal cancer patients, is associated with metastasis, hypoxia, IL1 $\beta$ , and anemia. *Biomed Res Int.* 2015;2015:523930
39. Neubauer K, Bednarz-Misa I, Walecka-Zacharska E, et al. Oversecretion and overexpression of nicotinamide phosphoribosyltransferase/pre-b colony-enhancing factor/visfatin in inflammatory bowel disease reflects the disease activity, severity of inflammatory response and hypoxia. *Int J Mol Sci.* 2019;20(1):166.

# Thermal effect of Er:YAG and Er,Cr:YSGG used for debonding ceramic and metal orthodontic brackets: An experimental analysis

Patrycja Downarowicz<sup>1,A–F</sup>, Paweł Noszczyk<sup>2,A–E</sup>, Marcin Mikulewicz<sup>1,C–F</sup>, Rafał Nowak<sup>3,C,E</sup>

<sup>1</sup> Department of Facial Abnormalities, Division of Maxillofacial Orthopaedics and Orthodontics, Wrocław Medical University, Poland

<sup>2</sup> Department of Building Physics and Computer Design Methods, Wrocław University of Science and Technology, Poland

<sup>3</sup> Department of Maxillofacial Surgery, Wrocław Medical University, Poland

A – research concept and design; B – collection and/or assembly of data; C – data analysis and interpretation; D – writing the article; E – critical revision of the article; F – final approval of the article

Advances in Clinical and Experimental Medicine, ISSN 1899–5276 (print), ISSN 2451–2680 (online)

*Adv Clin Exp Med.* 2020;29(5):557–563

## Address for correspondence

Patrycja Downarowicz  
E-mail: p.downarowicz@gmail.com

## Funding sources

None declared

## Conflict of interest

None declared

## Acknowledgements

The authors gratefully acknowledge the support of MEDIF Sp. z o.o. and MARKU DENTAL and their representatives, Aleksander Mieleśzko and Grzegorz Fąfara, for providing lasers used in this study.

Received on June 4, 2019

Reviewed on December 11, 2019

Accepted on March 10, 2020

Published online on May 12, 2020

## Cite as

Downarowicz P, Noszczyk P, Mikulewicz M, Nowak R. Thermal effect of Er:YAG and Er,Cr:YSGG used for debonding ceramic and metal orthodontic brackets: An experimental analysis. *Adv Clin Exp Med.* 2020;29(5):557–563. doi:10.17219/acem/118844

## DOI

10.17219/acem/118844

## Copyright

© 2020 by Wrocław Medical University

This is an article distributed under the terms of the Creative Commons Attribution 3.0 Unported (CC BY 3.0) (<https://creativecommons.org/licenses/by/3.0/>)

## Abstract

**Background.** In orthodontics, erbium (Er:YAG) lasers can be used for bracket debonding.

**Objectives.** To assess the changes in temperature of pulp and enamel during laser debonding of brackets.

**Material and methods.** A total of 13 brackets ( $n = 13$ ; 2 metal and 11 ceramic brackets) were bonded to 13 caries-free premolars extracted for orthodontic reasons. Brackets were irradiated with 2 lasers. Laser No. 1 was an erbium–chromium (Er,Cr:YSGG) laser (Waterlase Express; Biolase, Irvine, USA) with a wavelength of 2,780 nm at a power of 2.78–2.85 W, energy of 185–190 mJ, fluence of 10 ns, frequency of 25 Hz, pulse duration of 300  $\mu$ s, tip diameter of 0.6 mm, air/fluid cooling of 3.5 mL/s, and time of irradiation of 5–25 s. Laser No. 2 was an Er:YAG laser (LiteTouch; Light Instruments Ltd., Yokneam, Israel) with a wavelength of 2,940 nm at a power of 4 W, energy of 200 mJ, fluence of 10 ns, frequency of 20 Hz, pulse duration of 300  $\mu$ s, tip diameter of 0.8 mm, air/fluid cooling of 3.5 mL/s, and time of irradiation of 5–15 s. Two thermographic cameras (FLIR Zenmuse XT and FLIR P65; FLIR Systems, Wilsonville, USA) and type K thermocouple (Zhangzhou Weihua Electronic Co., Fujian, China) were used for precise temperature measurement on the surface of the teeth and inside them.

**Results.** When laser No. 1 was in use, the mean difference between the inner and outer temperature of the examined teeth (1.4°C) was higher than when the laser No. 2 was in use (0.6°C) ( $p = 0.0974$ ). The study found that the temperature inside the tooth did not increase, and it even decreased during treatment with Er:YAG laser using water cooling, provided that appropriate proportion of water and air was used. For laser No. 1, confidence interval (CI) was between 0.7 and 2.2 and for laser No. 2 it was between 0.500 and 1.23. Only experiment for ceramic brackets was described.

**Conclusions.** These findings confirm that the use of Er:YAG family lasers for orthodontic bracket debonding in an in vitro study is safe and effective.

**Key words:** thermography, enamel, orthodontic treatment, thermocouple, tooth temperature

## Introduction

Lasers are used in all areas of dentistry, ranging from the treatment of soft and hard tissues, periodontal and peri-implant therapy, infections caused by bacteria and fungi, to orthodontic treatment.<sup>1–6</sup>

Orthodontic treatment using fixed appliances with metal or ceramic brackets is a common therapy of malocclusion.<sup>7</sup> Removal of the bracket with conventional debonding pliers, however, can result in enamel cracks, pain and ceramic bracket damage.<sup>8</sup> The available single reports of *in vitro* studies using the 2,940 nm wavelength erbium (Er:YAG) lasers for ceramic bracket debonding indicate that the procedure is effective and safe for the pulp and enamel.<sup>9–14</sup> Lasers are effective in softening the adhesion at the bracket/resin interface by producing heat energy. Energy transfers into heat within the bonding material vapor and debond the brackets from the enamel.<sup>9</sup> Therefore, problems such as enamel break, bracket detachment and pain during debonding can be solved. The literature concerning the effect of the 2,780 nm wavelength erbium-chromium lasers (Er,Cr:YSGG) is scarce.<sup>15</sup> In addition, lasers have such advantages as decreasing debonding force and shortening debonding time.<sup>16</sup> The Er:YAG laser (2,940 nm) has a high absorbance coefficient in water.<sup>17</sup> Particular care should be taken to prevent thermal injury of the dental pulp with high-power lasers.<sup>18</sup> For example, an intrapulpal increase of 5.5°C causes pulpitis or pulp necrosis in 15% of irradiated teeth.<sup>19</sup> A temperature increase by 10°C on the outer root surfaces causes bone resorption and tooth ankylosis.<sup>20</sup> The use of high-power lasers requires well-defined parameters to prevent thermal damage and to ensure predictable debonding of brackets. However, there is no data on the effect of the 2,780 nm wavelength Er:YAG laser.

The objective of the research was to assess the changes in temperature of pulp and enamel during laser debonding of ceramic and metal brackets.

## Material and methods

### Sample preparation

Thirteen healthy human premolars, extracted as a part of orthodontic treatment, were immersed in 5% formalin solution for 24 h. All the teeth were removed on the same day before the experiment. They were kept at stable room temperature. After the 24-hour immersion, the enamel surface was polished with fluoride-free polishing paste (Super Polish; Kerr Hawe, Brea, USA) using the handpiece-attached prophylaxis brush, rinsed and air-dried.

### Bracket bonding procedure

Prior to laser exposure, metal (Mini Diamond Twin; Ormco, Glendora, USA) and esthetic (Inspire-ICE; Ormco) brackets were bonded (Primer Transbond XT and

Transbond XT; 3M Unitek, Maplewood, USA) on the same day. The polymerization of orthodontic adhesive was carried out for 20 s using a LED light-curing device. Next, the study teeth were immersed in a 5% formalin solution once again at stable room temperature for 48 h to ensure that bonding was complete prior to bracket debonding. Pulpotomy was performed in most studied teeth and pulp replaced with thermal compound to enable temperature measurements using a thermocouple within a pulp cavity. Tooth preparation protocol is shown in Fig. 1.

### Debonding protocol

This experimental *in vitro* study yielded specific settings of 2 lasers.

Laser No. 1 – Er,Cr:YSGG laser (Waterlase Express; Biolase, Irvine, USA) with a 2,780 nm wavelength, power of 2.78–2.85 W, energy of 185–190 mJ, frequency of 25 Hz, pulse duration of 300 µs, tip diameter of 0.6 mm, air/fluid cooling of 3.5 mL/s, and illumination time until spontaneous ceramic bracket detachment of 5–25 s.

Laser No. 2 – Er:YAG laser (LiteTouch; Light Instruments Ltd., Yokneam, Israel) with a 2,940 nm wavelength, power of 4 W, energy of 200 mJ, frequency of 20 Hz, pulse duration of 300 µs, tip diameter of 0.8 mm, air/fluid cooling

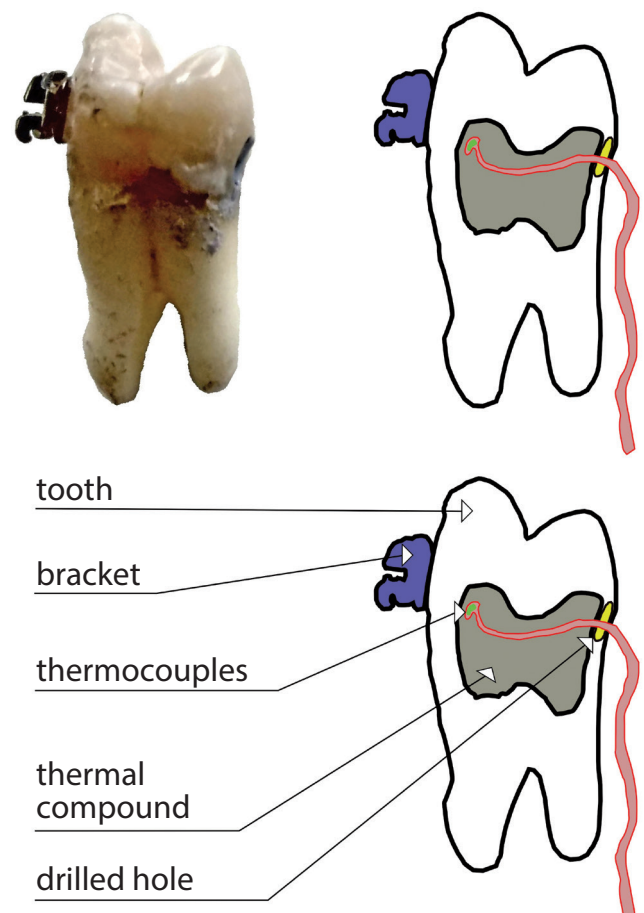


Fig. 1. Tooth preparation protocol



of 3.5 mL/s, and illumination time until spontaneous ceramic bracket detachment of 5–15 s.

The laser energy was applied from a distance of 1–2 mm. Ceramic brackets were illuminated centrally and with slight circular motion, whereas metal brackets were irradiated from all sides. All the samples were debonded with Er:YAG and Er:Cr:YSGG lasers on the same day.

### Temperature measurement

The temperature measurement followed a three-step procedure:

- temperature measurement prior to switching on the laser (20 s);
- temperature measurement during laser exposure. The exposure was continued either over a predefined amount of time or until the bracket detached, whichever shorter. This step lasted between 5 s and 150 s;
- temperature measurement after the laser was switched off, as the thermal balance between the tooth and the environment was being restored. This step lasted for a few minutes.

During each step of the procedure, the temperature on the surface of the tooth was measured using the thermographic camera every 10 s, whereas the temperature inside the tooth was measured using a thermocouple every 1 s.

If the bracket did not detach spontaneously within a few minutes following laser exposure, manual debonding was attempted. A following test stand was designed: 2 thermographic cameras, i.e., FLIR Zenmuse XT (FLIR Systems, Wilsonville USA) with a 640 × 512 pixel resolution and thermal sensitivity <50 mK, and FLIR P65 camera (FLIR Systems) with a 320 × 240 pixel resolution and thermal sensitivity <80 mK; relative humidity and ambient temperature sensor; and a temperature sensor attached to type K thermocouples (Zhangzhou Weihua Electronic Co., Fujian, China) (Fig. 1). The measurements recorded under different conditions are shown in Table 1.

### Statistical analysis

The obtained outcomes were subject to statistical analysis using STATISTICA v. 12.0 (StatSoft, Inc., Tulsa, USA) software and Student’s t-test ( $p = 0.0974$ ). The test for the assessment of normality was Kolmogorov–Smirnov (K–S).

### Results

When laser No. 1 was used, the outside temperature of the examined teeth (23.3°C) was significantly higher than their inner temperature (21.4°C) ( $p = 0.0004$ ). Using

Table 1. The measurements performed under different conditions.

Laser No. 1 – Waterlase Express, Er:Cr:YSGG, 2,780 nm (2.78 μm) wavelength, manufacturer: Biolase								
1	2	3	4	5	6	7	8	9
Tooth No.	laser exposure duration	energy	power	frequency	amount of water*	amount of air	bracket debonding	bracket type
[–]	[s]	[mJ]	[W]	[Hz]	[%]	[%]	[–]	[–]
1	30	120	3	25	5	10	manual, medium force	ceramic
2	30	120	3	25	5	10	manual, medium force	ceramic
3	30	120	3	25	0	10	manual, medium force	ceramic
4	15	180	2.7	25	80	60	manual, medium force	ceramic
5	10	190	2.85	25	80	60	detached spontaneously	ceramic
6	25	185	2.78	25	80	60	manual, low force	ceramic
7	5	185	2.78	25	80	60	detached spontaneously	ceramic
Laser No. 2 – Little Touch, Er:YAG, 2,940 nm (2.94 μm) wavelength								
1	2	3	4	5	6	7	8	9
Tooth No.	laser exposure duration	energy	power	frequency	amount of water and air*	nozzle type	bracket debonding	bracket type
[–]	[s]	[mJ]	[W]	[Hz]	[%]	[–]	[–]	[–]
8	15	200	4	20	50	red	detached spontaneously	ceramic
9 <sup>⊙</sup>	15	200	4	20	50	red	detached spontaneously	ceramic
10	75	200	4	20	50	yellow	manual, low force	ceramic
11	5	200	4	20	50	red	detached spontaneously	ceramic
12	120	200	4	20	50	red	manual, did not detach	metal
13	120	500	7.5	15	50	black	manual, did not detach	metal

\* 100% of air or water denotes maximum amount for a given device; \*\* the tooth was not filled with thermal compound – the pulp was not removed.

laser No. 2, the outside temperature of the examined teeth (24.7°C) was slightly higher than their inner temperature (24.2°C) ( $p = 0.1004$ ). When using laser No. 1, the median difference between the inner and outer temperatures of the examined teeth (1.4°C) was higher than when laser No. 2 was used (0.6°C) ( $p = 0.0974$ ).

The temperature changes over time both on the surface of the teeth and inside the teeth are presented in the Figures below. The temperature inside the tooth was shown

in Fig. 2 and 3. Figures 4 and 5 show temperature values measured on the surface of the teeth using the FLIR P65 thermographic camera (the Zenmuse XT thermographic camera was an additional, control camera). The temperature differences between the enamel and the pulp at the same time points were computed. Positive numbers indicate that the temperature of the enamel was higher than that of the pulp. The results are shown in Fig. 6 and 7.

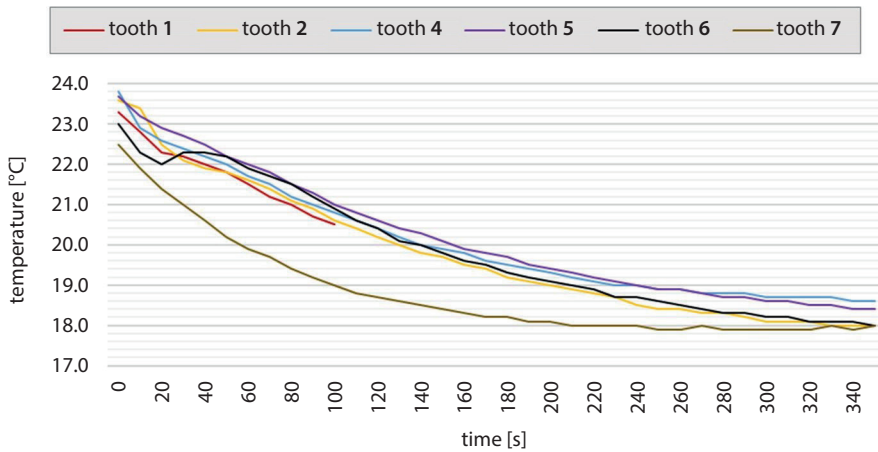


Fig. 2. The temperature inside the tooth during treatment with laser No. 1 measured using thermocouple – diagram close-up

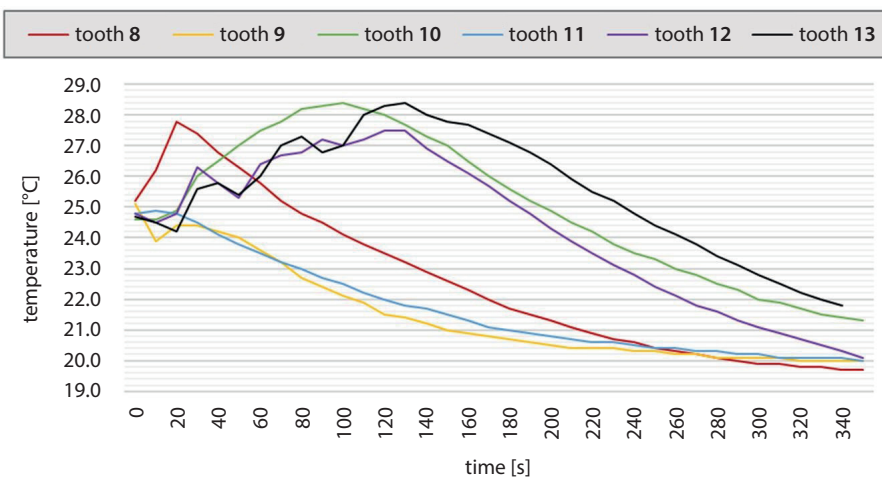


Fig. 3. The temperature inside the tooth during treatment with laser No. 2 measured using thermocouple

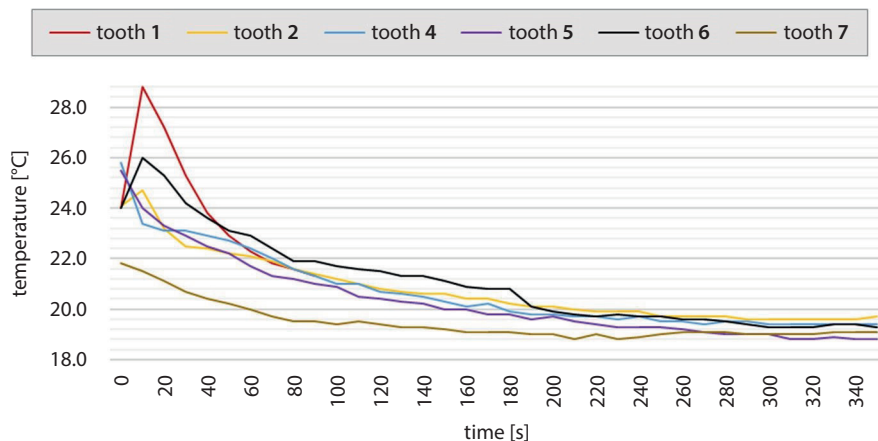


Fig. 4. The temperature on the surface of the tooth during treatment with laser No. 1 measured using thermographic camera – diagram close-up

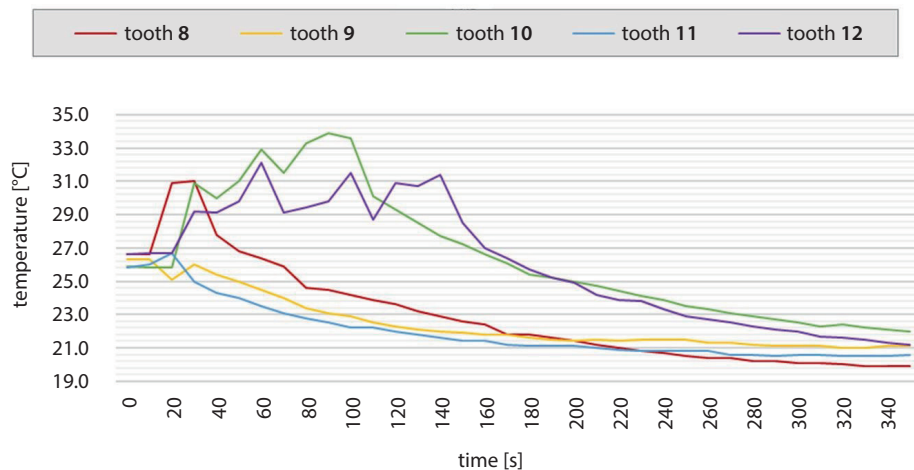


Fig. 5. The temperature on the surface of the tooth during treatment with laser No. 2 measured using thermographic camera – diagram close-up

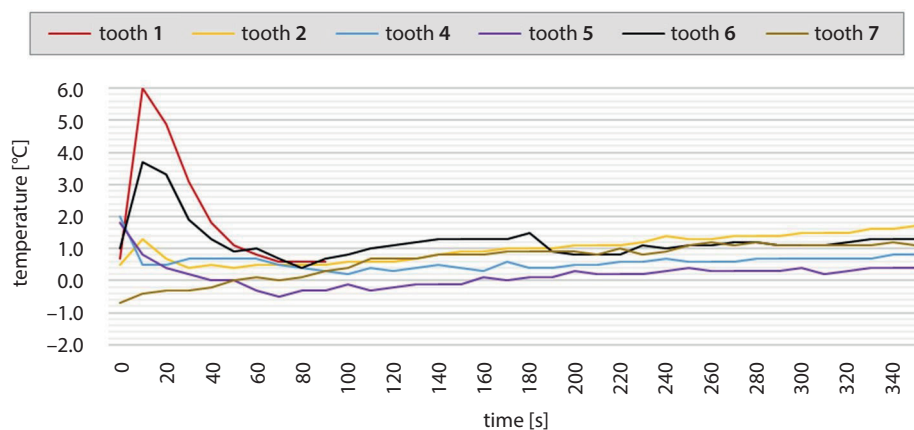


Fig. 6. Temperature differences between the enamel and pulp during exposure to laser No. 1 – diagram close-up

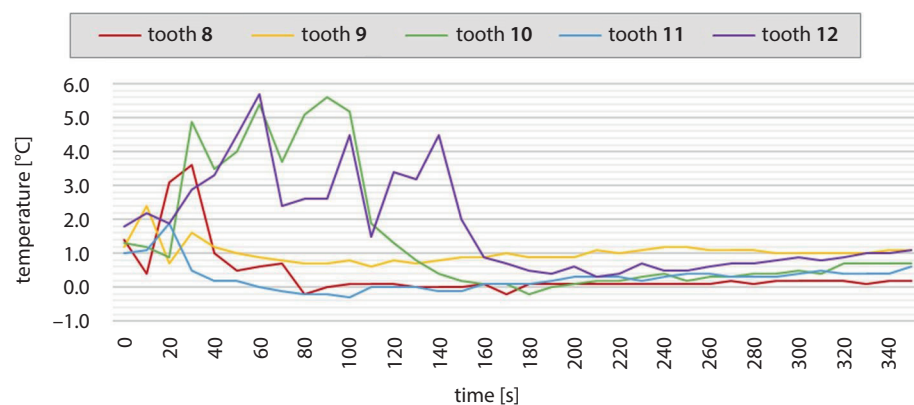


Fig. 7. Temperature differences between the enamel and pulp during exposure to laser No. 2 – diagram close-up

We found that laser debonding has caused lower temperature increase in dental pulp, which is a very good prognostic tool for in vivo study.

Our study described only the experiment for ceramic brackets.

The authors tried to debond 8 metal brackets using Er:YAG (4 brackets) and ER,Cr:YSGG (4 brackets) lasers, but neither debonded at any time (brackets were illuminated from all sides for 10–300 s). In our study, metal brackets were impossible to debond and that was the cause why the temperature was not checked. Only 2 metal brackets were measured to check the temperature.

## Discussion

The application of a laser for debonding orthodontic brackets has been investigated with regard to different wavelengths<sup>13,17</sup> and to different types of brackets, types of adhesive materials and lasing methods.<sup>13,20</sup> Our study contributes to the existing knowledge by testing the use of Er:YAG laser at the indicated parameters. Such laser supports debonding of dental brackets without significant damage to the dental pulp. Hamadah et al. used the 4.2 W laser power for 6 s in order to debond ceramic brackets and observed a temperature increase of 2.91–3.35°C.<sup>10</sup>

Nalbantgil et al., who used the 5 W Er:YAG laser power for 9 s on orthodontic brackets with and without water cooling, obtained similar results.<sup>11</sup> They reported that in the group with water cooling, the pulp temperature increase was lower (about 2.41°C) than in the group without water cooling (about 4.59°C). This has shown that simultaneous cooling the tooth surface with water spray is a necessary prerequisite for safe and effective debonding of orthodontic brackets. Dostálová et al.<sup>12</sup> concluded that there is a temperature increase of 2.0–3.2°C during laser debonding of both metal and ceramic brackets. The Er:YAG laser energy of 280 mJ was applied for 140 s at the frequency of 6 Hz. A temperature increase observed during debonding of metal brackets was lower than during the debonding of ceramic ones. An even lower temperature increase was observed following debonding of ceramic brackets using a new scanning laser method. There is no information in literature about the thermal effect of Er,Cr:YSGG laser used for debonding orthodontic brackets. In the study conducted by Zach and Cohen, the authors demonstrated that there is a pulp temperature increase of 1.8°C during laser bracket debonding.<sup>19</sup> Thus, they proved that laser debonding is safe for vital teeth, as only an increase of 5.5°C or more can cause pulpitis or pulp necrosis in 15% of laser-treated teeth. According to the newest research by Grzech-Leśniak et al., ceramic and metal brackets can be debonded using a laser at specific, predefined settings.<sup>9</sup> In this study, Er:YAG laser irradiation was associated with a slight, statistically nonsignificant increase in temperature during the orthodontic brackets debonding. These outcomes were statistically significantly higher in comparison with the ceramic brackets debonded using the scanning technique ( $p = 0.015$ ). The mean temperature gradient obtained for metal brackets was lower than for ceramic brackets. However, further in vivo studies are warranted to assess the impact of lasers on the rise of the temperature in the tooth and on the surface structure of the teeth as well.

The study contributes to the existing knowledge by testing the use of Er:YAG laser in ceramic and metal brackets debonding. The main finding of the study was that the Er:YAG laser supports debonding of dental brackets without significant damage to the enamel or the dental pulp. Findings regarding the use of the Er:YAG laser at the indicated parameters are important because of efficiency and safety of debonding.

The Er:YAG and Er,Cr:YSGG laser wavelengths both operate in the region of the major absorption peak for water and are the most suited to hard-tissue ablation treatments. The Er:YAG laser wavelength penetrates about 7 µm into the enamel and 5 µm into the dentin. The Er,Cr:YSGG laser wavelength penetrates deeper – 21 µm into the enamel and 15 µm into the dentin. Because of the higher absorption, the Er:YAG laser has a smaller penetration depth, and therefore, requires less time to ablate the tissue.<sup>21</sup>

Protecting the pulp is very important during debonding. Within the limitation of our ex vivo study, the outcomes suggest that it is safe to use lasers from the Er:YAG family during the removal of ceramic brackets. In our study, metal brackets were impossible to remove using lasers.

## Conclusions


The studied Er:YAG family lasers of 2 different wavelengths can be safely used for orthodontic bracket debonding with air and water cooling only.


During the treatment with laser No. 1 with cooling, not only did the temperature inside the tooth fail to increase, but it actually decreased, which appears promising for its potential in vivo use in the oral cavity. A temperature increase (up to about 3°C) followed by a subsequent drop was observed during the first stage of treatment with laser No. 2.


Ceramic brackets detach spontaneously significantly more often than metal brackets when using discussed laser parameters.

## ORCID iDs

Patrycja Downarowicz  <https://orcid.org/0000-0001-5411-4669>

Paweł Noszczyk  <https://orcid.org/0000-0003-2810-5165>

Marcin Mikulewicz  <https://orcid.org/0000-0001-5754-0284>

Rafał Nowak  <https://orcid.org/0000-0001-9375-0369>

## References

1. Grzech-Leśniak K. Making use of lasers in periodontal treatment: A new gold standard? *Photomed Laser Surg.* 2017;35(10):513–514.
2. Mizutani K, Aoki A, Coluzzi D, et al. Lasers in minimally invasive periodontal and peri-implant therapy. *Periodontol 2000.* 2016;71(1):185–216.
3. Grzech-Leśniak K, Sculean A, Gaspirc B. Laser reduction of specific microorganisms in the periodontal pocket using Er:YAG and Nd:YAG lasers: A randomized controlled clinical study. *Lasers Med Sci.* 2018; 33:1461–1470.
4. Grzech-Leśniak K, Matys J, Dominiak M. Comparison of clinical and microbiological effects of antibiotic therapy in periodontal pockets following laser treatment: In vivo study. *Adv Clin Exp Med.* 2018;27(9): 1263–1270.
5. Grzech-Leśniak K, Nowicka J, Pajęczkowska M, et al. Effects of Nd:YAG laser irradiation on the growth of *Candida albicans* and *Streptococcus mutans*: In vitro study. *Lasers Med Sci.* 2019;34(1):129–137.
6. Grzech-Leśniak K, Bericharit S, Dalal N, Mroccka K, Deeb JG. In vitro examination of the use of Er:YAG laser to retrieve lithium disilicate crowns from titanium implant abutments. *J Prosthodont.* 2019;28(6): 672–676. doi:10.1111/jopr.13077
7. Nishimura M, Sannohe M, Nagasaka H, Igarashi K, Sugawara J. Non-extraction treatment with temporary skeletal anchorage devices to correct a class II division 2 malocclusion with excessive gingival display. *Am J Orthod Dentofacial Orthop.* 2014;145(1):85–94.
8. Soltani MK, Barkhori S, Alizadeh Y, Golfeshan F. Comparison of debonding characteristics of the conventional metal and self-ligating brackets to enamel: An in vitro study. *Iran J Orthod.* 2014;9(3):e4842. doi:10.17795/ijo-3739
9. Grzech-Leśniak K, Matys J, Żmuda-Stachowiak D, et al. Er:YAG laser for metal and ceramic bracket debonding: An in vitro study on intrapulpal temperature. SEM and EDS analysis. *Photomed Laser Surg.* 2018; 36(11):595–600.
10. Hamadah O, Bachir W, Zamzam MK. Thermal effect of Er:YAG laser pulse durations on teeth during ceramic bracket debonding. *Dent Med Probl.* 2016;53(3):352–357.

11. Nalbantgil D, Tozlu M, Oztoprak MO. Pulpal thermal changes following Er:YAG laser debonding of ceramic brackets. *Sci World J.* 2014; 2014:912429. doi:10.1155/2014/912429
12. Dostálová T, Jelínková H, Remes M, Šulc J, Nemeč M. The use of the Er:YAG laser for bracket debonding and its effect on enamel damage. *Photomed Laser Surg.* 2016;34(9):394–399.
13. Dostálová T, Jelínková H, Šulc J, et al. Laser brackets debonding: Tm:YAP, Nd:YAG, and GaAs diode lasers evaluation. *Lasers in Dentistry.* 2009;XV 7162:71620C–71620C-6. doi:10.1117/12.808137
14. Sohrabi A, Jafari S, Kimyai S, Rikhtehgaran S. Er,Cr:YSGG laser as a novel method for rebonding failed ceramic brackets. *Photomed Laser Surg.* 2016;34(10):483–486.
15. Mirhashemi AH, Chiniforush N, Sharifi N, Hosseini AM. Comparative efficacy of Er,Cr:YSGG and Er:YAG lasers for etching of composite for orthodontic bracket bonding. *Lasers Med Sci.* 2018;33(4):835–841.
16. Sabuncuoğlu FA, Ersahan S, Ertürk E. Debonding of ceramic brackets by Er:YAG laser. *J Istanbul Univ Fac Dent.* 2016;50(2):24–30.
17. Eriksson AR, Albrektsson T. Temperature threshold levels for heat-induced bone tissue injury: A vital microscopic study in the rabbit. *J Prosthet Dent.* 1983;50(1):101–107.
18. Stein S, Kleye A, Schauseil M, Hellak A, Korbmacher-Steiner H, Braun A. 445-nm diode laser-assisted debonding of self-ligating ceramic brackets. *Biomed Tech (Berl).* 2017;62(5):513–520. doi:10.1515/bmt-2016-0027
19. Zach L, Cohen G. Pulp response to externally applied heat. *Oral Surg Oral Med Oral Pathol.* 1965;19:515–530.
20. Ozcan M, Finnema K, Ybema A. Evaluation of failure characteristics and bond strength after ceramic and polycarbonate bracket debonding: Effect of bracket base silanization. *Eur J Orthod.* 2008;30(2):176–182.
21. Diaci J, Gaspirc B. Comparison of Er:YAG and Er,Cr:YSGG lasers used in dentistry. *Journal of the Laser and Health Academy.* 2012;1:1–13.



# Upregulated sulfatase and downregulated MMP-3 in thoracic aortic aneurysm

Małgorzata Matusiewicz<sup>1,A–F</sup>, Maciej Rachwałik<sup>2,A–C,E,F</sup>, Małgorzata Krzystek-Korpacka<sup>1,B,C,E,F</sup>, Grzegorz Bielicki<sup>2,B,F</sup>, Izabela Berdowska<sup>1,C,E,F</sup>, Rafał Nowicki<sup>2,B,F</sup>, Andrzej Gamian<sup>1,3,A,E,F</sup>, Marek Jasiński<sup>2,C,E,F</sup>

<sup>1</sup> Department of Medical Biochemistry, Wrocław Medical University, Poland

<sup>2</sup> Department and Clinic of Cardiac Surgery, Wrocław Medical University, Poland

<sup>3</sup> Institute of Immunology and Experimental Therapy, Polish Academy of Sciences, Wrocław, Poland

A – research concept and design; B – collection and/or assembly of data; C – data analysis and interpretation; D – writing the article; E – critical revision of the article; F – final approval of the article

Advances in Clinical and Experimental Medicine, ISSN 1899–5276 (print), ISSN 2451–2680 (online)

*Adv Clin Exp Med.* 2020;29(5):565–572

## Address for correspondence

Małgorzata Matusiewicz

E-mail: malgorzata.matusiewicz@umed.wroc.pl

## Funding sources

Research grant from Wrocław Medical University, Poland (No. 1738).

## Conflict of interest

None declared

Received on November 12, 2019

Reviewed on March 1, 2020

Accepted on March 21, 2020

Published online on May 18, 2020

## Cite as

Matusiewicz M, Rachwałik M, Krzystek-Korpacka M, et al. Upregulated sulfatase and downregulated MMP-3 in thoracic aortic aneurysm. *Adv Clin Exp Med.* 2020;29(5):565–572. doi:10.17219/acem/119383

## DOI

10.17219/acem/119383

## Copyright

© 2020 by Wrocław Medical University

This is an article distributed under the terms of the Creative Commons Attribution 3.0 Unported (CC BY 3.0) (<https://creativecommons.org/licenses/by/3.0/>)

## Abstract

**Background.** Thoracic aortic aneurysm (TAA) formation is accompanied by degradation of extracellular matrix components (EMC). Numerous matrix metalloproteinases (MMPs) have been implicated in the process, but the involvement of MMP-3 remains unclear. Additionally, the changes in proteoglycan (PG) structure can alter the signal transduction pathways in TAA, though the enzymatic systems which originate them are not fully understood.

**Objectives.** To measure MMP-3 and sulfatase levels in aneurysmal tissue, comparing them with non-aneurysmal vessels, and to investigate possible correlations with patients' serum levels in order to evaluate their potential usefulness in aiding aneurysm detection and monitoring.

**Material and methods.** The study included 74 patients (TAA: n = 42; control group: n = 32). Sulfatase activity was measured colorimetrically and MMP-3 levels were measured immunoenzymatically.

**Results.** Sulfatase activities were higher ( $p = 0.03$ ) and MMP-3 concentrations lower ( $p = 0.014$ ) in aneurysmal tissue than in normal aortic tissue. Medium-sized dilatations were associated with lower tissue MMP-3 concentrations than small dilatations ( $p = 0.033$ ). No differences in sulfatase activity or MMP-3 concentration in the serum of TAA patients were observed in comparison with the controls. The serum and tissue levels of MMP-3 were correlated ( $r = 0.41$ ;  $p < 0.001$ ). The serum levels of MMP-3 were significantly lower in the female patients than in the male patients ( $p = 0.006$ ).

**Conclusions.** Our studies confirmed the lower MMP-3 levels in aneurysmal tissue, but the lack of a statistically confirmed reduction of MMP-3 in the blood serum seems to preclude its usefulness for diagnostic purposes. Our study points to the differences in MMP-3 behavior between TAA and abdominal aortic aneurysms. Significantly higher sulfatase activity in TAA tissue suggests a possible impact of sulfatase on signal transduction pathways involved in aneurysm formation.

**Key words:** metalloproteinases, ascending aortic aneurysm, matrix metalloproteinase-3, sulfatases, thoracic aortic aneurysm

## Introduction

Aortic aneurysms are localized dilatations of aorta exceeding 1.5 times its normal diameter, representing a loss of structural integrity of the vessels caused by changes in the composition of the extracellular matrix.<sup>1–3</sup> Tunica media, a middle layer of the aortic artery, contains elastin, collagen and smooth muscle cells (SMCs), as well as proteoglycans (PG) and glycoproteins; it is responsible for the mechanical properties of the aorta.<sup>1</sup> When thinning of the arterial wall occurs, the pressure of the flowing blood causes dilatations of the artery, ultimately leading to a rupture.<sup>2</sup> The thinning of the arterial wall is caused by degradation of the components of the extracellular matrix (ECM), mainly elastin, the degradation of which has been observed even in the early stages of aneurysm formation.<sup>3</sup> The degradation of ECM components is primarily conducted by matrix metalloproteinases (MMPs).

Matrix metalloproteinases are a group of zinc-containing endopeptidases which exhibit similarities in structure and an ability to degrade the components of ECM, such as collagen and elastin.<sup>4</sup> Numerous studies have been conducted to establish the role of MMPs in aneurysm formation.<sup>1,2</sup> Upregulation of MMP-2 and MMP-9 has been confirmed by studies in animal models of aneurysm, in cell cultures and in humans.<sup>5–12</sup> However, the data concerning MMP-3 is contradictory, and the role of this MMP in aneurysm formation remains unclear.

The MMP activity is under multilevel regulation involving, among other things, the presence of various growth factors. The availability of these growth factors depends on the composition of other elements of the ECM; i.e., PGs – and more precisely, on the state of their sulfation. By processing PG, sulfatases can enhance the level of certain growth factors, which in turn, through signal transduction, can enhance or inhibit the synthesis and activity of other enzymes, including MMPs. However, so far only limited studies have focused on this enzyme in connection to aneurysm formation.<sup>13</sup>

The prevalence of thoracic aortic aneurysm (TAA) in humans is increasing and is estimated to be around 4%; however, the mortality rate due to ruptured aortas is around 80–95%.<sup>14,15</sup> In cases of elective surgery, the mortality rate decreases to 5–7%.<sup>15</sup> Thus, there is a need for screening procedures which would allow for early, non-invasive detection of the disease. A better understanding of the molecular background of TAA could aid in finding possible candidates for indicators of the disease. However, despite the breadth of research on TAA, not many studies to date have been undertaken to directly correlate tissue levels of enzymes with their systemic levels, which might be crucial in establishing such biomarkers.

Therefore, the goals of our study were to determine the levels of MMP-3 and sulfatase in aneurysmal tissue, comparing them with non-aneurysmal vessels, and to correlate these values to those measured in the serum of the same patients in order to evaluate their possible

usefulness in aiding aneurysm detection and monitoring. We found that the concentrations of MMP-3 were down-regulated in aneurysmal tissue, especially in medium-sized aneurysms, while the tissue activity of sulfatase was up-regulated. Downregulation of MMP-3 might be a characteristic biochemical trait of TAA, distinguishing it from abdominal aneurysms in which MMP-3 upregulation has been observed. The differences in the serum levels of the 2 enzymes were not statistically significant, which seems to preclude their measurements for diagnostic purposes.

The study protocol was approved by the Medical Ethics Committee of Wrocław Medical University, Poland, and written informed consent was obtained from the patients.

## Material and methods

### Study population

A group of 42 patients admitted for surgery due to TAA was enrolled into the study. Patients with stenosis or vulvar insufficiency ( $n = 32$ ) served as a control group. There were 13 women and 29 men in the TAA group, and 10 women and 22 men in the control group ( $p = 0.821$ ). The mean age in the TAA group was 62 years (95% confidence intervals (95% CI) = 58–66) and 58 years (54–62) in the control group ( $p = 0.167$ ).

No patient in aneurysm group had a bicuspid aortic valve. The exclusion criteria also included the use of steroids or non-steroidal anti-inflammatory medication, or presence of malignancies of any type. Some of the patients were treated with angiotensin converting enzyme inhibitors (ACEIs) ( $n = 4$ ),  $\beta$ -adrenolytics ( $n = 11$ ) or both ( $n = 10$ ).

For analytical purposes, the patients were divided into subgroups according to aorta diameter: small ( $\leq 3.9$  cm), medium-sized (4.0–5.9 cm) and large ( $\geq 6.0$  cm).

### Material

Aneurysmal fragments were collected during open-heart surgery and immediately frozen in liquid nitrogen and stored at  $-80^{\circ}\text{C}$  for further analysis. These aorta samples are usually dissected as a routine part of the operation and are discarded. Fragments from patients with normal-sized aortas were dissected into small strips (5–7 mm  $\times$  2 cm). These harvestings did not interfere with the surgical closure of the aortotomy. Intraoperative photos of normal and ruptured aortas are presented in Fig. 1.

The tissue fragments were homogenized in 5 mM of Tris-HCl buffer (pH 7.0) using a FastPrep-24 homogenizer (MP Biomedicals, Solon, USA). Samples were subsequently centrifuged at  $14,000 \times g$  for 15 min and the supernatants were used for analysis. Blood samples were drawn with venous puncture in a fasting state. The serum samples were taken from clotted (30 min, room temperature) and centrifuged (15 min,  $1,500 \times g$ ) blood. The samples were then stored at  $-80^{\circ}\text{C}$  until analysis.



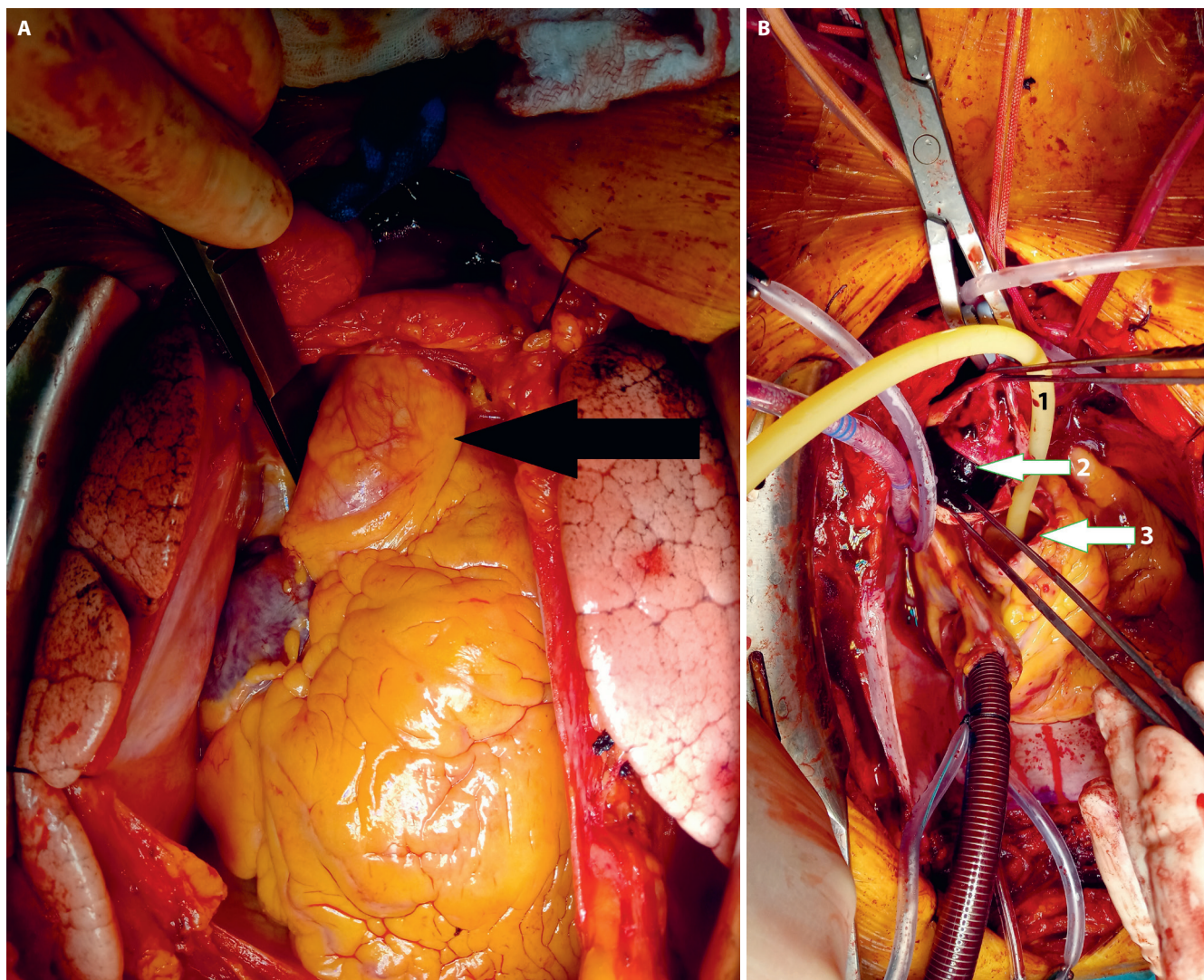


**Fig. 1.** A – normal-sized ascending aorta (black arrow), slightly elevated using surgical forceps; B – aortic dissection – intraoperative photo during the repair with cardiopulmonary bypass. Arrows indicate: 1 – false lumen of ruptured aortic aneurysm; 2 – true lumen of ruptured aortic aneurysm; 3 – foley catheter in true lumen of aortic aneurysm

## Analytical methods

### MMP-3

The MMP-3 concentrations were estimated using an enzyme double-antibody indirect immunoassay with Quantikine Human Total MMP-3 Immunoassay (R&D Systems, Minneapolis, USA) in accordance with the manufacturer's protocol. The MMP-3 concentration in the serum samples is expressed as ng/mL and in the homogenates as ng/g of protein.

### Sulfatase

Sulfatase activity was determined according to Singh et al.,<sup>16</sup> as all sulfatases in question display arylsulfatase activity.<sup>17</sup> Briefly, equal aliquots of serum and substrate solution (20 mM of p-nitrocatechol sulfate (Sigma-Aldrich, St. Louis,

USA)) were incubated for 4 h at 37°C and the reaction was stopped with 2.5 M of NaOH. The serum and control samples were run in duplicate. Sulfatase activity unit (U) was calculated as nmol of p-nitrocatechol liberated per 1 min with 1 L of serum (or 1 g of protein in case of homogenates).

### Protein concentration

The protein concentration of the tissue homogenates was estimated using the Bradford method (Pierce Coomassie Protein Assay Kit; Thermo Fisher Scientific, Rockford, USA).<sup>18</sup>

### Statistical analysis

Data distribution was tested using Kolmogorov–Smirnov test and the homogeneity of variances was tested using Levene's test. The data is presented as means with

95% confidence intervals (95% CI) and analyzed using the t-test for independent samples, with Welch correction for unequal variances if necessary or one-way analysis of variance (ANOVA) with Student–Neuman–Keuls's post hoc test. Correlation analysis was conducted using Pearson ( $r$ ) and Spearman ( $\rho$ ) correlation tests. Frequency analysis was conducted using  $\chi^2$  statistics. All calculated probabilities were two-tailed, and  $p$ -values  $\leq 0.05$  were considered statistically significant. The analyses were performed using MedCalc® v. 12.1.1.0 statistical software (MedCalc Software, Mariakerke, Belgium).

## Results

Sulfatase activity was significantly higher in the aneurysmal tissue than in the normal aortas (Fig. 2), with no difference between emergency and elective surgery ( $p = 0.423$ ). Enzyme activity tended to be higher in the medium-sized aneurysms than in the small and large aneurysms (Table 1). Tissue activity did not correlate with gender ( $p = 0.736$ ).

In the case of serum sulfatase activity, the differences between the TAA patients and the controls were not statistically significant (89.9 nmol/L (95% CI = 76–103) vs 79.9 nmol/L (95% CI = 69–91), respectively;  $p = 0.240$ ). Sulfatase activity in the serum tended to be higher among

women than men (97.8 nmol/L (95% CI = 80–115) vs 80 nmol/L (95% CI = 70–90);  $p = 0.06$ ). There was no correlation between the enzyme tissue and serum activity ( $r = 0.11$ ;  $p = 0.368$ ).

The concentrations of MMP-3 were significantly lower in aneurysmal tissue than in tissue from normal aortas (Fig. 3), but did not differ with respect to urgency of surgery ( $p = 0.436$ ). Medium-sized aneurysms had lower concentrations of the enzyme than small aneurysms (Table 1). The differences in enzyme level in the serum between TAA patients and controls did not reach statistical significance (6.6 ng/mL (95% CI = 5.4–7.8) vs 7.33 ng/mL (95% CI = 6.3–8.4);  $p = 0.381$ ). The MMP-3 serum levels were significantly lower in women than in men (5.28 ng/mL (95% CI = 3.9–6.7) vs 7.65 ng/mL (95% CI = 6.7–8.6);  $p = 0.006$ ), while the tissue level of the enzyme did not correlate with gender ( $p = 0.627$ ). The serum and tissue levels of the enzyme were correlated ( $r = 0.41$ ;  $p < 0.001$ ; Fig. 4).

Serum MMP-3 and sulfatase levels tended to negatively correlate, particularly in the male subjects ( $r = -0.33$ ;  $p = 0.026$ ) or the control subjects ( $r = -0.41$ ;  $p = 0.025$ ). Tissue enzyme levels did not show any correlation.

Since some of our patients received treatment, we evaluated the effect of ACEIs and  $\beta$ -adrenalytics on the enzymes in question. Neither of the drugs had any influence on the levels of sulfatase or MMP-3 in the tissue. In the case

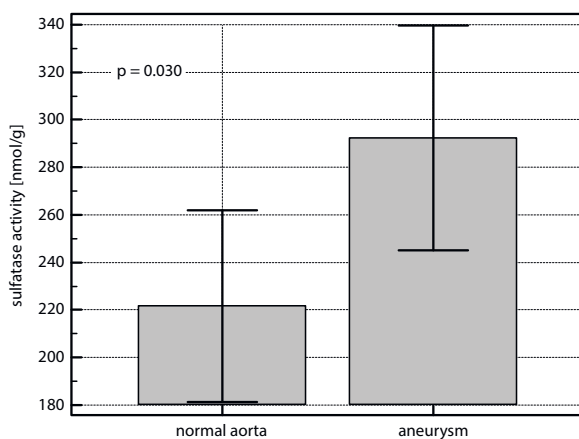


Fig. 2. Sulfatase activity in aneurysmal tissue ( $n = 42$ ) and normal aorta ( $n = 32$ ). Data is expressed as mean values with standard deviations (SD)

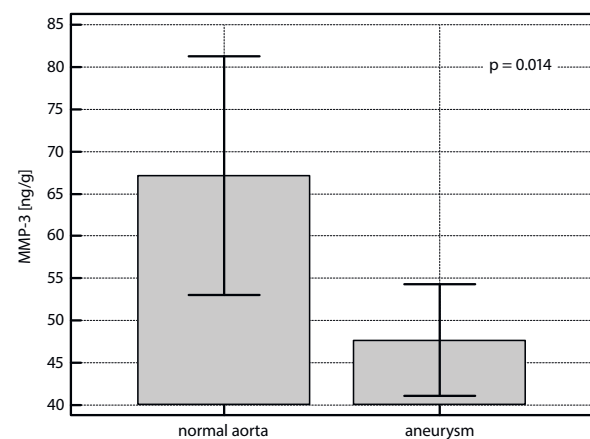


Fig. 3. MMP-3 concentration in aneurysmal tissue ( $n = 42$ ) and normal aorta ( $n = 32$ ). Data is expressed as mean values with standard deviations (SD)

Table 1. Sulfatase activity and MMP-3 concentration in relation to aorta diameter

Source	Enzyme	Aorta diameter			p-value
		$\leq 3.9$ mm ( $n = 32$ )	4.0–5.9 mm ( $n = 38$ )	$\geq 6.0$ mm ( $n = 4$ )	
Tissue	sulfatase [U]	222 (181–262)	294 (239–349)	216 (130–302)	0.086
	MMP-3 [ng/g]	63.13 (55.03–81.24)	47.29 (39.61–54.96) <sup>a</sup>	51.5 (25.37–77.63)	0.033*
Serum	sulfatase [U]	79.9 (69.3–90.5)	87.7 (74.1–101.3)	115.7 (0–260)	0.232
	MMP-3 [ng/mL]	7.33 (6.27–8.38)	6.69 (5.39–8.00)	5.53 (0–12.66)	0.581

Data is presented as means with 95% confidence intervals (95% CI) and was analyzed with one-way analysis of variance (ANOVA). \*  $p$ -values  $\leq 0.05$  were considered statistically significant; <sup>a</sup>statistically different from normal-sized aorta ( $\leq 3.9$  mm); MMP-3 – matrix metalloproteinase-3.

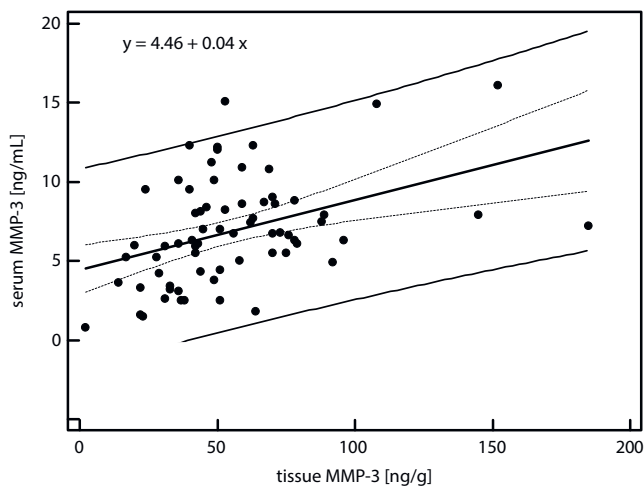


Fig. 4. The association between serum and tissue levels of matrix metalloproteinase-3 (MMP-3). Dashed regression line – 95% confidence interval (95% CI); solid regression line – 95% prediction interval

of serum, neither ACEIs nor  $\beta$ -adrenalytics had an influence on MMP-3 levels. However, serum sulfatase activity was significantly higher among patients who were treated with ACEIs than among the untreated group ( $p = 0.015$ ). When only patients without treatment were taken into consideration, there were no differences in serum sulfatase activity between the TAA and control groups ( $p = 0.878$ ).

## Discussion

The role of MMPs in the formation of aneurysms has been well documented. Conclusions have been drawn on the possible application of the findings of these studies in therapy and monitoring. However, it is impossible to directly measure the changes from the expression or activity of these enzymes in the affected tissue of a patient. Most of the studies on applying measurements of MMPs in the serum assume that tissue levels would be reflected on the systemic level, but there have been no studies to confirm this correlation so far. Therefore, our study was designed to measure the concentrations of one MMP – MMP-3 – in tissue fragments from aneurysmal and non-aneurysmal thoracic aortas and to correlate them with the serum levels of the same patients. To the best of our knowledge, our study is the first to demonstrate a direct correlation between tissue and serum levels of MMP-3. However, we also noted that despite the fact that MMP-3 was significantly lower in aneurysmal tissue, the differences in serum levels of the enzyme were not statistically significant.

The MMP-3, a stromelysin, is an enzyme whose role in aneurysm formation remains unclear. Apart from its direct role in the degradation of ECM elements, it also participates in the activation of other MMPs.<sup>4</sup> Little is known about signal transduction pathways which might lie at the onset and development of aneurysm formation,

but MMP-3 has been shown to cleave matrix components to release or activate various growth factors such as fibroblast growth factor (FGF), transforming growth factor- $\beta$  (TGF- $\beta$ ), heparin-binding epidermal growth factor (HB-EGF), or interleukin (IL)-1 $\beta$ .<sup>19–21</sup> Johnson et al. have recently demonstrated in their studies on MMP-3-knockout mice that MMP-3 is responsible for vascular SMC migration through MMP-9 activation and neointima formation.<sup>6</sup> Earlier studies also implicated this MMP in the cleavage of E-cadherin, and thus in the promotion of cellular aggregation.<sup>22</sup>

Unlike MMP-2 and MMP-9, the upregulation of which has been almost unanimously demonstrated in numerous studies,<sup>5–12</sup> the results coming from studies on MMP-3 are conflicting. Our study demonstrated decreased concentrations of MMP-3 in tissue homogenates from TAA, which is in agreement with a study by Ikonomidis et al.<sup>11</sup> Using immunoblotting and zymography, they noted lower levels of MMP-3 in tissue homogenates from patients with TAA. At the same time, they did not observe the same phenomenon in tissues from patients with Marfan syndrome – an inherited autosomal disorder characterized by a higher susceptibility to aneurysm formation. In their subsequent studies, the researchers also confirmed the lower MMP-3 concentrations in aneurysmal tissues, but only in the case of medium-sized TAAs (4.0–5.9 cm).<sup>23</sup> These results have been further supported by the *in vitro* studies on primary murine fibroblasts from normal and induced TAA.<sup>24</sup> The authors found not only different gene expressions in these 2 types of cells, but also phenotypic changes of fibroblasts during transformation from normal to aneurysmal tissue. However, these results are contradictory to data from a study on MMP-3-knockout mice, which exhibited reduced ascending and abdominal aortic aneurysm formation.<sup>25</sup> Similarly, the only study so far to assess the serum concentration of MMP-3, conducted by Karapanagiotidis et al., has reported increased concentrations of this MMP in TAA in comparison to healthy subjects.<sup>26</sup> Our research did not confirm their results – we observed a tendency towards lower MMP-3 serum concentrations in TAA patients. However, both studies indicated lower MMP-3 concentrations in women than in men. This fact may have influenced the results to a certain degree because Karapanagiotidis et al. included only 18 TAA patients – 14 of which were men – and their control group consisted of 12 women and only 3 men, while in our study the proportions of men and women in the study groups were more balanced. In the literature, abdominal aortic aneurysms demonstrate more uniform upregulation of MMP-3,<sup>27,28</sup> with the exception of a study by Patel et al., where MMP-3 was not detected in the SMCs from aneurysmal vessels.<sup>7</sup> It is possible that the profiles of MMP-3 concentration during the formation of ascending and abdominal aortic aneurysms differ, since the molecular composition varies between ascending, descending and abdominal aortas – as it has already been established – and the mechanisms

underlying aneurysm formation in these arteries can therefore involve different pathways<sup>1</sup>; this may explain the seemingly contradictory results in the studies on aneurysm. As has been recently reported, there are even differences in the patterns of MMP expression between TAA with and without a bicuspid valve.<sup>12</sup> Our study group was uniform in this respect, since none of the patients had a bicuspid aortic valve.

The SMCs seem to play a central role in the degenerative processes of blood vessels. They change their phenotype depending on the surrounding environment, and these changes influence their synthetic and migratory properties.<sup>2,24</sup> Aneurysmal tissue is characterized by fewer SMCs in the tunica media.<sup>3,29,30</sup> Therefore, it can be hypothesized that even if SMC expression of MMP-3 stays at the same level, a smaller number of these cells in aneurysmal tissue would result in an overall decrease in the protein level of the enzyme. The reduction of MMP-3 activity might be explained by inhibition from the overexpressed tissue inhibitors of metalloproteinases (TIMP). However, in our studies we measured the protein level of MMP-3, not its activity; therefore, the reduction cannot be explained by increased inhibition from TIMPs, especially since the method we used in the study measures both free MMP-3 and MMP-3/TIMP complexes.

Another possible explanation for the discrepancies in the reported MMP-3 levels might be the stage of aneurysm formation. It has been demonstrated that medium-sized aneurysms (4.0–5.9 cm) exhibited lower levels of MMP-3, while small ( $\leq 3.9$  cm) and large ( $\geq 6$  cm) aneurysms did not differ from non-aneurysmal tissues in respect to the concentration of this enzyme.<sup>23</sup> Our results partially corroborate these data – medium-sized aneurysms exhibited lower MMP-3 concentrations than small aneurysms. There was no statistical difference in MMP-3 concentration between large aneurysms and small or medium-sized aneurysms, which might be due to the small sample of large aneurysms in our study group. Further research monitoring the changes in aneurysm size, measured by ultrasound studies and MMP-3 concentration, might shed light on this problem. The positive correlation between tissue and serum levels which was established in this study indicates that measurements of serum MMP-3 concentration would reflect the changes of this MMP at the tissue level, but the lack of statistically confirmed differences between normal and TAA serum levels of this enzyme seems to imply that it is not suitable as a marker for diagnostic purposes. Nonetheless, this should be confirmed in larger-scale studies. Still, the downregulation of MMP-3 demonstrated by our and other studies seems to emerge as a characteristic molecular trait that distinguishes TAA from abdominal aortic aneurysm, in which upregulation of MMP-3 seems to be uniformly observed.









Collagen and elastin are responsible for the strength and elasticity of blood vessels, while the 3<sup>rd</sup> element of ECM – PGs – maintain the integrity of the arterial

wall, allow it to properly resist compressive forces, and serve as an anchor for a number of growth factors and regulators.<sup>31,32</sup> The PGs are composed of a core protein to which glycosaminoglycan (GAG) chains are attached. Changes in the composition of GAGs have been observed in the degenerative processes of the cardiovascular system, including aneurysm. Theocharis et al.<sup>33</sup> observed lower levels of heparan sulfate and chondroitin sulfate in abdominal aortic aneurysms in comparison to normal aortas. Their later studies indicated that aneurysmal tissue contains a reduced ratio of 6-sulfate to 4-sulfate disaccharides.<sup>34</sup> Moreover, while no changes in dermatan sulfate content have been noted, a decrease of oversulfated disaccharides – which are mainly present in this GAG – has been observed in aneurysmal tissue. The changes in composition and sulfation of PGs within the ECM has the potential to highly impact the structure and functioning of blood vessels. It has been documented that modulation of the fine structure of GAGs, including their sulfation, can influence signaling pathways.<sup>35,36</sup> Three groups of enzymes have been implicated in the remodeling of heparan sulfate PGs. Cell surface PGs can be cleaved by MMPs, their heparan sulfate chains can be further cut by heparanase, and endosulfatases can remove 6-O sulfate groups from trisulfated disaccharides.<sup>36</sup> The endosulfatases in question are a group of recently discovered extracellular enzymes which are able to remove sulfate groups from sulfate esters in ECM components. Since aneurysm formation is accompanied by a reduction in 6-sulfate GAGs, elevated levels of the enzymes responsible for sulfate group removal should be expected. We evaluated the activity of sulfatase and found that it was indeed significantly higher in the aneurysmal tissue as compared to normal tissue. To date, there has been only 1 other study indicating elevated sulfatase activity, though not in TAA but in abdominal aortic aneurysm.<sup>13</sup> The elevation of sulfatase in aneurysmal tissue, reducing the sulfation of PGs, may cause impaired binding of growth factors stored by the ECM and may initiate signaling pathways other than those active in normal aortas. It has been demonstrated that heparan sulfate PGs mediate the binding between latent TGF- $\beta$ -binding proteins (LTBP) and fibronectin.<sup>37</sup> It is now believed that dysregulated TGF- $\beta$  signaling lies at the bottom of aneurysm formation.<sup>38</sup> Alterations of TGF- $\beta$  signaling pathways have been demonstrated in a murine model for TAA.<sup>39</sup> It has been further suggested that the altered TGF- $\beta$  signaling might stimulate TAA development by the induction of myofibroblast differentiation from the fibroblasts which are replacing SMCs undergoing apoptosis, and might thus contribute to the changes in ECM composition.<sup>3</sup> The emergence of myofibroblasts has coincided with PG degradation.<sup>3</sup> It can therefore be hypothesized that the decreased sulfation of PGs can lead, via disrupted binding of LTBP to the ECM elements, to the excessive production of active TGF- $\beta$ , which in turn enters an alternative signaling pathway. However, it must also be noted that at this point

it is unclear whether the differentiation of myofibroblasts is a factor which contributes to aneurysm progression or as a repair process,<sup>3</sup> especially since it has also been suggested that the enhanced production of TGF- $\beta$  may play a protective role against aneurysm formation.<sup>40</sup> Cheung et al. also proposed that alterations in the TGF- $\beta$  signaling pathway and activation of MMPs may be an option in the management of congenitally related aortopathy.<sup>10</sup>

Our studies demonstrated that sulfatase activity in the tissue was not reflected in serum levels. Moreover, we noted that administration of ACEIs might influence serum levels of this enzyme. These 2 factors seem to preclude the application of systemic sulfatase in diagnostic procedures. However, the observed differences in sulfatase activity between normal and aneurysmal aortas indicate the need for further studies, which might shed further light on the molecular basis of aneurysm formation.

### ORCID iDs

Małgorzata Matusiewicz  <https://orcid.org/0000-0003-4624-0109>  
 Maciej Rachwalik  <https://orcid.org/0000-0001-9714-4059>  
 Małgorzata Krzystek-Korpacka  <https://orcid.org/0000-0002-2753-8092>  
 Grzegorz Bielicki  <https://orcid.org/0000-0003-0888-4229>  
 Izabela Berdowska  <https://orcid.org/0000-0002-0275-4522>  
 Rafał Nowicki  <https://orcid.org/0000-0002-3256-552X>  
 Andrzej Gamian  <https://orcid.org/0000-0002-2206-6591>  
 Marek Jasiński  <https://orcid.org/0000-0002-9989-7748>

### References

- Barbour JR, Spinale FG, Ikonomidis JS. Proteinase systems and thoracic aneurysm progression. *J Surg Res*. 2007;139(2):292–307.
- Curci JA. Digging in the “soil” of the aorta to understand the growth of abdominal aortic aneurysms. *Vascular*. 2009;17(Suppl 1):S21–S21.
- Jones JA, Beck C, Barbour JR, et al. Alterations in aortic cellular constituents during thoracic aortic aneurysm development: Myofibroblast-mediated vascular remodeling. *Am J Pathol*. 2009;175(4):1746–1756.
- Visse R, Nagase H. Matrix metalloproteinases and tissue inhibitors of metalloproteinases: Structure, function and biochemistry. *Circ Res*. 2003;92(8):827–839.
- Johnson C, Galis ZS. Matrix metalloproteinase-2 and -9 differentially regulate smooth muscle cell migration and cell-mediated collagen organization. *Arterioscler Thromb Vasc Biol*. 2004;24:54–60.
- Johnson JL, Dwivedi A, Somerville M, et al. Matrix metalloproteinase (MMP)-3 activates MMP-9 mediated vascular smooth muscle cell migration and neointima formation in mice. *Arterioscler Thromb Vasc Biol*. 2011;31(9):e35–e44.
- Patel MI, Melrose JJ, Ghosh P, Appleberg M. Increased synthesis of matrix metalloproteinases by aortic smooth muscle cells is implicated in the etiopathogenesis of abdominal aortic aneurysms. *J Vasc Surg*. 1996;24(1):82–92.
- Lesauskaite V, Tanganelli P, Sassi C, et al. Smooth muscle cells of the media in the dilatative pathology of ascending thoracic aorta: Morphology, immunoreactivity for osteopontin, matrix metalloproteinases, and their inhibitors. *Hum Pathol*. 2001;32(9):1003–1011.
- Sinha I, Bethi S, Cronin P, et al. A biologic basis for asymmetric growth in descending thoracic aortic aneurysms: A role for matrix metalloproteinase 9 and 2. *J Vasc Surg*. 2006;43(2):342–348.
- Cheung YF, Chow PC, So EK, Chan KW. Circulating transforming growth factor- $\beta$  and aortic dilation in patients with repaired congenital heart disease. *Sci Rep*. 2019;9(1):162. doi:10.1038/s41598-018-36458-1
- Ikonomidis JS, Jones JA, Barbour JR, et al. Expression of matrix metalloproteinases and endogenous inhibitors within ascending aortic aneurysms of patients with Marfan syndrome. *Circulation*. 2006;114(Suppl 1):I-365-I-370.
- Rabkin SW. Differential expression of MMP-2, MMP-9 and TIMP proteins in thoracic aortic aneurysm: Comparison with and without bicuspid aortic valve. A meta-analysis. *Vasa*. 2014;43(6):433–442.
- Kowalewski R, Sobolewski K, Małkowski A, Wolańska M, Gacko M. Evaluation of enzymes involved in proteoglycans degradation in the wall of abdominal aortic aneurysms. *J Vasc Res*. 2006;43(1):95–100.
- Lindholt JS, Juul S, Fasting H, Henneberg EW. Screening for abdominal aortic aneurysms: Single-centre randomized controlled trial. *BMJ*. 2005;330(7494):750. doi:10.1136/bmj.38369.620162.82
- Lindholt JS. Abdominal aortic aneurysms. *Dan Med Bull*. 2010;57:B4219.
- Singh J, Tavella D, Di Ferrante N. Measurements of arylsulfatases A and B in human serum. *J Pediatrics*. 1975;86(4):574–576.
- Morimoto-Tomita M, Uchimura K, Werb Z, et al. Cloning and characterization of two extracellular heparin-degrading endosulfatases in mice and humans. *J Biol Chem*. 2002;277(51):49175–49185.
- Bradford MM. A rapid and sensitive method for the quantitation of microgram quantities of protein utilizing the principle of protein-dye binding. *Anal Biochem*. 1976;72:248–254.
- Whitelock JM, Murdoch AD, Iozzo RV, Underwood PA. The degradation of human endothelial cell-derived perlecan and release of bound basic fibroblast growth factor by stromelysin, collagenase, plasmin, and heparanases. *J Biol Chem*. 1996;271(17):10079–10086.
- Imai K, Hiramatsu A, Fukushima D, Pierschbacher MD, Okada Y. Degradation of decorin by matrix metalloproteinases: Identification of the cleavage sites, kinetic analyses and transforming growth factor-beta 1 release. *Biochem J*. 1997;322(Pt 3):809–814.
- Suzuki M, Raab G, Moses MA, Fernandez CA, Klagsbrun M. Matrix metalloproteinase-3 releases active heparin-binding EGF-binding growth factor by cleavage at a specific juxtamembrane site. *J Biol Chem*. 1997;272(50):31730–31737.
- Noe V, Fingleton B, Jacobs K, et al. Release of an invasion promoter E-cadherin fragment by matrilysin and stromelysin-1. *J Cell Sci*. 2001;114(Pt 1):111–118.
- Ikonomidis JS, Jones JA, Barbour JR, et al. Expression of matrix metalloproteinases and endogenous inhibitors within ascending aortic aneurysms of patients with bicuspid and tricuspid aortic valves. *J Thorac Cardiovasc Surg*. 2007;133(4):1028–1036.
- Jones JA, Zavadzkas JA, Chang EI, et al. Cellular phenotype transformation occurs during thoracic aortic aneurysm development. *J Thorac Cardiovasc Surg*. 2010;140(3):653–659.
- Silence J, Lupu F, Collen D, Lijnen HR. Persistence of atherosclerotic plaque but reduced aneurysm formation in mice with stromelysin-1 (MMP-3) gene inactivation. *Arterioscler Thromb Vasc Biol*. 2001;21(9):1140–1145.
- Karapanagiotidis GT, Antonitsis P, Charokopos N, et al. Serum levels of matrix metalloproteinases-1, -2, -3 and -9 in thoracic aortic diseases and acute myocardial ischemia. *J Cardiovasc Surg*. 2009;4:59.
- Carrel TWG, Burnand KG, Wells GMA, Clements JM, Smith A. Stromelysin-1 (matrix metalloproteinase-3) and tissue inhibitor of metalloproteinase-3 are overexpressed in the wall of abdominal aortic aneurysms. *Circulation*. 2002;105(4):477–482.
- Hadi T, Boytard L, Silvestro M, et al. Macrophage-derived netrin-1 promotes abdominal aortic aneurysm formation by activating MMP3 in vascular smooth muscle cells. *Nat Commun*. 2018;9(1):5022. doi:10.1038/s41467-018-07495-1
- Della Corte A, Quarto C, Bancone C, et al. Spatiotemporal patterns of smooth muscle cell changes in ascending aortic dilatation with bicuspid and tricuspid aortic valve stenosis: Focus on cell-matrix signaling. *J Thorac Cardiovasc Surg*. 2008;135(1):8–18, e1–2.
- Rowe VL, Stevens SL, Reddick TT, et al. Vascular smooth muscle cell apoptosis in aneurysmal, occlusive, and normal human aortas. *J Vasc Surg*. 2000;31(3):567–576.
- Wight TN, Merrilees MJ. Proteoglycans in atherosclerosis and restenosis. Key roles for versican. *Circ Res*. 2004;94(9):1158–1167.
- Iozzo RV. The biology of small leucine-rich proteoglycans: Functional network of interactive proteins. *J Biol Chem*. 1999;274(27):18843–18846.
- Theocharis AD, Tsolakis I, Tsegenidis T, Karamanos NK. Human abdominal aortic aneurysm is closely associated with compositional and specific modifications at the glycosaminoglycan level. *Atherosclerosis*. 1999;145(2):359–368.

34. Theocharis AD, Theocharis DA, De Luca G, Hjerpe A, Karamanos NK. Compositional and structural alternations of chondroitin and dermatan sulfates during the progression of atherosclerosis and aneurismal dilatation of the human abdominal aorta. *Biochimie*. 2002;84(7):667–674.
35. Buono M, Cosma MP. Sulfatase activities towards the regulation of cell metabolism and signaling in mammals. *Cell Mol Life Sci*. 2010;67(5):769–780.
36. Sanderson RD, Yang Y, Kelly T, MacLeod V, Dai Y, Theus A. Enzymatic remodeling of heparan sulfate proteoglycans within the tumor microenvironment: Growth regulation and the prospect of new cancer therapies. *J Cell Biochem*. 2005;96(5):897–905.
37. Chen Q, Sivakumar P, Barley C, et al. Potential role for heparan sulfate proteoglycans in regulation of transforming growth factor- $\beta$  (TGF- $\beta$ ) by modulating assembly of latent TGF- $\beta$ -binding protein-1. *J Biol Chem*. 2007;282(36):26418–26430.
38. Powell JT, Länne T. Through thick and thin collagen fibrils, stress and aortic rupture: Another piece in the jigsaw. *Circulation*. 2007;115(21):2687–2688.
39. Jones JA, Barbour JR, Stroud RE, et al. Altered transforming growth factor-beta signaling in a murine model of thoracic aortic aneurysm. *J Vasc Res*. 2008;45(6):457–468.
40. Wang Y, Ait-Oufelia H, Herbin O, et al. TGF- $\beta$  activity protects against inflammatory aortic aneurysm progression and complications in angiotensin II-infused mice. *J Clin Invest*. 2010;120(2):422–432.

# Anatomy-related ratios predict colonoscopy incompleteness in similar examination conditions

Sławomir Woźniak<sup>1,A,C-F</sup>, Radosław Kempirski<sup>2,3,A-C,E,F</sup>,  
Joanna Grzelak<sup>4,C,E,F</sup>, Zygmunt Domagała<sup>1,E,F</sup>, Friedrich Paulsen<sup>5,E,F</sup>

<sup>1</sup> Department of Human Morphology and Embryology, Division of Anatomy, Wrocław Medical University, Poland

<sup>2</sup> 2<sup>nd</sup> Department and Clinic of Gastroenterology and Hepatology, Wrocław Medical University, Poland

<sup>3</sup> Medical Centre "Endomed", Wrocław, Poland

<sup>4</sup> Department of Oral Anatomy, Wrocław Medical University, Poland

<sup>5</sup> Institute of Functional and Clinical Anatomy, Friedrich–Alexander University Erlangen–Nürnberg, Erlangen, Germany

A – research concept and design; B – collection and/or assembly of data; C – data analysis and interpretation;  
D – writing the article; E – critical revision of the article; F – final approval of the article

Advances in Clinical and Experimental Medicine, ISSN 1899–5276 (print), ISSN 2451–2680 (online)

*Adv Clin Exp Med.* 2020;29(5):573–580

## Address for correspondence

Sławomir Woźniak  
E-mail: slawomir.wozniak@umed.wroc.pl

## Funding sources

None declared

## Conflict of interest

None declared

Received on November 27, 2019

Reviewed on January 19, 2020

Accepted on March 10, 2020

Published online on May 18, 2020

## Abstract

**Background.** Screening colonoscopy is one of the most popular modalities for screening and surveillance of colorectal cancer and other colon disorders.

**Objectives.** To introduce new ratios to predict the colonoscopy course in patients with similar characteristics.

**Material and methods.** Five hundred screening colonoscopies (252 females and 248 males) were performed by an experienced endoscopist. Incomplete colonoscopies (without pathologic findings, i.e., disease-unrelated) were included in the study. Collected data was used to determine new ratios.

**Results.** An examination was completed in 231 (91.7%) females (F) and 239 (96.4%) males (M). The majority of incomplete colonoscopies were discontinued in the sigmoid colon: 8 F (38.1%) and 4 M (44.4%) or in the descendsigmoid flexure: 4 F (19%) and 2 M (22.2%). We found statistically significant higher risk of incompleteness in females ( $p = 0.03$ ), patients after 2 or more surgical treatments ( $p = 0.007$ ) and in males with lower body mass index (BMI) ( $p = 0.01$ ) ( $\chi^2$  tests). Moreover, we discovered a statistically significant correlation with 2 or more previous surgical treatments in the female group ( $p = 0.02$ ) ( $\chi^2$  test). We calculated the incomplete colonoscopy anatomy-related (ICAR) and modified ICAR (MICAR) ratios. The range of ICAR and MICAR was 0–0.17; the number of incomplete examinations ranged from 0 to 1 failed out of 6 attempts (calculation:  $100:17 = 5.88$ ).

**Conclusions.** The ICAR and MICAR ratios reflect the various risk of colonoscopy incompleteness (i.e., disease-unrelated) and highlight the differences between patients in similar examination condition.

**Key words:** screening colonoscopy, incomplete colonoscopy, large intestine anatomy, colon anatomy-related incomplete colonoscopy

## Cite as

Woźniak S, Kempirski R, Grzelak J, Domagała Z, Paulsen F. Anatomy-related ratios predict colonoscopy incompleteness in similar examination conditions. *Adv Clin Exp Med.* 2020;29(5):573–580. doi:10.17219/acem/118847

## DOI

10.17219/acem/118847

## Copyright

© 2020 by Wrocław Medical University

This is an article distributed under the terms of the Creative Commons Attribution 3.0 Unported (CC BY 3.0) (<https://creativecommons.org/licenses/by/3.0/>)

## Introduction

The rectosigmoid flexure, right colic flexure, left colic flexure, and the descendosigmoid flexure constitute sections with significantly limited mobility and can be regarded as critical points (CPs) for colonoscopy progress. Except for the primary flexures, specified above, which are always present, we also encounter secondary flexures (intratransverse in the transverse colon and/or intrasigmoid in the sigmoid colon). Some of the angulations are bent at a very sharp (acute) angle. That flexures are a key obstacle when performing colonoscopy in patients.<sup>1</sup> The difficult colonic parts can be passed using special maneuvers, such as changing the patients' position or abdominal wall compression. The aim of these practices is to change the morphology of the colon segments and/or to correct looping of the endoscope.<sup>2</sup> The endoscopist's skills in advancing the scope are a key factor for managing the difficulties.<sup>3</sup> New scopes improvements, such as cuffs, caps and rings, are not always helpful.<sup>4</sup>

During 90% of all and 95% of screening colonoscopies (SCOs), the endoscope tip should be advanced into the cecum (with visualization the jejunocaecal valve). Such an examination is called a complete colonoscopy (CC). If the colonoscope advancing is stopped before reaching the cecum, the examination is classified as an incomplete colonoscopy (IC). In some patients, the reason for this lack of success remains unclear, although large intestine elongation and tortuosity are key causes.<sup>5–7</sup> The attempts to pass through the problematic colonic segment are usually repeated several times during a single examination, but at some stage the decision to abandon attempts to negotiate the obstacle must be made. Some authors suggest that prolonged examination time (over 30 min) and the inability to rotate the endoscope are the most important factors when making the decision to end the procedure.<sup>8</sup>

Screening colonoscopy is performed in patients without signs or symptoms suggesting colonic disease. During this procedure, the colonoscopist tends to diagnose the whole colon and if no pathology is found, the next routine SCO is scheduled within 10 years.<sup>9,10</sup> The examination is usually performed in the left lateral decubitus position, because the supine position impedes conducting a colonoscopy by deepening the intestine tortuosity.<sup>11,12</sup>

According to some authors, in hysterectomized female patients, a colonoscopy is more difficult to conduct,<sup>13,14</sup> although other studies do not confirm this statement.<sup>15</sup> A further patient related factor is intra-abdominal fatty tissue (less tissue correlates with examination difficulties).<sup>16,17</sup> The pain caused by peritoneal pulling and intestinal wall deformation is supposed to be one of the most frequent causes of ICs.<sup>18</sup>

We present some aspects that are not well known to specialists. The aim of this study was to introduce new ratios to predict the colonoscopy course. Moreover, we used these

ratios to estimate the chances for CC in patients with a history of abdominal and/or pelvic surgery.

## Material and methods

The patients participated spontaneously in the screening program sponsored by the Ministry of Health of the Republic of Poland. The eligible age range was 50–65 years (40–65 for patients with a history of a 1<sup>st</sup> degree relative with colorectal cancer).

### Study design

This is a six-month retrospective observational study (January to June, 2018), performed according to the Declaration of Helsinki and approved by the Bioethics Committee at Wrocław Medical University (No. 689/2018). Five hundred asymptomatic subjects (approval 252 female (F) and 248 male (M)) undergoing SCOs were included. Patients' medical history was analyzed, including previous surgical treatments. The patients underwent mostly classical surgical treatment (ST), and in some cases laparoscopic surgery (LS) (transabdominal or transvaginal approach). Surgical treatment means open abdomen, while LS surgery is carried out with small incisions (with laparoscopic equipment). The patients underwent the following: appendectomy (34 F, 30 M; among them ST – 32 F, 29 M; LS – 2 F and 1 M), cholecystectomy (20 F, 8 M; ST – 18 F, 7 M; LS – 2 F and 1 M), and cesarean sections (ST – 23). The other patients were treated because of uterine myomas (9 removals: ST – 8, LS – 1) and/or hysterectomy (10 F; ST – 9 and LS – 1 by abdominal approach), ovariectomy (ST – 9 F), linea alba, umbilical or inguinal herniotomy (ST – 4 F). Very few patients underwent other surgical operations – 3 F – adnexectomy (ST), partial gastrectomy (ST) and retroperitoneal tumor removal (ST).

The examination was always started in the patient's left lateral decubitus position. No general anesthesia was applied. If the colonoscopy progress was stopped, the subject position was changed or their abdominal wall compressions (to dislocate the colonic segments) were performed.

### Colonoscopies

Screening colonoscopies were performed in an outpatient clinic (Endomed, Wrocław, Poland) from Monday till Friday in the afternoon (between 3 p.m. and 7 p.m.). All the endoscopies were performed in similar examination conditions: the same sedation, scope and examiner. The examiner was an experienced specialist (over 10 years of endoscopy training; over 1,000 colonoscopies performed per year; cecum intubation rate over 95%; adenoma detection rate in SCOs over 30%; the skills of the gastroenterologist were certified by the Polish Society of Gastroenterology (Certificate of Advanced Skills in Colonoscopy)). Patients



were prepared using a split regimen of 4 L of PEG (polyethylene glycol) solution with standard diet before. Sedation for the examination included oral administration of 7.5 mg of midazolam 40 min before the procedure. Screening colonoscopies were performed with Pentax (Hoya Corporation, PENTAX Lifecare Division, Japan, Tokyo) endoscopes, series: EC-3890Fi2 (without stiffness control). Before the examination, written informed consent was obtained. Bowel preparation was evaluated with the Boston Bowel Preparation Scale. The preparation of the large bowel was either very good or good (8–9 or 6–7 points on the scale) in 419 (89.15%) of the subjects; in the remaining patients it was sufficient. Polyps found during examination, measuring less than 10 mm, were removed with an endoscopic snare (47 F, 68 M). In the case of larger polyps, a planned hospital polypectomy was scheduled (11 F, 19 M).

The location of the tip of the colonoscope was established using characteristic colon features and abdominal transillumination. The examinations were reported as CCs or ICs. Incomplete colonoscopies were divided into those where a pathological cause had been revealed (incomplete, pathological reasons colonoscopies – IPCs) and others (no reason for incompleteness, no pathology revealed, other than large intestine anatomy – IACs). The scope was then withdrawn during at least 6 min. No perforation or other serious post-examination complications were observed.

## Grouping of the patients

We grouped the patients according to gender, body mass index (BMI) and previous surgical treatments into clusters. The accumulated data was used to calculate ratios that “predict” the probability of performing ICs in patients with similar characteristics.

We performed calculations and created model curves of changing IAC risk in selected patients clusters, which can be used in subsequent examinations.

## Ratios

Two ratios were calculated (described by Woźniak et al.<sup>19</sup>) according to the formulas: 1. The IC anatomy-related ratio (ICAR) reflects the risk of incompleteness without showing the place of obstacle.

$$\text{ICAR} = \text{IAC} \div \text{CC}$$

IAC – number of incomplete colonoscopies with no pathology revealed; CC – the number of complete procedures.

## Interpretation of the ICAR index

The smaller its value, the lower the risk of the IAC. For example, hypothetically assuming: if 2 IACs occurred in a group of 100 examined persons, the calculated index value is 0.02 (quotient = 2 divided by 100). This value means that next IAC is expected in 1 future case out of 50 patients.

2. The modified IC anatomy-related ratio (MICAR) reflects the decreasing risk of stopping in subsequent large intestine segments after advancing them with scope.

$$\text{MICAR}_{cp} = \text{IAC}_{cp} \div \text{CC}$$

IAC<sub>cp</sub> – the number of IAC which occurred before an analyzed colonic segment. It is calculated by subtracting the number of IACs at critical points passed with the colonoscope from the total number of IACs; CC – the number of complete procedures.

## Interpretation of the MICAR index

The smaller the value, the lower the IAC risk. Hypothetical example: 100 examinations were performed in a homogenous cluster, out of which 6 were stopped at the left colic flexure and 7 at the right colic flexure (totally 13 IACs). As the scope approached the splenic flexure, the index value was 0.13 (quotient = 13 divided by 100); when it passed this bending, the index dropped to 0.07 (quotient = 7 divided by 100); after the right colic flexure, the value decreased to 0.0 (no failures after passing the RCF). The index value informs that in subsequent examinations, the discontinuation at the splenic flexure can happen in 1 out of 8 cases (MICAR 0.13; 100:13 = 7.69) and at the hepatic flexure 1 out of 15 cases (MICAR 0.07; 100:7 = 14.28); no stopping is expected after passing this critical point.

## Statistical analysis

The statistical analysis was carried out using STATISTICA v. 12 software (StatSoft, Inc., Tulsa, USA). The  $\chi^2$  test and Fisher's exact test were used for qualitative data analysis. The significance level for the study was  $p = 0.05$ . Based on the study calculations ( $p = 0.05$ ; test power goal 0.8), the minimal number of subjects to power the study was estimated at 102 for both genders (overall 204 patients are required). We decided to analyze a larger group consisting of 500 patients to provide homogenous conditions of the examinations (exclude the scope wear and tear).

## Results

The results are shown in Fig. 1. Detailed subjects' characteristics are shown in Table 1. In 4 male patients a neoplasm infiltration was found as a cause of incompleteness. Polyps were removed in 47 female (in 12 cases more than 1) and in 68 male patients (in 18 cases more than 1). Hospitalization was offered to 11 female and 19 male patients to address polyps bigger than 10 mm or the risk of complications (insufficient supervision after the procedure, suspected perforation or major bleeding after polypectomy).

In 26 IACs (21 F; 5 M) the colonoscopic progression was stopped before reaching the cecum. In the female group

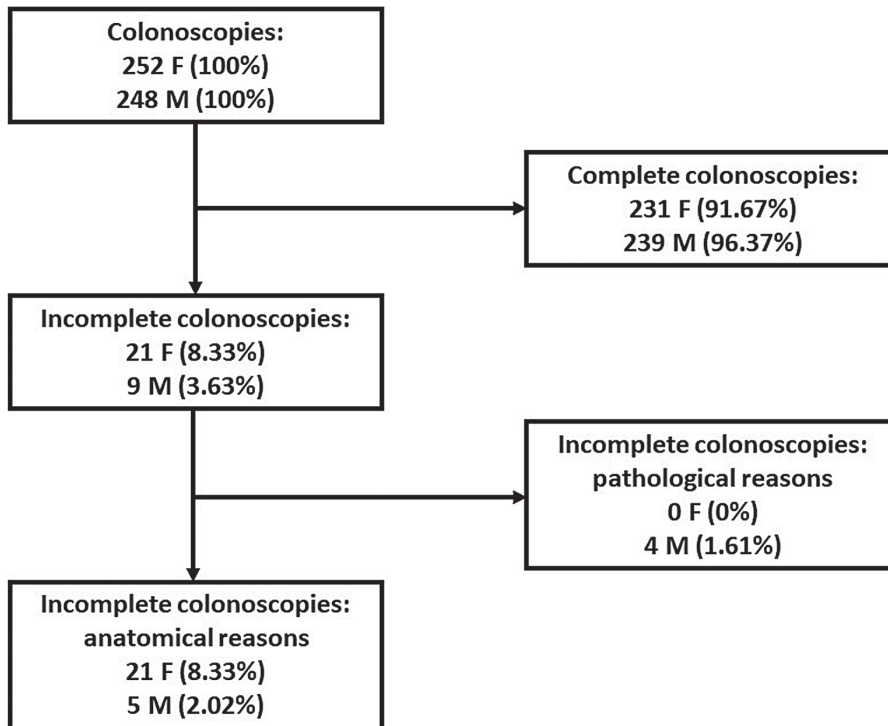


Fig. 1. Flowchart for study inclusion

Table 1. Characteristics of CCs and ICs subjects

Subject parameters	CCs		ICs (IPCs + IACs)		p-value (CCs vs ICs)		
	231 F	239 M	21 F	9 M	F and M together	F	M
Age [years] mean $\pm$ SD (40–65 years)	57.3 $\pm$ 5.83	56.9 $\pm$ 6.01	59 $\pm$ 4.29	57 $\pm$ 5.93	0.74	0.9	0.43
Weight [kg] mean $\pm$ SD (45–150 kg)	70.0 $\pm$ 12.5	88.9 $\pm$ 13.93	70.1 $\pm$ 13.75	89.1 $\pm$ 25.24*	0.15	0.76	0.05
Height [cm] mean $\pm$ SD (150–200 cm)	162.9 $\pm$ 5.5	176.6 $\pm$ 7	163.6 $\pm$ 5.04	175.9 $\pm$ 7.47	0.13	0.45	0.66
BMI mean $\pm$ SD	26.4 $\pm$ 4.49	28.4 $\pm$ 4.01	25.9 $\pm$ 5.36	27.9 $\pm$ 7.13	<b>0.03</b>	0.34	<b>0.01**</b>
After 1 PST n (%)	98 (42.4)	58 (24.3)	13 (61.9)	1 (11.1)	0.13	0.08	0.36
After at least 2 PSTs n (%)	24 (10.4)	8 (3.35)	4 (19.05)	0 (0.0)	<b>0.007</b>	<b>0.02</b>	0.82
After at least 1 PST in the pelvis	33 (14.3%)	0	6 (28.6%)	0	0.064	0.37	–

SD – standard deviation; CCs – complete colonoscopies; ICs – incomplete colonoscopies; IPCs – incomplete pathologic colonoscopies; IACs – incomplete “anatomy-related” colonoscopies; BMI – body mass index; PST – previous surgical treatment; F – female; M – male. Remarks: \* 1 subject weight was 150 kg; \*\* the lower the BMI, the higher the risk of IC. Statistically significant differences are highlighted in bold.

with IACs: 8 colonoscopies were stopped at the sigmoid colon, 4 at the descendsigmoid flexure or splenic flexure, 3 at the descending colon, and 1 at the hepatic flexure or transverse colon. In the male group: 2 at the descendsigmoid flexure, 1 at the sigmoid colon, descending colon or transverse colon.

We found statistically important differences between colonoscopy completeness and BMI ( $p = 0.03$ ), 2 or more previous surgical treatments ( $p = 0.007$ ) and female gender ( $p = 0.03$ ) ( $\chi^2$  test, respectively). Moreover, in the female

group, a statistically significant positive correlation with more than 1 previous surgical treatment was found ( $p = 0.02$ ;  $\chi^2$  test), but no correlation with surgery in the pelvis. There were no statistically significant differences between the completion of the examination and the height or age of the patients. Collected data was used to determine new ratios: initial MICAR value reflects the ICAR value (which is constant in analyzed subjects). The detailed parameters for female group in relation to PSTs are shown in Table 2.

**Table 2.** ICAR and MICAR values in female group in relation to previous surgical treatments

PSTs	Number of IACs and CCs	SCOs were stopped at:	Number of subjects	MICAR at subsequent critical points			
				ICAR = MICAR (SC)	MICAR (DSF)	MICAR (LCF)	MICAR (RCF)
0	8 IACs	SC	3	0.06	0.04	0.01	0.0
		DSF	1				
	133 CCs	DC	3				
		LCF	1				
1	9 IACs	SC	4	0.12	0.07	0.05	0.0
		DSF	1				
	74 CCs	LCF	3				
		TC	1				
At least 2	4 IACs	SC	1	0.17	0.125	0.04	0.04
	DSF	2					
At least 1 PST in lesser pelvis	24 CCs	RCF	1	0.14	0.1	0.04	0.02
		7 IACs	SC				
DSF	3						
50 CCs	TC	1					
		RCF	1				

PST – previous surgical treatment; IAC – incomplete anatomy-related colonoscopy; CC – complete colonoscopy; ICAR – incomplete anatomy-related colonoscopies ratio; MICAR – modified incomplete anatomy-related colonoscopies ratio; SC – sigmoid colon; DSF – descendsigmoid colon flexure; LCF – left colic flexure; TC – transverse colon; RCF – right colic flexure.

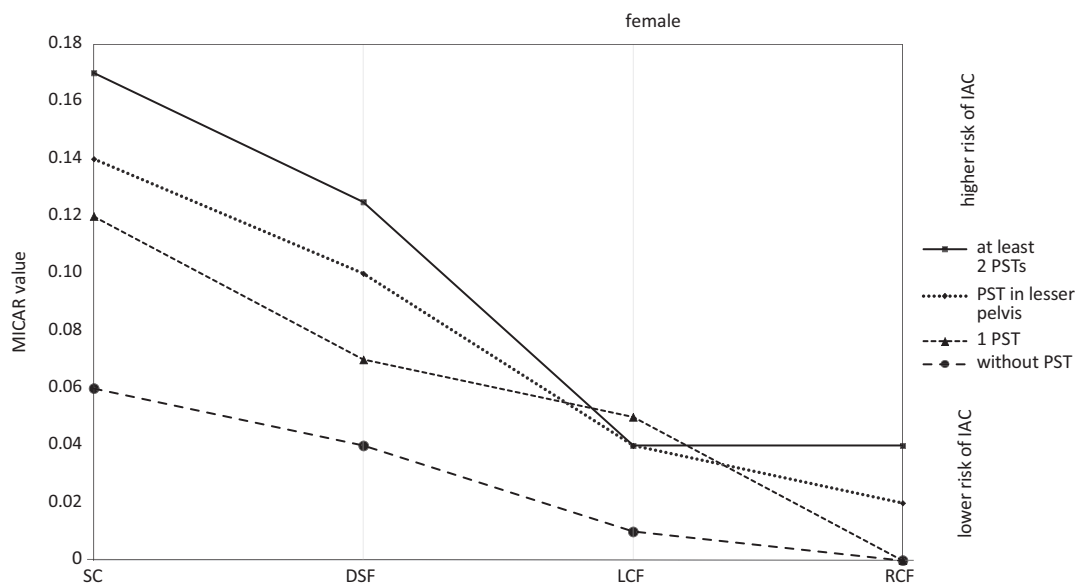


**Fig. 2.** MICAR in female patients with or without PSTs  
 SC – sigmoid colon; DSF – descendsigmoid flexure; LCF – left colic flexure; RCF – right colic flexure; IAC – incomplete anatomy-related colonoscopies; PST – previous surgery treatment.

In the cluster with at least 1 previous surgical treatment we defined a subgroup with at least 1 in the lesser pelvis (7 IACs and 50 CCs in this subgroup). Among the 7 IACs, 3 were stopped at the descendsigmoid flexure, 2 at the sigmoid colon, 1 at the transverse colon or right colic flexure, respectively; therefore, the ICAR was 0.14. The respective values of the ratios in the particular female groups are shown in Fig. 2.

In the analyzed group with a BMI below 25 and with at least 2 previous surgical treatments, we had 4 IACs and 24 CCs in the female subjects. In the subgroup of female

subjects with a BMI of at least 25 without previous surgical treatment, we had 6 IACs and 115 CCs. Figure 3 shows the ratios curve in these strongly different female subjects.

## Discussion

In our cohort, there were 8.3% incomplete examinations in female and 3.6% in male subjects. Some authors predict difficulties up to 10–20%, others in 5% of SCOs.<sup>5,7,18,20</sup> Our findings match these predictions.

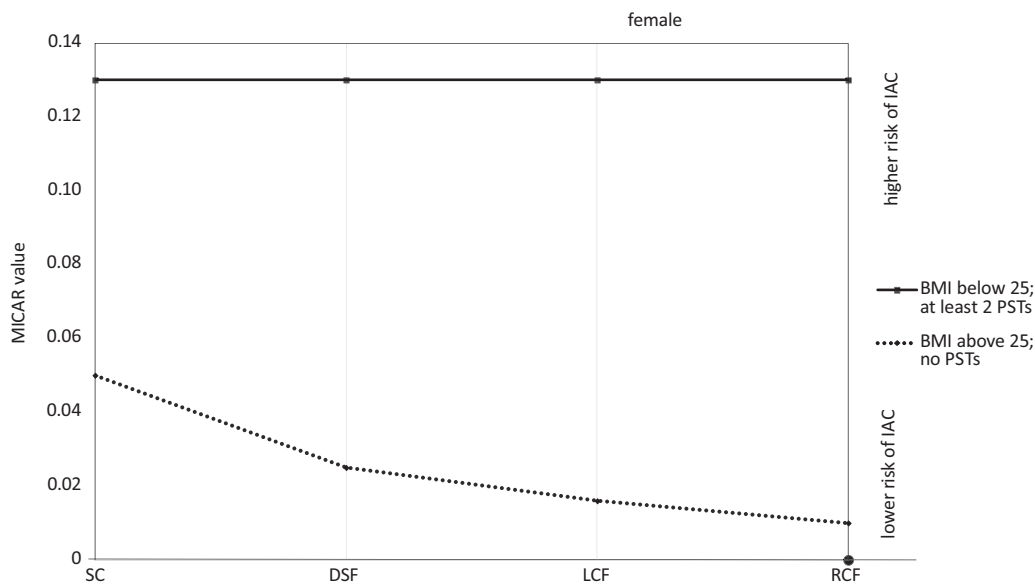


Fig. 3. MICAR in female subjects (BMI below 25 with 2 or more PSTs vs BMI above 25 without PSTs)

SC – sigmoid colon; DSF – descendosigmoid flexure; LCF – left colic flexure; RCF – right colic flexure; IAC – incomplete anatomy-related colonoscopies; PST – previous surgery treatment.

The advancing colonoscope encounters a series of acute flexures between contiguous colonic segments, either at the typical (the hepatic flexure, splenic flexure and descendosigmoid flexure) or at unexpected critical points – at the sigmoid or/and transverse colon. When the scope tip faces an acute flexure (defined as focal,  $<90^\circ$  angle bend of the colon), its progression is stopped. The mean supposed number of acute flexures is  $9.6 \pm 2.4^5$  and varies between patients. Rex et al. stated that the anatomical causes of difficulties in colonoscopy can be categorized into either an angulation and/or narrowing and/or redundancy of the colon.<sup>7</sup> Pushing the instrument further will lead to the scope looping proximal to the obstacle or to the development of tension in the intestinal wall (and in the mesentery if the colon is suspended on it), frequently causing the patient pain. Special maneuvers used in such cases (changing the patient's position and/or applying pressure to the abdominal wall and/or scope rotation to reduce the loop) are not always effective. Therefore, flexures and mobility remain key factors in “predicting” the course of a colonoscopy.

These factors are unchangeable, while those related to the endoscopist and the scope used can be modified (another operator can perform the examination successfully and/or a different colonoscope can be advanced in the colon with less difficulty). In our study, the same professional performed the examination with the same series of scopes. To assure the constant conditions, we did not use the pediatric colonoscopies or  $\text{CO}_2$  or/and water immersion techniques. Using abdominal compression maneuvers did not allow us to overcome the colonic obstacle in the IAC patients. By providing such conditions, we exclude certain variables, such as the wear and tear of scopes and different examiners' skills. Consequently, the large intestine anatomy was analyzed without significant confounding factors. Based on the results, we established the ratios reflecting the risk of ICs in subsequent subjects grouped according

to selected factors. In our opinion, this is the simplest and easiest way of showing the IAC risk to actual patients. Doctors routinely use descriptions of IC risk, such as odds ratio (OR) or hazard ratio, but the terms are not easily understood and accepted by patients.

We propose the ICAR and MICAR ratios for “predicting” the risk of incompleteness in “similar” subsequent patients. The 1<sup>st</sup> one reflecting the risk of general incompleteness without pointing at the specific point of stopping, while the 2<sup>nd</sup> one reflecting the risk of incompleteness at specific colonic segment. At the beginning of the colonoscopy, ICAR is equal to MICAR, while on subsequent critical points MICAR drops gradually.

In our study the ICAR ranged between 0.17 and 0.06, whereas MICAR ranged between 0.17 and 0.0. The interpretation of the ratio values is extremely easy. For example, in females with at least 2 previous surgical treatments, these values inform at the beginning of the procedure that we expect every 6<sup>th</sup> procedure (ICAR 0.17; calculation:  $100:17 = 5.88$ ) to be stopped before reaching the cecum. In a female without previous surgical treatment, we expect every 17<sup>th</sup> examination (ICAR 0.06;  $100:6 = 16.66$ ) to be incomplete. Saunders et al. stated that it is important to explain to the patient why difficulties sometimes occur during intubation.<sup>21</sup> We share the same opinion and propose an easy way to do so.

Rex et al. established that in lean women, a particularly sharp rectosigmoid angle is the reason for a more difficult colonoscopy course.<sup>7</sup> Loeve et al. found the S-shaped sigmoid colon, U-shaped left colic flexure, the wide U-shaped transverse colon and the U-shaped hepatic flexure as the most challenging part to pass with the scope.<sup>18</sup> We found the sigmoid colon and the descendosigmoid (in female and male patients) flexure as the most difficult segments to pass on colonoscopy. Khashab et al. established the mean number of sharp-angle flexures as  $10.9 \pm 2.4$  and pointed to the transverse colon as the main determinant in total

large intestine length differences between patients.<sup>22</sup> Philips et al., in contrast to the above statement, established that the rectosigmoid segment accounts for most of the variability in total colonic length.<sup>23</sup> According to Shah et al., problems with colonoscope advancing are mainly expected to occur in the sigmoid colon and/or in transverse colon.<sup>2</sup> We support the opinion that the sigmoid colon is the most problematic colonic segment.

Sadahiro et al. disclosed that older age is correlated with increased large intestine length and impaired intestine wall elasticity (in Japanese patients).<sup>24</sup> Such changes can lead to loop formation and make the colonoscopy course more difficult.<sup>16,25</sup> In our study, we have no statistically significant difficulties related to age; however, our subjects made up a specific group (40–65 years).

Some authors stated that performing a colonoscopy in females is more difficult.<sup>5,6,17,20,21,25</sup> This problem is related to the time needed to reach the cecum. Hsieh et al. and Krishnan et al. showed that in females this time is longer than in males.<sup>16,26</sup> We support that conclusion, because in our study female colonoscopy was more often incomplete due to anatomical reasons.

It should be added that all the examinations were performed in the afternoon, so differences in the time of day could not influence our results. Interestingly, afternoon colonoscopies are supposed to have lower intubation rates.<sup>27</sup>

The influence of previous surgical treatments on colonoscopy course is still unclear. Colonoscopy is more difficult to conduct in female patients who had previously undergone a hysterectomy,<sup>13,14</sup> although some studies do not confirm this claim.<sup>15</sup> Moreover, Garrett and Church established that posthysterectomy adhesions to the sigmoid colon make colonoscopy more difficult, but not in patients who were both hysterectomised and had their sigmoid colon resected.<sup>14</sup> We do not support that claim. In our group, the key factor was the number of previous surgical treatments; it did not matter whether the operation took place in lesser pelvis or abdominal cavity.

We support the statement that a higher BMI is an important factor in predicting a fast and problem-free colonoscopy course.<sup>16,17,25,26</sup> We observed a statistically significant incompleteness in males with a BMI below 25.

## Limitations

Our study has certain limitations. When the colonoscopy was stopped on a proximal critical point, we could not “predict” the course of the procedure on the next one. We could not totally exclude the individual sensitivity to pain – this factor can differ between patients. It is possible that the results would be different if other examination parameters (pediatric colonoscopies, water immersion or CO<sub>2</sub>) were employed during the procedure. And last, but not least, the endoscopist’s fatigue was not measured.

## Conclusions

The new ratios, ICAR and MICAR, are useful in “predicting” the colonoscopy course in the constant examination conditions. The curve derived from this indexes reflects a higher risk of large intestine anatomy-related colonoscopy incompleteness in patients, especially those with a history of 2 or more previous surgical treatments. There are no statistically significant differences between colonoscopy course and a history of 1 surgical operation (regardless whether conducted in the abdominal cavity or in the lesser pelvis)

## ORCID iDs

Sławomir Woźniak  <https://orcid.org/0000-0002-7450-7993>  
 Radosław Kempirski  <https://orcid.org/0000-0002-6030-2700>  
 Joanna Grzelak  <https://orcid.org/0000-0001-7957-1161>  
 Zygmunt Domagała  <https://orcid.org/0000-0002-2317-1932>  
 Friedrich Paulsen  <https://orcid.org/0000-0002-0527-0953>

## References

1. Woźniak S, Pytrus T, Kobierzycki C, Grabowski K, Paulsen F. The large intestine from fetal period to adulthood and its impact on the course of colonoscopy. *Ann Anat.* 2019;224:17–22.
2. Shah SG, Saunders BP, Brooker JC, Williams CB. Magnetic imaging of colonoscopy: An audit of looping, accuracy and ancillary maneuvers. *Gastrointest Endosc.* 2000;52(1):1–8.
3. Adler A, Wegscheider K, Lieberman D, et al. Factors determining the quality of screening colonoscopy: A prospective study on adenoma detection rates, from 12 134 examinations (Berlin Colonoscopy Project 3, BECOP-3). *Gut.* 2013;62(2):236–241.
4. Jain D, Sandhu N, Singhal S. New developments in mechanical enhancement of colonoscopy: Cuffs, caps and rings. *Digestion.* 2016; 93(3):234–247.
5. Eickhoff A, Pickhardt PJ, Hartmann D, Riemann JF. Colon anatomy based on CT colonography and fluoroscopy: Impact on looping, straightening and ancillary manoeuvres in colonoscopy. *Dig Liver Dis.* 2010;42(4):291–296.
6. Hanson ME, Pickhardt PJ, Kim DH, Pfaus PR. Anatomic factors predictive of incomplete colonoscopy based on findings at CT colonography. *AJR Am J Roentgenol.* 2007;189(4):774–779.
7. Rex DK. Achieving cecal intubation in the very difficult colon. *Gastrointest Endosc.* 2008;67(6):938–944.
8. Gan T, Yang JL, Wu JC, Wang YP, Yang L. When and why a colonoscopist should discontinue colonoscopy by himself? *World J Gastroenterol.* 2015;21(25):7834–7841.
9. Brenner H, Chang-Claude J, Jansen L, Knebel P, Stock C, Hoffmeister M. Reduced risk of colorectal cancer up to 10 years after screening, surveillance, or diagnostic colonoscopy. *Gastroenterology.* 2014; 146(3):709–717.
10. Floer M, Meister T. Endoscopic improvement of the adenoma detection rate during colonoscopy: Where do we stand in 2015? *Digestion.* 2016;93(3):202–213.
11. Alazmani A, Hood A, Jayne D, Neville A, Culmer P. Quantitative assessment of colorectal morphology: Implications for robotic colonoscopy. *Med Eng Phys.* 2016;38(2):148–154.
12. Pickhardt PJ, Bakke J, Kuo J, et al. Volumetric analysis of colonic distention according to patient position at CT colonography: Diagnostic value of the right lateral decubitus series. *AJR Am J Roentgenol.* 2014;203(6):W623–W628.
13. Clancy C, Burke JP, Chang KH, Coffey JC. The effect of hysterectomy on colonoscopy completion: A systematic review and meta-analysis. *Dis Colon Rectum.* 2014;57(11):1317–1323.
14. Garrett KA, Church J. History of hysterectomy: A significant problem for colonoscopists that is not present in patients who have had sigmoid colectomy. *Dis Colon Rectum.* 2010;53(7):1055–1060.
15. Lacasse M, Dufresne G, Jolicoeur E, et al. Effect of hysterectomy on colonoscopy completion rate. *Can J Gastroenterol.* 2010;24(6):365–368.

16. Hsieh YH, Kuo CS, Tseng KC, Lin HJ. Factors that predict cecal insertion time during sedated colonoscopy: The role of waist circumference. *J Gastroenterol Hepatol*. 2008;23(2):215–217.
17. Nagata N, Sakamoto K, Arai T, et al. Predictors for cecal insertion time: The impact of abdominal visceral fat measured by computed tomography. *Dis Colon Rectum*. 2014;57(10):1213–1219.
18. Loeve AJ, Fockens P, Breedveld P. Mechanical analysis of insertion problems and pain during colonoscopy: Why highly skill-dependent colonoscopy routines are necessary in the first place... and how they may be avoided. *Can J Gastroenterol*. 2013;27(5):293–302.
19. Woźniak S, Pytrus T, Woynarowski M, Pula B, Domagala Z, Iwanczak B. New colon anatomy-related ratios used to predict the course of colonoscopy in children. *Adv Clin Exp Med*. 2019;28(12):1–6.
20. Shah HA, Paszat LF, Saskin R, Stukel TA, Rabeneck L. Factors associated with incomplete colonoscopy: A population-based study. *Gastroenterology*. 2007;132(7):2297–2303.
21. Saunders BP, Fukumoto M, Halligan S, et al. Why is colonoscopy more difficult in women? *Gastrointest Endosc*. 1996;43(2 Pt 1):124–126.
22. Khashab MA, Pickhardt PJ, Kim DH, Rex DK. Colorectal anatomy in adults at computed tomography colonography: Normal distribution and the effect of age, sex, and body mass index. *Endoscopy*. 2009;41(8):674–678.
23. Phillips M, Patel A, Meredith P, Will O, Brassett C. Segmental colonic length and mobility. *Ann R Coll Surg Engl*. 2015;97(6):439–444.
24. Sadahiro S, Ohmura T, Yamada Y, Saito T, Taki Y. Analysis of length and surface area of each segment of the large intestine according to age, sex and physique. *Surg Radiol Anat*. 1992;14(3):251–257.
25. Chung GE, Lim SH, Yang SY, et al. Factors that determine prolonged cecal intubation time during colonoscopy: Impact of visceral adipose tissue. *Scand J Gastroenterol*. 2014;49(10):1261–1267.
26. Krishnan P, Sofi AA, Dempsey R, Alaradi O, Nawras A. Body mass index predicts cecal insertion time: The higher, the better. *Dig Endosc*. 2012;24(6):439–442.
27. Sanaka MR, Shah N, Mullen KD, Ferguson DR, Thomas C, McCullough AJ. Afternoon colonoscopies have higher failure rates than morning colonoscopies. *Am J Gastroenterol*. 2006;101(12):2726–2730.

# Evaluation of the association between angiotensin converting enzyme insertion/deletion polymorphism and the risk of endometrial cancer in and characteristics of Polish women

\*Grzegorz Raba<sup>1,A–F</sup>, \*Izabela Zawlik<sup>1,2,A,C–F</sup>, Marcin Braun<sup>3,C,E,F</sup>, Sylwia Paszek<sup>2,E,F</sup>, Natalia Potocka<sup>2,B,E,F</sup>, Marzena Skrzypa<sup>2,E,F</sup>, Bogdan Obrzut<sup>4,5,B,E</sup>, Marek Kluz<sup>1,B,E</sup>, Katarzyna Kluz<sup>1,B,E</sup>, Barbara Zych<sup>6,E,F</sup>, Magdalena Janowska<sup>7,B,E</sup>, Tomasz Kluz<sup>1,A,B,E</sup>

<sup>1</sup> Institute of Medical Sciences, College of Medical Sciences, University of Rzeszów, Poland

<sup>2</sup> Laboratory of Molecular Biology, Centre for Innovative Research in Medical and Natural Sciences, College of Medical Sciences, University of Rzeszów, Poland

<sup>3</sup> Department of Pathology, Chair of Oncology, Medical University of Lodz, Poland

<sup>4</sup> College of Medical Sciences, University of Rzeszów, Poland

<sup>5</sup> Department of Gynecology and Obstetrics, Provincial Clinical Hospital No. 2 in Rzeszów, Poland

<sup>6</sup> Institute of Health Sciences, College of Medical Sciences, University of Rzeszów, Poland

<sup>7</sup> Gynecology and Obstetrics Clinic, Frederic Chopin Clinical Provincial Hospital No. 1, Rzeszów, Poland

A – research concept and design; B – collection and/or assembly of data; C – data analysis and interpretation;

D – writing the article; E – critical revision of the article; F – final approval of the article

Advances in Clinical and Experimental Medicine, ISSN 1899–5276 (print), ISSN 2451–2680 (online)

Adv Clin Exp Med. 2020;29(5):581–585

## Address for correspondence

Izabela Zawlik

E-mail: izazawlik@yahoo.com

## Funding sources

This study was supported by funding from the University of Rzeszów, College of Medical Sciences. The study was performed within the project “Centre for Innovative Research in Medical and Natural Sciences” carried out by the University of Rzeszów, co-financed within the Regional Operational Program for Podkarpackie Province for the period 2007–2013, contract No. UDA-RPPK.01.03.00-18-004/12-00.

## Conflict of interest

None declared

\* Grzegorz Raba and Izabela Zawlik contributed equally to this work.

Received on December 4, 2019

Reviewed on February 2, 2020

Accepted on March 10, 2020

Published online on May 22, 2020

## Abstract

**Background.** Endometrial cancer is the most common malignant neoplasm of the female reproductive organs. A dysfunctional endometrial renin-angiotensin system (RAS) might contribute to the growth and spread of endometrial cancer. The RAS-related gene polymorphisms, including the polymorphism of insertion/deletion (I/D) in the angiotensin-converting enzyme (ACE) gene, influence RAS activity.

**Objectives.** In the present study, we examined the association between the I/D polymorphism of the ACE gene and endometrial cancer risk in Polish women.

**Material and methods.** Genotype analysis of the ACE I/D polymorphism was carried out using polymerase chain reaction (PCR) on 142 endometrial cancer type 1 patients and 68 cancer-free subjects. The results of the analyses were correlated with clinical data.

**Results.** The frequency of DD, DI and II ACE genotypes did not vary significantly between the experimental group and the control group (40 (28%), 61 (43%) and 41 (29%) vs 18 (26%), 31 (46%), and 19 (28%), respectively;  $p = 0.935$ ). In addition, the incidence of the DD, DI and II polymorphisms in the ACE gene did not vary significantly between the experimental subgroups when stratified by cancer grade – G1, G2 and G3 endometrioid carcinoma – and the control group. Furthermore, the ACE polymorphism was not significantly associated with hypertension, diabetes or lymph node metastasis.

**Conclusions.** The ACE I/D gene polymorphism was not associated with endometrial cancer risk or the clinicopathological features in Polish women.

**Key words:** endometrial cancer, molecular biology, ACE gene polymorphism

## DOI

10.17219/acem/118843

## Copyright

© 2020 by Wrocław Medical University

This is an article distributed under the terms of the Creative Commons Attribution 3.0 Unported (CC BY 3.0) (<https://creativecommons.org/licenses/by/3.0/>)

## Cite as

Raba G, Zawlik I, Braun M, et al. Evaluation of the association between angiotensin converting enzyme insertion/deletion polymorphism and the risk of endometrial cancer in and characteristics of Polish women. *Adv Clin Exp Med.* 2020;29(5):581–585. doi:10.17219/acem/118843

## Background

Endometrial cancer is the most common malignant neoplasm of the female reproductive organs. The incidence of endometrial cancer is increasing worldwide. Potential risk factors for this disease include diabetes, obesity, hypertension, and relative hyperestrogenism. All of these conditions are associated with activation of the renin-angiotensin system (RAS).<sup>1,2</sup> The RAS is an important aspect of the endocrine system that controls the fluid-electrolyte balance, aldosterone secretion and blood pressure regulation. Renin mediates the conversion of angiotensinogen (AGT) to angiotensin I (Ang I) and the protein des(Ang I)AGT. Both AGT and des(Ang I)AGT are non-inhibitory serpins that can inhibit angiogenesis. Angiotensin II is the most active protein of the RAS, and is converted from Ang I by angiotensin-converting enzyme (ACE) through the removal of 2 amino acids. Angiotensin II acts through angiotensin II receptor type 1 (AGTR1) to induce cell proliferation and angiogenesis.<sup>3</sup> As in all tissues, endometrial RAS is involved in the process of angiogenesis, neovascularization and cell proliferation.<sup>4</sup> Thus, endometrial RAS affects tumor growth and spread.

The role of overexpression of the proangiogenic and proliferation-stimulating Ang II/AGTR1 combination has been demonstrated in the pathogenesis of several cancers, including breast, lung, prostate, and cervical cancer.<sup>5</sup> Epidemiological data also supports the theory that the RAS plays a role in the formation of neoplasms. Pharmacological suppression of the RAS for the treatment of hypertension reduces the risk of cancer. The relative risk of reproductive tract cancer in women taking ACE inhibitors is 0.37 (0.12–0.87).<sup>6</sup> Experimental studies in a mouse model demonstrated that the administration of AGTR1 antagonists significantly reduces tumor growth in the progression of endometrial cancer.<sup>7</sup> Further, increased expression of Ang II, AGTR1, AGTR 2, vascular endothelial growth factor (VEGF), and the estrogen alpha receptor (NR3A1) has been observed in endometrial cancer tumors.<sup>8</sup> In addition, a strong positive correlation has been observed between the expression of Ang II, AGTR 1 and AGTR 2, and advancing tumor grade and stage.<sup>8</sup> Therefore, improper activation of the endometrial RAS may affect the formation and progression of endometrial cancer through the prorenin/ATP6AP2 and Ang II/AGTR1 pathways.

Excessive activation of the RAS may be observed more frequently in individuals with a single-nucleotide polymorphism (SNP) in the RAS system. The RAS-related gene polymorphisms influence RAS activity, including the polymorphism of insertion/deletion (I/D) in the ACE gene. The ACE gene encodes ACE type 1 and is located on the long arm of chromosome 17 (17q23), with a length of 21,000 base pairs (bp) comprised of 26 exons and 25 introns. Intron 16 of the ACE gene contains a restriction fragment length polymorphism (RFLP) based on the presence (insertion I) or absence (deletion D) of a 287-base-pair

non-sense DNA domain Alu repeat sequence (NCBI ref. SNP ID: rs1799752). There are 3 different ACE gene genotypes: D/D and I/I homozygotes and I/D heterozygotes. The D allele is associated with higher ACE activity in both the serum and tissue, in comparison with the I allele.<sup>9</sup> ACE I/D polymorphisms are associated with a risk for several types of cancer, including breast, prostate and hepatocellular cancer.<sup>10–12</sup> To the best of our knowledge, the only analysis of the ACE gene I/D polymorphism in patients with endometrioid cancer was presented by Freitas-Silva et al.,<sup>13</sup> who reported that the ACE polymorphism may be associated with the development of endometrial carcinoma and tumor onset in younger women. The clinical implications of the ACE I/D polymorphism on endometrial cancer have yet to be established. The aim of our study was to examine the association between the ACE I/D gene polymorphism and endometrial cancer risk and the clinicopathological features of the patients.

## Material and methods

### Subjects

The study included 210 Caucasian women: 142 with histopathologically confirmed endometrial cancer type 1 (study group) treated in the Clinical Departments of Gynecology and Obstetrics of Provincial Clinical Hospitals No. 1 and No. 2 in Rzeszów, Poland, and the Department of Gynecology and Obstetrics of the Provincial Hospital in Przemyśl, Poland. The control group comprised of 68 healthy women with no family history of cancer. The control group was recruited from among volunteers with negative results from prophylactic examinations in the Genetic Disorders Centre in Rzeszów. The study was carried out in 2017–2018. Peripheral blood samples were obtained from each individual and stored at –80°C prior to analysis. The exclusion criteria included a current or prior diagnosis of cancer of any type. The study was approved by the Local Bioethics Committee (approval No. 90/B/2016). Data concerning age, body mass index (BMI), comorbidities (diabetes, hypertension, etc.), hormone replacement therapy, tobacco smoking, and alcohol consumption were collected using a questionnaire.

### DNA isolation and molecular analysis

Genomic DNA was extracted from peripheral blood leukocytes using a rapid non-enzymatic method as reported by Lahiri et al.<sup>14</sup> The genotyping of the ACE rs1799752 (I/D) polymorphism was carried out using polymerase chain reaction (PCR), estimated by the presence or absence of the 287 bp sequence in intron 16. We determined the occurrence of the I/D polymorphism based on the presence of a fragment of 193 bp for the D allele and a fragment of 480 bp for the I allele. The ACE polymorphisms were



amplified using the PCR primers reported by Sanhueza et al.<sup>15</sup> The optimal conditions were determined to be initial denaturation at 95°C for 10 min followed by 30 cycles of denaturation at 95°C for 60 s, annealing at 64°C for 60 s, and extension at 72°C for 60 s, with a final extension at 72°C for 7 min. The PCR amplifications were performed in a T100™ Thermal Cycler (Bio-Rad, Hercules, USA). The amplification products were separated with electrophoresis through a 2% agarose gel (PB Genoplast Biochemicals, Rokocin, Poland) stained with Midori Green Stain (Nippon Genetics, Tokyo, Japan).

### Statistical analysis

The categorical variables are presented as numbers with percentages in brackets. Differences between the categorical variables were evaluated using Pearson’s  $\chi^2$  test. Continuous variables are presented as medians and interquartile ranges (IQR) in brackets. The Shapiro–Wilk test was used to assess the distribution of continuous variables. Due to a non-normal distribution, continuous variables were compared using the Mann–Whitney U test for 2 groups, or the Kruskal–Wallis one-way analysis of variance (ANOVA) with additional post hoc comparisons for 3 or more groups. A correction for multiple testing was applied. The Hardy–Weinberg equilibrium of allele frequencies was tested for using an online calculator (<http://www.oege.org/software/hwe-mr-calc.shtml>). The STATISTICA v. 12.5 PL package (StatSoft, Inc., Tulsa, USA) was used for other analyses. P-values of less than 0.05 were considered statistically significant.

### Results

Representative results of the *ACE* I/D polymorphism are shown in Fig. 1.

The frequencies of genotypes for the *ACE* I/D polymorphism among the study groups were consistent with

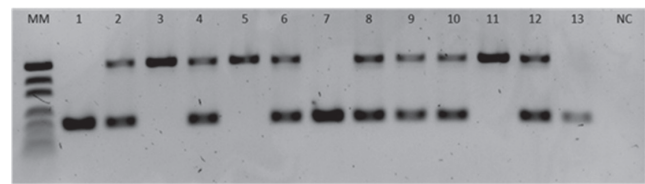


Fig. 1. Representative results of the insertion/deletion (I/D) polymorphism of a 287-bp fragment in intron 16 of the *ACE* gene

MM – DNA molecular mass markers (501, 404, 331, 242, 190, 147, and 110 bp); lanes 2, 4, 6, 8–10, and 12 I/D genotype (2 bands at 480 bp and 193 bp); lanes 3, 5 and 11 I/I genotype (1 band at 480 bp); lanes 1, 7 and 13 D/D genotype (1 band at 193 bp); NC – negative control.

Table 1. *ACE* insertion/deletion (I/D) genotype distributions in patients with endometrial cancer and controls

<i>ACE</i> I/D genotype	Experimental group n (% of the group)	Control group n (% of the group)	p-value
In the study:			
DD	40 (28)	18 (27)	0.935
ID	61 (43)	31 (46)	
II	41 (29)	19 (28)	
In perfect Hardy–Weinberg equilibrium:			
DD	35 (25)	16 (24)	1.000
ID	71 (50)	34 (50)	
II	36 (25)	18 (26)	

The parameters fulfil the criterion for Hardy–Weinberg equilibrium ( $p > 0.05$ ), confirming that both the experimental and control groups in the present study are representative.

Hardy–Weinberg equilibrium (Table 1). The BMI was significantly different between the experimental group (30.49 (26.99–34.67)) and control group (26.29 (24.15–27.74)) ( $p < 0.001$ ). There were no differences in BMI between DD, DI and II *ACE* polymorphisms in either the control or experimental group ( $p = 0.871$  and  $p = 1.000$ , respectively) (Table 2). The incidence of the DD, DI and II polymorphisms in the *ACE* gene did not vary significantly among

Table 2. Characteristics of the groups by insertion/deletion (I/D) polymorphism of the *ACE* gene

Factor	Group	Homozygotes DD median (IQR)	Heterozygotes ID median (IQR)	Homozygotes II median (IQR)	p-value
BMI	experimental	31.98 (28.3–35.16)	30.48 (27.0–34.67)	29.65 (26.18–33.85)	<0.001*
	control	26.55 (25.05–27.13)	26.45 (24.12–28.0)	25.41 (24.12–27.28)	
Number of births	experimental	2 (1–3)	2 (1–3)	2 (2–3)	0.067
	control	3 (1–4)	2 (2–3)	2 (1–3)	
Age at last menstruation [years]	experimental	50 (48–55)	52 (46–55)	50 (49–53)	0.132
	control	49 (47–53)	53 (49–54)	51 (48–55)	

\* In the post hoc analysis of the results, significant differences were only apparent between the cancer patients and the healthy controls, but BMI did not differ regarding *ACE* polymorphism. IQR – interquartile range; BMI – body mass index.

**Table 3.** Comparison of the incidence of the ACE insertion/deletion (I/D) polymorphism between endometrioid cancer grades 1–3 and the control group

Group	Homozygotes DD	Heterozygotes ID	Homozygotes II	p-value vs controls
Control group, n (%)	18 (26)	31 (46)	19 (28)	–
Experimental group, n (%)	40 (28)	61 (43)	41 (29)	0.935
G1, n (%)	16 (23)	28 (43)	23 (34)	0.754
G2, n (%)	16 (30)	26 (48)	12 (22)	0.764
G3, n (%)	8 (47)	5 (29)	4 (24)	0.244

**Table 4.** Incidence of hypertension, diabetes, and metastases in the retroperitoneal lymph nodes in women with endometrioid carcinoma in relation to ACE insertion/deletion (I/D) polymorphism

Disease	DD patients, n (%)	ID patients, n (%)	II patients, n (%)	p-value
Hypertension (n = 29)	8 (20.0)	13 (21.7)	8 (20.0)	0.971
Diabetes (n = 46)	13 (32.5)	18 (30.0)	15 (37.5)	0.730
Lymph node metastasis (n = 8)	3 (9.7)	4 (7.7)	1 (3.13)	0.570

the experimental group when stratified by cancer grade – G1, G2 and G3 endometrioid carcinoma – and the control group (Table 3). In women with endometrial cancer, the DD, DI and II polymorphisms in the ACE gene did not significantly affect the concurrent incidence of hypertension ( $p = 0.971$ ) or diabetes ( $p = 0.730$ ). The polymorphism type also did not significantly affect the presence of lymph node metastases ( $p = 0.570$ ; Table 4).

## Discussion

ACE I/D polymorphisms are a risk factor for many types of cancer.<sup>10–12,16</sup> Zhang et al. demonstrated that the ACE I/D polymorphism is associated with cancer risk in Caucasians in a meta-analysis of various adenocarcinomas, but they did not include studies of patients with endometrioid cancer.<sup>17</sup> Some other studies, however, have reported no association between ACE I/D polymorphism and cancer risk.<sup>18–21</sup> In the present study, we found no significant correlations between ACE I/D polymorphism and the incidence of endometrioid cancer, including cancer grades G1, G2 and G3. Moreover, we found no association between the ACE gene polymorphism and hypertension, diabetes, or metastases to the retroperitoneal lymph nodes. To the best of our knowledge, the only analysis of ACE gene I/D polymorphism in patients with endometrioid cancer was presented by Freitas-Silva et al., who suggested that ACE polymorphism is associated with the development of endometrial carcinoma in women younger than 63 years of age.<sup>13</sup> Their study was conducted on only 70 patients with endometrial cancer. Our results from 142 cases of endometrial cancer do not suggest any involvement of the ACE I/D polymorphism in the development and progression of endometrioid cancer, regardless of age (menopausal status). Previous studies have established that the ACE I/D polymorphism is functional.<sup>22,23</sup>

The lack of influence of the ACE I/D polymorphism on the biology of endometrioid cancer in the population of Polish Caucasians reported here proves that ACE I/D polymorphism alone cannot be a risk factor for endometrioid cancer.

One limitation of our study is the small sample size (a total of 210 women), which is important in research on polymorphisms. The Hardy–Weinberg equilibrium test, however, demonstrated that both the experimental group and the control group were representative. There are conflicting results describing the ACE I/D polymorphism as a risk factor in prostate cancer: some studies reported that the ACE I/D polymorphism is a risk factor, whereas other studies on other groups of patients found no such association.<sup>13,18</sup> On the basis of these findings, other genetic and environmental factors may influence the development of endometrioid cancer and the clinicopathological features.

## Conclusions

Our results revealed no association between the ACE I/D gene polymorphism and endometrial cancer risk or the basic clinicopathological features among Polish Caucasian women.

### ORCID iDs

Grzegorz Raba  <https://orcid.org/0000-0002-9196-8548>  
 Izabela Zawlik  <https://orcid.org/0000-0001-7992-9100>  
 Marcin Braun  <https://orcid.org/0000-0003-3804-7042>  
 Sylwia Paszek  <https://orcid.org/0000-0002-7865-2661>  
 Natalia Potocka  <https://orcid.org/0000-0002-5505-3922>  
 Marzena Skrzypa  <https://orcid.org/0000-0001-7674-5912>  
 Bogdan Obrzut  <https://orcid.org/0000-0002-1293-1860>  
 Marek Kluz  <https://orcid.org/0000-0003-2827-6984>  
 Katarzyna Kluz  <https://orcid.org/0000-0003-0145-4701>  
 Barbara Zych  <https://orcid.org/0000-0001-8008-6630>  
 Magdalena Janowska  <https://orcid.org/0000-0003-3132-6436>  
 Tomasz Kluz  <https://orcid.org/0000-0002-4798-3986>

## References

- Bokhman JV. Two pathogenetic types of endometrial carcinoma. *Gynecol Oncol.* 1983;15(1):10–17.
- Gorzelnia K, Janke J, Engeli S, Luft FC, Sharma AM. Upregulation of the AT(1) receptor human adipocytes by hydrocortisone. *J Hypertens.* 2002;20:543–543.
- Rigat B, Hubert C, Alhencgelas F, Cambien F, Corvol P, Soubrier F. An insertion deletion polymorphism in the angiotensin I-converting enzyme gene accounting for half the variance of serum enzyme levels. *J Clin Invest.* 1990;86(4):1343–1346.
- Li CB, Ansari R, Yu ZM, Shah D. Definitive molecular evidence of renin-angiotensin system in human uterine decidual cells. *Hypertension.* 2000;36(2):159–164.
- Deshayes F, Nahmias C. Angiotensin receptors: A new role in cancer? *Trends Endocrinol Metabol.* 2005;16(7):293–299.
- Lever AF, Hole DJ, Gillis CR, et al. Do inhibitors of angiotensin-I-converting enzyme protect against risk of cancer? *Lancet.* 1998;352(9123):179–184.
- Koyama N, Nishida Y, Ishii T, Yoshida T, Furukawa Y, Narahara H. Telmisartan induces growth inhibition, DNA double-strand breaks and apoptosis in human endometrial cancer cells. *PLoS One.* 2014;9(3):e93050.
- Piastowska-Ciesielska AW, Pluciennik E, Wojcik-Krowiranda K, Bienkiewicz A, Bednarek A, Ochedalski T. Analysis of the expression of angiotensin II type 1 receptor and VEGF in endometrial adenocarcinoma with different clinicopathological characteristics. *Tumor Biol.* 2012;33(3):767–774.
- Teranishi J, Yamamoto R, Nagasawa Y, et al. ACE insertion/deletion polymorphism (rs1799752) modifies the renoprotective effect of renin-angiotensin system blockade in patients with IgA nephropathy. *J Renin Angiotensin Aldosterone Syst.* 2015;16(3):633–641.
- Singh A, Srivastava N, Amit S, Prasad SN, Misra MP, Ateeq B. Association of AGTR1 (A1166C) and ACE (I/D) polymorphisms with breast cancer risk in North Indian population. *Transl Oncol.* 2018;11(2):233–242.
- Medeiros R, Vasconcelos A, Costa S, et al. Linkage of angiotensin I-converting enzyme gene insertion/deletion polymorphism to the progression of human prostate cancer. *J Pathol.* 2004;202(3):330–335.
- Yuan F, Zhang L-S, Li H-Y, Liao M, Lv M, Zhang C. Influence of angiotensin I-converting enzyme gene polymorphism on hepatocellular carcinoma risk in China. *DNA Cell Biol.* 2013;32(5):268–273.
- Freitas-Silva M, Pereira D, Coelho C, Bicho M, Lopes C, Medeiros R. Angiotensin I-converting enzyme gene insertion/deletion polymorphism and endometrial human cancer in normotensive and hypertensive women. *Cancer Genet Cytogenet.* 2004;155(1):42–46.
- Lahiri DK, Nurnberger JI. A rapid nonenzymatic method for the preparation of HMW DNA from blood for RFLP studies. *Nucleic Acids Res.* 1991;19(19):5444.
- Sanhueza JA, Zambrano T, Bahamondes-Avila C, Salazar LA. Association of anxiety-related polymorphisms with sports performance in Chilean long distance triathletes: A pilot study. *J Sports Sci Med.* 2016;15(4):554–561.
- Vairaktaris E, Yapijakis C, Tsigris C, et al. Association of angiotensin-converting enzyme gene insertion/deletion polymorphism with increased risk for oral cancer. *Acta Oncol.* 2007;46(8):1097–1102.
- Zhang K, Cheng D, Yi L, Shi H, Zhen G. Association between angiotensin I-converting enzyme gene polymorphism and susceptibility to cancer: A meta-analysis. *Int J Clin Exp Pathol.* 2014;7(9):6291–6300.
- Wang Z-Y, Li H-Y, Jiang Z-P, Zhou T-B. Relationship between angiotensin-converting enzyme insertion/deletion gene polymorphism and prostate cancer susceptibility. *J Cancer Res Ther.* 2018;14(Suppl):S375–S380.
- Li X-L, Zheng Z-J, Qu H-O. Lack of association of angiotensin-converting enzyme insertion/deletion polymorphism with breast cancer: An update meta-analysis based on 10405 subjects. *J Renin Angiotensin Aldosterone Syst.* 2015;16(4):1095–1100.
- Wang N, Yang D, Ji B, Li J. Angiotensin-converting enzyme insertion/deletion gene polymorphism and lung cancer risk: A meta-analysis. *J Renin Angiotensin Aldosterone Syst.* 2015;16(1):189–194.
- Alves Correa-Noronha SA, Ribeiro de Noronha SM, Alecrim C, et al. Association of angiotensin-converting enzyme I gene I/D polymorphism with endometrial but not with ovarian cancer. *Gynecol Endocrinol.* 2012;28(11):889–891.
- Xie Y, You C, Chen J. An updated meta-analysis on association between angiotensin I-converting enzyme gene insertion/deletion polymorphism and cancer risk. *Tumor Biol.* 2014;35(7):6567–6579.
- Li P, Cao L, Han X. Angiotensin-converting enzyme (ACE) I/D polymorphism is a risk factor of allergic rhinitis. *Cell Moll Biol.* 2017;63(8):48–50.



# Efficacy of intra-arterial lidocaine infusion in the treatment of cerulein-induced acute pancreatitis

Ryszard Antkowiak<sup>1,A–F</sup>, Łukasz Antkowiak<sup>2,A–F</sup>, Sławomir Grzegorzyn<sup>3,B–D</sup>, Klaudia Nalik-Iwaniak<sup>4,B,D</sup>, Natalia Kabała<sup>5,B,D</sup>, Zbigniew Arent<sup>4,B</sup>, Edyta Warmusz-Reichman<sup>6,B</sup>, Katarzyna Stęplewska<sup>7,C</sup>, Paweł Domosławski<sup>8,E,F</sup>

<sup>1</sup> Department of General and Multiorgan Surgery, 3<sup>rd</sup> Provincial Hospital, Rybnik, Poland

<sup>2</sup> Department of Pediatric Neurosurgery, Medical University of Silesia, Katowice, Poland

<sup>3</sup> Department of Biophysics, Medical University of Silesia, Zabrze, Poland

<sup>4</sup> Experimental and Innovative Medicine Centre, University of Agriculture, Kraków, Poland

<sup>5</sup> University Centre of Veterinary Medicine, University of Agriculture, Kraków, Poland

<sup>6</sup> Department of Histology and Embryology, Medical University of Silesia, Zabrze, Poland

<sup>7</sup> Department of Pathology, Institute of Medical Sciences, University of Opole, Poland

<sup>8</sup> Department of General, Gastroenterological and Endocrine Surgery, Wrocław Medical University, Poland

A – research concept and design; B – collection and/or assembly of data; C – data analysis and interpretation;

D – writing the article; E – critical revision of the article; F – final approval of the article

Advances in Clinical and Experimental Medicine, ISSN 1899–5276 (print), ISSN 2451–2680 (online)

*Adv Clin Exp Med.* 2020;29(5):587–595

## Address for correspondence

Łukasz Antkowiak

E-mail: lukaszantkowiak7@gmail.com

## Funding sources

None declared

## Conflict of interest

None declared

Received on April 6, 2020

Reviewed on April 22, 2020

Accepted on May 1, 2020

Published online on May 27, 2020

## Cite as

Antkowiak R, Antkowiak Ł, Grzegorzyn S, et al. Efficacy of intra-arterial lidocaine infusion in the treatment of cerulein-induced acute pancreatitis. *Adv Clin Exp Med.* 2020;29(5):587–595. doi:10.17219/acem/121932

## DOI

10.17219/acem/121932

## Copyright

© 2020 by Wrocław Medical University

This is an article distributed under the terms of the Creative Commons Attribution 3.0 Unported (CC BY 3.0) (<https://creativecommons.org/licenses/by/3.0/>)

## Abstract

**Background.** Disturbances in pancreatic microcirculation, beginning with vasoconstriction, are crucial in early pancreatitis and progression to necrotizing pancreatitis. Thus, vascular-targeted treatment aiming to restore a sufficient level of microcirculation through vasodilation would possibly reduce the severity of pancreatitis. Lidocaine is an anti-arrhythmic and local anesthetic drug, which also acts as a vasodilator at higher concentrations.

**Objectives.** To evaluate the efficacy of intra-arterial infusion of lidocaine into the celiac trunk in treatment of cerulein-induced acute pancreatitis.

**Material and methods.** Wistar rats ( $n = 20$ ) were randomly divided into 2 equal groups: the control group (NaCl group,  $n = 10$ ) and the study group (lidocaine group,  $n = 10$ ). All subjects underwent surgical intervention with intra-arterial infusion of 0.9% NaCl (control group) or 1% lidocaine hydrochloride (study group) into the celiac trunk. Blood samples were collected 5 times at regular intervals from each rat for amylase and lipase measurements. Histopathological analysis of the pancreas was performed.

**Results.** A total number of 16 rats (control group  $n = 7$ , study group  $n = 9$ ) were included. In the postoperative course, the study group (lidocaine group) revealed lower values of serum amylase and lipase levels compared to the control group (NaCl group), except the values at the 1<sup>st</sup> treatment point, which appeared 1 h after intraoperative drug injection. Significantly lower treatment endpoint levels of pancreatic enzymes were seen in the lidocaine group. Moreover, no differences were observed between the 1<sup>st</sup> and the last treatment point in the control group; however, these differences were significant for both enzymes in the study group. Histopathology revealed reduced pancreatitis severity in the study group compared to the controls.

**Conclusions.** Intra-arterial lidocaine infusion into the celiac trunk decreases pancreatitis severity. What is more, this study demonstrates the relevance of early vasodilation in the therapy of acute pancreatitis.

**Key words:** acute pancreatitis, lidocaine, regional arterial infusion, microcirculation

## Introduction

Acute pancreatitis is defined as an inflammatory process of the pancreas.<sup>1</sup> The annual incidence of acute pancreatitis is 34 per 100,000 and is expected to increase.<sup>2,3</sup> Severe pancreatitis associated with local and further systemic complications affects 20% of patients with acute pancreatitis. Mortality rises from 1.5% in mild to 5–17% in severe pancreatitis.<sup>4</sup> These considerably increased rates indicate the necessity and importance of developing methods of preventing severe pancreatitis. Molecular mechanism indicates that acinar cell injury with subsequent intracellular activation of enzymes is a trigger of further autodigestion of pancreatic parenchyma and local inflammatory response.<sup>5</sup> Consequent vessels injury causes increased vascular permeability with development of edema involving pancreatic parenchyma, vasoconstriction with long-lasting pancreatic hypoperfusion and ischemia, which can eventually lead to necrotizing pancreatitis.<sup>6</sup> Acute pancreatitis can progress from local inflammatory response to systemic inflammatory response syndrome (SIRS), eventually leading to organ failure (OR).<sup>7</sup> The pancreas is very sensitive to ischemia; hence, sufficient blood flow plays a very important role in its homeostasis and the prevention of inflammatory conditions.<sup>8</sup> Moreover, there are studies indicating that patients with hypovolemia and shock were diagnosed with subclinical pancreatitis.<sup>6,9</sup> Previous studies indicated that the decrease of pancreatic blood flow is an initial event in the development of acute pancreatitis.<sup>10,11</sup> Early vasoconstriction is a trigger of further microvascular disturbances in the so-called ischemia–reperfusion phenomenon.<sup>12</sup> They are said to be fundamental in the progression into severe and necrotizing pancreatitis and are described as crucial initiators of systemic inflammation.<sup>13</sup> To our knowledge, no studies concerning targeted vasodilating treatment have been conducted. In order to induce vasodilation, lidocaine solution was infused intra-arterially. Lidocaine is an antiarrhythmic and local anesthetic drug, which, depending on its concentration, may have an absolutely distinct impact on vascular smooth muscle cells. Lidocaine is reported to have vasoconstricting action at low concentrations and acts as a vasodilator at higher concentrations.<sup>14</sup> Thus, we hypothesized that infusion of lidocaine in the adequate dose would dilate arterioles and consequently reduce the severity and progression of pancreatitis. The aim of our study was to evaluate the efficacy of topical intra-arterial infusion of a high-concentration lidocaine solution into the celiac trunk in treating cerulein-induced acute pancreatitis in rats.

## Material and methods

The experiment was conducted after the approval of II Local Ethical Committee for animal experiments operating at the Institute of Pharmacology of the Polish Academy

of Sciences. All procedures were implemented in compliance with the Polish and European law (EU Directive 2010/63 on the protection of animals used for scientific purposes and the Act of January 15, 2015 on the protection of animals used for scientific or educational purposes).

## Animals and animal care conditions

The project was carried out on a group of 20, 12-week old, male albino Wistar rats. The experiment was performed in Experimental and Innovative Medicine Centre at the University of Agriculture in Kraków, Poland. Rats were housed in the animal house in standardized conditions: temperature 20–24°C, humidity 50–60%, lighting 130–325 lux, and noise level <30 dB. Controlled lighting provided 12/12 light/dark cycle. Ventilation of the holding rooms ensured the air circulation with air exchange 10 times per hour. The environmental conditions were monitored on a daily basis. Rats were housed in conventional cages in groups of 2 compatible individuals. The cages were provided with nesting materials and environmental enrichments adapted to the species. Rats were provided with laboratory animal feed and water ad libitum. Animals were checked daily by a qualified person. All procedures were carried out by an adequately educated, trained and competent staff. Prior to the beginning of the project, the animals underwent 7-day quarantine. During this period, they were subjected to handling carried out by an experienced staff. After the quarantine, the rats were divided randomly into 2 equal groups: the control group (NaCl group, n = 10) and the study group (lidocaine group, n = 10).

## Animals inclusion criteria

Rats were included in a postexperimental analysis if all of the following criteria were fulfilled: 1) no sudden death of uncertain origin within the time of the experiment; and 2) complete number of 5 blood samplings.

## Induction of acute pancreatitis

All 20 animals after determination of body weight (b.w.) received subcutaneously 20 µg/kg b.w. cerulein every hour for 4 consecutive hours (80 µg/kg b.w. in total per animal).

## Blood collection

Blood samples for biochemical analyses of serum amylase and lipase levels were collected 5 times in case of each animal from both groups. Constantly for all measurements, a total volume of 0.2 mL blood was taken from the great saphenous vein or caudal vein. First sample (M1) was taken before cerulein injection to determine the reference values of serum amylase and lipase. Second sample (M2) was collected 6 h after the last cerulein injection in particular animal (at 10<sup>th</sup> h after beginning of cerulein administration

**Table 1.** Blood sampling timing and their purposefulness. Point "0" indicates the moment before cerulein administration, when the blood was collected in order to establish the initial amylase and lipase levels

Sample	Blood tests time point	Aim of the sampling
M1	0	enzymes initial levels (reference)
M2	10 <sup>th</sup>	enzymes levels at the point when pancreatitis was already evoked – just before intraoperative drug infusion
M3	11 <sup>th</sup>	enzymes levels 1 h after operation (the 1 <sup>st</sup> treatment point)
M4	13 <sup>th</sup>	enzymes levels 3 h after operation (the 2 <sup>nd</sup> treatment point)
M5	15 <sup>th</sup>	enzymes levels 5 h after operation (treatment endpoint)

in each rat). Immediately after that, blood sampling surgery was started and then an intraoperative drug infusion was made. After termination of the surgery, the following blood tests were performed: 1 h (M3), 3 h (M4) and 5 h (M5) after intraoperative intra-arterial application of adequate solution (NaCl in controls, lidocaine in study group). The summary of blood collection procedure is presented in Table 1.

## General anesthesia procedure

The surgical procedures were carried out under general anesthesia. After applying a dose of 10 mg/kg b.w. ketamine (Bioketan; Vetoquinol Biowet, Gorzów Wielkopolski, Poland), the rats were given isoflurane (Isotek; Laboratorios Karizoo, Barcelona, Spain) during the whole procedure. The animals were treated with preemptive and postoperative analgesia – a dose of 0.05 mg/kg b.w. buprenorphine (Bupaq; Richter Pharma, Wels, Austria).

## Surgical procedure and intraoperative injection of NaCl/lidocaine

Under general anesthesia, in order to open the abdominal cavity, a 5 cm long skin incision extending from the xiphoid process was performed. After bowel irrigation, the inferior vena cava was exposed and protected from desiccation. Guided by vena cava location, which was left laterally, deeper penetration into abdominal cavity exposed the abdominal aorta with its branches (celiac trunk, superior mesenteric artery, renal arteries). Superiorly to the point where the celiac trunk branches and superiorly to the superior mesenteric artery branch, the aorta was freed from adhesions and prepared for temporal aorta occlusion with the insertion of suspensions (superiorly and inferiorly to celiac trunk branch). Subsequently, 2 vascular clamps were inserted in the prepared places in order to close the aorta completely, with the celiac trunk branch being located in the middle between these clamps, thus enabling injection. Preoperatively prepared 0.9% NaCl solution (0.5 mL/kg b.w.) in the control group

and a 1% lidocaine hydrochloride solution (5 mg/kg b.w. accounting for 10<sup>4</sup> µg/mL drug concentration) in the experimental group was injected slowly, exactly in the area of celiac trunk branching, within the timespan of approx. 1 min. Hemostatic materials were placed on the injection point immediately after the needle was extracted and the vascular clamps were subsequently removed from the aorta. Hemostatic materials were applied for around 3–5 min to support hemostasis and, after ascertaining that the bleeding stopped, the abdominal cavity was prepared for closure with hemostatics left inside. The skin was closed using single non-absorbable sutures. Surgical intervention was complete.

## Euthanasia

After the last blood collection, the animals were euthanized with an anesthetic overdose. They were subjected to isoflurane and then a lethal dose of 300 mg/kg b.w. pentobarbital (Morbital; Biowet Puławy, Puławy, Poland) was administered. After confirming the cessation of vital signs, laparotomy was conducted to collect the pancreas from each animal for further histopathological examination.

## Histopathological examination

The pancreas of each rat was fixed with a standard method in 10% formalin solution and embedded in paraffin blocks. Slices, 5 µm in thickness, were cut and routinely stained with hematoxylin and eosin (H&E). Histologic examination was carried out by an experienced pathologist who was unaware of the distribution of subjects in each group. Histopathologic examination assessed semi-quantitatively the extent of necrosis, edema, hemorrhage, vacuolization, and leukocyte infiltration, as it was described in the previous study.<sup>15</sup> The following scale was used to evaluate the severity of these features: 0 – feature was not observed, no changes, 1 – mild changes, 2 – moderate changes, 3 – severe changes.

## Statistical analysis

The statistical analysis was performed with the use of STATISTICA v. 13.1 software (StatSoft, Inc., Tulsa, USA). The normality of the variable distributions was tested using the Shapiro–Wilk test.

The t-test for independent variables was performed to test the differences between the means of the study and the control groups. The non-parametric Mann–Whitney U test was used in cases where one of the comparable variables was lacking normality. The nonparametric Friedman analysis of variance (ANOVA) test for repeatable measurements was used to determine the statistical significance of differences in a series of dependent variables of the control or study group. The significance level  $\alpha < 0.05$  was adopted.

## Results

Sixteen Wistar rats (control group  $n = 7$ , study group  $n = 9$ ) were finally included in the study and further analysis. Four animals (3 from the control group and 1 from study group) from 20 participating had to be excluded from the study because of early death, which precluded the possibility of obtaining a complete number of 5 measurements. Serum amylase and lipase levels for both groups: control (NaCl group) and study (lidocaine group) are presented in Tables 2 and 3. No statistical significance

**Table 2.** Amylase values measurements in the control and the study group through the entire preoperative (M1–M2) and postoperative course (M3–M5)

Blood sample	Control group (NaCl group)		Study group (lidocaine group)	
	mean [U/L]	SD [U/L]	mean [U/L]	SD [U/L]
M1	651.43	83.57	645.56	51.979
M2	39933	15103	49357	5776
M3	17969	4862	18691	3142.2
M4	15974	3219	15311	868
M5	16010	6412	10488	1247.5

SD – standard deviation.

**Table 3.** Lipase values measurements in the control and the study group through the entire preoperative (M1–M2) and postoperative course (M3–M5)

Blood sample	Control group (NaCl group)		Study group (lidocaine group)	
	mean [U/L]	SD [U/L]	mean [U/L]	SD [U/L]
M1	10.29	1.92	9.52	1.273
M2	1860.7	886.38	2090.3	371.54
M3	743.56	217.44	681.21	186.229
M4	605.74	107.49	498.48	109.248
M5	568.31	228.43	262.48	59.486

SD – standard deviation.

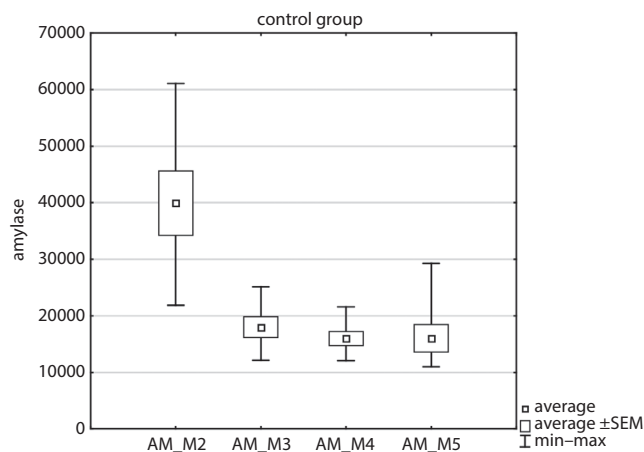


**Fig. 1.** Kinetics of amylase values in the control group measured from pancreatitis point (M2) through entire postoperative course (M3–M5)

**Table 4.** Comparison of amylase and lipase levels between the control and the study group before induction of pancreatitis (M1), when pancreatitis was evoked (M2) and at the treatment endpoint (M5)

Variable	Control group (NaCl group)		Study group (lidocaine group)		p-value
	mean [U/L]	SD [U/L]	mean [U/L]	SD [U/L]	
Amylase M1	651.43	83.57	645.56	51.979	0.9182
Lipase M1	10.29	1.92	9.52	1.273	0.1416
Amylase M2	39933	15103	49357	5776	0.2105
Lipase M2	1860.7	886.3	2090.3	371.54	0.5360
Amylase M5	16010	6412	10488	1247.5	<b>0.005921</b>
Lipase M5	568.31	228.43	262.48	59.49	<b>0.001645</b>

SD – standard deviation; bold values denote statistical significance at the  $p < 0.05$  level.

was found in the initial enzymes levels (M1, reference enzyme levels) between the 2 groups and in the levels after the induction of pancreatitis (M2) between 2 groups as well (Table 4). Differences in M2–M5 series were significant in both control (amylase  $p < 0.05$ ; lipase  $p < 0.05$ ) and the study group (amylase  $p < 0.05$ ; lipase  $p < 0.05$ ); however, differences checked in M3–M5 series revealed significance only in the study group (Table 5). That observation indicates that the significance obtained in M2–M5 series in the controls is caused mainly by a parameter drop between M2 and M3 (Fig. 1–4). Significant differences between M4 and M5 only in the study group reveal the general decreasing tendency in the pancreas inflammation parameters (Fig. 5,6).

Intergroup comparison of M5 parameters (Table 4) showed significant differences for both amylase (controls mean: 16,010 U/L; study mean: 10,488 U/L) and lipase (controls mean: 568.31 U/L; study mean: 262.48 U/L). Moreover, no differences were observed between the 1<sup>st</sup> treatment point (M3) and the last treatment point (M5) in the control group; however, these differences were significant

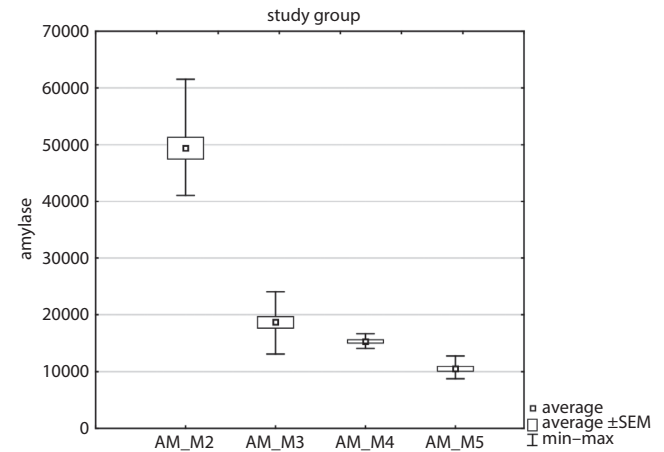


**Fig. 2.** Kinetics of amylase values in the study group measured from pancreatitis point (M2) through entire postoperative course (M3–M5)



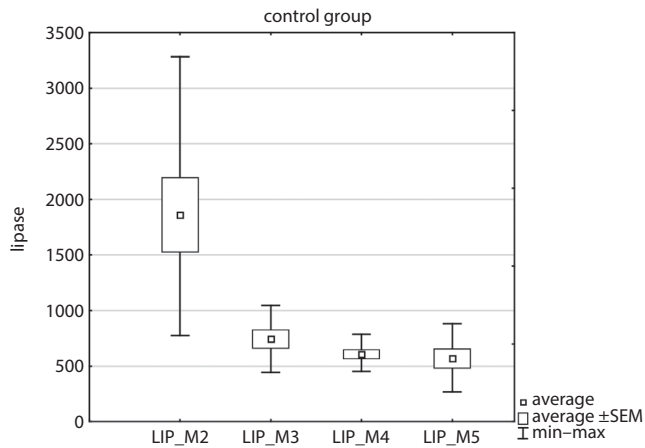


Fig. 3. Kinetics of lipase values in the control group measured from pancreatitis point (M2) through entire postoperative course (M3–M5)

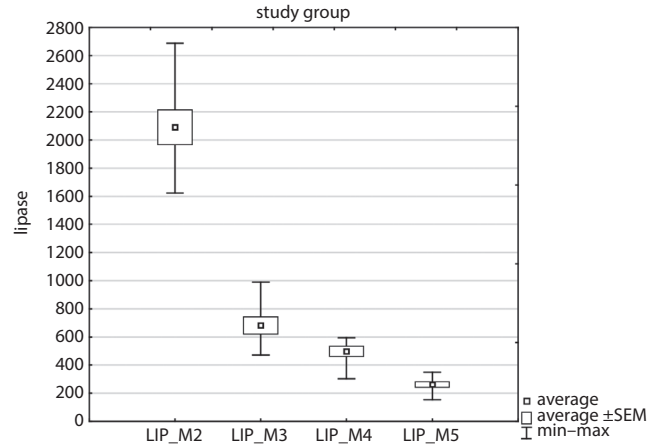


Fig. 4. Kinetics of lipase values in the study group measured from pancreatitis point (M2) through entire postoperative course (M3–M5)

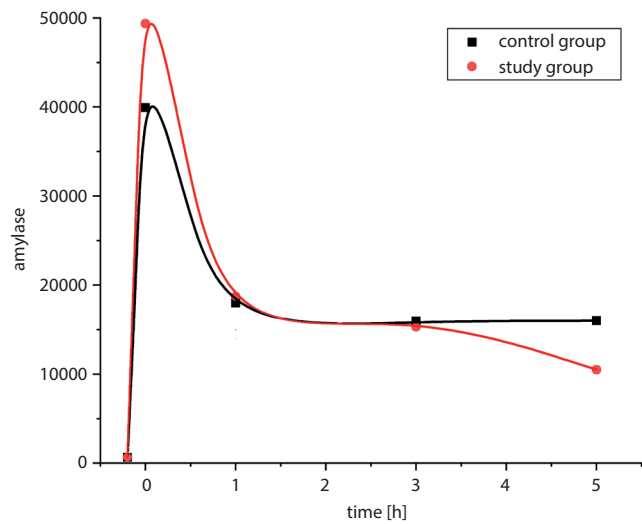


Fig. 5. Differences of amylase absolute values between control and study group in the entire preoperative (M1–M2) and postoperative course (M3–M5)

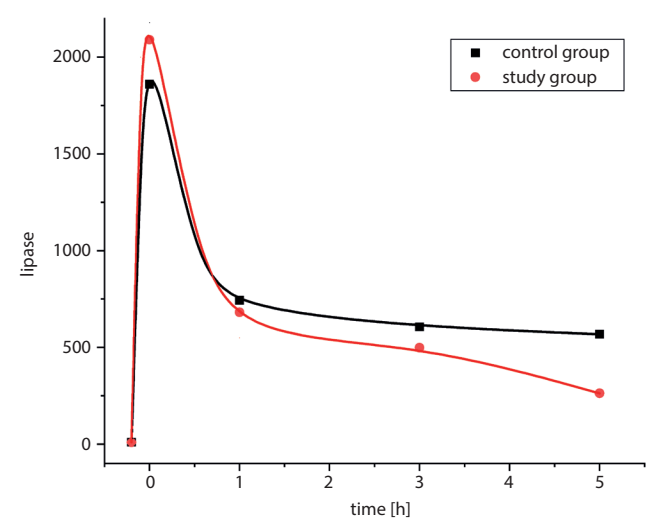


Fig. 6. Differences of lipase absolute values between control and study group in the entire preoperative (M1–M2) and postoperative course (M3–M5)

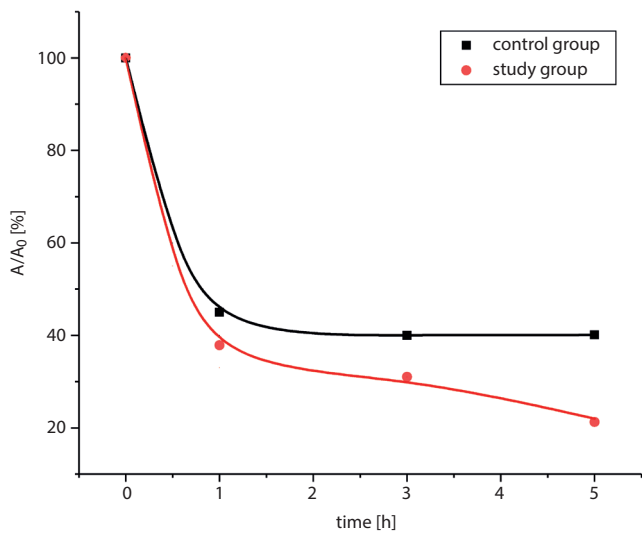


Fig. 7. Percentage differences of amylase values between control and study group in the entire postoperative course (M3–M5) with reference to values obtained at pancreatitis point (M2)

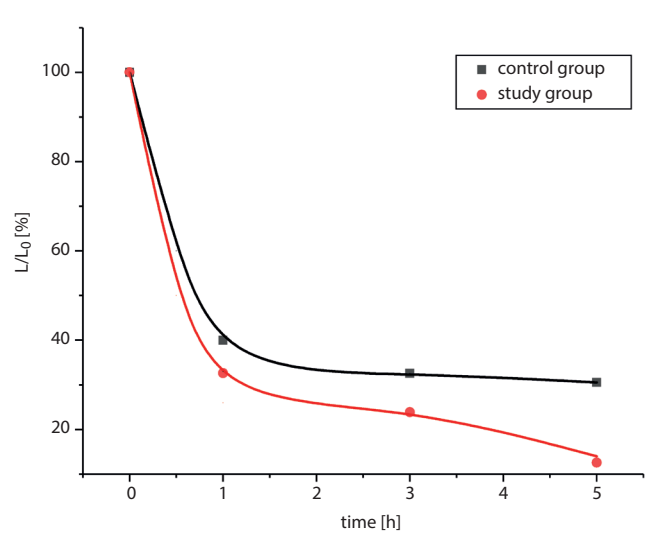


Fig. 8. Percentage differences of lipase values between control and study group in the entire postoperative course (M3–M5) with reference to values obtained at pancreatitis point (M2)

**Table 5.** Statistical analysis of intragroup differences between both enzyme levels in the particular periods. M2–M5 are values from pancreatitis point until the treatment endpoint; M3–M5 are values from the 1<sup>st</sup> treatment point until the treatment endpoint; M2–M3 are values from the pancreatitis point until the 1<sup>st</sup> treatment point; M3–M4 are values from the 1<sup>st</sup> treatment point until the 2<sup>nd</sup> treatment point; M4–M5 are values from the 2<sup>nd</sup> treatment point until the last treatment point

Series of measurements	Amylase		Lipase	
	control group (NaCl group)	study group (lidocaine group)	control group (NaCl group)	study group (lidocaine group)
	p-values			
M2–M5	<b>0.00197</b>	<b>0.00001</b>	<b>0.00319</b>	<b>0.00001</b>
M3–M5	0.15612	<b>0.00030</b>	0.249655	<b>0.00030</b>
M2–M3	<b>0.006693</b>	<b>0.000000</b>	<b>0.012695</b>	<b>0.000003</b>
M3–M4	<b>0.02982</b>	<b>0.01963</b>	0.080211	<b>0.01963</b>
M4–M5	0.735317	<b>0.00270</b>	0.742494	<b>0.00270</b>

Bold values denote statistical significance at the  $p < 0.05$  level.

**Table 6.** Comparison between the 1<sup>st</sup> treatment point (M3) and the last treatment point (M5) in both groups for both enzyme values

Variable	Control group (NaCl group)		Study group (lidocaine group)	
	mean	p-value	mean	p-value
Amylase M3	17969	0.498963	18691	<b>0.00270</b>
Amylase M5	16010		10488	
Lipase M3	743.56	0.249655	681.2	<b>0.00270</b>
Lipase M5	568.31		262.5	

Bold values denote statistical significance at the  $p < 0.05$  level.

in the study group (Table 6), thus clearly indicating that the study group (lidocaine group) responded much better to the given therapy than the control group (NaCl group).

According to Fig. 7, the decrease in amylase levels from the induction of pancreatitis (M2) to the final treatment point (M5) amounted to 60% in the control group and 79% in the study group. Respectively, lipase decrease reached 70% in the NaCl group and 87% in the lidocaine group (Fig. 8).

Histopathological analysis revealed lower intensity of necrosis, edema, hemorrhage, and vacuolization in the study group compared to the control group. However, leukocyte infiltration was similar in both groups (Fig. 9,10). Results of histopathological examination of all pancreatic tissue specimens from both groups, presented as ranges of values of assessed features, are shown in Table 7.

**Table 7.** Ranges of values of microscopic features severity in pancreas H&E specimens in the control and the study group

Group	Necrosis	Edema	Hemorrhage	Vacuolization	Leukocyte infiltration
Control group (n = 7)	0–2	0–2	0–3	0–3	0–2
Study group (n = 9)	0–1	0–1	0–1	0–1	0–2

H&E – hematoxylin and eosin.

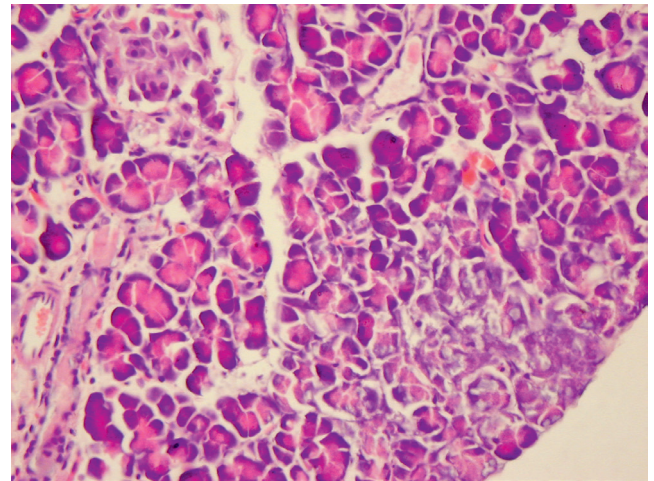


**Fig. 9.** Pancreas with necrosis and edema in the control group (H&E, magnification  $\times 400$ )

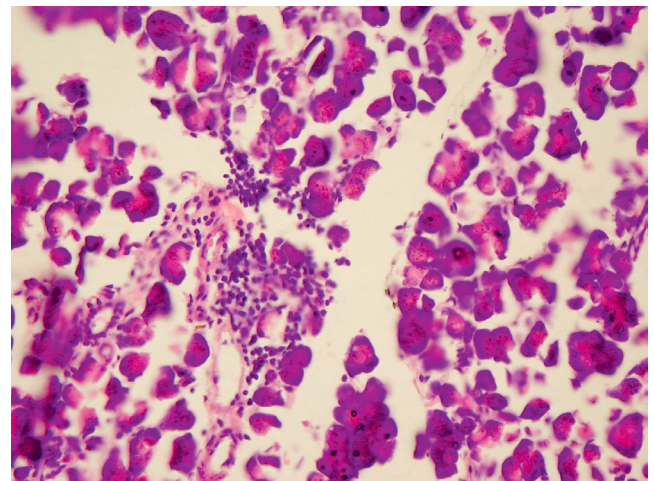


**Fig. 10.** Pancreas with leukocyte infiltration in the study group (H&E, magnification  $\times 200$ )

## Discussion

Lidocaine is a local anesthetic and antiarrhythmic drug, which additionally has a dual action on vessels. It causes vasoconstriction at low drug concentrations ( $10^3 \mu\text{g/mL}$  and lower), but acts as a vasodilator at higher concentrations ( $10^4 \mu\text{g/mL}$ ).<sup>14,16</sup> Newton et al. indicated that vasodilation caused by lidocaine can also be mediated by the local production of nitric oxide in endothelium.<sup>17</sup> Furthermore, lidocaine has an anti-inflammatory activity, thus reducing cytokine-induced injury of endothelial and vascular

smooth muscle cells. It has already been reported that mitochondrial adenosine triphosphate-sensitive potassium channels (KATP), which are present in both endothelial and vascular smooth muscle cells, mediate cellular protection.<sup>18</sup> Lidocaine induces KATP channels activity and, thereby, functions as an important anti-apoptotic factor. Vasodilating and cell-protecting properties of lidocaine have a positive impact on endothelial and vascular smooth muscle cells; hence, the application of that drug is an effective means of preventing pancreatic tissue hypoperfusion and subsequent irreversible exacerbation of pancreatitis. Due to the dual action of lidocaine, topical application was performed to gain the highest possible concentration in the pancreatic microcirculation. Action of intravenously administered lidocaine on vessels was described by Johns et al. and resulted in vasoconstriction.<sup>14</sup> Moreover, local intra-arterial infusion of lidocaine solution at concentration of  $10^3$   $\mu\text{g}/\text{mL}$  and lower caused considerable vasospasm too. Thus, we applied lidocaine solution at  $10^4$   $\mu\text{g}/\text{mL}$  concentration which was previously confirmed to cause significant dilation of arterioles.<sup>14</sup> This study was conducted using currently available intra-arterial drug administration method known as Continuous Regional Arterial Infusion (CRAI). The CRAI is a therapeutic method introduced in Japan in 1996. Its advantage over the intravenous method comes from the possibility of applying local intra-arterial infusion of selected substance, and gaining almost 10 times higher drug concentration in the pancreatic vessels.<sup>19</sup> Many studies concerning the difference between CRAI and the intravenous method indicated univocally the advantage of CRAI in acute pancreatitis therapy.<sup>19,20</sup> Taking into consideration the dual action of lidocaine, intra-arterial CRAI method was chosen to obtain high lidocaine concentrations in the celiac trunk, this ultimately led to vasorelaxation of arterioles in pancreatic microcirculation.

The pathophysiology of acute pancreatitis is substantially understood; however, exact cellular mechanisms are still not completely known.<sup>21</sup> There is a consensus that intra-acinar trypsinogen activation is a trigger of pancreatic tissue injury, finally resulting in activation of enzymes stored in granules.<sup>22</sup> Furthermore, some authors indicate that activation of NF $\kappa$ B in acinar cells is the second major parallel mechanism observed in the early pancreatitis.<sup>5</sup> Moreover, activation of NF $\kappa$ B is the most important factor inducing inflammation in pancreatitis and is also responsible for subsequent systemic inflammatory response.<sup>23</sup> These 2 pathways seem to be initiated independently. Trypsinogen-activation induces pancreatic damage and acinar cell death in early stages; however, NF $\kappa$ B-modulated inflammation is essential in later phases.<sup>24</sup> Enzyme-induced acinar cell injury leads to outflow of digestive enzymes into parenchyma, causing autodigestion of pancreatic tissue and injury to the vessels.<sup>7</sup> Subsequent inflammation-induced disturbances of pancreatic vessels are crucial for disease progression. Early endothelial injury leads to changes

in the structure of pancreatic arterioles by initiating increased permeability, thrombi formation and release of vasoconstricting endothelin.<sup>18,25,26</sup> The pancreas is extremely susceptible to ischemia. Some studies revealed subclinical pancreatitis in patients with hypovolemia or shock.<sup>9</sup> That mechanism can be explained by the characteristics of pancreatic microcirculation. Every pancreatic lobule is supplied by a single arteriole, which branches after entering the lobule. The interlobular artery has no anastomoses with other vessels and is described as an end artery.<sup>22</sup>

Vasoconstriction seems to be an early event of pancreatitis, which inevitably leads to ischemia, necrosis, circulatory obstruction, and systemic complications.<sup>27,28</sup> A study conducted by Klar et al. confirms the presence of arterioles vasoconstriction, which is visible in the direct area of pancreatitis. These findings were visualized using low contrast enhancement in the computed tomography. This method additionally confirmed histologically observed microcirculatory disturbances.<sup>11</sup> Zhou et al. stated that an arteriolar sphincter injury caused by the inflammatory process in the pancreatic parenchyma leads to vasospasms and is the primary factor of microcirculation disturbances. Pancreatic edema and intravascular emboli are followed by secondary changes, appearing after arteriolar sphincter injury.<sup>29</sup> Disturbances in microcirculation, despite being already present in mild pancreatitis, are characteristic for severe acute pancreatitis. In the latter phase, however, they are no longer associated with reversible changes in the pancreas. The mechanism called ischemia–reperfusion is an early occurring event responsible for further pancreatic hypoperfusion in acute pancreatitis. It is believed to be a crucial factor in the gradual progression of pancreatitis severity. Vasospasm affecting precapillary arterioles is responsible for early pancreatitis phase – ischemia.<sup>12</sup> Nitric oxide as a potent vasodilating factor is released by an intact endothelium. It affects the conditions of the vessels and reduces prothrombotic events.<sup>30</sup> Endothelial injury induces the production of endothelin, which is known to be a long-acting vasoconstrictor.<sup>25</sup> Imbalance between nitric oxide and endothelin plays a crucial role in the previously described induction of vasospasm.<sup>12</sup> Additionally, trypsin, elastase, phospholipase A<sub>2</sub>, and activated neutrophils subsequently increase vascular permeability both locally and systemically.<sup>31,32</sup> Erosions in the vascular walls, caused by released pancreatic enzymes, are responsible for the occurrence of significant vasospasm, reduction of pancreatic blood flow, induction of hypercoagulability, and elevation in blood viscosity resulting in substantial pancreas hypoperfusion.<sup>6</sup> Topical loss of endothelial barrier mechanisms can allow blood and large molecules such as activated proteases to infiltrate the pancreatic tissue, causing further cell injury, local pancreatic hemorrhages and pancreatic edema.<sup>7</sup> Systemic changes in vascular permeability considerably distort central hemodynamics in severe acute pancreatitis by increasing extravascular fluids penetration, which leads to ascites, pleural exudation,

hypotony, and eventually shock.<sup>33</sup> Adhesion of leukocytes to the endothelium especially in postcapillary venules is not present in the vasoconstricting – ischemic – phase. It only appears in the second, reperfusion–vasodilating – phase.<sup>12,22</sup> Reperfusion with oxygen inflow induces production of free radicals and leukocyte activation. It is also suggested that leukocyte, and platelets destroy pancreas in the reperfusion phase and are responsible for noticeable worsening of the disease course.<sup>12</sup> Furthermore, short-term vasoconstriction causes reversible changes in pancreatic morphology and physiology, while a long-lasting spasm leads to irreversible histological changes and necrotizing pancreatitis.<sup>25</sup> Our study demonstrates that early improvement of pancreatic microcirculation by induced vasodilation could be a beneficial and promising therapy; however, it requires further validation. We found out that histological changes, such as necrosis, edema and hemorrhages, were more prevalent in the control group than in the study group (lidocaine group). The presented results indicate that vasodilation caused by lidocaine decreased disease severity. These findings confirm the necessity of prompt vasodilation at the early stage of pancreatitis in order to prevent irreversible microcirculatory changes in the pancreas. According to demonstrated pathophysiology of acute pancreatitis, vasodilation should be considered the primary treatment option. It is worth mentioning that improved hypoperfusion is associated with lower levels of trypsinogen activation peptide, which correlates with the severity of pancreatitis.<sup>4</sup> Microvascular disturbances are not limited only to the pancreas. It is suggested that systemic inflammatory response syndrome (SIRS) and subsequent organ failure (OR) derive from intensive and prolonged intrapancreatic leukocyte–endothelium interactions, hypercoagulability, thrombi formation, and an increase in platelet count.<sup>8,34</sup>

These factors are likely to influence the condition of other organs, which has already been confirmed by thrombi found in the vascular bed of the spleen and lungs.<sup>35</sup>










To date, only a few studies dealing with the improvement of pancreatic blood flow were performed.<sup>36,37</sup> However, to our knowledge, this is the first study of a new method that aims to restore adequate microcirculation by vasodilation, and enables effective treatment at the first phase of pancreatitis. Vascular disturbances seem to be crucial in the development and progression of acute pancreatitis with further systemic complications. Thus, numerous authors indicate the relevance of pancreatic blood flow improvement.<sup>10,12,22,29,38</sup> Previous studies focused on restoring sufficient vascular architecture by administering heparin, endothelin receptor antagonists and PAF, or by performing aggressive fluid resuscitation.<sup>6</sup> Ke et al. indicated the important role of low-molecular-weight heparin in attenuating necrosis and restoring pancreatic perfusion, which leads to the improvement of microcirculation.<sup>36</sup> Endothelin participates in the progression of pancreatitis

by its vasoconstricting action and subsequent hypoperfusion.<sup>33,38,39</sup> It was shown that blockage of endothelin receptor (ET-A) increases blood flow and decreases vascular permeability.<sup>37</sup> Bradykinin and PAF antagonists were linked with decreased pancreatitis severity, also owing to the improvement of pancreatic blood flow, a decrease in vascular permeability and a reduction of leukocyte adhesion.<sup>6,22</sup> Fluid therapy, when initiated in a very early stage of pancreatitis, can presumably improve clinical course by enhancing microcirculation.<sup>40</sup> These experimental methods, although promising, need further validation and their effectiveness should be compared with lidocaine efficacy. We hypothesize that a combination of lidocaine with some of the other previously tested drugs can presumably turn out to be more effective than therapy with lidocaine alone. This could be explained by the feasible increase in the availability of infused therapeutics due to enhanced pancreatic blood flow caused by vasodilating action of lidocaine. We hope that our findings will contribute to introducing an innovative acute pancreatitis treatment method.

## Conclusions

Intra-arterial lidocaine infusion into the celiac trunk decreases pancreatitis severity. What is more, this study demonstrates the relevance of early vasodilation induction in the therapy of acute pancreatitis. To our knowledge, this is the first study describing a new method that aims to restore adequate pancreatic blood flow by inducing vasodilation in the early, vasoconstricting phase of acute pancreatitis. Further comparative human studies need to be conducted in order to precisely assess the long-term therapeutic effect of lidocaine and to confirm the efficacy of this method in treating acute pancreatitis.

### ORCID iDs

Ryszard Antkowiak  <https://orcid.org/0000-0003-1377-1608>  
 Łukasz Antkowiak  <https://orcid.org/0000-0003-0145-4680>  
 Sławomir Grzegorzczyn  <https://orcid.org/0000-0002-5248-3505>  
 Klaudia Nalik-Iwaniak  <https://orcid.org/0000-0003-3140-7172>  
 Natalia Kabała  <https://orcid.org/0000-0001-5707-7349>  
 Zbigniew Arent  <https://orcid.org/0000-0002-5997-2555>  
 Edyta Warmusz-Reichman  <https://orcid.org/0000-0002-1061-807X>  
 Katarzyna Stęplewska  <https://orcid.org/0000-0002-0971-2317>  
 Paweł Domosławski  <https://orcid.org/0000-0003-1903-0843>

### References

1. Goodchild G, Chouhan M, Johnson GJ. Practical guide to the management of acute pancreatitis. *Frontline Gastroenterol.* 2019;10(3): 292–299. doi:10.1136/flgastro-2018-101102
2. Machicado JD, Papachristou GI. Pharmacologic management and prevention of acute pancreatitis. *Curr Opin Gastroenterol.* 2019;35(5): 460–467. doi:10.1097/MOG.0000000000000563
3. Garg PK, Singh VP. Organ failure due to systemic injury in acute pancreatitis. *Gastroenterology.* 2019;156(7):2008–2023. doi:10.1053/j.gastro.2018.12.041
4. Chatila AT, Bilal M, Guturu P. Evaluation and management of acute pancreatitis. *World J Clin Cases.* 2019;7(9):1006–1020. doi:10.12998/wjcc.v7.i9.1006

5. Sah RP, Garg P, Saluja AK. Pathogenic mechanisms of acute pancreatitis. *Curr Opin Gastroenterol.* 2012;28(5):507–515. doi:10.1097/MOG.0b013e3283567f52
6. Cuthbertson CM, Christophi C. Disturbances of the microcirculation in acute pancreatitis. *Br J Surg.* 2006;93(5):518–530. doi:10.1002/bjs.5316
7. Bhatia M, Wong FL, Cao Y, et al. Pathophysiology of acute pancreatitis. *Pancreatol.* 2005;5(2–3):132–144. doi:10.1159/000085265
8. Menger MD, Plusczyk T, Vollmar B. Microcirculatory derangements in acute pancreatitis. *J Hepatobiliary Pancreat Surg.* 2001;8(3):187–194. doi:10.1007/s005340170015
9. Warshaw AL, O'Hara PJ. Susceptibility of the pancreas to ischemic injury in shock. *Ann Surg.* 1978;188(2):197–201. doi:10.1097/00000658-197808000-00012
10. Kinnala PJ, Kuttala KT, Grönroos JM, Havia TV, Nevalainen TJ, Niinikoski JH. Pancreatic tissue perfusion in experimental acute pancreatitis. *Eur J Surg.* 2001;167(9):689–694. doi:10.1080/11024150152619345
11. Klar E, Messmer K, Warshaw AL, Herfarth C. Pancreatic ischaemia in experimental acute pancreatitis: Mechanism, significance and therapy. *Br J Surg.* 1990;77(11):1205–1210. doi:10.1002/bjs.1800771104
12. Vollmar B, Menger MD. Microcirculatory dysfunction in acute pancreatitis. A new concept of pathogenesis involving vasomotion-associated arteriolar constriction and dilation. *Pancreatol.* 2003;3(3):181–190. doi:10.1159/000070727
13. Foitzik T, Eibl G, Hotz B, et al. Persistent multiple organ microcirculatory disorders in severe acute pancreatitis: Experimental findings and clinical implications. *Dig Dis Sci.* 2002;47(1):130–138. doi:10.1023/a:1013284008219
14. Johns RA, DiFazio CA, Longnecker DE. Lidocaine constricts or dilates rat arterioles in a dose-dependent manner. *Anesthesiology.* 1985;62(2):141–144. doi:10.1097/00000542-198502000-00008
15. Kim KH, Lee MG, Kim DG. The cholecystokinin receptor antagonist L-364,718 reduces taurocholate-induced pancreatitis in rats. *Int J Pancreatol.* 1996;20(3):205–211. doi:10.1007/BF02803770
16. Satoh K, Kamada S, Kumagai M, Sato M, Kuji A, Joh S. Effect of lidocaine on swine lingual and pulmonary arteries. *J Anesth.* 2015;29(4):529–534. doi:10.1007/s00540-014-1965-9
17. Newton DJ, McLeod GA, Khan F, Belch JJ. Mechanisms influencing the vasoactive effects of lidocaine in human skin. *Anaesthesia.* 2007;62(2):146–150. doi:10.1111/j.1365-2044.2006.04901.x
18. de Klaver MJ, Buckingham MG, Rich GF. Lidocaine attenuates cytokine-induced cell injury in endothelial and vascular smooth muscle cells. *Anesth Analg.* 2003;97(2):465–470. doi:10.1213/01.ane.0000073162.27208.e9
19. Piaszcik M, Rydzewska G, Milewski J, et al. The results of severe acute pancreatitis treatment with continuous regional arterial infusion of protease inhibitor and antibiotic: A randomized controlled study. *Pancreas.* 2010;39(6):863–867. doi:10.1097/MPA.0b013e3181d37239
20. Mikami Y, Takeda K, Matsuda K, et al. Rat experimental model of continuous regional arterial infusion of protease inhibitor and its effects on severe acute pancreatitis. *Pancreas.* 2005;30(3):248–253. doi:10.1097/01.mpa.0000153328.54569.28
21. Manohar M, Verma AK, Venkateshaiah SU, Sanders NL, Mishra A. Pathogenic mechanisms of pancreatitis. *World J Gastrointest Pharmacol Ther.* 2017;8(1):10–25. doi:10.4292/wjgpt.v8.i1.10
22. Sunamura M, Yamauchi J, Shibuya K, et al. Pancreatic microcirculation in acute pancreatitis. *J Hepatobiliary Pancreat Surg.* 1998;5(1):62–68. doi:10.1007/pl00009952
23. Rakoncay Z Jr, Hegyi P, Takács T, McCarroll J, Saluja AK. The role of NF- $\kappa$ B activation in the pathogenesis of acute pancreatitis. *Gut.* 2008;57(2):259–267. doi:10.1136/gut.2007.124115
24. Dawra R, Sah RP, Dudeja V, et al. Intra-acinar trypsinogen activation mediates early stages of pancreatic injury but not inflammation in mice with acute pancreatitis. *Gastroenterology.* 2011;141(6):2210–2217.e2. doi:10.1053/j.gastro.2011.08.033
25. Plusczyk T, Witzel B, Menger MD, Schilling M. ETA and ETB receptor function in pancreatitis-associated microcirculatory failure, inflammation, and parenchymal injury. *Am J Physiol Gastrointest Liver Physiol.* 2003;285(1):G145–G153. doi:10.1152/ajpgi.00181.2002
26. Laude K, Beauchamp P, Thuillez C, Richard V. Endothelial protective effects of preconditioning. *Cardiovasc Res.* 2002;55(3):466–473. doi:10.1016/s0008-6363(02)00277-8
27. Kusterer K, Poschmann T, Friedemann A, Enghofer M, Zandler S, Usadel KH. Arterial constriction, ischemia-reperfusion, and leukocyte adherence in acute pancreatitis. *Am J Physiol.* 1993;265(1 Pt 1):G165–G171. doi:10.1152/ajpgi.1993.265.1.G165
28. Plusczyk T, Westermann S, Rathgeb D, Feifel G. Acute pancreatitis in rats: Effects of sodium taurocholate, CCK-8, and Sec on pancreatic microcirculation. *Am J Physiol.* 1997;272(2 Pt 1):G310–G320. doi:10.1152/ajpgi.1997.272.2.G310
29. Zhou ZG, Chen YD, Sun W, Chen Z. Pancreatic microcirculatory impairment in experimental acute pancreatitis in rats. *World J Gastroenterol.* 2002;8(5):933–936. doi:10.3748/wjg.v8.i5.933
30. Ghimire K, Altmann HM, Straub AC, Isenberg JS. Nitric oxide: What's new to NO? *Am J Physiol Cell Physiol.* 2017;312(3):C254–C262. doi:10.1152/ajpcell.00315.2016
31. Anderson MC, Schoenfeld FB, Iams WB, Suwa M. Circulatory changes in acute pancreatitis. *Surg Clin North Am.* 1967;47(1):127–140. doi:10.1016/s0039-6109(16)38138-5
32. Eibl G, Buhr HJ, Foitzik T. Therapy of microcirculatory disorders in severe acute pancreatitis: What mediators should we block? *Intensive Care Med.* 2002;28(2):139–146. doi:10.1007/s00134-001-1194-1
33. Foitzik T, Eibl G, Hotz HG, Faulhaber J, Kirchengast M, Buhr HJ. Endothelin receptor blockade in severe acute pancreatitis leads to systemic enhancement of microcirculation, stabilization of capillary permeability, and improved survival rates. *Surgery.* 2000;128(3):399–407. doi:10.1067/msy.2000.107104
34. Aggarwal A, Manrai M, Kochhar R. Fluid resuscitation in acute pancreatitis. *World J Gastroenterol.* 2014;20(48):18092–18103. doi:10.3748/wjg.v20.i48.18092
35. Ranson JH, Lackner H, Berman IR, Schinella R. The relationship of coagulation factors to clinical complications of acute pancreatitis. *Surgery.* 1977;81(5):502–511.
36. Ke L, Ni HB, Tong ZH, Li WQ, Li N, Li JS. Efficacy of continuous regional arterial infusion with low-molecular-weight heparin for severe acute pancreatitis in a porcine model. *Shock.* 2014;41(5):443–448. doi:10.1097/SHK.0000000000000129
37. Eibl G, Hotz HG, Faulhaber J, Kirchengast M, Buhr HJ, Foitzik T. Effect of endothelin and endothelin receptor blockade on capillary permeability in experimental pancreatitis. *Gut.* 2000;46(3):390–394. doi:10.1136/gut.46.3.390
38. Zhou ZG, Chen YD. Influencing factors of pancreatic microcirculatory impairment in acute pancreatitis. *World J Gastroenterol.* 2002;8(3):406–412. doi:10.3748/wjg.v8.i3.406
39. Inoue K, Hirota M, Kimura Y, Kuwata K, Ohmuraya M, Ogawa M. Further evidence for endothelin as an important mediator of pancreatic and intestinal ischemia in severe acute pancreatitis. *Pancreas.* 2003;26(3):218–223. doi:10.1097/00006676-200304000-00002
40. Singh VK, Gardner TB, Papachristou GI, et al. An international multicenter study of early intravenous fluid administration and outcome in acute pancreatitis. *United European Gastroenterol J.* 2017;5(4):491–498. doi:10.1177/2050640616671077



# Macrophage migration inhibitory factor gene polymorphisms as exacerbating factors of apical periodontitis

Andrea Freer-Rojas<sup>1,A,B,D</sup>, Luis Carlos Martínez-Garibay<sup>1,A,B,D</sup>, Fernando Torres-Méndez<sup>1,A,C</sup>, Claudia Edith Dávila-Pérez<sup>1,A,C</sup>, Gabriel Alejandro Martínez-Castañón<sup>2,E,F</sup>, Nuria Patiño-Marín<sup>2,E,F</sup>, Jorge Alejandro Alegría-Torres<sup>3,4,A,C-F</sup>

<sup>1</sup> Department of Endodontics, Dental School, Autonomous University of San Luis Potosí, Mexico

<sup>2</sup> Clinical Research Laboratory, Program of Doctorate in Dental Sciences, Autonomous University of San Luis Potosí, Mexico

<sup>3</sup> Department of Pharmacy, University of Guanajuato, Mexico

<sup>4</sup> Molecular Nutrition Research Laboratory, LIMON, University of Central Mexico UCEM, San Luis Potosí, Mexico

A – research concept and design; B – collection and/or assembly of data; C – data analysis and interpretation;

D – writing the article; E – critical revision of the article; F – final approval of the article

Advances in Clinical and Experimental Medicine, ISSN 1899–5276 (print), ISSN 2451–2680 (online)

Adv Clin Exp Med. 2020;29(5):597–602

## Address for correspondence

Jorge Alegría-Torres

E-mail: ja.alegriatorres@ugto.mx

## Funding sources

None declared

## Conflict of interest

None declared

Received on June 27, 2018

Reviewed on July 30, 2018

Accepted on April 29, 2020

Published online on May 19, 2020

## Abstract

**Background.** Two polymorphisms in the macrophage migration inhibitory factor (*MIF*) gene have been associated with inflammatory diseases (-794 CATT5–8 and -173G>C); however, so far there are no reports of studies related to oral health.

**Objectives.** To genotype the -794 CATT5–8 and -173G>C *MIF* polymorphisms in Mexican patients with apical periodontitis as a genetic risk of exacerbation.

**Material and methods.** The study involved 120 patients with apical periodontitis: 60 with a diagnosis of acute apical periodontitis (Group A) and 60 without previous episodes of exacerbation (Group B). Allelic discrimination was performed from peripheral blood DNA; the repeat polymorphism -794 CATT5–8 was genotyped with sequencing, while the -173G>C polymorphism was determined using real-time polymerase chain reaction (RT-PCR) using TaqMan probes. The associations between *MIF* polymorphisms, haplotypes and the risk of exacerbated apical periodontitis were assessed.

**Results.** The allele CATT7 was associated with the risk of a stage of acute inflammation (OR = 4.13; 95% CI = 1.82–9.63;  $p < 0.001$ ). Regarding the -173G >C polymorphism, a process of inflammation exacerbation was only associated with the CC genotype (OR = 4.1; 95% CI = 1.02–20.84;  $p = 0.045$ ). The analysis of the haplotype showed that the combination CATT7/C increases the risk of exacerbation of apical periodontitis (OR = 3.57; 95% CI = 1.038–13.300;  $p = 0.021$ ).

**Conclusions.** The polymorphisms -794 CATT5–8 and -173G>C *MIF* seem to significantly influence the development of a state of exacerbated inflammation in patients with apical periodontitis.

**Key words:** apical periodontitis, genetic polymorphisms, macrophage migration inhibitory factor

## Cite as

Freer-Rojas A, Martínez-Garibay LC, Torres-Méndez F, et al. Macrophage migration inhibitory factor gene polymorphisms as exacerbating factors of apical periodontitis. *Adv Clin Exp Med.* 2020;29(5):597–602. doi:10.17219/acem/121508

## DOI

10.17219/acem/121508

## Copyright

© 2020 by Wrocław Medical University

This is an article distributed under the terms of the Creative Commons Attribution 3.0 Unported (CC BY 3.0) (<https://creativecommons.org/licenses/by/3.0/>)

## Introduction

Periodontitis is an inflammatory condition which affects areas such as the gingivae, periodontal ligaments and alveolar bones because of viral or bacterial infections. In acute episodes, there is pain because of an increase in hypersensitivity to touch.<sup>1</sup> According to several studies, the prevalence of periodontitis increases with age and could be a problem in more than 60% of the world population.<sup>2–4</sup> When acute inflammation becomes apparent in the tissue, cells of the immune system such as macrophages, lymphocytes and plasma cells are wrapped in collagenous connective tissue as part of the antimicrobial response. As a result, the cytokines block not only the osteoclastic activity but also bone reabsorption, leading to asymptomatic latent or inactive granuloma without visible changes in a radiographic image.<sup>1</sup>

When the balance of the periapical area is broken, bacterial proliferation can be triggered towards the radicular conduct and periapical tissues, with subsequent exacerbation of chronic periodontitis, which manifests itself in the formation of a secondary abscess.<sup>5</sup> In this process, interleukins such as tumor necrosis factor  $\alpha$  (TNF- $\alpha$ ), interleukin 1b (IL-1b), IL-6, and IL-8 intervene as mediators of inflammation.<sup>6</sup> The macrophage migration inhibitory factor (MIF) is another regulatory cytokine of the innate immune response expressed by macrophages, monocytes, B cells and dendritic cells as well as granulocytes.<sup>7,8</sup>

The MIF is considered an important component in the defense against bacterial infections, since this cytokine promotes the release of pro-inflammatory molecules<sup>9,10</sup>; however, its overexpression could lead to an acute exacerbated response. In fact, MIF has been used as a biomarker of diseases with a relevant inflammatory component.<sup>11,12</sup>

Two polymorphisms located in the promotor region of the *MIF* gene are associated with inflammatory diseases. First, the short tandem repeat CATT<sub>5–8</sub> is a tetranucleotide that is repeated between 5 and 8 times in position -794; increases in the numbers of repetitions produce a corresponding increase in MIF promoter activity.<sup>13</sup> On the other hand, C-173G, a single nucleotide polymorphism (SNP), acts to enhance the union of the transcription factor AP4 and the subsequent overexpression of MIF.<sup>14</sup> Both polymorphisms have been studied as factors related to the pathogenesis of sepsis, severe acute respiratory syndrome, asthma, arthritis, glomerulonephritis, and inflammatory bowel disease.<sup>12,15</sup>

However, we have found no scientific reports that associate MIF polymorphisms with acute inflammatory processes in the oral cavity. Therefore, the goal of this study was to evaluate the risk of exacerbation in Mexican patients with a diagnosis of apical periodontitis by analyzing the distribution of alleles, genotypes and haplotypes in 2 groups: patients without previous episodes of exacerbation, and patients with a medical history of exacerbation.

## Material and methods

### Characteristics of the study groups

A cross-sectional study of 120 patients including 46 males (38.3%) and 74 females (61.7%) between 18 and 72 years of age diagnosed with apical periodontitis at the endodontic clinic at the University of San Luis Potosí, Mexico, was carried out. Anthropometric data and clinical histories were collected from all patients. The individuals were classified into 2 groups according to clinical assessment.

Group A included 60 patients with pulp necrosis associated with acute apical abscess or phoenix abscess. Symptoms could vary from moderate to severe, including intraoral/extraoral edema, exudate, tumefaction, and pain on palpation or percussion. In severe cases, fever and/or lymphadenopathy could also be observed. When the diagnosis was acute apical abscess, no periapical lesion could be detected radiographically, while for a phoenix abscess, a periapical lesion could be greater than 2 mm.

Group B also included 60 patients with chronic apical periodontitis, but without a previous history of exacerbation. A negative response to a cold thermic test was diagnosed as pulp necrosis. The patients could have mild or no pain on palpation or percussion. Radiographically, a periapical lesion with a diameter wider than 2 mm needed to be detected.

This project was previously approved by the bioethics committee at the Autonomous University of San Luis Potosí (approval No. CEJ-FE-009-014), and informed consent was obtained from all the participants prior to initiating our study. All the procedures performed were in accordance with the 1964 Helsinki Declaration and its later amendments or comparable ethical standards.

### DNA purification

DNA was isolated from blood obtained by venous puncture and preserved at  $-80^{\circ}\text{C}$  in accordance with a previously described protocol.<sup>16</sup> Briefly, 1 mL of blood was treated with a pH 7.5 lysis solution (0.3 M sucrose, 10 mM Tris-HCl pH 7.5, 5 mM MgCl<sub>2</sub>, and 1% Triton X-100). Leukocytes were obtained with centrifugation and washed with the lysis solution. Subsequently, the pellet was suspended in 10 mM Tris-HCl pH 8 and lysed with 20 mg/mL laundry detergent. Proteins were precipitated with 5 M NaCl and the supernatant was treated with cold 96% ethanol. The DNA was washed with 70% ethanol and suspended in nuclease-free water. The samples were analyzed with the help of a UV-spectrophotometer at 260 nm and 280 nm. The ratio of the absorbance at 260 nm and 280 nm (A<sub>260/280</sub>) was used as indicator of purity of DNA; a value between 1.4 and 2 was considered acceptable. The DNA samples were standardized to a final concentration of 30 ng/ $\mu\text{L}$  and frozen until use. All the reagents were purchased from Sigma-Aldrich (St. Louis, USA).



## Genotyping

CATT<sub>5–8</sub> repetitions in the position -794 of the *MIF* gene were identified with sequencing from a polymerase chain reaction (PCR) product obtained using the following oligonucleotides: (F) 5'-TGTCCTCTTCCTGCTATGTC/(R) 5'-CACTAATGGTAAACTCGGGG -3'.<sup>17</sup> The final volume of each PCR was 25 µL with the following composition: 5 µL 5 × iProof<sup>TM</sup> HF Buffer (BioLabs, Cambridge, USA), 120 ng of DNA and 0.125 µL of Taq polymerase (1.25 units). For each primer, the final concentrations were 200 nM and 200 µM for deoxynucleotide triphosphates (dNTPs) (BioLabs). The amplification conditions were 1 cycle at 95°C for 1 min; 35 cycles at 95°C for 30 s, 60°C for 30 s and 72°C for 30 s; and finally, 1 cycle at 72°C for 2 min. All PCR assays were performed in duplicate in a T100<sup>TM</sup> Thermal Cycler (Bio-Rad Laboratories Inc., Hercules, USA). The amplification products were previously verified in 3% agarose gel electrophoresis, and the sequencing service was provided by LANBAMA (IPICYT, San Luis Potosí, Mexico).

The *MIF* -173G>C polymorphism was detected with real-time PCR (RT-PCR) using allele-specific oligonucleotide probes for both wild-type and mutant alleles, labeled with different fluorescent tags. The primers used were as follows: (F) 5'-CCAGCAACCGCCGCTAAG-3'/(R) 5'-TGCG-GACTAACATCGGTGA-3', and the probe for the -173G allele was [Q705]-ACCGCTCCAACCTGTT-[BHQ2], while the probe for the -173C allele was [Cy5]-CCGCTCCAAGCT-GTT-[BHQ2]. The primers and probes were designed by RealTimeDesign software and purchased from BioSearch Technologies Inc. (Petaluma, USA). The qPCR was carried out with 30 ng of genomic DNA. Each sample (10 µL) was analyzed in duplicate and contained 5 µL of iQTM Multiplex Powermix (Bio-Rad) and 300 nmol of each primer and probe. The PCR cycles were programmed on a CFX96 Touch Real-time PCR detection system (Bio-Rad) and consisted of hot-start incubation (95°C, 3 min) and amplification for 45 cycles (95°C, 15 s; 59°C, 1 min). Genotypes were distinguished by post-read PCR fluorescence of normalized reported values for wild-type and mutant alleles. The genotype of each sample was determined using a multicomponent algorithm, generating 3 allelic clusters: GG, GC and CC genotypes.

## Statistical analysis

Geometric means and standard deviations (SD) were calculated for continuous variables, percentages by gender and frequencies for alleles, genotypes and haplotypes. Comparisons of means between the 2 study groups were analyzed using the Mann–Whitney U test, while differences in the distribution of alleles and genotypes were analyzed using the  $\chi^2$  test. The Hardy–Weinberg equilibrium for the alleles was measured using the  $\chi^2$  test, and the linkage disequilibrium (LD) between the loci was calculated using a 2-locus LD calculator.

The association magnitude was quantified with odds ratios (OR) with 95% confidence intervals (95% CI) to calculate the risk of exacerbation of apical periodontitis. A binomial logistic regression analysis was used after categorization by alleles, genotypes and haplotypes, considering the clinical diagnosis as a dependent variable with a binary outcome (acute vs chronic apical periodontitis). Results were considered statistically significant when  $p < 0.05$ . All the analyses were performed with an IBM SPSS v. 19.0 statistic software package (IBM Corp., Armonk, USA).

## Results

A total of 120 patients with diagnoses of apical periodontitis were included in this study, 50% with a history of at least 1 acute episode (Group A) and the other half with chronic apical periodontitis without exacerbations (Group B). The percentages of women and men were 62.7 and 37.3, respectively; the average age was 36.4 years. With respect to the body mass index (BMI), 43.2% corresponded to normal weight, 35.2% to overweight and 21.6% to obesity. Age, the proportion of women and men and BMI did not differ between the 2 groups when the data was statistically analyzed. These results are summarized in Table 1.

The allelic and genotyping frequencies, as well as the distribution of them between the 2 study groups, are shown in Table 2. In the case of the *MIF* -794 CATT<sub>5–8</sub> polymorphisms, frequencies of 0.23, 0.57 and 0.2 were found for CATT<sub>5</sub>, CATT<sub>6</sub> and CATT<sub>7</sub>, respectively; the CATT<sub>8</sub>

Table 1. Characteristics of the study population

Variable	Total n = 120 mean (min–max) (%)	Group A (AP*) n = 60 mean (min–max) (%)	Group B (CP*) n = 60 mean (min–max) (%)	p-value
Age mean (min–max)	36.4 (12–72)	37.4 (18–69)	35.6 (12–72)	0.45 <sup>a</sup>
Women	62.7	50	74	0.13 <sup>b</sup>
Men	37.3	50	26	–
BMI, mean (min–max)	26.7 (18.4–46.3)	27.1 (18.4–36.6)	26.4 (18.4–46.3)	0.33 <sup>a</sup>
Normal weight	43.2	37.5	48.2	–
Overweight	35.2	41.7	29.6	–
Obesity	21.6	20.8	22.2	0.64 <sup>b</sup>

<sup>a</sup>Mann–Whitney U test; <sup>b</sup> $\chi^2$  test; \*AP – acute periapical periodontitis; CP – chronic periapical periodontitis; BMI – body mass index.

**Table 2.** Allelic and genotypic frequencies of -794 CATT<sub>5-8</sub> and G-173C *MIF* polymorphisms in the study group

<i>MIF</i> polymorphism	Total n (%)	Group A (AP*) n	Group B (CP*) n	p-value <sup>b</sup>
<b>-794 CATT<sub>5-8</sub></b>				
Allele				
CATT <sub>5</sub>	55 (23)	16	39	0.001
CATT <sub>6</sub>	136 (57)	73	63	
CATT <sub>7</sub>	49 (20)	31	18	
CATT <sub>8</sub>	0	0	0	
Genotype				
CATT 5/5	12 (10)	3	9	0.060
CATT 5/6	26 (22)	8	18	
CATT 5/7	5 (4)	2	3	
CATT 6/6	50 (42)	30	20	
CATT 6/7	10 (8)	5	5	
CATT 7/7	17 (14)	5	12	
<b>G-173C</b>				
Allele				
G	150 (62.5)	68	82	0.125
C	90 (37.5)	50	40	
Genotype				
GG	43 (36)	19	24	0.122
GC	64 (53)	30	34	
CC	13 (11)	10	3	

<sup>b</sup> $\chi^2$  test; \*AP – acute periapical periodontitis; CP – chronic periapical periodontitis.

allele was not found in any of the participants. Regarding the -173G>C polymorphism, the frequencies for G and C alleles were 0.625 and 0.375, respectively, following the Hardy–Weinberg equilibrium ( $\chi^2 = 2.28$ ,  $p = 0.13$ ). Both *MIF* polymorphisms were found in linkage disequilibrium ( $D' = 0.635$ ,  $r^2 = 0.179$ ,  $\chi^2 = 17.72$ ). When the distribution of alleles and genotypes of -794 CATT<sub>5-8</sub> and -173G>C variants were analyzed between the 2 study groups, we found that only the CATT polymorphism had a different statistically significant distribution between the groups ( $p = 0.001$ ).

Odds ratios were measured for *MIF* polymorphisms according to the classification of apical periodontitis (acute vs chronic). As shown in Table 3, an association was established in individuals carrying the alleles -794 CATT<sub>6</sub> (OR = 2.8; 95% CI = 1.44–5.62;  $p = 0.002$ ) and CATT<sub>7</sub> (OR = 4.13; 95% CI = 1.82–9.63;  $p < 0.001$ ), while no association with the -173C allele was found. The analysis by genotype showed that the CATT risk alleles are associated with acute episodes of apical periodontitis only in a homozygous model. In fact, CATT7/7 had a greater strength of association and increased odds with respect to CATT6/6 (OR = 4.39, 95% CI = 1.09–22.28 and  $p = 0.03$  vs OR = 6.65, 95% CI = 1.29–42.49 and  $p = 0.02$ ). In the case of the -173C/C genotype, an association was

**Table 3.** Analysis of the association of *MIF* alleles and genotypes with the risk of exacerbation of periapical periodontitis

<i>MIF</i> polymorphisms	OR (95% CI)	p-value
<b><i>MIF</i> alleles</b>		
<b>-784 CATT<sub>5-8</sub></b>		
CATT <sub>5</sub>	1	–
CATT <sub>6</sub>	2.8 (1.44–5.62)	0.002
CATT <sub>7</sub>	4.13 (1.82–9.63)	<0.001
<b>-173G/C</b>		
G	1	–
C	0.81 (0.52–1.28)	0.18
<b><i>MIF</i> genotypes</b>		
<b>-784 CATT<sub>5-8</sub></b>		
5/5	1	–
5/6	1.32 (28.00–7.48)	0.74
5/7	1.91 (0.16–20.30)	0.58
5/5	1	–
6/6	4.39 (1.09–22.28)	0.03
6/7	3.11 (1.63–6.10)	<0.001
7/7	6.65 (1.29–42.49)	0.02
<b>-173G/C</b>		
GG co-dominant	1	–
GC	1.18 (0.54–2.60)	0.67
CC	4.1 (1.02–20.84)	0.045
GG dominant	1	–
GC+CC	1.36 (0.64–2.91)	0.42
GG+GC recessive	1	–
CC	3.9 (1.064–18.50)	0.019

OR – odds ratio.

observed in a homozygous model (OR = 4.1; 95% CI = 1.02–20.84;  $p = 0.045$ ) as well as a recessive model (OR = 3.9; 95% CI = 1.064–18.500;  $p = 0.019$ ).

An analysis of haplotypes was conducted considering the -794CATT<sub>5</sub>/-173G combination as a reference (Table 4).

**Table 4.** Haplotype frequencies of the -784 CATT<sub>5-8</sub> and -173G/C *MIF* polymorphisms and the risk of exacerbation of periapical periodontitis

Haplotype	Acute cases	Chronic cases	OR (95% CI)	p-value
CATT <sub>5</sub> /G	10	27	1	–
CATT <sub>6</sub> /G	42	43	1.6 (0.67–4.16)	0.13
CATT <sub>7</sub> /G	18	12	2.15 (0.85–7.58)	0.046
CATT <sub>5</sub> /C	7	12	0.99 (0.28–3.42)	0.49
CATT <sub>6</sub> /C	30	20	2.51 (0.96–6.83)	0.03
CATT <sub>7</sub> /C	13	6	3.57 (1.038–13.3)	0.021
Total	120	120	–	–

In our results, the CATT<sub>7</sub>/G and CATT<sub>6</sub>/C haplotypes had statistically significant associations with exacerbations of periodontitis (OR = 2.15, 95% CI = 0.85–7.58 and  $p = 0.046$  vs OR = 2.51, 95% CI = 0.96–6.83 and  $p = 0.03$ , respectively). However, the OR for the CATT<sub>7</sub>/C haplotype was greater than the other 2 combinations, taking into consideration that both *MIF* alleles were associated with a higher risk of inflammation (OR = 3.57; 95% CI = 1.038–13.300;  $p = 0.021$ ).

## Discussion

Both *MIF* -794 CATT<sub>5-8</sub> and -173G>C polymorphisms have been related to the risk of increasing the severity of the inflammatory response.<sup>12,15,18</sup> Consequently, we studied both variants as genetic risk factors for exacerbation of inflammation in patients with apical periodontitis. When patients with acute apical periodontitis and chronic apical periodontitis were compared, no correlations were observed in terms of age, sex or BMI in either study group; therefore, possible effects of age, sex or obesity on the exacerbation of periodontitis were ruled out (Table 1). The most frequent allele was CATT<sub>6</sub> (57%), while the CATT<sub>8</sub> allele was not detected, which is consistent with previous reports carried out in the Mexican population.<sup>19,20</sup> Regarding *MIF* -173G>C polymorphism, a frequency of 37.5% for risk allele C was found. This was slightly higher than previously reported for the Mexican population, in which a value around 30% has been observed; however, those studies were carried out in other geographical regions of Mexico.<sup>21–23</sup> The -794 CATT alleles showed a significant difference in distribution between the 2 groups, in contrast with the -173G>C allele, which did not show a different proportion between the acute and chronic groups (Table 2).

The genetic risk of exacerbated apical periodontitis is analyzed in Table 3, noting that CATT<sub>6</sub> and CATT<sub>7</sub> carriers have almost 3 or 4 times higher potential risk of developing an episode of acute apical periodontitis than CATT<sub>5</sub> carriers do; however, either a homozygous condition or CATT<sub>6</sub>/7 combination seems to be necessary for an acute episode. Indeed, the homozygous carriers of CATT<sub>7</sub> showed the highest risk of exacerbation, with an OR value of 6.6 (95% CI = 1.29–42.49;  $p = 0.02$ ). In fact, the CATT<sub>6</sub>/7 genotype has been considered a vulnerability factor for other health risks in the Mexican population, such as acute coronary syndrome and rheumatoid arthritis.<sup>19,20</sup>

On the other hand, risk allele C for the *MIF* -173 polymorphism was only associated with acute apical periodontitis in a homozygous condition (OR = 4.1; 95% CI = 1.02–20.84;  $p = 0.045$ ), but has also been observed in a recessive model where GG+GC genotypes were used as references (OR = 3.9; 95% CI = 1.064–18.500;  $p = 0.019$ ). Very recently, several studies have reported that the C allele in the *MIF* -173

position represents a genetic risk factor associated with diverse disorders or diseases, such as osteoporosis<sup>24</sup>; pulmonary arterial hypertension in patients with systemic sclerosis<sup>25</sup>; tuberculosis<sup>26</sup>; fibrosis in biliary atresia patients<sup>27</sup>; breast cancer, especially among older patients<sup>28</sup>; childhood asthma<sup>29</sup>; and autoimmune hepatitis with acute symptomatic presentation.<sup>30</sup> However, differences in allele frequency among racial groups is a factor to be considered when interpreting the results. In the present study, none of these diseases was reported by carriers of the -173C allele.

When a haplotype analysis was performed considering all the allele combinations between -794 CATT and -193 G>C *MIF* polymorphisms (Table 4), the association of CATT<sub>7</sub> and -173C showed the greatest risk of exacerbating periodontitis, which concurs with other studies where the CATT<sub>7</sub>/-173C haplotype has been shown to be related to an increased inflammatory process.<sup>12,19</sup> Particularly, the CATT<sub>7</sub>/-173C combination has been considered a risk factor for death in carriers with severe sepsis,<sup>31</sup> as well as a risk factor for inflammatory polyarthritis.<sup>32</sup>

Since *MIF* -794 CATT<sub>7</sub> and -173C polymorphisms can modify the gene expression and therefore the production of MIF, carriers of this allele combination would have higher levels of circulating MIF, with a consequent predisposition to an increased response to inflammatory processes<sup>13,31,33</sup>; however, plasma MIF levels were not determined in this study. More investigations into the role of MIF in the development and severity of apical periodontitis as well as the genetic predisposition to exacerbation are needed.

## Conclusions

Although several studies have shown that MIF plays a role in the pathogenesis of apical periodontitis as a promoter of other pro-inflammatory molecules,<sup>7,9,10,34</sup> *MIF* polymorphisms have only been studied in systemic types of inflammatory disorders, such as sclerosis, tuberculosis, fibrosis, and asthma.<sup>25–27,29</sup> Very few studies have looked at *MIF* polymorphisms in diseases of the oral cavity.<sup>35</sup> There are few reports in the literature about polymorphisms in pro-inflammatory cytokine genes related to apical periodontitis.<sup>36–38</sup> This study is the first report where a positive association has been found between acute stages in patients with apical periodontitis and -794 CATT<sub>7</sub> and *MIF* -173C polymorphisms.

## References

- Nair PN. Apical periodontitis: A dynamic encounter between root canal infection and host response. *Periodontol* 2000. 1997;13:121–148.
- Kirkevang LL, Vaeth M, Hörsted-Bindslev P, Wenzel A. Longitudinal study of periapical and endodontic status in a Danish population. *Int Endod J*. 2006;39(2):100–107.
- Jiménez-Pinzón A, Segura-Egea JJ, Poyato-Ferrera M, Velasco-Ortega E, Ríos-Santos JV. Prevalence of apical periodontitis and frequency of root-filled teeth in an adult Spanish population. *Int Endod J*. 2004; 37(3):167–173.

4. Hussein FE, Liew AK, Ramlee RA, Abdullah D, Chong BS. Factors associated with apical periodontitis: A multilevel analysis. *J Endod*. 2016;42(10):1441–1445.
5. Abbott PV. Classification, diagnosis and clinical manifestations of apical periodontitis. *Endod Topics*. 2014;8(1):36–54.
6. Jakovljevic A, Knezevic A, Karalic D. Pro-inflammatory cytokine levels in human apical periodontitis: Correlation with clinical and histological findings. *Aust Endod J*. 2015;41(2):72–77.
7. Calandra T, Roger T. Macrophage migration inhibitory factor: A regulator of innate immunity. *Nat Rev Immunol*. 2003;3(10):791–800.
8. Donn RP, Ray DW. Macrophage migration inhibitory factor: Molecular, cellular and genetic aspects of a key neuroendocrine molecule. *J Endocrinol*. 2004;182(1):1–9.
9. Onodera S, Nishihira J, Iwabuchi K, et al. Macrophage migration inhibitory factor up-regulates matrix metalloproteinase-9 and -13 in rat osteoblasts: Relevance to intracellular signaling pathways. *J Biol Chem*. 2010;277(10):7865–7874. doi:10.1074/jbc.M106020200
10. Toh M, Aeberli D, Lacey D, et al. Regulation of IL-1 and TNF receptor expression and function by endogenous macrophage migration inhibitory factor. *J Immunol*. 2006;177(7):4818–4825.
11. Grieb G, Merk M, Bernhagen J, Bucala R. Macrophage migration inhibitory factor (MIF): A promising biomarker. *Drug News Perspect*. 2010;23(4):257–264.
12. Renner P, Roger T, Calandra T. Macrophage migration inhibitory factor: Gene polymorphisms and susceptibility to inflammatory diseases. *Clin Infect Dis*. 2005;41(Suppl 7):S513–519.
13. Baugh JA, Chitnis S, Donnelly SC. A functional promoter polymorphism in the macrophage migration inhibitory factor (MIF) gene associated with disease severity in rheumatoid arthritis. *Genes Immun*. 2002;3(3):170–176.
14. Bucala R. MIF alleles and the regulation of the host response. In: Bucala R, ed. *The MIF Handbook*. Hackensack, NJ: World Scientific Publishing Company; 2012.
15. Bucala R. MIF alleles, and prospects for therapeutic intervention in autoimmunity. *J Clin Immunol*. 2013;33(Suppl 1):S72–78.
16. García-Sepulveda CA, Carrillo-Acuña E, Guerra-Palomares SE, Barriga-Moreno M. Maxiprep genomic DNA extractions for molecular epidemiology studies and biorepositories. *Mol Biol Rep*. 2010;37(4):1883–1890.
17. Matia-García I, Salgado-Goytia L, Muñoz-Valle JF, et al. Macrophage migration inhibitory factor promoter polymorphisms (-794 CATT 5-8 and -173 G>C): Relationship with mRNA expression and soluble MIF levels in young obese subjects. *Dis Markers*. 2015;46:1208. doi:10.1155/2015/461208
18. Falvey JD, Bentley RW, Merriman TR, et al. Macrophage migration inhibitory factor gene polymorphisms in inflammatory bowel disease: An association study in New Zealand Caucasians and meta-analysis. *World J Gastroenterol*. 2013;19(39):6656–6664.
19. Llamas-Covarrubias MA, Valle Y, Bucala R, et al. Macrophage migration inhibitory factor (MIF): Genetic evidence for participation in early onset and early stage rheumatoid arthritis. *Cytokine*. 2013;61(3):759–765.
20. Valdés-Alvarado E, Muñoz-Valle JF, Valle Y, et al. Association between the -794 (CATT)5-8 MIF gene polymorphism and susceptibility to acute coronary syndrome in a Western Mexican population. *J Immunol Res*. 2014;2014:704854. doi:10.1155/2014/704854
21. De la Cruz-Mosso U, Bucala R, Palafox-Sánchez CA, et al. Macrophage migration inhibitory factor: Association of -794 CATT5-8 and -173 G>C polymorphisms with TNF- $\alpha$  in systemic lupus erythematosus. *Hum Immunol*. 2014;75(5):433–439. doi:10.1016/j.humimm.2014.02.014
22. Morales-Zambrano R, Bautista-Herrera LA, De la Cruz-Mosso U, et al. Macrophage migration inhibitory factor (MIF) promoter polymorphisms (-794 CATT5-8 and -173 G>C): association with MIF and TNF $\alpha$  in psoriatic arthritis. *Int J Clin Exp Med*. 2014;7(9):2605–2614.
23. Martínez-Guzmán MA, Alvarado-Navarro A, Pereira-Suárez AL, Muñoz-Valle JF, Fafutis-Morris M. Association between STR -794 CATT5-8 and SNP -173 G/C polymorphisms in the MIF gene and lepromatous leprosy in Mestizo patients of western Mexico. *Hum Immunol*. 2016;77(10):985–989. doi:10.1016/j.humimm.2016.07.006
24. Ozsoy AZ, Karakus N, Tural S, et al. Influence of the MIF polymorphism -173G>C on Turkish postmenopausal women with osteoporosis. *Z Rheumatol*. 2017;77(7):629–632. doi:10.1007/s00393-017-0382-5
25. Bossini-Castillo L, Campillo-Davó D, López-Isac E, et al; Spanish Scleroderma Group. An MIF promoter polymorphism is associated with susceptibility to pulmonary arterial hypertension in diffuse cutaneous systemic sclerosis. *J Rheumatol*. 2017;44(10):1453–1457.
26. Naderi M, Hashemi M, Ansari H. Macrophage migration inhibitory factor -173 G>C polymorphism and risk of tuberculosis: A meta-analysis. *EXCLI J*. 2017;16:313–320. doi:10.17179/excli2016-662
27. Sadek KH, Ezzat S, Abdel-Aziz SA, Alaraby H, Mosbeh A, Abdel-Rahman MH. Macrophage migration inhibitory factor (MIF) gene promoter polymorphism is associated with increased fibrosis in biliary atresia patients, but not with disease susceptibility. *Ann Hum Genet*. 2017;81(5):177–183.
28. Lin S, Wang M, Liu X, et al. Association of genetic polymorphisms in MIF with breast cancer risk in Chinese women. *Clin Exp Med*. 2017;17(3):395–301.
29. El-Adly TZ, Kamal S, Selim H, Botros S. Association of macrophage migration inhibitory factor promoter polymorphism -173G/C with susceptibility to childhood asthma. *Cent Eur J Immunol*. 2016;41(3):268–272.
30. Assis DN, Takahashi H, Leng L, Zeniya M, Boyer JL, Bucala R. A macrophage migration inhibitory factor polymorphism is associated with autoimmune hepatitis severity in US and Japanese patients. *Dig Dis Sci*. 2016;61(12):3506–3512.
31. Lehmann LE, Book M, Hartmann W, et al. A MIF haplotype is associated with the outcome of patients with severe sepsis: A case control study. *J Transl Med*. 2009;7:100.
32. Barton A, Lamb R, Symmons D, et al. Macrophage migration inhibitory factor (MIF) gene polymorphism is associated with susceptibility to but not severity of inflammatory polyarthritis. *Genes Immun*. 2003;4(7):487–491.
33. Qian L, Wang XY, Thapa S, et al. Macrophage migration inhibitory factor promoter polymorphisms (-794 CATT5-8): Relationship with soluble MIF levels in coronary atherosclerotic disease subjects. *BMC Cardiovasc Disord*. 2017;17(1):144.
34. Liu L, Peng B. The expression of macrophage migration inhibitory factor is correlated with receptor activator of nuclear factor kappa b ligand in induced rat apical lesions. *J Endod*. 2013;39(8):984–989.
35. Heidari Z, Mahmoudzadeh-Sagheb H, Hashemi M, Ansarimoghaddam S, Moudi B, Sheibak N. Association of macrophage migration inhibitory factor gene polymorphisms with chronic periodontitis in a South Eastern Iranian population. *Dent Res J (Isfahan)*. 2017;14(6):395–402.
36. de Sá AR, Moreira PR, Xavier GM, et al. Association of CD14, IL1B, IL6, IL10 and TNF $\alpha$  functional gene polymorphisms with symptomatic dental abscesses. *Int Endod J*. 2007;40(7):563–572.
37. Amaya MP, Criado L, Blanco B, et al. Polymorphisms of pro-inflammatory cytokine genes and the risk for acute suppurative or chronic nonsuppurative apical periodontitis in a Colombian population. *Int Endod J*. 2013;46(1):71–78.
38. Aminoshariae A, Kulild JC. Association of functional gene polymorphism with apical periodontitis. *J Endod*. 2015;41(7):999–1007.

# Annexin V in children with idiopathic nephrotic syndrome treated with cyclosporine A

Anna Jakubowska<sup>A–D</sup>, Katarzyna Kiliś-Pstrusińska<sup>A,C–F</sup>

Department and Clinic of Pediatric Nephrology, Wrocław Medical University, Poland

A – research concept and design; B – collection and/or assembly of data; C – data analysis and interpretation; D – writing the article; E – critical revision of the article; F – final approval of the article

Advances in Clinical and Experimental Medicine, ISSN 1899–5276 (print), ISSN 2451–2680 (online)

*Adv Clin Exp Med.* 2020;29(5):603–609

## Address for correspondence

Anna Jakubowska  
E-mail: an.jakubow@gmail.com

## Funding sources

None declared

## Conflict of interest

None declared

Received on March 13, 2020  
Reviewed on March 19, 2020  
Accepted on April 30, 2020

Published online on May 28, 2020

## Abstract

**Background.** Treatment with cyclosporine A (CsA), a calcineurin inhibitor, is effective in children with difficult idiopathic nephrotic syndrome (INS). Prolonged CsA treatment can result in several adverse effects, the most significant being nephrotoxicity (CsAN). The plasma and urine levels of the proteins annexin V (AnV) and uromodulin (UM) were investigated in order to assess their usefulness as indicators of early-stage CsAN. Uromodulin is considered a distal tubular damage marker. Annexin V is present in the distal tubules.

**Objectives.** To measure AnV in children with INS receiving CsA treatment and to assess the usefulness of this biomarker for monitoring CsAN and as an indicator of changes in the distal tubules of the nephron.

**Material and methods.** The prospective study included 30 patients with INS and 22 controls. Plasma and urinary AnV levels were measured 3 times: before CsA treatment, and after 6 and 12 months of therapy. The AnV levels were compared to those of UM.

**Results.** The urinary AnV and UM levels were significantly higher in the INS patients before CsA therapy in comparison to the reference group. A progressive increase of urinary AnV was observed after 6 and 12 months of therapy. Urinary UM only increased after 6 months. No significant correlations were found between plasma and urinary concentrations of the proteins studied.

**Conclusions.** The increased urinary excretion of AnV in children with INS receiving CsA treatment may suggest its usefulness as an early marker of subclinical CsAN. Annexin V seems to be a more sensitive indicator of tubular damage in the course of CsA therapy than UM, though large, multicenter studies are needed.

**Key words:** children, idiopathic nephrotic syndrome, cyclosporine nephrotoxicity, urine biomarkers

## Cite as

Jakubowska A, Kiliś-Pstrusińska K. Annexin V in children with idiopathic nephrotic syndrome treated with cyclosporine A. *Adv Clin Exp Med.* 2020;29(5):603–609. doi:10.17219/acem/121519

## DOI

10.17219/acem/121519

## Copyright

© 2020 by Wrocław Medical University  
This is an article distributed under the terms of the Creative Commons Attribution 3.0 Unported (CC BY 3.0) (<https://creativecommons.org/licenses/by/3.0/>)

## Introduction

Idiopathic nephrotic syndrome (INS) is the most common form of primary glomerulopathy in children. Although treating INS with glucocorticosteroids leads to remission in approx. 80% of children with INS, this disease is marked by a tendency towards relapses and steroid dependence. Moreover, primary corticosteroid resistance can reach as high as 45%, and a high risk of developing end-stage kidney failure has been noted (30–40% of children, over 10 years of observation).<sup>1–4</sup> In cases with a history of nephrotic syndrome and frequent relapses, steroid-dependent nephrotic syndrome (SDNS) or steroid-resistant nephrotic syndrome (SRNS), alternative treatments are employed, including the use of cyclosporine A (CsA).

It is estimated that CsA therapy leads to remission in 80–100% of cases of SDNS and in 30% of cases of SRNS. However, the length of CsA treatment is still controversial. Short-term therapies are associated with frequent relapses after the treatment ends, while the administration of drugs at low dosages for 18 months does not provide satisfactory results.<sup>5</sup> Fears of administering CsA long-term mainly stem from its nephrotoxicity (CsAN).

The early clinical and laboratory indicators of cyclosporine toxicity have not yet been clearly determined. Due to individuals' varying sensitivity to the toxic effects of the drug – independent of the dosage – monitoring CsA concentration in the serum does not guarantee the safety of this therapy. An increase in the serum creatinine concentration and a decrease in glomerular filtration rate (GFR) may not be observed until advanced, irreversible changes have taken place in the kidney. Kidney biopsy and histological evaluation of kidney tissue allow for a reliable assessment of the extent of kidney damage, though this is an invasive examination – a fact which prevents the use of biopsy for continuous monitoring. Therefore, markers of early kidney damage are sought after, as they would help to improve this therapy. One such marker may be annexin V (AnV), which belongs to the family of annexins, the cytoplasmic calcium-binding proteins.<sup>6,7</sup>

Annexin V, with a molecular weight of 32–35 kDa, occurs in large amounts in the cells of the distal tubules and the glomeruli epithelium.<sup>8</sup> It is widely used in many fields of medicine as a marker of apoptosis. It has been helpful in explaining many processes which occur in the kidneys, including acute kidney injury and diabetic nephropathy.<sup>9,10</sup> Moreover, its usefulness as a biochemical marker of atherosclerosis has been assessed in patients with chronic kidney disease (CKD)<sup>11</sup> and AnV has also been measured in studies on the causes behind impaired immunity in CKD patients.<sup>12</sup>

The aim of this study was to assess AnV concentrations in the plasma and urine of children with INS, depending on the disease history (steroid dependence or steroid resistance) and treatment (steroids or CsA), and to determine the usefulness of the abovementioned markers for monitoring CsAN, determining the prognosis of the disease course,

and indicating changes in the distal tubules of the nephron. Values of AnV concentration have been compared to concentrations of uromodulin (UM) as another marker of distal tubule damage.

## Material and methods

The study involved 52 children: 30 children with INS at the age of  $9.08 \pm 3.99$  years and 22 children with primary mono-symptomatic nocturnal enuresis at the age of  $10.50 \pm 3.39$  years (reference group). The INS diagnosis was based on the criteria of the International Study of Kidney Disease in Children.<sup>13</sup> Initially, all patients with INS were treated using glucocorticosteroids (prednisone, pulses with methylprednisolone). In accordance with the criteria of the non-profit organization Kidney Disease Improving Global Outcomes from 2012, 22 patients were diagnosed with SDNS and 8 patients with SRNS. The average duration of the disease before the introduction of CsA treatment in the entire nephrotic syndrome group was  $4.55 \pm 3.41$  years, while it was  $5.99 \pm 2.81$  years in the SDNS group and  $0.56 \pm 0.36$  years in the SRNS group. Twenty-two children were subjected to kidney biopsy before CsA therapy was initiated. Histopathological examination revealed changes which are typical of minimal change disease in 14 children, mesangial proliferation in 5 patients and focal segmental glomerulosclerosis in 1 patient. In 2 cases, kidney biopsy proved to be non-diagnostic. A biopsy was not performed in 6 patients because the typical clinical course of the disease was enough to diagnose INS. In 2 cases, the parents did not consent to the procedure.

## Methodology of the study

A prospective study was conducted. The observation time of the INS patients was 12 months. In all children with INS, blood and urine were collected before CsA was administered, and then again after 6 and 12 months of the therapy. The abovementioned time points were labelled I, II and III, respectively. In children from the reference group, blood and urine samples were collected in the morning during other routinely performed examinations, and the measurements were performed once.

In all patients, fasting blood samples were drawn from the ulnar vein. Plasma samples were obtained after centrifugation and transferred to separate test tubes to be stored at  $-80^{\circ}\text{C}$  prior to the assay. Urine samples were collected from the first morning portion of the urine, on the day of blood collection. After centrifugation at 3,000 rpm for 15 min, the precipitate was removed and the supernatant was frozen and stored at  $-80^{\circ}$  prior to biomarker measurement.

In each patient, the concentrations of AnV and UM were measured in plasma and urine with the use of the enzyme-linked immunosorbent assay (ELISA) method (eBioscience BMS252/BMS252TEN; Thermo Fisher Scientific, Waltham,

USA). The ratio of AnV and UM to creatinine was assessed. In serum, the concentrations of urea, creatinine, uric acid, total protein, albumin, and total cholesterol were assessed; in urine, the concentrations of creatinine and protein were determined using standard laboratory methods. The GFR was estimated based on Schwartz’s equation.<sup>14</sup>

The study was approved by the Ethical Committee of Wrocław Medical University, Poland (approval No. 169/2008). The parents of all subjects were fully informed about the study, and written consent forms were obtained.

### Statistical analysis

The results are presented as mean value ± standard deviation (SD) or median value and quartile range. Differences with a significance level of  $p < 0.05$  were considered to be statistically significant.

The normality of data distribution was verified using the D’Agostino–Pearson test. Depending on the normality of the data distribution and the homogeneity of the variance, the analysis of differences between 2 variables was conducted using Student’s t-test (data with normal distribution), the Welch test (normal data without variance homogeneity) or the Mann–Whitney U test (data which does

not meet the assumptions regarding normality of distribution). The significance of differences between the variables at specific time points was analyzed using a paired analysis of variance (ANOVA) test with Greenhouse–Geisser estimation or the Friedman test. Additionally, the post hoc analysis was conducted using multiple iterations of Student’s t-test or the Wilcoxon test (for ANOVA and Friedman, respectively) for paired data. In both cases, Bonferroni correction was applied.

### Results

During the 12-month observation, no disorders of the excretory function of the kidneys were observed in any of the patients with INS. Serum urea, creatinine and uric acid concentration did not differ significantly in different time points, and no differences were noted in regard to GFR (Table 1). Blood CsA concentrations remained within the therapeutic range ( $65.2 \pm 31.4$  ng/mL).

In the group of INS patients, before the introduction of CsA, the concentrations of AnV and UM were significantly higher than in the reference group (Table 2). Plasma AnV concentrations rose gradually during the observation period, and their values significantly differed between

**Table 1.** Plasma creatinine concentrations and GFR in patients with INS at 3 time points: before CsA (I) treatment, and after 6 (II) and 12 (III) months of CsA therapy

Parameter	Time point			p-value <sup>a</sup>
	I	II	III	
	mean ±SD median (1–3 quartile)	mean ±SD median (1–3 quartile)	mean ±SD median (1–3 quartile)	
Creatinine in plasma [mg/dL]	0.50 ±0.14 0.48 (0.41–0.59)	0.47 ±0.13 0.44 (0.40–0.53)	0.54 ±0.15 0.49 (0.45–0.62)	0.11
GFR [mL/min/1.73 m <sup>2</sup> ]	147 ±34.7 145 (127–163)	142 ±47.3 150 (129.3–177)	137.5 ±33.6 151 (102–160)	0.74

<sup>a</sup> comparison of values at 3 time points; p-value – level of significance; highlighted  $p < 0.05$ ; GFR – glomerular filtration rate; INS – idiopathic nephrotic syndrome; CsA – cyclosporine A.

**Table 2.** Comparison of AnV and UM concentrations in plasma (p) and urine (u) between group of children with INS before CsA treatment and the reference group

Parameter	Children with INS (n = 30) mean ±SD median (1–3 quartile)	Reference group (n = 22) mean ±SD median (1–3 quartile)	p-value
p AnV [ng/mL]	30.81 ±1.62 31.08 (29.38–32.32)	18.10 ±1.04 18.04 (17.23–19.11)	0.0001
p UM [ng/mL]	11.28 ±0.60 11.40 (10.80–11.81)	6.21 ±0.94 6.38 (5.32–7.07)	0.0001
u AnV/u creatinine [ng/mg]	15.28 ±2.31 14.61 (13.58–16.91)	5.37 ±0.28 5.36 (5.20–5.48)	0.0001
u UM/u creatinine [ng/mg]	4.93 ±0.88 4.80 (4.15–5.45)	1.93 ±0.22 1.92 (1.82–2.04)	0.0001
u total protein/u creatinine [mg/mg]	5.14 ±9.41 0.85 (0.00–5.81)	0.06 ±0.02 0.00 (0.00–0.00)	0.0005

p – plasma; u – urine; p – level of significance; highlighted  $p < 0.05$ . SD – standard deviation; INS – idiopathic nephrotic syndrome; UM – uromodulin; AnV – annexin V; CsA – cyclosporine A.

**Table 3.** Concentration values of studied variables in plasma (p) and urine (u) of the patients suffering from INS in 3 time points: before CsA treatment (I), and after 6 (II) and 12 (III) months of therapy

Parameter	Time point			p-value <sup>a</sup>
	I	II	III	
	mean ±SD median (1–3 quartile)	mean ±SD median (1–3 quartile)	mean ±SD median (1–3 quartile)	
p AnV [ng/mL]	30.81 ±1.62 31.08 (29.38–32.32)	38.22 ±2.46 38.5 (37.84–39.09)	39.35 ±1.23 39.33 (38.63–39.8)	<0.0001
p UM [ng/mL]	11.28 ±0.60 11.40 (10.80–11.81)	13.95 ±0.16 13.98 (13.9–14.06)	13.95 ±0.21 14.0 (13.92–14.09)	<0.0001 *
u AnV/u creatinine [ng/mg]	15.28 ±2.31 14.61 (13.58–16.91)	16.69 ±1.68 16.05 (15.55–7.68)	17.09 ±1.56 16.77 (15.79–18.22)	<0.0001
u UM/u creatinine [ng/mg]	4.93 ±0.88 4.80 (4.15–5.45)	6.63 ±0.85 6.34 (5.92–7.34)	6.41 ±0.93 6.33 (5.75–7.09)	<0.0001 *

<sup>a</sup> comparison of values at 3 time points; p-value – level of significance; highlighted p < 0.05; \*I vs II and I vs III; SD – standard deviation; UM – uromodulin; AnV – annexin V.

all time points in the study. Plasma UM concentrations in the group of children with INS before CsA were significantly lower than in subsequent time points of the therapy. No statistically significant difference in the concentration of this protein was noted after 6 or 12 months of treatment (Table 3). Urine AnV concentration in the INS group was significantly higher after 6 months of CsA treatment, compared to the baseline values. A further increase in the concentration of this protein was observed after 12 months of therapy ( $p < 0.0001$ ; Fig. 1). Urine UM concentrations after 6 and 12 months of therapy were significantly higher than the values from before the treatment, but the differences of urine UM after 6 and 12 months of administering the drug were not statistically significant (Fig. 2).

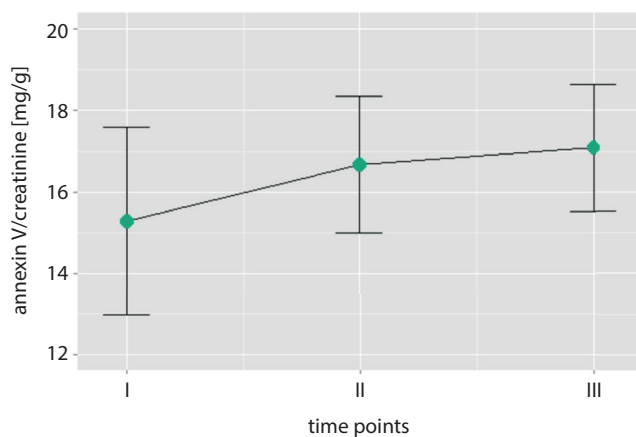


**Fig. 1.** Comparison of urine AnV concentrations in INS patients at 3 time points: before CsA treatment (I) and after 6 (II) and 12 (III) months of therapy

### Correlations between the studied variables in the group of INS patients before the start of CsA treatment (time point I)

Before the CsA therapy, there were no statistically significant correlations noted between plasma (p) AnV and UM concentrations and the concentrations of these proteins in the urine (u): pAnV vs uAnV –  $r = -0.12$ ,  $p = 0.52$ ; and pUM vs uUM –  $r = 0.02$ ,  $p = 0.93$ . Likewise, there were no statistically significant correlations found between the concentrations of AnV and UM in the plasma ( $r = -0.20$ ,  $p = 0.29$ ), while on the other hand there was significant correlation noted between studied proteins in the urine (uAnV vs uUM  $r = 0.67$ ,  $p < 0.0001$ ; Fig. 3). No significant correlations were found concerning urine AnV and UM in regard to the urine protein.

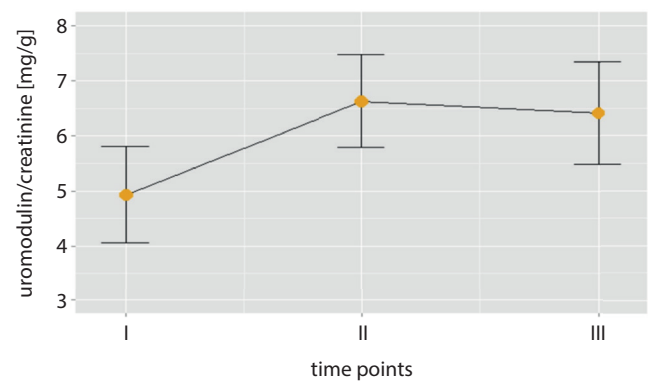


**Fig. 2.** Comparison of urine UM concentrations in INS patients at 3 time points: before CsA treatment (I) and after 6 (II) and 12 (III) months of therapy



### Correlations between the studied variables in the INS patients after 6 and 12 months of CsA treatment (time points II and III)

After 6 and 12 months of CsA treatment, there were no statistically significant correlations between the concentrations of the variables of interest in the plasma and urine, or between the concentrations of AnV and UM in the plasma. Statistically significant correlations were noted between the concentrations of AnV and UM in the urine ( $r = 0.68$  and  $r = 0.64$  after 6 and 12 months, respectively;  $p < 0.0001$ ; Fig. 3).

No correlation was found between urine AnV and UM concentrations and blood CsA concentration, after either 6 or 12 months of the treatment. At the selected time points, no significant correlations were found between the urine AnV and UM and proteinuria.

The AnV concentrations measured in the urine of patients with INS before CsA treatment and after 6 and 12 months of therapy did not correlate with the GFRs, assessed at 3 time points. There was also no correlation between serum CsA concentration and eGFR (Table 4).

No significant differences were noted between the SDNS patients and the SRNS patients in terms of the selected parameters in the plasma and urine.

### Discussion

Our study showed significantly higher concentrations of AnV in the plasma and urine of children with INS in comparison with the healthy children, which suggests the involvement of this protein in the pathomechanism of the disease. Similarly, other authors have found higher concentrations of AnV in the urine of patients suffering from primary glomerulopathies, and in patients with other diseases which affect the kidneys.<sup>15</sup>

The pathomechanism of the increased AnV concentrations in patients with kidney diseases is not clear. The protein occurs in the kidneys primarily in the distal tubules and epithelial cells of Bowman’s capsule.<sup>8,16</sup> According to Matsuda et al., the increase of its concentration in the urine may indicate damage to those parts of the nephron, just as, e.g., lysosomal enzymes (NAG) or small-molecule proteins, such as  $\alpha_1$ -microglobulin and  $\beta_2$ -microglobulin, are markers of disorders in the proximal tubules.<sup>16</sup> The experimental glomerulonephritis in rats showed high concentrations of AnV in the urine, concurrent with increased secretion of B NAG isoenzyme.<sup>16</sup> Annexin V was found on the luminal surface of the cell membranes of the distal tubules and in their lumen, and outflow of this protein from the tubule cells was observed.

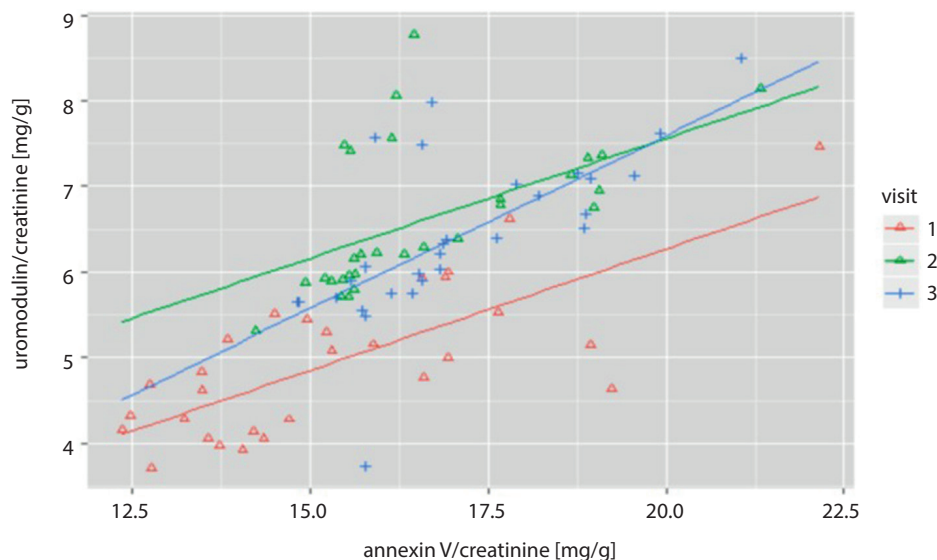


Fig. 3. Correlations between urinary concentrations of AnV and UM in INS patients at 3 time points

Table 4. Correlations between concentrations of AnV, CsA and GFR of the patients suffering from INS in 3 time points: before CsA treatment (I), and after 6 (II) and 12 (III) months of therapy

Parameter	GFR I [mL/min/1.73 m <sup>2</sup> ]	GFR II [mL/min/1.73 m <sup>2</sup> ]	GFR III [mL/min/1.73 m <sup>2</sup> ]
u AnV/u creatinine [ng/mg]	$r = 0.06$ $p = 0.77$	$r = -0.3$ $p = 0.26$	$r = -0.37$ $p = 0.18$
CsA [ng/mL]	–	$r = -0.28$ $p = 0.36$	$r = -0.15$ $p = 0.59$

GFR – glomerular filtration rate; AnV – annexin V; CsA – cyclosporine A; INS – idiopathic nephrotic syndrome; u – urine; p – level of significance; highlighted  $p < 0.05$ .

Moreover, a relationship was found between the concentration of AnV in the urine and the degree of kidney tissue damage.

The previously cited work of Matsuda et al.<sup>15</sup> reported AnV concentrations in the urine of patients with nephrotic syndrome, lupus nephritis, IgA nephropathy, and CKD, as well as in healthy people. Significantly higher concentrations of AnV were noted in the first 2 groups of patients compared to the others, and the highest levels were found in the patients with nephrotic syndrome. This is consistent with our observations of children with INS. Similar results were presented by Simsek et al. in a study on children with nephrotic syndrome.<sup>18</sup> Their research also confirms our observations regarding plasma AnV concentration (higher in sick children than in healthy children) and the lack of correlation between concentrations of AnV in the plasma and urine.

The origin of AnV excreted with urine has not yet been determined. The lack of a correlation between concentrations of AnV in the plasma and the urine suggests that the increased urine AnV concentration in INS cannot be regarded as a consequence of increased excretion by the basal membrane of the glomeruli. This is also supported by the fact that we did not find a correlation between AnV excretion in the urine and proteinuria. This is consistent with the study by Simsek et al.,<sup>18</sup> though it differs from the observations of Matsuda et al. regarding adults.<sup>15</sup> These authors have shown a positive correlation with proteinuria (defined as the concentration of protein in urine) and suggested that a high concentration of AnV in the urine may be an indicator of acute kidney damage, resulting in proteinuria. This difference of observations may be due, as other authors have pointed out,<sup>18</sup> to age-dependent kidney function and metabolism. It may also be a consequence of the methods used and the method of assessing the amount of protein in the urine. In our study, the protein to creatinine concentration ratio has been calculated in urine, which increases the reliability of results.

The reason for the increased plasma AnV concentrations in children suffering from INS that we observed is unclear. It is known that the basic pathophysiological role of this protein is associated with cell apoptosis, and that higher indicators of apoptosis of circulating lymphocytes have been reported in children with nephrotic syndrome.<sup>19</sup> The protein also occurs in leukocytes and platelets, and disorders of these cells are one element of the syndrome.<sup>15,20</sup> The wide variance of AnV concentration in the plasma of healthy people which has been observed by other authors additionally supports the idea that there are many determinants of these markers.<sup>18</sup> Therefore, AnV concentration in the urine may better reflect kidney changes than concentrations in the plasma, especially since some researchers did not observe any differences in the level of this protein between sick and healthy people at all.<sup>21</sup>

In recent years, more and more emphasis has been placed on changes in the distal tubules in the course of nephrotic

syndrome.<sup>22,23</sup> For example, Tudpor et al.,<sup>24</sup> in an animal model of nephrotic proteinuria, demonstrated its negative impact on the distal tubules by changes in TRVP5, leading to disorders of the intercellular transport of  $Ca^{+2}$ . In these processes, which involve the protein kinase C, the AnV may play a regulating role.<sup>25</sup>

We did not find differences in urine AnV concentrations between patients suffering from SRNS and SDNS. On the other hand, Simsek et al. demonstrated higher AnV concentrations in the urine of patients suffering from SRNS than in patients with SSNS.<sup>18</sup> It is difficult to compare these results to those of our study. Our study involves children with SDNS and SRNS, in which the vast majority of kidney biopsies found changes typical of minimal change disease and mesangial proliferation. However, most of the kidney biopsies of children with SRNS studied by Turkish authors displayed focal segmental glomerulosclerosis (FSGS).<sup>18</sup> It is known that in the course of nephrotic syndrome in children, there may be a noticeable evolution of morphological images of the kidney biopsies; therefore, we cannot exclude the different degrees of advancement of glomerulopathy in the study groups, hence the different observations. On the basis of their research, Simsek et al. suggested that AnV in the urine may be an indicator of steroid resistance and that it may be significant in predicting the disease course.<sup>18</sup> The results of our own study, however, suggest that the measuring AnV in the urine as a predictor of the response to steroid treatment in children with INS requires further research on larger samples. In the study by Simsek et al., the analysis covered the data from 23 children with SSNS and 22 with SRNS, while in our study, the group of children with SRNS consisted of only 8 children and the majority of the study group (22 patients) were children with SDNS.<sup>18</sup>

In this study, we did not find a statistically significant difference in the concentrations of AnV and UM in the urine among the children with SRNS and SDNS, either before the start of CsA therapy or during the treatment. This finding suggests a lack of association between possible CsAN and resistance to steroid treatment. The views of Sinha et al. on this matter are different, though, because they believe that starting resistance to steroids is one of the risk factors of CsAN, while the others include duration of the disease, massive proteinuria and hypertension during therapy.<sup>26</sup> These differing observations may result from the different characteristics of the patients with SRNS: none of them showed hypertension or severe proteinuria. It should be also noted that in other studies concerning CsAN, the response to steroid treatment was not described as a risk factor for adverse effects of the drug.

In our study, we attempted to assess the usefulness of AnV as a marker in children suffering from INS and being treated with CsA. We reported an increasing value of AnV concentration in the urine of sick patients in subsequent months of CsA therapy. While taking into account the fact that the children were in nephrotic syndrome


remission, the observed increase in the concentration of this protein, assessed after 6 months and 12 months of treatment, may indicate the ongoing processes that damage the cells of distal tubules and may be the result of the nephrotoxicity effect of the drug. In this study, we related the AnV concentrations to the concentrations of UM, a glycoprotein with a molecular weight of 80–90 kDa which is produced almost exclusively by the cells of the distal tubules and the ascending limb of the loop of Henle.<sup>27</sup> We found higher concentrations of UM in the urine of sick children before the introduction of CsA therapy than in healthy children, which may confirm that the distal tubules are damaged in the course of the underlying disease. The treatment with CsA resulted in further increases in this protein level after 6 months of treatment. This finding suggests that despite remission of the disease, there is a progression of changes in the distal tubules due to the side effect of the drug. However, the values of UM concentration in the urine after an additional 6 months were stable, unlike in the case of AnV. Perhaps AnV is not only an early, but also a sensitive marker of CsAN. Its usefulness as a marker in children with INS and undergoing treatment with calcineurin inhibitors requires further studies. It would be interesting to perform a study concerning AnV in children with different histopathological types of nephrotic syndrome. This is one of the limitations of our study. It should also take into account the issue of response to steroids (resistance/dependency) as a risk factor for nephrotoxicity of the drug.

## Conclusions

An increase in urine AnV concentration can be found in children with INS and being treated with CsA, which suggests that AnV may be useful as a marker for monitoring the therapy. Increased excretion of the proteins of the distal tubules in the urine of patients suffering from INS and undergoing CsA treatment, in the absence of other indicators of CsAN, indicates that as early as after 6 months of pharmacotherapy, functional impairment of the kidney tubules may occur. Annexin V seems to be a more sensitive indicator of changes in the distal tubules in cyclosporine therapy than UM. The usefulness of AnV as an indicator in the urine of children suffering from INS and treated with calcineurin inhibitors requires further studies.

### ORCID iDs

Anna Jakubowska  <https://orcid.org/0000-0002-7732-3487>

Katarzyna Kiliś-Pstrusińska  <https://orcid.org/0000-0001-7352-6992>

### References

- Zagury A, Oliveira AL, Montalvão JA, et al. Steroid-resistant idiopathic nephrotic syndrome in children: Long-term follow-up and risk factors for end-stage renal disease. *J Bras Nefrol.* 2013;35(3):191–199.
- Mekahli D, Liutkus A, Ranchin B, et al. Long-term outcome of idiopathic steroid-resistant nephrotic syndrome: A multicenter study. *Pediatr Nephrol.* 2009;24(8):1525–1532.
- Catran DC, Rao P. Long-term outcome in children and adults with classic focal segmental glomerulosclerosis. *Am J Kidney Dis.* 1998;32(1):72–79.
- Kim JS, Bellw CA, Silverstein DM, Aviles DH, Boineau FG, Vehaskari VM. High incidence of initial and late steroid resistance in childhood nephrotic syndrome. *Kidney Int.* 2005;68(3):1275–1281.
- Ishikura K, Ikeda M, Hattori S, et al. Effective and safe treatment with cyclosporine in nephrotic children: A prospective, randomized multicenter trial. *Kidney Int.* 2005;73(10):1167–1173.
- Gerke V, Moss SE. Annexins: From structure to function. *Physiol Rev.* 2002;82(2):331–371.
- Lizarbe MA, Barrasa JI, Olmo N, Gavilanes F, Turnay J. Annexin–phospholipid interactions: Functional implications. *Int J Mol Sci.* 2013;14(2):2652–2683.
- Marchewka Z. Low molecular weight biomarkers in the nephrotoxicity. *Adv Clin Exp Med.* 2006;15(6):1129–1138.
- Wever KE, Wagener FA, Frielink C, et al. Diannexin protects against renal ischemia reperfusion injury and targets phosphatidylserines in ischemic tissue. *PLoS One.* 2011;6(8):e24276. doi:10.1371/journal.pone.0024276
- Bamri-Ezzine S, Ao ZJ, Londoño I, Gingras D, Bendayan M. Apoptosis of tubular epithelial cells in glycogen nephrosis during diabetes. *Lab Invest.* 2003;83(7):1069–1080.
- Emanuel VL, Mnuskina MM, Smirnov AV, et al. Annexin-5 as a biochemical marker of early vascular disorders under chronic disease of kidneys [in Russian]. *Klin Lab Diagn.* 2013;4:9–10.
- Meier P, Dayer E, Blanc E, Wauters JP. Early T cell activation correlates with expression of apoptosis markers in patients with end-stage renal disease. *J Am Soc Nephrol.* 2002;13(1):204–212.
- International Study of Kidney Disease in Children. Primary nephrotic syndrome in children: Clinical significance of histopathologic variants of minimal change and of diffuse mesangial hypercellularity. A Report of the International Study of Kidney Disease in Children. *Kidney Int.* 1981;20(6):765–771.
- Schwartz GJ, Brion LP, Spitzer A. The use of plasma creatinine concentration for estimating glomerular filtration rate in infants, children, and adolescents. *Pediatr Clin North Am.* 1987;34(3):571–590.
- Matsuda R, Kaneko N, Horikawa Y, et al. Measurement of urinary annexin V by ELISA and its significance as a new urinary marker of kidney disease. *Clin Chim Acta.* 2000;298(1–2):29–43.
- Matsuda R, Kaneko N, Horikawa Y, et al. Localization of annexin V in rat normal kidney and experimental glomerulonephritis. *Res Exp Med (Berl).* 2001;200(2):77–92.
- Tomlinson PA. Low molecular weight proteins in children with renal disease. *Pediatr Nephrol.* 1992;6(6):565–571.
- Simsek B, Buyukcelik M, Soran M, et al. Urinary annexin V in children with nephrotic syndrome: A new prognostic marker? *Pediatr Nephrol.* 2008;23(1):79–82.
- Zachwieja J, Dworacki G, Bobkowski W, Dobrowolska-Zachwieja A, Zaniew M, Maciejewski J. Increased apoptosis of peripheral blood lymphocytes in children with nephrotic syndrome. *Pediatr Nephrol.* 2002;17(3):197–200.
- Sinha A, Bagga A. Nephrotic syndrome. *Indian J Pediatr.* 2012;79(8):1045–1055.
- Kaneko N, Matsuda R, Hosoda S, Kajita T, Ohta Y. Measurement of plasma annexin V by ELISA in the early detection of acute myocardial infarction. *Clin Chim Acta.* 1996;251(1):65–80.
- Chugh SS, Clement LC, Macé C. New insights into human minimal change disease: Lessons from animal models. *Am J Kidney Dis.* 2012;59(2):284–292.
- Zhang S, Audard V, Fan Q, Pawlak A, Lang P, Sahali D. Immunopathogenesis of idiopathic nephrotic syndrome. *Contrib Nephrol.* 2011;169:94–106.
- Tudpor K, Laínez S, Kwakernaak AJ, et al. Urinary plasmin inhibits TRPV5 in nephrotic-range proteinuria. *J Am Soc Nephrol.* 2012;23(11):1824–1834.
- Schlaepfer DD, Jones J, Haigler HT. Inhibition of protein kinase C by annexin V. *Biochemistry.* 1992;31(6):1886–1891.
- Sinha A, Sharma A, Mehta A, et al. Calcineurin inhibitor induced nephrotoxicity in steroid resistant nephrotic syndrome. *Indian J Nephrol.* 2013;23(1):41–46.
- Devuyst O, Dahan K, Pirson Y. Tamm–Horsfall protein or uromodulin: New ideas about an old molecule. *Nephrol Dial Transplant.* 2005;20(7):1290–1294.



# Kidney transplantation and other methods of renal replacement therapy in children: 30 years of observations in one center

Anna Medyńska<sup>A–F</sup>, Katarzyna Kiliś-Pstrusińska<sup>A–F</sup>, Irena Makulska<sup>C,F</sup>, Danuta Zwolińska<sup>E,F</sup>

Department of Pediatric Nephrology, Wrocław Medical University, Poland

A – research concept and design; B – collection and/or assembly of data; C – data analysis and interpretation; D – writing the article; E – critical revision of the article; F – final approval of the article

Advances in Clinical and Experimental Medicine, ISSN 1899–5276 (print), ISSN 2451–2680 (online)

*Adv Clin Exp Med.* 2020;29(5):611–613

## Address for correspondence

Katarzyna Kiliś-Pstrusińska

E-mail: katarzyna.kilis-pstrusinska@umed.wroc.pl

## Funding sources

None declared

## Conflict of interest

None declared

Received on March 20, 2020

Reviewed on April 14, 2020

Accepted on May 1, 2020

Published online on May 28, 2020

## Abstract

**Background.** Kidney transplantation (Tx) is regarded as the optimal treatment method for renal replacement therapy (RRT) for end-stage renal disease (ESRD) patients. Children qualified for Tx should receive the organ as soon as possible in order to improve their chances for healthy development. In our center, RRT for children with ESRD has been conducted for 36 years: hemodialysis (HD) since 1982, peritoneal dialysis (PD) since 1992 and the first transplant in 1987.

**Objectives.** To analyze the rates of different RRT methods in children with ESRD. Special attention was paid to Tx.

**Material and methods.** We compared the rates of RRT methods over 3 subsequent decades (1987–1996, 1997–2006 and 2007–2017).

**Results.** In the period analyzed, 153 children aged from 2 weeks to 18 years were dialyzed. The mean age of the start of RRT was 9.4 years. In 80 children (52.2%), first method was HD, while in 73 patients (47.7%) it was PD. In 25 children, the type of dialysis was changed. Kidney transplantation was performed in 40%, 60.34% and 73% of patients dialyzed in the periods 1987–1996, 1997–2006 and 2007–2017, respectively. The average waiting time for a transplant in the abovementioned decades was 2.25 years, 2.65 years and 1.97 years, respectively. Three children underwent transplantation with a family donor; 1 boy received a transplanted kidney and liver. Two children underwent a preemptive transplant from a deceased donor.

**Conclusions.** The percentage of children with ESRD treated with Tx continues to increase, but in our assessment, it still remains too low. Among the types of dialysis, PD was much more frequently used, which is consistent with pediatric recommendations. Small number of transplants from a living donor and preemptive transplants indicates the need to promote organ donation in Polish society.

**Key words:** renal replacement therapy, kidney transplantation, children

## Cite as

Medyńska A, Kiliś-Pstrusińska K, Makulska I, Zwolińska D.

Kidney transplantation and other methods of renal replacement therapy in children: 30 years of observations in one center.

*Adv Clin Exp Med.* 2020;29(5):611–613.

doi:10.17219/acem/121928

## DOI

10.17219/acem/121928

## Copyright

© 2020 by Wrocław Medical University

This is an article distributed under the terms of the Creative Commons Attribution 3.0 Unported (CC BY 3.0)

(<https://creativecommons.org/licenses/by/3.0/>)

## Introduction

Kidney transplantation (Tx) is undoubtedly the best method for renal replacement therapy (RRT) in children with end-stage renal disease (ESRD).<sup>1</sup> In addition to the benefits that are universal for all kidney recipients, organ transplantation in children allows for the best physical development possible when it comes to chronic illness, as well as for noticeable benefits in the child's intellectual and social development. In the last 2 decades, the survival of patients who have been kidney recipients has improved significantly, as new groups of children are eligible for treatment with this method (e.g., patients who lost a transplant or who have been recipients of another transplant). The first pediatric patients were included in the RRT in the 1960s.<sup>2</sup> In our clinic, hemodialysis (HD) has been available since 1982 and peritoneal dialysis (PD) since 1992. The first patient from our clinic received a transplant 30 years ago. Since then, the number of transplants in children treated for ESRD has been rising steadily, but many of them stay on the waiting list for a long time.

## Objectives

The aim of the study was to assess the rates of Tx treatment in children with ESRD in comparison with other methods of chronic RRT. We analyzed the data of patients treated between 1987 and 2017; in particular, we compared the transplants conducted over 3 subsequent decades.

## Patients and methods

We analyzed the data of patients treated with RRT in the period of 1987–2017.

The following factors were taken into account: the children's age, the children's age when dialysis began, the type of dialysis (HD or PD) used as the first method of RRT, possible alterations in the type of dialysis therapy, and the cause of ESRD. In the group of patients treated with Tx, we analyzed the following factors: the age at which the kidney was transplanted, the waiting time for Tx and the type of transplantation (transplantation from a deceased donor, from a living donor, or preemptive transplant).

The collective data analysis compared RRT over 3 decades: 1987–1996, 1997–2006 and 2007–2017. In the group of dialyzed patients, in the 2<sup>nd</sup> or 3<sup>rd</sup> decade, those who started dialysis in the given period and those who continued it from the previous decade were distinguished. In particular decades, the number of transplants was referred to the total number of patients dialyzed during the specified period. Among the transplanted patients, the group of children was separated from the group of adults. The latter included patients who, after reaching the age of 18, were further dialyzed at the pediatric

station and were transplanted under their care. The percentage of transplants in a given period was determined by referring the number of Tx to the number of dialyzed patients, regardless of the date of their inclusion in the dialysis program.

## Results

In the period studied, 153 children aged from 2 weeks to 18 years (mean age: 10.17 ± 5.63 years) were dialyzed; the average age of the start of RRT was 9.4 years. The causes of ESRD were as follows: 49% – congenital anomalies of the kidney and the urinary tract, 40% – glomerulonephritis and 11% – other causes. In 80 children (52.2%), the method utilized first was HD, while in 73 children (47.7%) it was PD. In 25 children, the type of dialysis was changed.

In the period of 1987–1996, 41 children were hemodialyzed and 9 children were treated with PD. In the next decade, 26 children underwent RRT with HD, while 32 children were treated with PD. In 2007–2017, 13 children were treated with HD and 32 children were treated with PD. In the 1<sup>st</sup> decade, Tx was performed in 14 children (including 13 on HD and 1 on PD) and in 6 young adults. In the next decade, Tx was carried out in 12 children treated with HD and in 17 who were treated with PD and started dialysis in this period. In addition, 6 patients who had undergone dialysis in the previous decade received a transplant (3 children and 3 young adults). Between 2007 and April 2017, hemodialysis was initiated in 13 children, whereas PD treatment was started in 32 patients. During this period, Tx was performed in 6 children treated with HD and in 17 children treated with PD. Similarly to the previous decade, transplants were also conducted in 8 children and 2 young adults who had started dialysis therapy earlier.

In total, Tx was performed in 20 (40%), 35 (60.34%) and 33 (73%) of patients who were dialyzed in 1987–1996, 1997–2006 and 2007–2017, respectively. The average waiting time for a transplant in the abovementioned decades was 2.25 years, 2.65 years and 1.97 years, respectively (range: 6 months–10 years).

Among our patients, a transplantation from a family member in the analyzed period was performed only in 3 children who were dialyzed in the period of 1997–2006, which constitutes 1.96% of all patients on RRT in the entire period analyzed. One patient underwent a kidney and liver transplant. In the years 2007–2017, a preemptive transplant from a deceased donor (1.3%) was performed in 2 children.

## Discussion

End-stage renal failure in children is much less common than in adults, with an incidence rate of 5–10 per million each year.<sup>3</sup> The causes of ESRD in the pediatric

population are primarily congenital anomalies of the kidney and the urinary tract (CAKUT), followed by glomerulonephritis and other diseases.<sup>4</sup> Among our pediatric patients, structural abnormalities of the urinary system were also the most common causes: we found them to be the cause in 49% of children.

The ten-year survival rate is about 80% in children with ESRD. However, the risk of death for dialyzed children remains 30 times higher than in the general population.<sup>5</sup> Of all the methods of RRT, Tx is unquestionably the best method for ensuring proper physical and social development and for significantly improving quality of life.<sup>1</sup>

In Poland, about 100 children are waiting for Tx, and the number of transplants is 35–45 per year. In 2015, 91 children were waiting for Tx and 35 transplants were carried out – 28 from deceased donors and the rest from living donors.<sup>6</sup> The average waiting time for a transplant is about 2 years, which is confirmed by our observations. In Poland, since January 1, 2016, the organ allocation system has been changed: currently, a donor up to the age of 18 is considered a donor for a child, a policy which may shorten the waiting time for organs among children.

The use of modern immunosuppression has improved the long-term prognosis for maintaining renal function after transplantation; it is 90–92% after 1 year and 75–80% after 5 years.<sup>7</sup>

A preemptive Tx helps to prevent complications and the burden of dialysis. It also ensures better patient survival than any type of dialysis.<sup>5,8</sup> Unfortunately, about 80% of children require an initial period of dialysis in preparation of Tx, or after its loss.<sup>9</sup>

In a study conducted by Amaral et al. on a very large group of children (7,527) who received transplants in the USA from 2000 to 2012, it was shown that preemptive transplants from both living and deceased donors ensure longer graft survival and reduce the mortality of patients.<sup>8</sup> In our group of children, a preemptive transplant from a deceased donor was performed in only 2 children (i.e., 1.3%). In research by Amaral et al., the vast majority of patients receiving a transplant before the start of dialysis received kidneys from living donors (66% of all preemptive transplants), which was not confirmed in our small group of children.

Transplantation from a living donor not only provides for preemptive transplantation, but it also has a number of other benefits. Such a graft has a longer survival rate than grafts from a deceased donor.<sup>1</sup> The biological quality of the kidney is better, which is associated with a shorter time of cold ischemia,<sup>1</sup> and there is no brain-death-related damage to the graft, which occurs in deceased donors.<sup>10</sup> Also, immunological matching remains at a more compatible level.

In our group of patients, a living donor transplant (from a family member) was performed in 3 children (during

the 2<sup>nd</sup> decade of observation), which is a small percentage (1.96%) of all transplanted patients. In a study conducted by Perez-Bertolez et al., the rate of living donor transplants reached 38.27%.<sup>11</sup>


According to the North American Pediatric Renal Trials and Collaborative Studies, living donor transplants accounted for 61% of the total transplants in 2001 and dropped to 37% in 2007.<sup>12</sup>

## Summary


Kidney transplantation continues to be the best option available for RRT in children. In subsequent decades, the number of transplants among our patients has increased. However, it should be emphasized that the number of children who start dialysis therapy has also increased. In the authors' opinion, it is important to promote organ donation, family donation in particular, among patients and their families.

### ORCID iDs

Anna Medyńska  <https://orcid.org/0000-0001-8191-045X>

Katarzyna Kiliś-Pstrusińska  <https://orcid.org/0000-0001-7352-6992>

Irena Makulska  <https://orcid.org/0000-0001-8324-274X>

Danuta Zwolińska  <https://orcid.org/0000-0002-6714-3992>

### References

1. Roach JP, Bock M, Goebel J. Pediatric kidney transplantation. *Semin Pediatr Surg.* 2017;26:233–240.
2. Chesnaye NC, van Stralen KJ, Bonthuis M, Harambat J, Groothoff JW, Jager KJ. Survival in children requiring chronic renal replacement therapy. *Pediatr Nephrol.* 2018;33:585–594.
3. Van Arendonk KJ, Boyarsky BJ, Orandi BJ, et al. National trends over 25 years in pediatric kidney transplant outcomes. *Pediatrics.* 2014; 133(4):594–601.
4. Harambat J, van Stralen KJ, Kim JJ, Tizard EJ. Epidemiology of chronic kidney disease in children. *Pediatr Nephrol.* 2012;27(3):363–373.
5. McDonald SP, Craig JC. Long-term survival of children with end-stage renal disease. *N Engl J Med.* 2004;350(26):2654–2662.
6. [Poltransplant. Biuletyn Informacyjny, nr 1 (23), 2015. ISSN 1428-0825]. [http://www.poltransplant.pl/Download/biuletyn2015\\_www.pdf](http://www.poltransplant.pl/Download/biuletyn2015_www.pdf). Accessed on December 15, 2019.
7. Grenda R, Kaliciński P. Organ transplantation in children. Kidney transplantation. An overview. In: Cierpka L, Durlík M, eds. *Clinical Transplantation.* Poznań, Poland: Termedia; 2015:223–233.
8. Amaral S, Sayed BA, Kutner N, Patzer RE. Preemptive kidney transplantation is associated with survival benefits among pediatric patients with end stage renal disease. *Kidney Int.* 2016;90(5):1100–1108.
9. Chesnaye N, Bonthuis M, Schaefer F, et al. Demographics of paediatric renal replacement therapy in Europe: A report of the ESPN/ERA-EDTA registry. *Pediatr Nephrol.* 2014;29(12):2403–2410.
10. Jochmans I, Watson CJ. Taking the heat out of organ donation. *N Engl J Med.* 2015;373(5):477–478.
11. Perez-Bertolez S, Barrero R, Fijo J, et al. Outcomes of pediatric living donor kidney transplantation: A single-center experience. *Pediatr Transplant.* 2017;21(3):1–6.
12. Smith JM, Martz K, Blydt-Hansen TD. Pediatric kidney transplant practice patterns and outcome benchmarks, 1987–2010: A report of the North American Pediatric Renal Trials and Collaborative Studies. *Pediatr Transplant.* 2013;17(2):149–157.





# Classification algorithm of patients with endometriosis: Proposal for tailored management

Stefano Cosma<sup>A,D,F</sup>, Chiara Benedetto<sup>C,E,F</sup>

Gynecology and Obstetrics, Department of Surgical Sciences, City of Health and Science, University of Torino, Italy

A – research concept and design; B – collection and/or assembly of data; C – data analysis and interpretation; D – writing the article; E – critical revision of the article; F – final approval of the article

Advances in Clinical and Experimental Medicine, ISSN 1899–5276 (print), ISSN 2451–2680 (online)

*Adv Clin Exp Med.* 2020;29(5):615–622

## Address for correspondence

Stefano Cosma

E-mail: stefano.cosma@unito.it

## Funding sources

None declared

## Conflict of interest

None declared

Received on June 1, 2019

Reviewed on October 21, 2019

Accepted on March 10, 2020

Published online on May 21, 2020

## Abstract

Endometriosis is a pseudoneoplastic disease that has a significant personal and social impact. Unlike other neoplastic diseases, its management is burdened by uncertainty and controversy. The aim of this article is to furnish clinicians with a simple, useful and updated tool to select an appropriate diagnostic-therapeutic care pathway for affected women. Guidelines and recommendations cite advances in diagnostics, novel medications and optimized assisted reproductive techniques; however, such advancements have not simplified the management of endometriosis, since they often lack an integrated, multidisciplinary view of diagnostic, therapeutic and reproductive scenarios that inevitably overlap in the management of the disease. We selected and compared major society guidelines on the diagnosis and treatment of endometriosis. Three international and 5 national guidelines were analyzed. The overlapping recommendations were extracted and mapped, developing a simplified diagnostic-therapeutic care pathway in the form of an algorithm. We subdivided the patient population attending our tertiary referral center according to 4 decision nodes: type (deep infiltrating endometriosis or isolated endometrioma); stage (I–IV according to the revised American Society for Reproductive Medicine classification); predominant health problem (pain or infertility); and fertility potential of the couple (normal/abnormal screening fertility). We identified 9 classes, each corresponding to a suggested mode of treatment (medical, surgical or assisted reproductive technique) according to the most recent evidence published. This simplified scheme is designed to standardize treatment and is intended for use as a tool in diagnostic and therapeutic planning with a view to reduce inappropriate treatment.

**Key words:** laparoscopy, infertility, endometrioma, deep endometriosis, endometriosis management

## Cite as

Cosma S, Benedetto C. Classification algorithm of patients with endometriosis: Proposal for tailored management.

*Adv Clin Exp Med.* 2020;29(5):615–622.

doi:10.17219/acem/118849

## DOI

10.17219/acem/118849

## Copyright

© 2020 by Wrocław Medical University

This is an article distributed under the terms of the Creative Commons Attribution 3.0 Unported (CC BY 3.0) (<https://creativecommons.org/licenses/by/3.0/>)

## Introduction

The care of patients with deep endometriosis requires treatment in a specialist referral center, where gynecologists collaborate in multidisciplinary teams and evaluate their work in a volume that is sufficient to maintain their high surgical skills. Such centers, designated in the literature as centers of excellence because they operate according to principles of evidence-based medicine, provide for cooperation between gynecologist (group coordinator); pelvic sonographer and radiologist; gynecologist from the assisted reproductive technologies (ART) services; gynecologic/colorectal/urologic laparoscopic surgeon; anesthetist for pain management; psychologist; professional nurse; and (ideally) a neurologist and a patient association representative.<sup>1–3</sup>

The complex nature of such a system leaves it prone to error. Diagnostic Therapeutic Care Pathways (DTCP) were developed to improve reproducibility and uniformity in the delivery of healthcare services and to minimize the occurrence of adverse events. They contextualize treatment guidelines for a disease within the reality of a hospital organization, while taking account of the resources available in order to achieve the best outcome (efficacy), with the best clinical practice (appropriateness), while optimizing resources and time (efficiency).

Endometriosis is estimated to affect 10% of women between the age of 20 and 40 years; about 20% of women are diagnosed with deep endometriosis. The social cost of the disease, in terms of illness and loss of work productivity, is over \$ 9,911 per patient per year.<sup>4</sup> The reasons supporting the choice of disease for which a DTCP can be constructed rest on priority criteria: impact on the health of the individual and the community; presence of specific guidelines; variability and unevenness in the delivery of services; and economic impact. Endometriosis meets these criteria and represents an ideal candidate for establishing a DTCP.

This paper aims to present a simplified algorithm we developed and adopted as DTCP in our tertiary referral center for the management of patients with endometriosis. The scheme, based on published data and the latest major society international guidelines, may serve as a template for developing local care pathways.

## Material and methods

A literature search was conducted for society guidelines for the clinical management of patients with endometriosis published in the last 5 years. Three international societies in the field of endometriosis, reproductive medicine and gynecology, and 5 national societies were included: the World Endometriosis Society (WES, 2017),<sup>5</sup> the European Society of Human Reproduction and Embryology (ESHRE, 2014),<sup>6</sup> the International Federation of Gynecology and Obstetrics (FIGO, 2016),<sup>7</sup> the Society of Obstetricians and

Gynaecologists of Canada (SOGC, 2010),<sup>8</sup> the American College of Obstetricians and Gynecologists (ACOG, 2010),<sup>9</sup> the National Institute for Health and Care Excellence (NICE, 2017),<sup>1</sup> the French College of Gynecologists and Obstetricians (CNGOF, 2018),<sup>10</sup> and the Italian Society of Gynecology and Obstetrics (SIGO, 2018).<sup>11</sup> The society recommendations were compared and presented systematically as an algorithm, along with the quality of evidence<sup>6,8–11</sup> and strength of recommendation.<sup>6,8,10,11</sup>

## Results

### Algorithm

The best way to illustrate a care pathway, essentially a series of decision nodes, is an algorithm, since it gives an overview of the entire course of decision-making. The algorithm (Fig. 1) shows how the clinician, following a course through 4 decision nodes (checkpoints), is able to subdivide the patient population into 9 classes (A–I), each requiring a specific care pathway. The diagnostic checkpoints and therapeutic classes are described below.

### Diagnostic checkpoints

#### Check 1

On the basis of findings from accurate history taking,<sup>1,6–8</sup> self-report questionnaire (Endometriosis Health Profile EHP-30),<sup>12</sup> rectovaginal exam,<sup>6,8</sup> and transvaginal sonography,<sup>1,6,9,13</sup> the gynecologist will be able to discriminate between peritoneal (superficial or deep) endometriosis and isolated endometrioma(s). A transvaginal sonography exam should be performed by the coordinating gynecologist and include consultation, according to standard protocol.<sup>14,15</sup> Ovarian endometriomas are often markers of a more extensive disease.<sup>8</sup> When the 2 ovaries adhere posteriorly to the uterus in the cavity of Douglas, they appear as “kissing ovaries” on the sonogram. This necessitates ruling out deep pelvic endometriosis with bowel and tubal involvement (20% and 90%, respectively).<sup>16</sup> When ovarian and deep endometriosis are present, the latter is prioritized in the management pathway.

#### Check 1bis

When endometriosis has been found, the coordinating gynecologist stages the disease or orders further tests to stage it. If first-line investigations (history, consultation, transvaginal sonography) are inconclusive, second-line diagnostic tests should be ordered, e.g., pelvic magnetic resonance imaging (MRI) with contrast if organ involvement is suspected (bowel, bladder, ureters).<sup>17</sup> If bowel stenosis is suspected, double-contrast barium enema and/or computed axial tomography (CT) of the colon, eventually

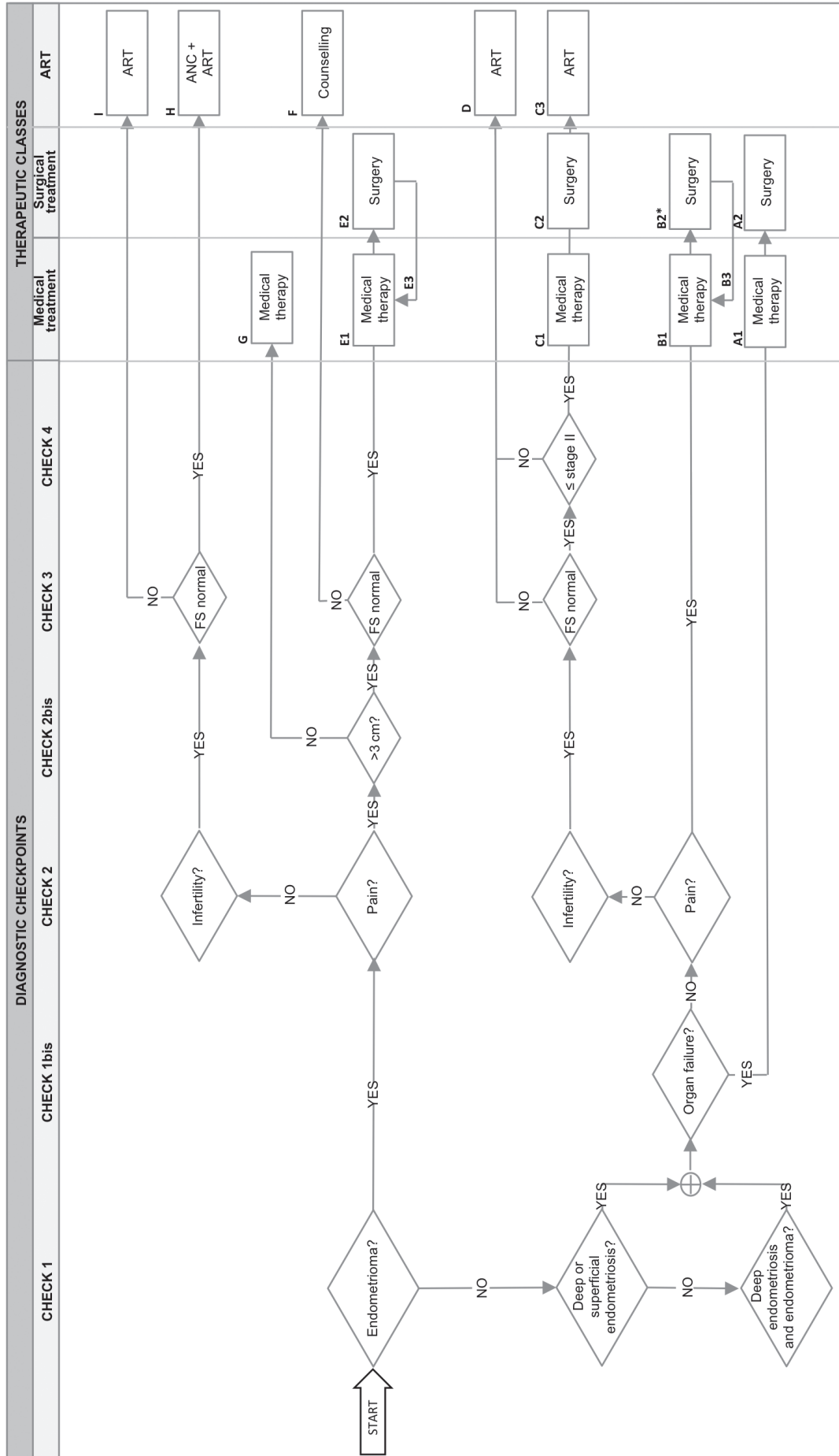


Fig. 1. Classification algorithm of patients with endometriosis (arrow: flowchart starting point)

FS – fertility screening; ANC – attempts of natural conception; ART – assisted reproductive technologies; \* if medical treatment fails.

with virtual colonoscopy, can be ordered.<sup>1,8</sup> Cystoscopy can be useful to rule out bladder trigone involvement.<sup>1,8</sup> If hydronephrosis is suspected, renal scintigraphy will yield useful information on residual renal function. Imaging with <sup>16</sup>α-[<sup>18</sup>F]-fluoroestradiol positron-emission tomography/CT has been shown useful in discriminating between scar tissue and endometriotic tissue in patients with a history of surgery and in the diagnosis of sites of extrapelvic disease. Its use is still limited to clinical studies, however.<sup>18</sup>

## Check 2

Endometriosis causes pain and infertility. Pain manifests with dysmenorrhea in 80% of women and with dyspareunia in 30%. Between 30% and 50% of women will be affected by infertility, defined as the inability to conceive after 1 year of regular, unprotected intercourse. The monthly pregnancy rate is 2–10% compared to the 15–20% rate for the healthy population.<sup>19</sup> It is essential for the following decision node to understand the main reason why the patient sought consultation (pain or infertility) in order to meet her health needs.<sup>1</sup>

## Check 2bis

Most guidelines set an endometrioma size of 3 cm as a cut-off value for clinical decision-making.<sup>6,8,14</sup>

## Check 3

Since endometriosis affects women of reproductive age and ovarian surgery invariably leads to the depletion of oocytes, the reproductive state of the woman and her partner should be evaluated. Fertility tests include the level of anti-Müllerian hormone (AMH) in the blood, sonohysterosalpinography (SSG) and sperm test.<sup>10</sup> Fertility screening (FS) comprises these tests. We will use the term “subfertile” to identify women who are infertile but with normal fertility screening test results.

## Check 4

The most widely used endometriosis classification is the revised American Society for Reproductive Medicine (r-ASRM) system issued in 1997 that uses 4 stages according to local spread of the disease (I – minimal, II – mild, III – moderate, IV – severe).<sup>20</sup> Other, more recent systems are the Enzian classification<sup>21</sup> and the Endometriosis Fertility Index (EFI).<sup>22</sup> All 3 have attracted criticism for the poor correlation between disease stage and symptoms and their inability to predict disease stage. Nonetheless, until new systems become available, it is recommended that patients undergoing surgery be evaluated according to the 4-stage r-ASRM classification and that those with deep endometriosis not yet treated surgically be evaluated according to the Enzian classification; finally, patients in

whom fertility is a priority should be assessed according to the EFI.<sup>5</sup>

## Therapeutic classes

### Class A – patients with organ failure due to deep endometriosis

#### A1

In cases of deep endometriosis involving the bowel, bladder or ureters, 3-month therapy with gonadotropin-releasing hormone (GnRH) analogues can be considered before surgery.<sup>1,23</sup>

#### A2

Surgical treatment is indicated and necessary in cases of severe infiltrating or stenosing disease involving the bowel, bladder, ureters, or pelvic nerves.<sup>8</sup>

### Class B – symptomatic patients with superficial or deep endometriosis

#### B1

Progestin or combined estrogen/progestin therapy can be considered as first-line treatment in patients with symptomatic endometriosis since it has been demonstrated effective in relieving dysmenorrhea (decrease from 3 to 9 points out of 10 on the visual analogue scale (VAS)), dyspareunia and chronic pelvic pain in patients with disease involving the rectum, vagina and rectovaginal septum (RVS). There is no evidence for recommending therapy only to reduce lesion volume in order to prevent surgical complications.<sup>10</sup>

Since there is no significant difference in efficacy between hormone therapies, the choice should be based on safety parameters (e.g., risk of venous or arterial thrombosis), tolerability and costs. There is consensus on first prescribing progestins, then combined estrogen/progestin therapy as first-line therapeutic options. The GnRH agonist therapy or Danazol, though equally effective, should be considered second-line treatment owing to their side effects.<sup>11,24</sup>

Progestins can be administered via oral, intrauterine, intramuscular (IM) or subcutaneous (SC) route. The 2 oral progestins most widely studied for their effect on deep endometriosis are norethindrone acetate (NETA) and dienogest. A recent observational study showed that the two have a substantially similar benefit and that dienogest has better tolerability. The NETA has androgenic activity, is partially metabolized into estrogen, which should protect against bone loss during prolonged therapy, and has greater progestin effects than dienogest,<sup>25</sup> which has mainly antiandrogenic effects. Although the lowest dose approved by the U.S. Food and Drug Administration (FDA) for NETA is 5 mg daily, excellent results have been obtained with half the dose (2.5 mg daily). Dienogest can provide an effective long-term therapeutic option.<sup>26,27</sup> A daily dose of 2 mg was found to be significantly superior

to placebo and equally effective as GnRH agonists in relieving pain.<sup>8,28</sup> Desogestrel<sup>29</sup> is another oral progestin that has been shown to reduce pain in patients with endometriosis of the RVS by 2 points on a VAS pain scale.<sup>10</sup>

Levonorgestrel-releasing intrauterine system (LNG-IUS) can be considered in patients with endometriosis of the RVS and adenomyosis, who no longer seek conception and do not tolerate systemic progestin administration.<sup>30</sup> The lower amount of progestin released in the bloodstream through the IUD reduces the risk of systemic side effects.

Depot medroxyprogesterone acetate (DMPA), IM or SC formulation is poorly manageable because its action can persist for more than 3 months after IM injection and the lack of androgenic properties increases the risk of bone mineral density loss and hypokalemia during prolonged use. Estrogen/progestins can be administered by oral, vaginal or transdermal route with equal efficacy.<sup>1,4,17,24</sup>

Preparations with a lower percentage of ethinylestradiol and containing second-generation progestins should be preferred. They can be administered cyclically or continuously. Continuous administration is preferable when the prevalent symptom is dysmenorrhea.

The GnRH agonists relieve endometriosis-related pain, although there is limited evidence regarding dosage and duration of treatment<sup>31</sup> (strength of recommendation A).<sup>6</sup> A GnRH agonist should never be used for prolonged periods without the addition of estrogen therapy (e.g., 1 mg of 17- $\alpha$  estradiol or equivalent).<sup>8,9</sup> The GnRH agonists do not cause flare-ups, have a rapid effect and suppress the pituitary gland in a dose-dependent manner. The FDA has recently approved their use (Elagolix) for the treatment of moderate-to-severe pain (dose 150 mg daily or 200 mg twice daily).<sup>32</sup>

In women with endometriosis of the RVS refractory to medical or surgical treatment, aromatase inhibitors with combined estrogen/progestin therapy or progestin therapy alone or with GnRH analogues can be considered as they have been shown to reduce endometriosis-related pain<sup>33</sup> (strength of recommendation B).<sup>6</sup>

## B2

Between 1/4 and 1/3 of patients do not respond to medical therapy, probably because of progesterone resistance.<sup>34,35</sup> Surgical treatment of endometriosis is indicated in patients with pelvic pain who do not respond to, decline or have contraindications to medical therapy in order to relieve endometriosis-related pain and improve the patient's quality of life (evidence level IIIA)<sup>6,9</sup> (strength of recommendation B).<sup>8</sup>

The goal of conservative surgery is to remove endometriotic lesions, restore normal anatomy, and preserve visceral innervation and fertility.<sup>8,11,36</sup> Shaving, discoid and segmental resection are the most used techniques in the surgical management of intestinal endometriosis.<sup>37</sup> There is evidence for the superiority of the laparoscopic over the laparotomic approach in the treatment of pelvic

endometriosis, independent of disease severity, as long as surgery is performed in a referral center highly specialized in endoscopic pelvic surgery and by surgeons expert in treatment of the disease<sup>11</sup> (evidence level IIIA).<sup>8</sup> Non-conservative surgical treatment (hysterectomy and adnexectomy) is reserved for cases with pain refractory to medical and surgical therapy and in women in perimenopause who do not desire future pregnancies. In such cases, visible endometriosis must be completely removed.<sup>1,6,11</sup>

## B3

After excisional surgery, hormone therapy should be considered to prolong the benefits obtained with surgery and to prevent disease recurrence<sup>38</sup> (evidence level A).<sup>6</sup>

## Class C – subfertile patients with early stage endometriosis

### C1

Because adequate evidence is lacking in subfertile women with endometriosis, we recommend against prescribing hormone therapy before any intervention to improve spontaneous pregnancy rates. The only benefit of prescription is pain relief (strength of recommendation, good practice point (GPP)).<sup>6</sup>

### C2

In subfertile women with r-ASRM stage I/II endometriosis, ablative or excision laparoscopy of endometriotic lesions raises the pregnancy rate as compared to diagnostic laparoscopy alone<sup>39,40</sup> (evidence level I)<sup>8</sup> (strength of recommendation A).<sup>6</sup> Eight patients need to be treated to achieve pregnancy in 1 of them. It would be more sensible to propose surgical treatment in young patients (<37 years) with a brief duration of infertility (<4 years), presence of ovulatory cycles, normal uterine anatomy, and partner's normal sperm function.<sup>8</sup>

### C3

If spontaneous conception does not occur within 6 months after surgery, ART should be advised.<sup>11</sup> In infertile women with r-ASRM stage I/II endometriosis, it is reasonable to propose within 6 months after surgery a cycle of ovarian stimulation followed by intrauterine insemination (IUI) rather than further expectant management.<sup>41</sup> The pregnancy rate in such cases is similar to that reported for infertility of unknown origin<sup>42</sup> (strength of recommendation C).<sup>6</sup>

## Class D – subfertile patients with advanced stage endometriosis and infertile patients with endometriosis

In subfertile women with r-ASRM stage III/IV endometriosis, there are no controlled studies comparing reproductive outcome after surgery and after expectant management. Prospective cohort studies showed a higher crude

spontaneous pregnancy rate after laparoscopic surgery than after expectant management.<sup>43,44</sup> However, the benefit of reproductive outcome obtained from surgical eradication of deep endometriosis compared to expectant management before ART has not yet been clearly established (strength of recommendation C).<sup>6</sup> The literature contains no randomized studies; there are only 2 prospective cohort studies that showed conflicting results. While some data suggests that surgical resection of endometriosis can improve the pregnancy rate, ovarian damage with decrease in the number of antral follicles can occur after the procedure.<sup>45,46</sup> The pregnancy rate after ART in women with deep endometriosis is the same as that after ART for other indications<sup>47</sup> (strength of recommendation C).<sup>6</sup> An improved outcome of ART after GnRH analogue therapy for 3–6 months before ART was mentioned in a single report and not confirmed to date.<sup>23</sup> Currently, there is weak evidence for the utility of this therapy (strength of recommendation B).<sup>6</sup>

#### **Class E – symptomatic patients with endometrioma size >3 cm and normal FS**

##### **E1**

Preoperative medical therapy should be understood as symptomatic and not cytoreductive since the lesions do not regress completely<sup>48</sup> and resume their metabolic activity when therapy is stopped.<sup>11,49</sup> Nonetheless, a recent study reported a marked reduction in cyst dimension after dienogest therapy.<sup>26</sup>

##### **E2**

It is reasonable to propose enucleation of endometriomas >3 cm in symptomatic women<sup>6</sup> with intact ovarian reserve, large unilateral cysts, or radiologically or clinically suspected cysts.<sup>34</sup> Compared with vaporization or coagulation of the cyst bed, excision of endometriotic cysts is better for reducing the number of recurrences, and the persistence/onset of pelvic pain.<sup>9</sup> It is also associated with a higher rate of spontaneous pregnancy in the short and long term<sup>50,51</sup> (evidence level I)<sup>8</sup> (strength of recommendation A and B).<sup>6</sup>

##### **E3**

In patients who do not desire future pregnancies, postoperative hormone therapy can be proposed, since it has demonstrated a lower recurrence rate (evidence level IA),<sup>8</sup> independent of the type of progestin used.<sup>11</sup>

#### **Class F – symptomatic patients with endometrioma size >3 cm and abnormal fertility tests**

Laparoscopic stripping is associated with a reduction in ovarian reserve, which is quantifiable with a mean postoperative decrease in AMH of 1.13 ng/mL.<sup>52,53</sup> Patients with

endometrioma had significantly lower AMH levels than age-matched patients with no endometrioma, irrespective of the type of surgery, and reduced response to ovarian stimulation in the presence of large cysts.<sup>34</sup> Patients with symptomatic ovarian endometriosis, especially if bilateral, should be adequately counseled on the risks of reduced ovarian function or premature ovarian failure. The risks of surgery should be weighed against the benefits in women with a history of ovarian surgery<sup>6</sup> or low AMH levels (near 1 ng/mL). An option in selected cases is preservation of fertility via cryopreservation of ovarian cortical fragments or mature oocytes obtained with superovulatory induction and transvaginal ultrasound-guided oocyte retrieval.<sup>11,55</sup> Alcohol sclerosing therapy is a technique alternative to laparoscopic enucleation and may be considered in such circumstances, though it has not been tested in adequately sized patient samples in randomized prospective trials.<sup>10</sup>

#### **Class G – symptomatic patients with endometrioma size <3 cm**

In cases of endometrioma size <3 cm, watchful waiting and medical therapy for pain relief are recommended (evidence level IA).<sup>8</sup>

#### **Class H – subfertile patients with endometrioma**

Young women with regular menstrual cycles in whom endometrioma is incidentally discovered, without signs of malignancy, and with good ovarian reserve should be encouraged to conceive naturally for a limited amount of time.<sup>34</sup> If, however, natural conception fails and a course of ART is planned, excisional surgery can be considered to improve follicular access.<sup>6,8</sup>

#### **Class I – infertile patients with endometrioma**

In infertile patients with endometrioma size >3 cm, there is no evidence that cystectomy before ART improves the pregnancy rate<sup>42,56</sup> (strength of recommendation A).<sup>6</sup> The results of ART are similar for women with and those without endometrioma, even if the number of oocytes retrieved is smaller, indicating a reduced ovarian reserve.<sup>11,57</sup>

Atypical endometriomas or cysts with suspicious appearance absent, and asymptomatic women of advanced reproductive age with reduced ovarian reserve, bilateral endometriomas or a history of ovarian surgery may benefit from direct access to ART since surgery may further compromise ovarian function and delay the start of treatment.<sup>34</sup> Improved outcome after ART following GnRH analogue therapy for 3–6 months before starting ART therapy was reported in 1 study and never replicated<sup>23</sup>; further findings are awaited. Currently, there is weak evidence for the utility of this therapy (strength of recommendation B).<sup>6</sup> Outcome after ART is poorer for women with concomitant deep endometriosis.<sup>58</sup>

## Discussion

Due to the poor correlation with disease symptoms as well as a lack of predictive prognosis and unclear pathways of treating pelvic pain and infertility, the current classification systems for endometriosis, which are based on disease extension, continue to attract criticism. Adamson stated that a good classification system is one that provides a simple description of the disease, correlates well with the pain and infertility experienced by women, and predicts response to pain relief, infertility and recurrence of post-treatment symptoms.<sup>59</sup>

As the primary goal is treating the patient rather than the disease, we developed a patient-based classification system concerning patients' health needs, identifying them as possible determinants of therapeutic choices. Personalized medicine emphasizes the customization of health-care, where decisions and practices are tailored to individual patients whenever possible to improve tolerability and compliance.<sup>60</sup> However, unless details are provided on the parameters that lead to personalized choices, a generic appeal to personalized therapy risks turning into a justification for empiricism. Indeed, in clinical practice, physicians are more comfortable with pursuing these goals if pragmatic aids, such as predefined algorithms, are provided. Therefore, it is advisable to set up a clear decision-making process for complex situations in a complex environment.


In medicine, algorithm-based practice implies that the sequence is strictly followed and that the physician does not base primary decisions on individual patient characteristics. Conversely, a patient-tailored approach adopts a treatment strategy based on the individual patient's specific disease situation. Our algorithm was set up in an attempt to merge patient-related parameters (pain, pregnancy desire and fertility status) with disease-related parameters (superficial or deep endometriosis vs isolated endometrioma, disease staging), bearing in mind that a patient-tailored approach and an algorithm-based decision-making are not mutually exclusive but rather complementary.


For planning and analyzing the feasibility of DTCP in a referral center, the subdivision in patient groups is crucial to help clinicians to determine their own adherence to the management pathway and to monitor the quality of care through patient's outcomes. For instance, on the basis of the current literature on women with endometriosis, population A should be expected not to exceed 5% of the total<sup>37</sup>; population B2 to be about 25% of population B1<sup>35</sup>; and populations C3, D and H/I to have pregnancy rates  $\geq 35\%$ ,  $\geq 30\%$  and  $\geq 30\%$ , respectively.<sup>57,60</sup>

Though established in gynecological oncology, DTCP have not yet become part of clinical practice in the management of benign gynecological conditions. The algorithm presented in this article has the potential to help the clinician reduce interindividual variability and ensure

patient-tailored treatment. We are confident that the dissemination and adoption of this management tool may, through consistent implementation, lead to the standardization of care.

## ORCID iDs

Stefano Cosma  <https://orcid.org/0000-0003-0563-0071>

Chiara Benedetto  <https://orcid.org/0000-0003-1514-4771>

## References

1. Endometriosis: Diagnosis and management (NG73). London, UK: National Institute for Health and Care Excellence; 2017.
2. Saridoglu E, Byrne D. The British Society for Gynaecological Endoscopy Endometriosis Centres Project. *Gynecol Obstet Invest.* 2013; 76(1):10–13.
3. D'Hooghe T, Hummelshoj L. Multi-disciplinary centres/networks of excellence for endometriosis management and research: A proposal. *Hum Reprod.* 2006;21(11):2743–2748.
4. Soliman AM, Yang H, Du EX, Kelley C, Winkel C. The direct and indirect costs associated with endometriosis: A systematic literature review. *Hum Reprod.* 2016;31(4):712–722.
5. Johnson NP, Hummelshoj L, Adamson GD, et al; World Endometriosis Society Sao Paulo Consortium. World Endometriosis Society Consensus on the Classification of Endometriosis. *Hum Reprod.* 2017;32(2): 315–324.
6. Dunselman GA, Vermeulen N, Becker C, et al; European Society of Human Reproduction and Embryology. ESHRE guideline: Management of women with endometriosis. *Hum Reprod.* 2014;29(3):400–412.
7. Adamson GD. *Endometriosis: Medical and Surgical Management of Pain and Infertility.* London, UK: International Federation of Gynecology and Obstetrics (FIGO); 2016.
8. Leyland N, Casper R, Laberge P, Singh SS; SOGC. Endometriosis: Diagnosis and management. *J Obstet Gynaecol Can.* 2010;32(7 Suppl 2): S1–32.
9. Practice Bulletin No. 114: Management of endometriosis. *Obstet Gynecol.* 2010;116(1):223–236.
10. Collinet P, Fritel X, Revel-Delhom C, et al. Management of endometriosis: CNGOF/HAS clinical practice guidelines. *J Gynecol Obstet Hum Reprod.* 2018;47(7):265–274.
11. Diagnosi e trattamento dell'endometriosi. SIGO, AOGO, AGUI. Rome, Italy: Italian Society of Gynecology and Obstetrics (SIGO); 2018.
12. Jones G, Jenkinson C, Kennedy S. Evaluating the responsiveness of the Endometriosis Health Profile Questionnaire: The EHP-30. *Qual Life Res.* 2004;13(3):705–713.
13. Hudelist G, Ballard K, English J, et al. Transvaginal sonography vs clinical examination in the preoperative diagnosis of deep infiltrating endometriosis. *Ultrasound Obstet Gynecol.* 2011;37(4):480–487.
14. Guerriero S, Condous G, van den Bosch T, et al. Systematic approach to sonographic evaluation of the pelvis in women with suspected endometriosis, including terms, definitions and measurements: A consensus opinion from the International Deep Endometriosis Analysis (IDEA) group. *Ultrasound Obstet Gynecol.* 2016;48(3):318–332.
15. Exacoustos C, Malzoni M, Di Giovanni A, et al. Ultrasound mapping system for the surgical management of deep infiltrating endometriosis. *Fertil Steril.* 2014;102(1):143–150.e2.
16. Ghezzi F, Raio L, Cromi A, et al. "Kissing ovaries": A sonographic sign of moderate to severe endometriosis. *Fertil Steril.* 2005;83(1):143–147.
17. Bazot M, Daraï E. Diagnosis of deep endometriosis: Clinical examination, ultrasonography, magnetic resonance imaging, and other techniques. *Fertil Steril.* 2017;108(6):886–894.
18. Cosma S, Salgarello M, Ceccaroni M, et al. Accuracy of a new diagnostic tool in deep infiltrating endometriosis: Positron emission tomography-computed tomography with 16α-[18F]fluoro-17β-estradiol. *J Obstet Gynaecol Res.* 2016;42(12):1724–1733.
19. Hughes EG, Fedorkow DM, Cillins JA. A quantitative overview of controlled trials in endometriosis-associated infertility. *Fertil Steril.* 1993; 59(5):963–970.
20. American Society for Reproductive Medicine. Revised American Society for Reproductive Medicine classification of endometriosis. *Fertil Steril.* 1997;67(5):817–821.

21. Haas D, Wurm P, Shamiyeh A, Shebl O, Chvatal R, Oppelt P. Efficacy of the revised Enzian classification: A retrospective analysis. Does the revised Enzian classification solve the problem of duplicate classification in rASRM and Enzian? *Arch Gynecol Obstet*. 2013;287(5):941–945.
22. Adamson GD, Pasta DJ. Endometriosis fertility index: The new, validated endometriosis staging system. *Fertil Steril*. 2010;94(5):1609–1615.
23. Sallam HN, Garcia-Velasco JA, Dias S, Arici A. Long-term pituitary down-regulation before in vitro fertilization (IVF) for women with endometriosis. *Cochrane Database Syst Rev*. 2006;1:CD004635.
24. Vercellini P, Somigliana E, Viganò P, Abbiati A, Barbara G, Crosignani PG. Endometriosis: Current therapies and new pharmacological developments. *Drugs*. 2009;69(6):649–675.
25. Hapgood JP, Africander D, Louw R, Ray RM, Rohwer JM. Potency of progestogens used in hormonal therapy: Toward understanding differential actions. *J Steroid Biochem Mol Biol*. 2013;142:39–47.
26. Petraglia F, Hornung D, Seitz C, et al. Reduced pelvic pain in women with endometriosis: Efficacy of long-term dienogest treatment. *Arch Gynecol Obstet*. 2012;285(1):167–173.
27. Sugimoto K, Nagata C, Hayashi H, Yanagida S, Okamoto A. Use of dienogest over 53 weeks for the treatment of endometriosis. *J Obstet Gynaecol Res*. 2015;41(12):1921–1926.
28. Strowitzki T, Marr J, Gerlinger C, Faustmann T, Seitz C. Dienogest is as effective as leuprolide acetate in treating the painful symptoms of endometriosis: A 24-week, randomized, multicentre, open-label trial. *Hum Reprod*. 2010;25(3):633–641.
29. Leone Roberti Maggiore U, Remorgida V, Scala C, Tafi E, Venturini PL, Ferrero S. Desogestrel-only contraceptive pill versus sequential contraceptive vaginal ring in the treatment of rectovaginal endometriosis infiltrating the rectum: A prospective open-label comparative study. *Acta Obstet Gynecol Scand*. 2014;93(3):239–247.
30. Petta CA, Ferriani RA, Abrao MS, et al. Randomized clinical trial of a levonorgestrel-releasing intrauterine system and a depot GnRH analogue for the treatment of chronic pelvic pain in women with endometriosis. *Hum Reprod*. 2005;20(7):1993–1998.
31. Brown J, Pan A, Hart RJ. Gonadotrophin-releasing hormone analogues for pain associated with endometriosis. *Cochrane Database Syst Rev*. 2010;12:CD008475.
32. Taylor HS, Giudice LC, Lessey BA, et al. Treatment of endometriosis-associated pain with elagolix, an oral GnRH antagonist. *N Engl J Med*. 2017;377(1):28–40.
33. Ferrero S, Gillott DJ, Venturini PL, Remorgida V. Use of aromatase inhibitors to treat endometriosis-related pain symptoms: A systematic review. *Reprod Biol Endocrinol*. 2011;9:89.
34. The effect of surgery for endometriomas on fertility: Scientific Impact Paper No. 55. *BJOG*. 2018;125(6):e19–e28.
35. Cakmak H, Taylor HS. Molecular mechanisms of treatment resistance in endometriosis: The role of progesterone-HOX gene interactions. *Semin Reprod Med*. 2010;28(1):69–74.
36. Ceccaroni M, Clarizia R, Bruni F, et al. Nerve-sparing laparoscopic eradication of deep endometriosis with segmental rectal and parametrial resection: The Negrar method. A single-center, prospective, clinical trial. *Surg Endosc*. 2012;26(7):2029–2045.
37. Donnez O, Roman H. Choosing the right surgical technique for deep endometriosis: Shaving, disc excision, or bowel resection? *Fertil Steril*. 2017;108(6):931–942.
38. Furness S, Yap C, Farquhar C, Cheong Y. Pre and post-operative medical therapy for endometriosis surgery. *Cochrane Database Syst Rev*. 2004;3:CD003678.
39. Jacobson TZ, Duffy JM, Barlow D, Koninckx PR, Garry R. Laparoscopic surgery for pelvic pain associated with endometriosis. *Cochrane Database Syst Rev*. 2014;8:CD001300.
40. Nowroozi K, Chase JS, Check JH, Wu CH. The importance of laparoscopic coagulation of mild endometriosis in infertile women. *Int J Fertil*. 1987;32(6):442–444.
41. Tummon IS, Asher LJ, Martin JS, Tulandi T. Randomized controlled trial of superovulation and insemination for infertility associated with minimal or mild endometriosis. *Fertil Steril*. 1997;68(1):8–12.
42. Werbrouck E, Spiessens C, Meuleman C, D'Hooghe T. No difference in cycle pregnancy rate and in cumulative live-birth rate between women with surgically treated minimal to mild endometriosis and women with unexplained infertility after controlled ovarian hyperstimulation and intrauterine insemination. *Fertil Steril*. 2006;86(3):566–571.
43. Olive DL, Stohs GF, Metzger DA, Franklin RR. Expectant management and hydrotubations in the treatment of endometriosis-associated infertility. *Fertil Steril*. 1985;44(1):35–41.
44. Nezhat C, Crowgey S, Nezhat F. Videolaserectomy for the treatment of endometriosis associated with infertility. *Fertil Steril*. 1989;51(2):237–240.
45. Bianchi PH, Pereira RM, Zanatta A, Alegretti JR, Motta EL, Serafini PC. Extensive excision of deep infiltrative endometriosis before in vitro fertilization significantly improves pregnancy rates. *J Minim Invasive Gynecol*. 2009;16(2):174–180. Erratum in: *J Minim Invasive Gynecol*. 2009;16(5):663.
46. Papaleo E, Ottolina J, Viganò P, et al. Deep pelvic endometriosis negatively affects ovarian reserve and the number of oocytes retrieved for in vitro fertilization. *Acta Obstet Gynecol Scand*. 2011;90(8):878–884.
47. Prefumo F, Rossi AC. Endometriosis, endometrioma, and ART results: Current understanding and recommended practices. *Best Pract Res Clin Obstet Gynaecol*. 2018;51:34–40.
48. Muzii L, Di Tucci C, Achilli C, et al. Continuous versus cyclic oral contraceptives after laparoscopic excision of ovarian endometriomas: A systematic review and meta-analysis. *Am J Obstet Gynecol*. 2016;214(2):203–211.
49. Vercellini P, Viganò P, Somigliana E, Fedele L. Endometriosis: Pathogenesis and treatment. *Nat Rev Endocrinol*. 2014;10(5):261–275.
50. Carmona F, Martínez-Zamora MA, Rabanal A, Martínez-Román S, Balasch J. Ovarian cystectomy versus laser vaporization in the treatment of ovarian endometriomas: A randomized clinical trial with a five-year follow-up. *Fertil Steril*. 2011;96(1):251–254.
51. Hart RJ, Hickey M, Maouris P, Buckett W. Excisional surgery versus ablative surgery for ovarian endometriomata. *Cochrane Database Syst Rev*. 2008;2:CD004992.
52. Raffi F, Metwally M, Amer S. The impact of excision of ovarian endometrioma on ovarian reserve: A systematic review and meta-analysis. *J Clin Endocrinol Metab*. 2012;97(9):3146–3154.
53. Somigliana E, Benaglia L, Paffoni A, Busnelli A, Viganò P, Vercellini P. Risks of conservative management in women with ovarian endometriomas undergoing IVF. *Hum Reprod Update*. 2015;21(4):486–499.
54. Donnez J, Dolmans MM. Cryopreservation and transplantation of ovarian tissue. *Clin Obstet Gynecol*. 2010;53(4):787–796.
55. Benschop L, Farquhar C, van der Poel N, Heineman MJ. Interventions for women with endometrioma prior to assisted reproductive technology. *Cochrane Database Syst Rev*. 2010;11:CD008571.
56. Donnez J, Wyns C, Nisolle M. Does ovarian surgery for endometriomas impair the ovarian response to gonadotropin? *Fertil Steril*. 2001;76(4):662–665.
57. Hamdan M, Dunselman G, Li TC, Cheong Y. The impact of endometrioma on IVF/ICSI outcomes: A systematic review and meta-analysis. *Hum Reprod Update*. 2015;21(6):809–825.
58. Ballester M, Oppenheimer A, Mathieu d'Argent E, et al. Deep infiltrating endometriosis is a determinant factor of cumulative pregnancy rate after intracytoplasmic sperm injection/in vitro fertilization cycles in patients with endometriomas. *Fertil Steril*. 2012;97(2):367–372.
59. Adamson GD. Endometriosis classification: An update. *Curr Opin Obstet Gynecol*. 2011;23(4):213–220.
60. Harb HM, Gallos ID, Chu J, Harb M, Coomarasamy A. The effect of endometriosis on in vitro fertilisation outcome: A systematic review and meta-analysis. *BJOG*. 2013;120(11):1308–1320.



# The role of genetic factors in carpal tunnel syndrome etiology: A review

Andrzej Żyluk<sup>A–F</sup>

Clinic of General and Hand Surgery, Pomeranian Medical University in Szczecin, Poland

A – research concept and design; B – collection and/or assembly of data; C – data analysis and interpretation; D – writing the article; E – critical revision of the article; F – final approval of the article

Advances in Clinical and Experimental Medicine, ISSN 1899–5276 (print), ISSN 2451–2680 (online)

*Adv Clin Exp Med.* 2020;29(5):623–628

## Address for correspondence

Andrzej Żyluk  
E-mail: [azyluk@hotmail.com](mailto:azyluk@hotmail.com)

## Funding sources

None declared

## Conflict of interest

None declared

Received on May 6, 2019

Reviewed on December 12, 2019

Accepted on March 10, 2020

Published online on May 14, 2020

## Abstract

The direct causes of idiopathic carpal tunnel syndrome (CTS) still remain obscure. It has been suggested that the pathology of tendons and other connective tissue structures within the carpal tunnel may be involved in its etiology. The objective of this study was to review the literature about the potential role of genetic factors in the etiology of CTS. Three different mechanisms are suspected to be involved in genetic predisposition to CTS: collagen synthesis, collagen degradation and protection against oxidative stress effect in connective tissue. Several gene groups are involved in the regulation and modulation of these mechanisms, and the research reviewed in this study showed their possible effect on the development of CTS. Variants within the *COL1A1*, *COL5A1* and *COL11A1* genes – encoding the synthesis of minor collagen subtypes – may potentially be involved, as they alter the mechanical properties of tendons and other connective tissue structures within the carpal tunnel. The collagen within connective tissue structures is also remodeled by matrix metalloproteinases (MMPs), so variants of these genes have also been investigated for their possible role in the risk of CTS development. Next, the variants of genes encoding glutathione S-transferase (GST) synthesis were found to be involved in the etiology of CTS. The findings from the abovementioned studies provide reliable information on the potential role of genetic risk factors in the development of CTS.

**Key words:** genetic factors, collagen synthesis, gene variants, carpal tunnel syndrome etiology

## Cite as

Żyluk A. The role of genetic factors in carpal tunnel syndrome etiology: A review. *Adv Clin Exp Med.* 2020;29(5):623–628.  
doi:10.17219/acem/118846

## DOI

10.17219/acem/118846

## Copyright

© 2020 by Wrocław Medical University

This is an article distributed under the terms of the Creative Commons Attribution 3.0 Unported (CC BY 3.0) (<https://creativecommons.org/licenses/by/3.0/>)

## Introduction

Carpal tunnel syndrome (CTS) is the most common compression neuropathy in the upper limbs. Mechanical compression and local ischemia result in symptoms of paresthesia (numbness and tingling), pain, and sensory and motoric disturbance along the median nerve.<sup>1</sup> The pathogenesis of most cases of CTS has not been determined. In the “idiopathic” syndrome, the direct cause of the increased pressure in the carpal tunnel is unknown. Among numerous concepts on pathogenesis of CTS, the possible involvement of tendons and/or other connective tissue structures within the carpal tunnel structure has been proposed.<sup>2–4</sup> Considering the proximity of the 9 flexor tendons and the thick flexor retinaculum to the median nerve within the limited space of the carpal tunnel, it is not unlikely that pathology of these tendons or the retinaculum may contribute to CTS pathology. This concerns possible genetic factors which may influence the characteristics and regulation of collagen fibrils, which are the basic ingredient of connective tissue structures such as tendons, ligaments and bones.

Collagen is not a homogenous substance. Several subtypes of collagen have been identified, but type I is the one most commonly found in all connective tissue structures. Although the collagen fibril consists predominantly of type I collagen, several other quantitatively minor collagens, including types V, XI and XII, have been identified. These types were suspected as playing a possible role in regulating the formation and maintaining the structural integrity of the collagen fibril and surrounding matrix.<sup>2</sup> It has also been postulated that collagen types V and XI interact to regulate fibrillogenesis (the size and assembly of fibrils) during tendon development.<sup>5</sup> Characteristic features of collagen, such as elasticity and endurance, may be related to the proportions of the minor types of collagen composing the fibrils of tendons and filaments. Changes in these properties may translate into modulation of pressure in the carpal tunnel, followed by the development of compression of the median nerve. Previous studies showed a relationship between variants in genes encoding the production and degradation of collagen and some inflammatory/overuse diseases of the connective tissue and increased risk of traumatic damage to the tendons and ligaments.<sup>6–10</sup> The results of these studies prompted investigators to search for a possible association between selected gene variants and the risk of developing CTS.

Another mechanism which may be involved in the etiology of CTS is the activity of matrix metalloproteinase (MMP) genes.<sup>11</sup> It has been shown that the products of these genes play an important role in connective tissue remodeling through collagen fibril degradation. Previous studies showed an association between variants of these genes and tendon and ligament diseases, as well as susceptibility to tendon and ligament injury.<sup>12–16</sup>

Oxidative stress is another mechanism suspected to be involved in the etiology of CTS. It was found to play a role in the development of systemic inflammatory diseases, diabetes and some malignancies. Previous research showed that oxidative stress as a result of overproduction of reactive oxygen and hydroxyl free radicals in synovial connective tissue around the carpal tunnel may result in tissue damage, edema and subsequent development of compression of the median nerve.<sup>17</sup> Glutathione S-transferases (GST) are a large family of isoenzymes involved in the defense mechanisms against reactive oxidative stress. Variants in genes encoding production of these proteins were investigated as playing a possible role in the development of CTS.<sup>18</sup>

The objective of this study was to review the literature on the potential role of genetic factors in the etiology of CTS.

## Material and methods

This article presents a review of the published literature from PubMed and MEDLINE databases on the role of genetic factors in the etiology of CTS. A search for Cochrane Reviews was performed, but we were unable to identify any relevant reviews on this topic. The keywords used when searching for articles were as follows: carpal tunnel pathomechanism, genetics, collagen synthesis, polymorphism, molecular mechanisms, COL genes, MMP genes, and oxidative stress. We attempted to ascertain the role of selected factors – such as collagen, MMP and GST gene variants – as risk factors in the development of CTS.

## Results

### The role of collagen gene variants

Previous studies have found that variants within the genes encoding for synthesis of collagen types I, V, XI, and XII may be implicated in their potential role in various musculoskeletal soft tissue disorders. It was shown that a variant within *COL1A1*, which encodes for  $\alpha 1$  chain of type I collagen of type I collagen, is the functional Sp1 binding site polymorphism (rs1800012, G/T). The TT genotype was associated with the mechanical properties of tendons and ligaments, specifically with greater endurance of the anterior cruciate ligament in the knee joint.<sup>8</sup> Likewise, variants of the *COL5A1* (rs71746744) and *COL11A1* (rs3753841, T/C and rs1676486, C/T) genes – encoding for type V and XI collagen – are involved in modulating the risk of chronic Achilles tendinopathy.<sup>7</sup> The results of these studies prompted investigators to search for potential associations between variants of genes encoding for synthesis of minor collagen types and the risk of CTS development.

The following associations were found:

1. The presence of the T allele of the *COL11A1* gene (rs1676486) has been reported to be associated with decreased  $\alpha 1$ (XI) collagen chain production, and by implication type XI collagen synthesis might be involved in the etiology of CTS.<sup>7,10</sup>

2. The presence of T-C (AGGG) variants (rs3753841, rs1676486 and rs1746744) of the *COL5A1* and *COL11A1* genes is associated with altered mRNA stability, which results in altered type V and XI collagen synthesis. Both types of collagen regulate collagen fibril assembly and diameter; thus, these variants could alter the mechanical properties of tendons and other connective tissue structures within the carpal tunnel, which may be implicated in the etiology of CTS.<sup>3,7</sup>

3. A significant association has been found between the single-nucleotide polymorphism TT of *COL11A1* (rs3753841, T/C) and increased risk of CTS development. This variant, located in exon 52, results in a non-synonymous amino acid exchange of leucine to proline at position 1323 of the  $\alpha 1$ (XI) chain, whereas the rs1676486 variant located in exon 62 results in amino acid substitution from proline to serine at position 1535. The combination of alleles from these variants could potentially cause conformational changes in type XI collagen with a potential effect on the structural and functional properties of new collagen fibrils. These changes, through their effect on tendons and other connective tissue structures in the carpal tunnel, may be further implicated in the etiology of CTS.<sup>10</sup>

4. The abovementioned minor T allele variant of *COL1A1* (rs1800012, G/T), which encodes for the  $\alpha 1$  chain of type I collagen, was significantly associated with an increased risk of CTS among women. The substitution of a tyrosine with a guanine nucleotide within the Sp1 binding site of intron 1 of *COL1A1* has been suggested to result in an increased binding affinity for transcription factor Sp1. This results in *COL1A1* gene expression and the overproduction of type I collagen homotrimers consisting of 3  $\alpha 1$  chains. Increased amounts of type I collagen homotrimers in tendons and other connective tissue structures is believed to change their mechanical characteristics in terms of susceptibility to injury. These changes may also be implicated in the development of increased pressure in the carpal tunnel.<sup>3,6</sup>

Dada et al. reported the results of their genetic studies performed on a self-reported Colored South African population. One hundred and three participants with a history of carpal tunnel release surgery and 150 matched control participants, without any reported history of CTS symptoms, were genotyped for *COL1A1* rs1800012 (G/T), *COL11A1* rs3753841 (T/C), *COL11A1* rs1676486 (C/T), *COL11A2* rs1799907 (T/A), and *COL12A1* rs970547 (A/G). It was shown that the TT variant of *COL11A1* rs3753841 was statistically significantly overrepresented among CTS patients in comparison with the control group (21.4% vs 7.9%;  $p = 0.004$ ). A trend for the T minor allele

to be overrepresented in the CTS group ( $p = 0.055$ ) was also observed with statistically significant differences ( $p = 0.036$ ) when only women were considered in the analysis. The authors believe that constructed inferred variants, including the previously mentioned *COL5A1* gene variant rs71746744 (AGGG), suggest that gene–gene interactions between *COL5A1* and *COL11A1* modulate the risk of developing CTS.<sup>3</sup>

Findings from the abovementioned studies provide reliable information on the potential role of genetic risk factors and the possible role of variations of collagen fibril composition in the etiology of carpal tunnel syndrome. Genetic factors can potentially be included in models developed to identify individuals at risk of CTS.

### The effect of variants of MMP genes on chromosome 11q22

In the previous paragraph, the association between some variants of genes encoding the synthesis of collagen and the risk of developing CTS was discussed. However, the final properties of collagen are also related to other factors. The collagen fibrils within connective tissue structures are remodeled by a family of endopeptidases called MMPs,<sup>11</sup> among other proteins. The following roles of MMPs in the modulation of collagen degradation have been identified<sup>12–15</sup>:

- MMP3 and MMP10 are involved in the degradation of several collagens, including type V, proteoglycans and other extracellular matrix proteins.
- These MMPs also have the potential to activate several pro-MMPs.
- MMP1 is responsible for degrading the triple-helical region in most collagens.
- MMP12 is responsible for degrading elastin and other extracellular matrix proteins.

Several studies have reported a significant association of *MMP3* gene variants with chronic Achilles tendinopathy: AA *MMP3* rs679620 (A/G, E45 K), CC *MMP3* rs591058 (T/C) and AA *MMP3* rs650108 (G/A).<sup>13</sup> An inferred haplotype constructed from MMP variants *MMP10* rs486055 (C/T, R5 3), *MMP1* rs1799750 (G/GG), *MMP3* rs679620 (A/G), and *MMP12* rs2276109 (A/G), which are clustered together on chromosome 11q22, was found to be associated with modulation of the risk of anterior cruciate ligament ruptures in the knee joint.<sup>14,16</sup> Considering the potential effect of MMPs on homeostasis of soft tissue and their structures (tendons and ligaments), studies were commenced to investigate a possible association between various MMP variants and the risk of CTS development. The 4 variants of MMPs were particularly suspected because of previously reported associations with other musculoskeletal diseases and because of their potential functions – the ability to degrade various types of collagens. The *MMP1* rs1799750 (G/GG) variant consists of the presence (GG) or absence (G) of an extra guanine

nucleotide at position 1607 bp. The GG variant creates an Ets binding site that leads to increased transcription of the *MMP1* gene compared to the allele without an extra G nucleotide. The *MMP12* rs2276109 (A/G) variant modulates the binding of the transcription factor activator AP-1 protein, which regulates *MMP12* expression. Variants *MMP3* rs679620 and *MMP10* rs486055 result in a single-nucleotide substitution that causes an amino acid change in proteins – the products of these genes.<sup>11,15</sup> The specific consequences of these amino acid substitutions are unknown, but previous studies have suggested potential associations with tendon and ligament diseases, susceptibility to tendon and ligament injuries, and the risk of CTS development.

Burger et al. reported the results of genetic studies on a self-reported Colored South African population: 97 women with clinically and electrophysiologically confirmed CTS and 131 healthy volunteers without any history of CTS symptoms were genotyped for 4 MMP gene variants: *MMP10* rs486055 (C/T), *MMP1* rs1799750 (G/GG), *MMP3* rs679620 (A/G), and *MMP12* rs2276109 (A/G). The results of this genotyping showed no independent association between these gene variants and CTS (negative outcome). Furthermore, no significant association was found between any of the inferred haplotypes constructed from these variants and CTS.<sup>12</sup> However, this finding does not exclude other variants within the same or other MMP genes within this locus from potentially being associated with the risk of CTS. Several other MMP genes, including *MMP7*, *MMP8*, *MMP13*, and *MMP20*, are located on the long arm of chromosome 11, close to the previously investigated genes. The *MMP3* 5A/6A variant has been associated with several multifactorial conditions and was found to be involved in the regulation of MMP gene expression.<sup>16</sup> The authors suggest that these gene variants may be reasonable CTS candidates for future studies. Also, the use of next-generation sequencing technologies, i.e., targeted sequencing, in identifying additional potentially associated variants within the MMP cluster may yield positive results. It should be noted that the abovementioned study was based on a specific population and that the number of participants was relatively small. Therefore, further studies of other variants of the roles of MMP genes in modulating the risk of development of CTS, based on a European population and involving a greater cohort of patients, seems to be justified.

## The role of GST variants

Another mechanism suspected to be involved in the development of idiopathic CTS is oxidative stress as a result of overproduction of free oxygen ( $\cdot\text{O}$ ) and hydroxyl ( $\cdot\text{OH}$ ) radicals in the sub-synovial soft tissue of tendons and ligaments.<sup>17,18</sup> Increased synthesis or insufficient elimination of reactive oxygen species (ROS) may cause damage to soft tissue structures and may be an underlying mechanism in the development of systemic inflammatory

diseases and malignancies. There are several substances known as antioxidants or radical scavengers which exhibit properties that eliminate free radicals, including vitamins (C, D and E), amino acids (N-acetylcysteine), hormones (steroids), and mannitol. There are also several enzymes with this potential, such as peroxidase, catalase and GSTs (oddly enough, hydroxyl radicals do not have their own natural detoxifying mechanisms). The GSTs are a large family of isoenzymes involved in the defense mechanism against the cytotoxic activity of ROS by inactivating their secondary metabolites. The most investigated isoenzyme members of this family are GST-mu1 (GSTM1), GST-theta1 (GSTT1) and GST-pi1 (GSTP1). They are suspected of playing a protective role against oxidative stress-related development of systemic inflammatory diseases and malignancies.<sup>19</sup> The most common GSTM1 and GSTT1 polymorphisms are deletions in these genes, resulting in a lack of enzyme function. Another frequent polymorphism in this group is *GSTP1* Ile105Val, of which the Ile105Val/Val (AG) and Ile105Val/Val (GG) variants result in reduced enzymatic activity in comparison with that of the Ile105Val/Val (AA) variant.<sup>20</sup> Several studies have demonstrated an association between some GST family isoenzyme variants and rheumatoid diseases, diabetes and malignancies in whose pathogenesis ROS are involved.<sup>19</sup> The results of these studies prompted investigators to search for potential associations between variants of GST genes and the risk of developing CTS.

Eroğlu et al. reported the results of their study of the incidence of 3 GST variants – *GSTM1*, *GSTT1* and *GSTP1* Ile105Val – in a Turkish population of CTS patients and controls (n = 140 and n = 97, respectively). The incidence of *GSTT1* and *GSTM1* variants was determined using the polymerase chain reaction (PCR) method, whereas PCR-restriction fragment length polymorphism (PCR-RFLP) was used to detect the *GSTP1* Ile105Val variant. The researchers found a statistically significant (p = 0.01) higher incidence of the *GSTM1*-null variant in CTS patients compared to the healthy controls. Moreover, the *GSTM1*-null variant was associated with an approximately twofold increase in the risk of CTS. The combination of the *GSTM1*-null and *GSTT1* variants was also more prevalent in CTS patients, but it was of borderline statistical significance (p = 0.045) and did not increase the risk of CTS development. The authors also reported a statistically significant association between greater clinical severity of CTS (in terms of higher Levine questionnaire scores) in patients with the *GSTP1* Ile/Val and Val/Val variants compared to *GSTP1* Ile/Ile, which was more frequent in patients with clinically milder disease.<sup>18</sup> The authors suggest that future studies investigating the potential role of GST variants in the development of CTS are justified.

Fernandez-de-Las-Penas et al. investigated the association of the Val158Met polymorphism with treatment outcomes in 120 female patients with CTS who received either surgery or manual therapy. The patients were randomly allocated to the treatment methods: 60 patients received

3 sessions of manual therapy and 60 underwent carpal tunnel release (n = 60). The rs4680 genotypes were determined after amplifying the Val158Met polymorphism with PCR. The subjects were classified according to their Val158Met polymorphism: Val/Val, Val/Met or Met/Met. Final outcomes were assessed 12 months after the intervention. No interaction was observed between the Val158Met genotype and any outcome: pain, symptom or function severity.<sup>21</sup>

Cevik et al. investigated the influence of interleukin 1 (IL-1) receptor antagonist (IL-1Ra) and angiotensin-converting enzyme (ACE) I/D polymorphisms on the susceptibility to CTS in 158 patients and 151 healthy controls. No statistically significant association was found between gene polymorphisms and the risk of developing CTS.<sup>22</sup>

## Discussion

Three different mechanisms are thought to be involved in genetic predisposition to CTS: collagen synthesis, collagen degradation and protection against the effects of oxidative stress in connective tissue. Several gene groups are involved in the regulation and modulation of these mechanisms and the studies presented herein demonstrated that they may be associated with the etiology of CTS. There are some interesting aspects of the disease which suggest the potential effect of genetic predispositions to its development<sup>23–25</sup>:

- early onset of CTS in adolescents and young adults;
- familial occurrence – most of the members of the family have been affected;
- familial occurrence – higher incidence of the condition among relatives of some patients than in the general population;
- bilateral manifestation of CTS.

None of studies conducted to date have dealt with these specific aspects of the syndrome; therefore, additional investigations in this field seem to be promising. Another unexplored aspect of the genetic predisposition to CTS is that most studies have been based on non-European populations (South African, Turkish and Brazilian). It is known that the incidence of specific mutations may differ among races, so investigation into the abovementioned associations between selected gene variants and the risk of CTS in Caucasians seems to be justified.

## Conclusions

The findings from the studies reviewed in this paper provide reliable information on the potential role of genetic risk factors in the development of CTS. None of the studies conducted to date have dealt with these specific aspects of the syndrome, thus additional studies in this field seem to be appropriate.

## ORCID iDs

Andrzej Żyluk  <https://orcid.org/0000-0002-8299-4525>

## References

1. Puchalski P, Żyluk P, Szlosser Z, Żyluk A. Factors involving the clinical profile of carpal tunnel syndrome. *Handchir Mikrochir Plast Chir.* 2018;50(1):8–13.
2. Burger M, de Wet H, Collins M. The *BGN* and *ACAN* genes and carpal tunnel syndrome. *Gene.* 2014;551(2):160–166.
3. Dada S, Burger MC, Massij F, de Wet H, Collins M. Carpal tunnel syndrome: The role of collagen gene variants. *Gene.* 2016;587(1):53–58. doi:10.1016/j.gene.2016.04.030
4. Burger M, de Wet H, Collins M. The *COL5A1* gene is associated with increased risk of carpal tunnel syndrome. *Clin Rheumatol.* 2014;34(4):767–774.
5. Wenstrup RJ, Smith SM, Florer JB, et al. Regulation of collagen fibril nucleation and initial fibril assembly involves coordinate interactions with collagens V and XI in developing tendon. *J Biol Chem.* 2011;286(23):20455–20465.
6. Ficek K, Cieszyk O, Kaczmarczyk M, et al. Gene variants within the *COL1A1* gene are associated with reduced ACL injury in professional soccer players. *J Sci Med Sport.* 2013;16(5):396–400.
7. Hay M, Patricos J, Collins R, et al. Association of type XI collagen genes with chronic Achilles tendinopathy in independent populations from South Africa and Australia. *Br J Sports Med.* 2013;47(9):569–574.
8. Posthumus M, September AV, Keegan M, et al. Genetic risk factors for anterior cruciate ligament ruptures: *COL1A1* gene variant. *Br J Sports Med.* 2009;43(5):352–356.
9. Posthumus M, September AV, O’Cuinneagain D, van der Merwe W, Schwellnus MP, Collins M. The association between the *COL12A1* gene and anterior cruciate ligament ruptures. *Br J Sports Med.* 2010;44(16):1160–1165.
10. Mio F, Chiba K, Hirose Y, et al. A functional polymorphism in *COL11A1*, which encodes the alpha 1 chain of type XI collagen, is associated with susceptibility to lumbar disc herniation. *Am J Hum Genet.* 2007;81(6):1271–1277.
11. Pasternak B, Aspenberg P. Metalloproteinases and their inhibitors: Diagnostic and therapeutic opportunities in orthopedics. *Acta Orthop.* 2009;80(6):693–703.
12. Burger MC, De Wet H, Collins M. Matrix metalloproteinase genes on chromosome 11q22 and risk of carpal tunnel syndrome. *Rheumatol Int.* 2016;36(3):413–419. doi:10.1007/s00296-015-3385-z
13. Raleigh SM, van der Merwe L, Ribbans WJ, Smith RK, Schwellnus MP, Collins M. Variants within the *MMP3* gene are associated with Achilles tendinopathy: Possible interaction with the *COL5A1* gene. *Br J Sport Med.* 2009;43(7):514–520.
14. Posthumus M, Collins M, van der Merwe L, et al. Matrix metalloproteinase genes on chromosome 11q22 and the risk of ACL rupture. *Scand J Med Sci Sport.* 2012;22(4):523–533.
15. Somerville RP, Oblader SA, Aptek SS. Matrix metalloproteinases: Old dogs with new tricks. *Genome Biol.* 2003;4(6):216. doi:10.1186/gb-2003-4-6-216
16. Malila S, Yuktanandana P, Saowaprut S, Jiamjarasrangi W, Honsawek S. Association between matrix metalloproteinase-3 polymorphism and ACL ruptures. *Genet Mol Res.* 2011;10(4):4158–4165.
17. Kim JK, Koh YD, Hann HJ, Kim MJ. Oxidative stress in sub-synovial connective tissue of idiopathic carpal tunnel syndrome. *J Orthop Res.* 2010;28(11):1463–1468.
18. Eroğlu P, Erkol İnal E, Sağ ŞÖ, Görükmez Ö, Topak A, Yakut T. Associations analysis of GSTM1, T1 and P1 Ile105Val polymorphisms with carpal tunnel syndrome. *Clin Rheumatol.* 2016;35(5):1245–1251. doi:10.1007/s10067-014-2855-0
19. Board PG, Menon D. Glutathione transferases, regulator of cellular metabolism and physiology. *Biochem Biophys Acta.* 2013;1830(5):3267–3288.
20. Ali-Osman F, Akande O, Antoun G, Mao XJ, Buolamwini J. Molecular cloning, characterization and expression in *Escherichia coli* of full-length cDNAs of three human GSTP1 variants: Evidence of catalytic activity of encoded proteins. *J Biol Chem.* 1007;272(15):10004–10012.

21. Fernandez-de-Las-Penas C, Ambite-Quesada S, Fahandezh-Saddi Díaz H, Paras-Bravo P, Palacios-Cena D, Cuadrado ML. The Val158Met polymorphism of the catechol-O-methyltransferase gene is not associated with long-term treatment outcomes in carpal tunnel syndrome: A randomized clinical trial. *PLoS One*. 2018;13(10):e0205516. doi:10.1371/journal.pone.0205516
22. Cevik B, Tekcan A, Inanir A, Kurt SG, Yigit S. The investigation of association between IL-1Ra and ACE I/D polymorphisms in carpal tunnel syndrome. *J Clin Lab Anal*. 2018;32(1):e22204. doi:10.1002/jcla.22204
23. Puchalski P, Szlosser Z, Żyluk A. Familial occurrence of carpal tunnel syndrome. *Neurol Neurochir Pol*. 2019;53(1):43–46. doi:10.5603/PJNNS.a2019.0004
24. Gossett JG, Chance PF. Is there a familial carpal tunnel syndrome? An evaluation and literature review. *Muscle Nerve*. 1998;21(11):1533–1536.
25. Alford JW, Weiss AP, Akelman E. The familial incidence of carpal tunnel syndrome in patients with unilateral and bilateral disease. *Am J Orthop (Belle Mead NJ)*. 2004;33(8):397–400.

# The significance of angiotensin II type 1 receptor (AT1 receptor) in renal transplant injury

Agnieszka Sas-Strózik<sup>A–F</sup>, Magdalena Krajewska<sup>E,F</sup>, Mirosław Banasik<sup>A–F</sup>

Department of Nephrology and Transplantation Medicine, Wrocław Medical University, Poland

A – research concept and design; B – collection and/or assembly of data; C – data analysis and interpretation; D – writing the article; E – critical revision of the article; F – final approval of the article

Advances in Clinical and Experimental Medicine, ISSN 1899–5276 (print), ISSN 2451–2680 (online)

*Adv Clin Exp Med.* 2020;29(5):629–633

## Address for correspondence

Agnieszka Sas-Strózik  
E-mail: a\_sas@op.pl

## Funding sources

The research was financially supported by the Ministry of Health subvention according to number STM.C160.20.115 from the IT Simple system of Wrocław Medical University.

## Conflict of interest

None declared

Received on March 19, 2020

Reviewed on April 25, 2020

Accepted on April 29, 2020

Published online on May 27, 2020

## Abstract

Humoral response beyond human leukocyte antigen (HLA) is of great interest in the transplant community. We decided to summarize the data on a new antigenic target called angiotensin II type 1 receptor (AT1 receptor). Non-HLA antibodies can now be detected in routine clinical care of patients after transplantation, but their role is not fully understood. Numerous analyses showed that non-HLA response may exert a higher risk of allograft rejection and allograft loss independently of the HLA system. Non-HLA response may even have a higher rate of antibody-mediated rejection. Information regarding antigen target, as well as the pathophysiology of its antibodies and diagnostic tools, is essential for a better understanding of non-HLA humoral response. Angiotensin II type 1 receptors are the most recognized target for non-HLA antibodies. Anti-AT1R Abs (anti-angiotensin II type 1-receptor-activating antibodies) may identify renal transplant patients at higher risk of graft rejection and loss. The presence of AT1 receptor expression analyzed together with anti-AT1R Abs should be considered for better transplant immunological risk assessment. Further assessment is required for a better understanding and to create appropriate therapeutic strategies.

**Key words:** angiotensin AT1 receptor, non-HLA antibodies, anti-AT1R Abs, antibody-mediated rejection, renal transplantation

## Cite as

Sas-Strózik A, Krajewska M, Banasik M. The significance of angiotensin II type 1 receptor (AT1 receptor) in renal transplant injury. *Adv Clin Exp Med.* 2020;29(5):629–633. doi:10.17219/acem/121510

## DOI

10.17219/acem/121510

## Copyright

© 2020 by Wrocław Medical University

This is an article distributed under the terms of the Creative Commons Attribution 3.0 Unported (CC BY 3.0) (<https://creativecommons.org/licenses/by/3.0/>)

## Introduction

Antibody-mediated rejection (AMR) is currently the main cause of graft loss.<sup>1</sup> The influence of anti-HLA antibodies on transplant injury is well known and described as humoral theory of transplantation.<sup>2–4</sup> Recently, non-HLA antibodies have been more often considered an additional factor which may have a negative impact on the transplant.<sup>5</sup> The search for the role of these antibodies in renal transplant rejection has become more vital and has led to the discovery of many specific targets of their binding, other than HLA. Non-HLA antigens may be expressed on endothelial and epithelial cells but also parenchymal cells and circulating immune cells, which may be objectives for non-HLA antibodies. Among them, antibodies directed against angiotensin II type 1 receptor (anti-AT1R Abs) seem to be more important and should be considered a potential cause of transplant injury. Anti-AT1R Abs were described as associated with allograft rejection.<sup>6–8</sup> It seems possible that circulating anti-AT1R Abs might indicate renal transplant recipients at an increased risk of graft rejection and loss who are not discovered by the HLA system.

In this review, we discussed the significance of AT1 receptor as a potential target for anti-AT1R Abs. We also analyzed the pathomechanism of transplant injury and clinical consequences of the damage. Finally, we considered potential diagnostic implementation and therapeutic implications.

## AT1 receptor as a potential target for non-HLA antibodies

The distribution of AT1 receptors occurs in many organs and, after activation by angiotensin II, has an impact on the vasoconstriction of vascular smooth muscle cells, sodium reabsorption in proximal tubules and aldosterone secretion in the adrenal cortex.<sup>9,10</sup>

Angiotensin II type 1 receptor (AT1 receptor) is G protein-coupled receptor that contains 7 transmembrane loops with the antibody binding place located on the second loop.<sup>11</sup> It is activated by angiotensin II, which mediates some physiological and pathophysiologic processes with arterial blood pressure or water-salt balance.<sup>12</sup> The human gene for AT1 receptor is located on chromosome 3 and contains 4 exons.<sup>13</sup> There are some polymorphisms of AT1 receptors but the most known is A1166C, which is connected with increased sensitivity to angiotensin II and cardiovascular and renal insufficiency.<sup>14</sup> The stimulation of AT1 receptors by anti-AT1R Abs involves the activation of nuclear factor- $\kappa$ B and causes inflammatory response.<sup>15</sup> Stimulation of higher receptors has also been revealed due to cardiovascular complications connected with remodeling in heart, kidney and vessels, and caused increased mortality and morbidity.<sup>16</sup>

Many studies have shown that the significant presence of anti-AT1R Abs before transplantation is an important risk factor of graft loss.<sup>7,17</sup> Some studies have also revealed a potential influence of a higher level of anti-AT1R Abs on graft failure and worse functioning of renal transplant.<sup>6,18</sup> In their study, Dragun et al. presented 16 allograft recipients with refractory rejection and malignant hypertension and anti-AT1R Abs but without donor HLA-specific antibodies (HLA-DSAs).<sup>15</sup>

These findings challenged us to analyze the presence of AT1 receptors in renal transplant biopsies.<sup>19</sup> As far as we know, nobody has analyzed AT1 receptors in renal transplant biopsies for cause (deterioration in function or proteinuria), so this research was pioneering. We detected positive immunostaining of AT1 receptors in tubular epithelium in 26.3% (42/118) of patients who had indication biopsy. The expression was estimated based on a three-step scale described as lack of expression (0), low immunoreactivity (1) and high expression (2). The expression was assessed as high in 7 patients and as low in 35 patients. What seems to be of high clinical significance is that one-year post-biopsy graft loss in patients with AT1 receptors expression in tubules was significantly higher compared to patients without such expression.<sup>19</sup>

The analysis of 156 renal transplant patients for the expression of the AT1 receptor and, additionally, the presence of anti-AT1R Abs showed that AT1 receptors are also detected in other renal compartments.<sup>20</sup> In this group, 6 patients had positive expression in microcirculation (glomeruli and peritubular capillaries), which was connected with antibody-mediated rejection and high graft loss.

## Pathomechanism of injury

Non-HLA antibodies, like anti-AT1R Abs, can be present before transplantation or occur de novo after transplantation.<sup>21</sup> Many papers have revealed that when HLA antibodies and non-HLA antibodies occur together, they can cause much shorter graft survival compared to the situation when only 1 group of these antibodies is present.<sup>7</sup> This is attributed to their synergistic impact on the structure of the endothelium. It is assumed that HLA antibodies cause endothelial damage and, as a result, autoantigens are exposed, which can lead to the formation of autoantibodies.<sup>22</sup> On the other hand, non-HLA antibodies may provoke an inflammatory response and this process can cause upregulation of HLA expression; in consequence, the graft becomes more prone to alloimmune response.<sup>23</sup>

Angiotensin II type 1 receptor is prevalent on vascular endothelium and performs many significant functions. For example, it stimulates angiotensin II both in physiological and pathophysiological ways.<sup>12</sup> It is involved in vasoconstriction, blood pressure regulation, and water and salt balance. It is the main mediator of oxidative stress and reduced activity of nitric oxide (NO). Angiotensin II causes



endothelial dysfunction and stimulates pro-inflammation in vascular smooth muscle cells.<sup>24</sup> It is thought that an increased level of angiotensin II may lead to acute ischemic complications. It can stimulate local metalloproteinases and, in the end, provoke high possibility of rupture.<sup>25</sup>

Stimulation of AT1 receptors by autoantibodies induces phosphorylation of the ERK1/2 pathway in the endothelium. It raises the binding activity of transcription factor nuclear factor- $\kappa$ B and activator-protein 1. This process may result in the synthesis of proteins, cell migration, inflammation and fibrosis.<sup>26,27</sup> Dragun et al. revealed that only IgG1 and IgG3 subclasses can cause this type of agonistic effect.<sup>15</sup>

Due to their noticeable role in many molecular processes, anti-AT1R Abs are considered to be a significant risk factor in vascular diseases such as pre-eclampsia, systemic sclerosis and malignant hypertension.<sup>28,29</sup>

## The clinical significance of AT1 receptors in renal transplantation

The first report about the impact of antibodies against angiotensin II type-1 receptor (anti-AT1R Abs) appeared in a study by Dragun et al., which indicated the influence of these antibodies on the kidney antibody-mediated rejection, where the presence of anti-AT1R Abs with the absence of anti-HLA was detected in 16 patients with progressive graft failure after renal transplantation.<sup>15</sup>

The presence of anti-AT1R Abs before the transplantation is a separate risk factor for graft failure both shortly after transplantation and in later outcome.<sup>30</sup> Many studies have shown that patients with the anti-AT1R Abs (+) had a worse graft function and more frequent graft loss than the groups of patients where anti-AT1R Abs were absent.<sup>6,31</sup>

Giral et al. in their research focused on the presensitization against AT1 receptors and its impact on graft survival and the risk of acute rejection.<sup>7</sup> The study involved 599 patients who underwent renal transplantation. A higher level of anti-AT1R Abs was identified in 283 patients (47.2%) before renal transplantation. The study assumed an elevated level of anti-AT1R Abs as  $>10$  U/L. In the risk group, where anti-AT1R Abs were positive, the probability of graft failure was 2.6-fold higher 3 years after transplantation and 1.9-fold higher risk of acute rejection during the first 4 months after transplantation. Therefore, a high level of anti-AT1R Abs should be considered a significant risk factor for rejection.

The occurrence of anti-AT1R Abs in renal transplant recipients seems to greatly affect graft survival and is an additional factor of graft rejection in patients with a higher immunological risk.

Antibodies against AT1 receptors may develop in many pathways. The transplant process itself can cause increased

expression of AT1 receptors; ischemia and reperfusion injury by oxidative stress may also lead to an immune response.<sup>23</sup>

The pre-transplant presence of anti-AT1R Abs may be significant in predicting anti-AT1R Ab-related rejection.<sup>34</sup> The evaluation of antibody-mediated rejection (AMR) risk based solely on the HLA pre-sensitization seems to be inadequate. In a study by Taniguchi et al., 351 patients after renal transplantation were taken into consideration. The patients were divided into a group with abnormal biopsies ( $n = 134$ ) and a control group ( $n = 217$ ).<sup>6</sup> Anti-AT1R Abs were detected using quantitative enzyme-linked immunosorbent assay (ELISA) test. A positive level of those antibodies was assumed to be 15–25 U/mL and a negative one  $<10$  U/mL. Of all the patients, 17% ( $n = 60$ ) had a positive level of anti-AT1R Abs. Thirty-five of those patients were anti-AT1R Abs-positive only at the time before transplantation and 1 patient from this group lost his graft. However, the remaining 25 patients, who were anti-AT1R Abs-positive, both before and after transplantation, had significantly greater graft loss. In the group of patients ( $n = 11$ ) in which anti-AT1R Abs occurred de novo, the graft loss was observed in 64% of the patients ( $n = 7$ ). In the group of patients with abnormal biopsies, 14% (19/134) of patients were pre-transplant positive and 84% (16/19) of them stayed positive also after transplantation. In the control group, 19% of the patients (41/217) were anti-AT1R Abs-positive before transplantation, but only 22% (9/41) of them maintained the positive level of those antibodies after transplantation. Graft outcome revealed that 79% (19/24) of the group of patients with abnormal biopsies with post-transplant anti-AT1R Abs-positive had lost their grafts, whereas in the control group, there were no cases of graft loss ( $p < 0.001$ ). Another factor investigated in this study was the influence of anti-AT1R Abs on graft survival with the presence or absence of donor-specific antibodies (DSA). It was observed that the worst graft survival was in the group of patients who presented both post-transplant anti-AT1R Abs and DSA ( $p = 0.007$ ). The study concluded that despite the role of HLA antibodies on graft failure, non-HLA antibodies like anti-AT1R Abs also have a significant influence on graft function deterioration and, finally, rejection.

In the analysis of 117 patients after renal transplantation, arteritis in renal biopsy was significantly more frequent in anti-AT1R Abs (+) group (3/27, 11.1%) than in anti-AT1R Abs (–) group (1/90, 1.1%) ( $p = 0.038$ ). The study showed that the pre-transplant presence of anti-AT1R Abs can influence the graft function as an independent risk factor, which can result in earlier graft failure, rejection and graft loss.<sup>8</sup>

Our very last analysis of the expression of AT1 receptor together with its antibodies in patients who had a renal transplant indication biopsy showed that the presence of anti-AT1R Abs in serum together with the expression of AT1 receptor in transplant biopsy was associated with a significantly higher graft loss.<sup>20</sup>

Anti-AT1R Abs may possibly identify renal transplant recipients at high risk of allograft rejection and loss independently of the HLA system. In the analysis of 1,845 renal transplant recipients, donor-specific HLA antibodies (DSA) and anti-AT1R Abs were measured at the time of the first acute rejection episode or 1 year after transplantation.<sup>32</sup> Transplant biopsy was performed to assess the rejection phenotype and endothelial activation. The analysis showed that 371 (20.1%) participants had anti-AT1R Abs, 334 (18.1%) had DSA and 133 (7.2%) had both.



Additionally, patients with anti-AT1R Abs had a higher rate of antibody-mediated rejection compared to participants without anti-AT1R Abs. Among 77 renal transplant recipients with histological features of AMR but without DSAs, 51 (66.2%) had anti-AT1R Abs. What is more, anti-AT1R Abs-associated rejection was marked by a higher level of endothelial-associated transcripts and lack of complement deposition in allograft capillaries.

Monitoring of non-HLA anti-AT1R Abs, in addition to the current immunologic assessment of renal transplant recipients, may have clinical significance in graft protection. Understanding complement-independent anti-AT1R Abs-mediated rejection may help to create a new therapeutic approach targeting circulating anti-ATR Abs to improve allograft survival. Nowadays, the therapeutic strategy in recipients with antibody-mediated rejection involves removing circulating DSA, blocking the DSA effects, and reducing the production of antibodies.<sup>33</sup> The identification of anti-AT1R Abs may significantly affect the clinical routine care of transplant recipients, as it may facilitate the development of therapeutic strategies. Further research should evaluate the usefulness of current therapies, such as plasma exchange and IVIG, which are standard care in the therapy of patients with anti-HLA AMR. Potential therapeutic strategies may include a selective blockade of AT1 receptors using sartans.<sup>5,32,34,35</sup> However, no clinical trial has been presented to prove the potential benefit of such approaches.

## Conclusions

Angiotensin II type 1 receptors are an important target for non-HLA antibodies, which may cause injury of renal transplant. Independently of the HLA system, monitoring of anti-AT1R Abs may recognize renal transplant patients who are at a higher risk of graft rejection and loss. The presence of AT1 receptor expression in renal biopsy analyzed together with anti-AT1R Abs should be considered for better transplant immunological risk assessment.

### ORCID iDs

Agnieszka Sas-Strózik  <https://orcid.org/0000-0002-1068-0893>  
 Magdalena Krajewska  <https://orcid.org/0000-0002-2632-2409>  
 Mirosław Banasik  <https://orcid.org/0000-0002-0588-1551>

## References

- Sellares J, de Freitas DG, Mengel M, et al. Understanding the causes of kidney transplant failure: The dominant role of antibody-mediated rejection and nonadherence. *Am J Transplant.* 2012;12(2):388–399.
- Terasaki PI. Humoral theory of transplantation. *Am J Transplant.* 2003; 3(6):665–673.
- Cai J, Terasaki PI. Humoral theory of transplantation: Mechanism, prevention, and treatment. *Hum Immunol.* 2005;66(4):334–342.
- Terasaki PI, Cai J. Humoral theory of transplantation: Further evidence. *Curr Opin Immunol.* 2005;17(5):541–545.
- Dragun D, Philippe A, Catar R. Role of non-HLA antibodies in organ transplantation. *Curr Opin Organ Transplant.* 2012;17(4):440–445.
- Taniguchi M, Rebellato LM, Cai J, et al. Higher risk of kidney graft failure in the presence of anti-angiotensin II type-1 receptor antibodies. *Am J Transplant.* 2013;13(10):2577–2589.
- Giral M, Foucher Y, Dufay A, et al. Pretransplant sensitization against angiotensin II type 1 receptor is a risk factor for acute rejection and graft loss. *Am J Transplant.* 2013;13(10):2567–2576.
- Banasik M, Boratynska M, Koscielska-Kasprzak K, et al. The influence of non-HLA antibodies directed against angiotensin II type 1 receptor (AT1R) on early renal transplant outcomes. *Transpl Int.* 2014;27(10): 1029–1038.
- Gasc JM, Shanmugam S, Sibony M, Corvol P. Tissue-specific expression of type 1 angiotensin II receptor subtypes. An in situ hybridization study. *Hypertension.* 1994;24(5):531–537.
- Gurley SB, Riquier-Brison ADM, Schnermann J, et al. AT1A angiotensin receptors in the renal proximal tubule regulate blood pressure. *Cell Metab.* 2011;13(4):469–475.
- Reinsmoen NL, Lai CH, Heidecke H, et al. Anti-angiotensin type 1 receptor antibodies associated with antibody-mediated rejection in donor HLA antibody negative patients. *Transplantation.* 2010; 90(12):1473–1477.
- Hunyady L, Catt KJ. Pleiotropic AT1 receptor signaling pathways mediating physiological and pathogenic actions of angiotensin II. *Mol Endocrinol.* 2006;20(5):953–970.
- Dragun D. Humoral responses directed against non-human leukocyte antigens in solid-organ transplantation. *Transplantation.* 2008; 86(8):1019–1025.
- Miller JA, Scholey JW. The impact of renin-angiotensin system polymorphisms on physiological and pathophysiological processes in humans. *Curr Opin Nephrol.* 2004;13(1):101–106.
- Dragun D, Muller DN, Brasen JH, et al. Angiotensin II type 1-receptor activating antibodies in renal-allograft rejection. *NEJM.* 2005;352(6): 558–569.
- Dzau VJ. Theodore Cooper Lecture: Tissue angiotensin and pathobiology of vascular disease: A unifying hypothesis. *Hypertension.* 2001;37(4):1047–1052.
- Banasik M, Boratynska M, Koscielska-Kasprzak K, et al. Non-HLA antibodies: Angiotensin II type 1 receptor (anti-AT1R) and endothelin-1 type A receptor (anti-ETAR) are associated with renal allograft injury and graft loss. *Transplant Proc.* 2014;46(8):2618–2621.
- Banasik M, Boratynska M, Koscielska-Kasprzak K, et al. The impact of de novo donor-specific anti-human leukocyte antigen antibodies on 5-year renal transplant outcome. *Transplant Proc.* 2013;45(4): 1449–1452.
- Sas A, Donizy P, Koscielska-Kasprzak K, et al. Histopathological relevance of angiotensin II type 1 receptor in renal transplant biopsy. *Transplant Proc.* 2018;50(6):1847–1849.
- Sas-Strózik A, Donizy P, Koscielska-Kasprzak K, et al. Angiotensin II type 1 receptor (AT1R) expression in renal transplant biopsies and anti-AT1R antibodies in serum indicates the risk of transplant loss. *Transplant Proc.* <https://doi.org/10.1016/j.transproceed.2020.01.126>
- Michielsen LA, van Zuilen AD, Krebber MM, Verhaar MC, Otten HG. Clinical value of non-HLA antibodies in kidney transplantation: Still an enigma? *Transplantation Rev.* 2016;30(4):195–202.
- Wang S, Zhang C, Wang J, et al. Endothelial cells in antibody-mediated rejection of kidney transplantation: Pathogenesis mechanisms and therapeutic implications. *J Immunol Res.* 2017;2017:8746303.
- Reinsmoen NL. Role of angiotensin II type 1 receptor-activating antibodies in solid organ transplantation. *Hum Immunol.* 2013;74(11): 1474–1477.

24. Kranzhofer R, Schmidt J, Pfeiffer CA, Hagl S, Libby P, Kubler W. Angiotensin induces inflammatory activation of human vascular smooth muscle cells. *Arterioscler Thromb Vasc Biol.* 1999;19(7):1623–1629.
25. Rouet-Benzineb P, Gontero B, Dreyfus P, Lafuma C. Angiotensin II induces nuclear factor – kappa B activation in cultured neonatal rat cardiomyocytes through protein kinase C signaling pathway. *J Mol Cell Cardiol.* 2000;32(10):1767–1778.
26. Oliveira L, Costa-Neto CM, Nakaie CR, Schreier S, Shimuta SI, Paiva AC. The angiotensin II AT1 receptor structure-activity correlations in the light of rhodopsin structure. *Physiol Rev.* 2007;87(2):565–592.
27. Zhang H, Unal H, Gati C, et al. Structure of the angiotensin receptor revealed by serial femtosecond crystallography. *Cell.* 2015;161(4):833–844.
28. Xia Y, Kellems RE. Angiotensin receptor agonistic autoantibodies and hypertension: Preeclampsia and beyond. *Circ Res.* 2013;113(1):78–87.
29. Crowley SD, Gurley SB, Herrera MJ, et al. Angiotensin II causes hypertension and cardiac hypertrophy through its receptors in the kidney. *PNAS.* 2006;103(47):17985–17990.
30. Banasik M, Boratynska M, Koscielska-Kasprzak K, et al. Long-term follow-up of non-HLA and anti-HLA antibodies: Incidence and importance in renal transplantation. *Transplant Proc.* 2013;45(4):1462–1465.
31. Fuss A, Hope CM, Deayton S, et al. C4d-negative antibody-mediated rejection with high anti-angiotensin II type I receptor antibodies in absence of donor-specific antibodies. *Nephrology (Carlton).* 2015;20(7):467–473.
32. Lefaucheur C, Viglietti D, Bouatou Y, et al. Non-HLA agonistic anti-angiotensin II type 1 receptor antibodies induce a distinctive phenotype of antibody-mediated rejection in kidney transplant recipients. *Kidney Int.* 2019;96(1):189–201.
33. Velidedeoglu E, Cavallé-Coll MW, Bala S, Belen OA, Wang Y, Albrecht R. Summary of 2017 FDA Public Workshop: Antibody-mediated rejection in kidney transplantation. *Transplantation.* 2018;102(6):e257–e264. doi:10.1097/TP.0000000000002141
34. Carroll RP, Riceman M, Hope CM, et al. Angiotensin II type-1 receptor antibody (AT1Rab) associated humoral rejection and the effect of peri operative plasma exchange and candesartan. *Hum Immunol.* 2016;77(12):1154–1158.
35. Weidanz JA, Jacobson LM, Muehrer RJ, et al. ATR blockade reduces IFN-gamma production in lymphocytes in vivo and in vitro. *Kidney Int.* 2005;67(6):2134–2142.

